4

A FAILURE CRITERION FOR BRICKWORK IN AXIAL COMPRESSION

A Thesis submitted for the Degree of

Doctor of Philosophy

of the

UNIVERSITY OF EDINBURGH

by

CHENG-LIM KHOO, B.E., D.I.C., M.I.C.E., C.Eng.

Department of Civil Engineering & Building Science

February 1972

CONTENTS

6.2/

ACKNOWLEDGEMENTS

I wish to thank Professor A.W. Hendry, Ph.D., D.Sc., F.R.S.E., F.I.C.E., F.I.Struct.E. for the opportunity to undertake this research under his personal supervision.

Thanks are also due to the University of Singapore for their generous approval in granting me leave of absence from employment to pursue this work, and to the British Ceramic Research Association for their financial assistance.

The excellent co-operation given to me by the Technical Staff of the Civil Engineering Department is gratefully acknowledged. The skilful presentation of the thesis manuscript is the work of Mrs. G. Temple.

Finally, I would like to extend my appreciation to my wife for her constant encouragement during these years, and to our children, Li-Min and Li-Chung, without whom this thesis might have been completed perhaps a shade earlier.

PRINCIPAL NOTATIONS

The following symbols have been used in this thesis:

A	Area of element.
a	Semi-major axis of ellipse, or internal radius of pipe.
$[B]$	Matrix of co-ordinates of nodal points in element.
$[B^T]$	Transpose of matrix $[B]$.
b	Semi-minor axis of ellipse, or external radius of pipe.
c	Compressive stress.
c_o	Uniaxial compression strength.
D	Diameter of cylindrical specimen, or depth of specimen.
$[D]$	Matrix of elastic constants of element material.
d_b	Thickness of brick.
d_m	Thickness of mortar joint.
E_t	Elastic modulus of brick in tension.
$[F]^e$	Matrix of nodal forces in element.
$[K]$	Stiffness matrix for complete structure.
k	Coefficient in tensile splitting test formula.
k	Stiffness matrix for element.
k_r, k_θ	Coefficients in formula for pipe subject to internal pressure.
L	Width of specimen.
l	Length of specimen.
m	Ratio of semi-minor to semi-major axes of ellipse.
P	Knife-edge load in tensile splitting test.
p	Internal pressure in pipe.
r	Radius of any point in pipe.
s_o	Shear strength of material at zero normal stress.

t/

t	Tensile stress.
t_b	Lateral tensile stress in brick.
t_o	Tensile strength of brick.
V_f	Volume fraction of coarse aggregates in concrete mix.
α	Mortar/brick thickness ratio, or eccentric angle of ellipse.
β	Inclination of normal to the plane to major principal stress.
$[\delta]^e$	Matrix of displacements of nodal points in element.
$[\varepsilon]^e$	Matrix of strains in element.
σ	Normal stress.
σ_o	Uniaxial compression strength.
$\sigma_1, \sigma_2, \sigma_3$	Major, intermediate, minor principal stresses respectively.
σ_b	Tangential stress on the boundary of elliptical flaw.
σ_m	Lateral compressive stress in mortar.
σ_r	Radial stress in pipe.
$\sigma_x, \sigma_y, \sigma_z$	Normal stresses in x, y, z directions respectively.
σ_θ	Circumferential stress in pipe.
$[\sigma]^e$	Matrix of stresses in element.
τ	Shear stress.
τ_{xy}	Shear stress in xy-plane.
μ	Coefficient of internal friction of material, or Micro-strain (10^{-6})

ABSTRACT

The object of this thesis is to establish a failure criterion for brickwork in axial compression.

Chapter 1 introduces the problem of brickwork in compression and reviews previous investigations carried out in this area. It outlines the proposed failure theory for brickwork in compression, and finally lists the experimental and theoretical investigations to be undertaken in order to provide information required to formulate the proposed criterion.

The general behaviour of brittle materials under the action of complex stresses and the existing theories developed to explain their failure mechanism are discussed in Chapter 2.

In Chapter 3, tests carried out on one-third scale model bricks to determine its biaxial compression-tension failure envelope are described. Certain observations concerning the basic strength properties of bricks are noted.

An alternative method of determining the biaxial compression-tension strength relationship for ceramic material is carried out using clay pipe specimens; details of these experiments are given in Chapter 4.

A study of the behaviour of brickwork mortar in a state of triaxial compression is recorded in Chapter 5.

Chapter 6 presents a finite element analysis of the lateral stress distribution in brickwork under axial compression, the results of which clarified the mode of failure observed in axially-loaded brickwork.

Using information gathered from investigations undertaken in earlier chapters, the proposed failure criterion for brickwork in axial compression/

compression is developed in Chapter 7. A favourable comparison of the brickwork compressive strength exists between theoretical predictions given by the failure theory and experimental results obtained from crushing tests on brickwork prisms. The theory is also successfully tested against data on the compressive strength of brickwork taken from selected publications.

The general conclusions arising from this research are listed in Chapter 8 which includes some suggestions for further work.

CHAPTER 1 - BRICKWORK IN COMPRESSION

1.1 INTRODUCTION

Investigation into the loadbearing strength of brickwork was undertaken from time to time many decades ago, but it was only as recent as the late forties that loadbearing brickwork came under serious study. The revived interest in loadbearing brickwork was prompted by the realisation that structural brickwork could, under favourable circumstances, be an economic proposition for high-rise structures, exemplified aptly in the erection of multi-storey buildings in loadbearing brickwork in Switzerland and elsewhere.

The compressive strength of brickwork was certainly the first aspect of structural brickwork to be examined.

In the early stages of the investigation into the compressive strength of brickwork, research programmes were concerned mainly in gathering reliable experimental data with which to update existing provisions in the code of practice whose recommendations were long recognised to be unduly conservative. Little effort was made at this point to achieve a theoretical solution which could describe the behaviour of brickwork in compression. Even so, there were several useful observations which resulted from this phase of brickwork research.

The first was the awareness that the traditional treatment of brickwork as approximating to a homogenous material is far from reality, and that in brickwork one is dealing with a two-phase assemblage of brick and mortar whose carrying capacity under stress will be determined by the interaction of the strength properties of its two constituent materials.

It was/

It was also observed that a brickwork panel axially loaded to destruction produced vertical cracks in the brick elements. This suggests the existence of a lateral tensile stress within the brick, which is rightly subscribed to the different lateral strain characteristics of brick and its horizontal mortar joint, the mortar joint tending to expand laterally more than the brick and in so doing induces a lateral tension in the brick element. This observation is indeed the single most important contribution towards the understanding of the failure mechanism of brickwork in compression, and has since become the central concept in later attempts to derive an analytical solution to the problem.

In the course of experimentation, it was noted that there are various factors which influence the compressive strength of brickwork. It is obvious that a stronger brick produces a higher brickwork compressive strength. Similarly, a richer mortar mix will lead to an increased brickwork strength. Less apparent, however, is the observation that a higher bearing capacity of brickwork is achieved if the mortar joint thickness is kept to a minimum. Like any long column subject to the effect of buckling, the compressive strength of a brick wall is reduced with increasing slenderness ratio. The quality of workmanship has been found to influence greatly the strength of brickwork. However, since the standard of workmanship in research work is usually satisfactory, the workmanship factor is not a consideration in the correlation of laboratory results.

While the effect of the above mentioned factors on the compressive strength of brickwork has been firmly established, there are other factors whose influence on brickwork strength is not so conclusive. Whether the/

Whether the presence of perpends - vertical mortar joints - in brickwork does in fact weaken brickwork in compression is not proven, although it has been mentioned that the effect is negligible in conventional masonry bonds. Another yet undetermined factor is the effect of using perforated and frogged bricks in brickwork. It appears that so long as the degree of perforation is low and the layout and the shape of the perforations do not result in points of stress concentration within the brick, the crushing strength of brickwork is much the same as that made of solid bricks of the same strength. In regard to frogged bricks, the behaviour of the interlocking action of mortar in the frogged area of the brick is currently not known.

In the absence of an analytical solution, empirical relationships, either graphical or algebraic, derived from the results obtained in experiments, have been put forward to show the variation of brickwork compressive strength with a given factor. For example, it has been suggested that the brickwork compressive strength varies as the square root of its brick crushing strength. This relationship may only apply to the type of mortar and its joint thickness used in that series of experiments. Whether the relationship can be extended to include other mortar mixes and joint thicknesses is doubtful. In otherwords, empirical relationships derived from test data are often limited in scope, and needless to say, it is an immense task on the basis of experimental work alone to be able to provide empirical expressions which can cater for the large number of permutations in brickwork strength arising from the various factors affecting the compressive strength of brickwork.

The need/

The need to establish an analytical solution which can account for all known factors which contribute to the compressive strength of brickwork is more than just a matter of academic curiosity. The possibility of introducing, for instance, horizontal reinforcement as a means to enhance the loadbearing strength of brickwork in compression can gain no headway until the behaviour of unreinforced brickwork is fully understood.

Looking wider afield, the search for a substitute to Portland cement mortar is more likely to succeed if the desirable characteristics of a joint material in brickwork are first determined, and this requires a complete understanding of the behaviour of mortar in brickwork which only a proven theory can afford.

Recent years have seen a few but growing number of attempts to arrive at a failure criterion for brickwork in compression which can adequately explain not only the manner in which but also the extent to which a particular factor, such as mortar joint thickness, influences the crushing strength of brickwork. In nearly all of these attempts, the failure criterion has been developed, in part or whole, on the assumption of an elastic behaviour in brick and mortar. It is precisely the inelastic behaviour of the materials, particularly of mortar approaching failure, which determines principally the strength of brickwork in compression. Consequently, these failure theories have been found to be inadequate.

It is the objective of this thesis to establish an acceptable failure criterion for brickwork in compression with a different approach from that of the elastic theory.

1.2 REVIEW OF PREVIOUS WORK

This section contains a literature review of work carried out on the compressive strength/

compressive strength of axially loaded brickwork beginning from the early fifties. Reference may be made to the publications of Morsy[40] and of Monk[39] for information concerning work done prior to this date.

In a paper to the Institution of Civil Engineers, London in 1950, Davey & Thomas[16] described the testing carried out at the Building Research Station to determine, among other things, the relationship between the strength of brick and of mortar, and the strength of brickwork. They pointed out the significant influence of the mortar upon the crushing strength of brickwork piers, and arising from the experimental results, advised against the use of a mortar "stronger than is just necessary to give the optimum strength of brickwork". Using the data acquired in this investigation, Thomas[53] in 1953 criticised the conservative provisions contained in the Code of Practice CP 111 (1948) "Structural Recommendations for Loadbearing Walls", especially in the use of high strength bricks. In his opinion, with these bricks, the permissible brickwork stresses might well be increased by 50 to 75%. This brought about the increased values of permissible stresses for brickwork in the revision in 1964 of CP 111.

The first attempt to develop a theoretical expression for the strength of brickwork in compression was made by Haller[24] in 1960 on the assumption of an elastic behaviour in brickwork. However, he was quick to admit the limitation of his formula, acknowledging the inelastic behaviour of brickwork approaching failure. In the same paper, based upon results derived from some crushing tests on brickwork, Haller evolved an empirical expression which related brickwork strength to strength of brick and of mortar.

Beginning in/

Beginning in 1963, the Structural Clay Products Research Foundation in the United States began a series of brickwork tests designated as the "National Testing Program", the results of which were published in a series of SCPRF Research Reports. In Report No. 1[42] of the program, small scale specimens were tested to determine the influence of brick properties, mortar properties and the thickness of joints on the strength of brickwork. Experimental data indicated that higher brickwork compressive strengths were associated with higher brick and mortar strengths, and that an inverse linear relationship existed between the brickwork compressive strength and the thickness of mortar joints.

In a number of crushing tests on storey-height brickwalls in 1965, Prasan et al.[46] observed that the mode of failure in brickwalls under compression was by transverse splitting, and this suggested the importance of the tensile strength of brick and also of the properties of the horizontal mortar joints in determining the strength of the brickwork. Increases in brickwork strength of over 60% were observed when every bed joint was reinforced horizontally.

Extending the study undertaken by Prasan above, Bradshaw & Hendry[5] in 1967 carried out further tests on the crushing strength of storey-height brickwalls, and the outcome of the tests were largely in agreement with earlier results. Empirical formulae derived from these tests suggested the strength of brickwork in compression to be proportional to the square root of the brick strength, and to the cube or fourth root of the mortar strength. In other words, the influence of mortar strength upon brickwork strength was less than that of brick strength.

A failure/

A failure theory for the compressive strength of brickwork was formulated by Sinha & Hendry[50] in 1966. The analysis assumed an elastic behaviour of brickwork, and predicted the compressive strength at first crack.

In a paper to the International Conference on Masonry Structural Systems in 1967, Hilsdorf[25] outlined a new approach towards the development of a failure criterion for brickwork in compression, in which the compressive strength of brickwork is determined by the interaction of the strength properties of brick and of mortar under their appropriate state of complex stresses. However, due to a lack of information concerning the behaviour of brick and mortar materials under combined stresses, the merit of this method of analysis was not apparent.

Sinha[48, 49] in 1968 devised a direct tensile test for one-sixth scale model bricks, and hence was able to relate the compressive strength of brickwork to the tensile strength of brick, a relationship which he found to be linear.

The performance of walls built of wirecut bricks with and without perforations was comprehensively investigated by West et al.[62] in 1968. The investigation showed that so long as the degree of perforation in bricks was low and the shape of the perforations did not result in points of stress concentration, brickwork built with perforated bricks performed under compression as well as those built with solid bricks.

Morsy[40] in 1968 produced a formula for the compressive strength of brickwork which took into account the effect of the presence of vertical mortar joints in brickwork. Computations using this formula which assumed an elastic behaviour of brickwork did not yield acceptable values.

At the British Ceramic Society's 3rd Symposium on Loadbearing Brickwork held in November 1968, Lenczner[35] presented a failure theory for axially-loaded brickwork which is derived entirely on the assumption of elastic behaviour in brickwork.

Lastly, Francis et al.[19] in 1970 developed a failure theory for brickwork in compression which was partly based on the elastic theory and partly based on an arbitrarily assumed linear failure envelope for brick under biaxial compression-tension. Since the behaviour of brickwork near ultimate stress is principally inelastic, this approach is of doubtful value.

1.3 AN OUTLINE OF THE PROPOSED FAILURE THEORY FOR BRICKWORK IN COMPRESSION

It was pointed out in the concluding part of Section 1.1 that the existing failure theories describing the compressive strength of brickwork have been found to be unsatisfactory. This is because these failure theories have been developed on the assumption of an elastic behaviour in brick and mortar. In reality, both brick and mortar are not truly elastic in behaviour, particularly so for mortar near ultimate stress. In fact, it is the inelastic behaviour of mortar approaching failure which governs principally the compressive strength of brickwork. Another criticism levelled at these elastic failure theories is that they ignore the important fact that the properties of brittle materials, a category to which brick and mortar belong, alter under different states of applied stresses. For example, the values of the elastic constants, say, for mortar under uniaxial compression differ from those under triaxial compression.

The aim of this research, therefore, is to formulate an acceptable failure criterion/

failure criterion for brickwork in compression which can account for all the various factors known to affect the compressive strength of brickwork. If this is achieved, it will then be possible to predict from a given set of brick and mortar parameters the compressive strength of brickwork.

This thesis adopts what may be termed the "strength" approach in which the failure criterion is essentially determined by the strength properties of brick and mortar in the state of complex stresses in which they exist in axially-loaded brickwork. This "strength" approach has the distinct advantage over the elastic theory approach in that it deals with the strength values of brick and mortar and these are readily and accurately measurable quantities, whereas the elastic theory requires the determination of the elastic constants of brick and mortar, and being inelastic materials, these not only vary according to the level of applied stress but are hardly measurable near ultimate load.

More important however, the "strength" approach accounts for the change in material property of the brick and mortar in a state of multiaxial stress, which is indeed a typical feature in the behaviour of brittle materials.

It is felt necessary to give, at this point, an outline of the proposed failure criterion for brickwork in axial compression so that the reader may appreciate the objective behind each phase of the research programme as listed in Section 1.4. A complete development of the failure criterion will, of course, be detailed in a later chapter.

In order not to introduce peripheral factors which may complicate the basic problem, the investigation will be confined to the study of the behaviour of stack-bonded brickwork prisms (i.e of one brick unit with no perpends), as shown in Fig. 1.1(a), subject to axial compression using solid/

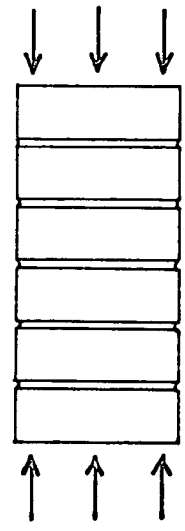

Fig 1.1(a) Brickwork Prism under Axial Load

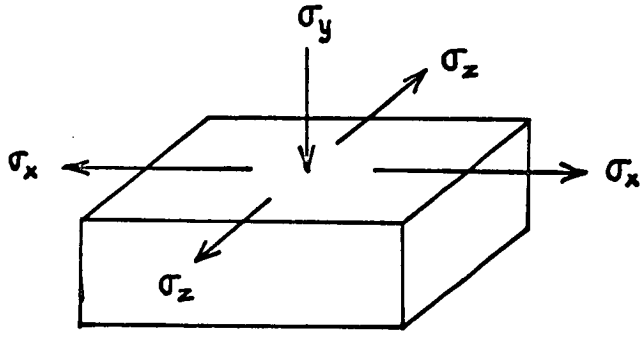

Fig 1.1(b) Brick Element under Vertical Compression & Bi-Lateral Tension

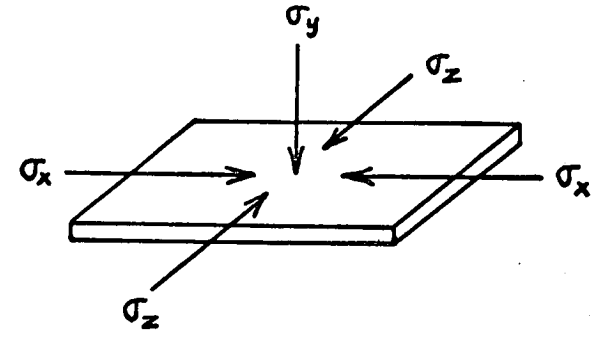

Fig 1.1(c) Mortar Joint under Triaxial Compression

sion using solid bricks (i.e. non-perforated and with no frogs). This eliminates consideration of the influence of mortar perpends, perforations and frogs on the brickwork compressive strength.

Fig. 1.1(a) shows a brickwork prism acted upon by an axial compressive load. If no bond or friction exists at the brick-mortar interface, both the brick and the mortar will be free to expand laterally on their own, the mortar expanding laterally more than the brick. However, in reality, the coefficient of friction between brick and mortar being high, about 0.7, there can be no slippage between brick and mortar under a compressive load. (It can be shown that under any given vertical compression, the lateral force resulting from the differential lateral strain between brick and mortar is always less than the limiting friction at the brick-mortar interface.) This being so, a brick unit in addition to being compressed vertically is also acted upon by a pair of lateral tensions at the brick-mortar interface, the bi-lateral tension being the result of the differential lateral strain between the brick and the mortar joint, see Fig. 1.1(b). Similarly, the mortar joint in addition to a vertical compression is acted upon by a pair of lateral compressive stresses at the brick-mortar interface, see Fig. 1.1(c).

In other words, the state of stress existing in a brick element within a brickwork prism under compression is one of vertical compression and bi-lateral tension, and that of the mortar joint is one of triaxial compression.

The development of stresses in a brick element in a brickwork prism subject to axial compression is best illustrated graphically. Fig. 1.2 shows the assumed failure envelope for brick in a state of biaxial compression-tension, since the lateral tensile stresses in the x and z directions,/

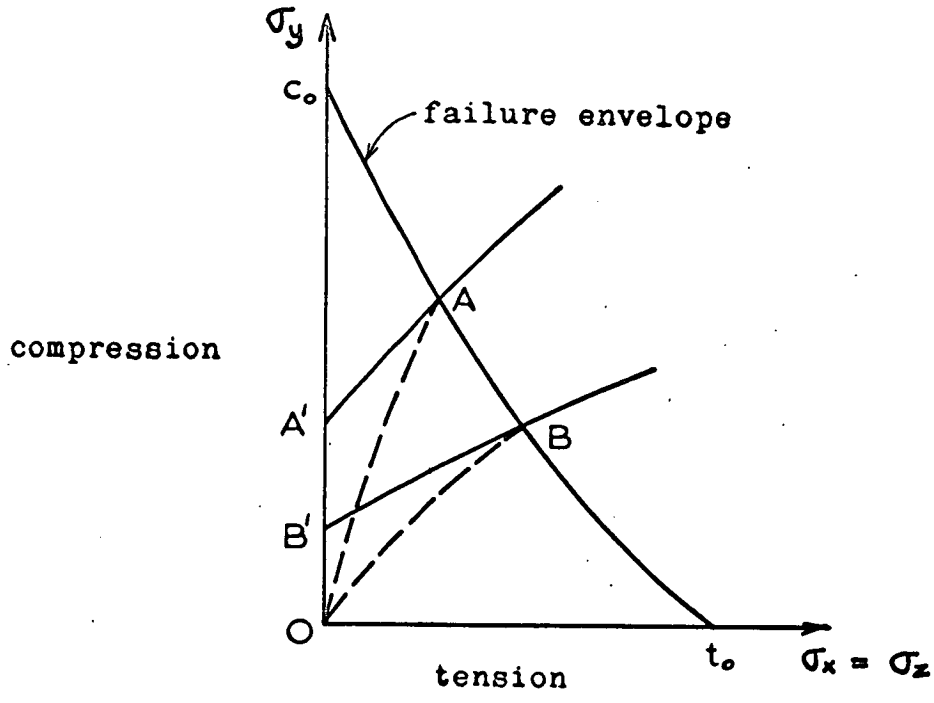

Fig 1.2 Failure Envelope for Brick in Biaxial Compression - Tension

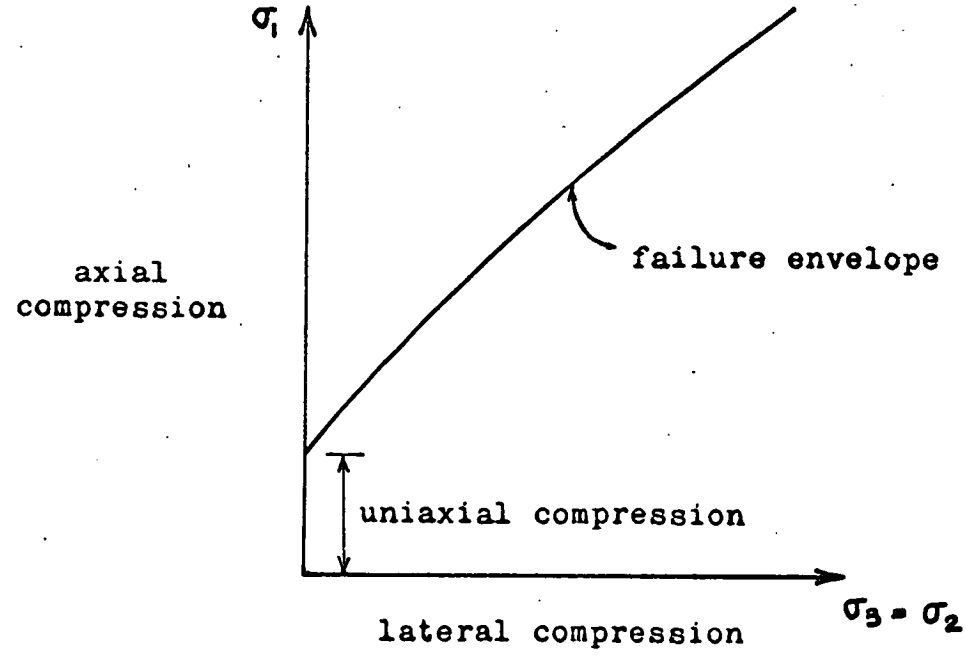

Fig 1.3 Failure Envelope for Mortar in Triaxial Compression

directions, σ_x and σ_z, are equal. c_o and t_o are the uniaxial compressive and tensile strengths of brick respectively. Any state of stress to the right of this curve denotes failure. The exact profile of the failure envelope is presently unknown. The experimental work for this thesis will include its determination.

As the vertical compression acting on the brickwork prism increases, the state of stress in the brick element proceeds along the dashed line OA in Fig. 1.2. Failure occurs within the brick element when the line OA intersects the failure envelope at A, and hence the compressive strength of the brickwork prism is given by the ordinate of the point A. The stress path taken by the line OA is solely determined by the properties of the mortar joint under triaxial compression and the ratio of the thicknesses of the mortar joint to the brick unit. For a weaker mortar whose lateral strain is greater under load, the stress path travels along the lower line OB in Fig. 1.2, where B denotes the state of stress within the brick element at failure. Similarly, the compressive strength of the brickwork prism is given by the ordinate of the point B.

It is possible to determine the points of intersection A and B on the failure envelope from a study of the behaviour of the mortars under a state of triaxial compression which we will consider next.

The effect of a lateral compressive pressure on a brittle material, such as mortar, in triaxial compression is to increase its ultimate crushing strength substantially. A schematic representation of the failure envelope for mortar in triaxial compression is given in Fig. 1.3. Much work has been done in this area for concrete where it is found that the major principal stress at failure is increased by approximately four times the confining pressure. There are a few similar experiments/

similar experiments carried out on cement mortar. However no investigation into the behaviour of brickwork mortar under triaxial compression has been undertaken so far. Therefore, it is necessary to establish the principal stress relationship for brickwork mortar in triaxial compression experimentally, and this will be carried out in the proposed testing programme.

A study of the behaviour of the brickwork mortars in triaxial compression will enable curves A'A and B'B in Fig. 1.2 to be drawn. These curves are, of course, modified to account for the ratio of brick to mortar thicknesses in order to satisfy the equilibrium of lateral forces in the brickwork prism. The ultimate strengths of the brickwork prism are represented by the compressive stresses at the points of intersection, A and B, between the failure envelope for brick and the curves A'A and B'B.

Up to this stage, it has been implicitly assumed that the lateral stresses in both the brick and the mortar joint are uniformly distributed throughout their thicknesses. In actuality, the stresses resulting from the differential lateral strains between the brick and the mortar elements act along the interfaces of the brick and the mortar joint. In what manner these shear stresses along the brick-mortar interface are distributed is presently not clear. The lateral tensile stress distribution within each of these elements will depend upon how these stresses at the interface are distributed, in addition to the geometry of the brick unit and the mortar joint.

1.4 PROPOSED RESEARCH AND TESTING PROGRAMME

It is now apparent that in order to formulate the proposed failure hypothesis for brickwork in compression, information pertaining to the behaviour/

the behaviour of brick and mortar under their appropriate states of stress are necessary, and also information concerning the lateral stress distribution within these elements.

In this research it is proposed to investigate:

(a) the behaviour of brick under a state of compression-tension-tension stresses

(b) the behaviour of brickwork mortar under a state of triaxial compression

(c) the lateral stress distribution on brick and mortar elements in brickwork under axial compression.

In regard to (a) above, since it has not been possible to devise a testing method which can produce a state of compression-tension-tension stresses in brick, the study is confined to a two-dimensional state of biaxial compression-tension stresses.

As brick is not a castable material like concrete, the choice of testing methods which can generate a state of biaxial compression-tension stresses in brick is very limited. The range of testing methods available will be discussed in greater length in Section 2.4 which deals with the biaxial compression-tension of brittle materials. In the light of this limitation, it was decided to carry out the biaxial compression-tension tests on bricks by the two methods listed below:

(1) Direct Compression and Tension

In this method, in addition to a direct tension applied to a briquet specimen horizontally, the specimen is vertically compressed at the same time. The details of the experimental technique and the test results are given in Chapter 3.

(2) Hollow Cylinders/

(2) Hollow Cylinders

In this method, a fluid pressure is applied to the core of a ceramic pipe. This internal pressure produces a circumferential lateral tension in the pipe. At the same time, the pipe is compressed along its longitudinal axis. The details of the experiments and the test results are discussed in Chapter 4.

The triaxial compression of brickwork mortar, would be carried out in a standard high pressure triaxial equipment. The details of the experiments and the test results are given in Chapter 5.

A theoretical analysis of the lateral stress distribution within brick and mortar elements in brickwork subject to axial compression would be investigated by the method of finite element analysis. This is discussed in Chapter 6.

Lastly, a series of compression tests would be carried out on brickwork prisms built with one-third scale model bricks of various strengths using standard brickwork mortar mixes. The crushing strengths of these prisms would then be compared with the predicted strengths derived from the proposed failure theory.

1.5 SUMMARY

(1) Failure in brickwork under axial compression is initiated by vertical tensile cracking in the brick elements. This is the result of the differential lateral strains in brick and mortar.

(2) Factors affecting the compressive strength of brickwork are brick and mortar strengths, the ratio of brick to mortar thicknesses, its slenderness ratio, and the quality of workmanship.

(3) The influence of other factors on brickwork strength such as the presence of perpends, perforations and frogs in bricks are not conclusively established.

(4) Existing failure theories for brickwork in compression, derived from an assumption of elastic behaviour of brick and mortar, are unsatisfactory.

(5) A "strength" approach is adopted for the proposed failure criterion in which the compressive strength of brickwork is determined by the strength properties of brick and mortar in their appropriate states of complex stresses.

(6) Formulation of the proposed failure criterion for brickwork in compression requires the following information, the determination of which would be carried out in the proposed testing and research programme:

(a) the behaviour of brick under a state of biaxial compression-tension stresses

(b) the behaviour of brickwork mortar under a state of triaxial compression

(c) the lateral stress distribution within the brick and the mortar elements in brickwork under axial compression.

CHAPTER 2 - FAILURE CRITERIA OF BRITTLE MATERIALS UNDER COMPLEX STRESSES

2.1 BEHAVIOUR OF BRITTLE MATERIALS

The need to establish a failure criterion which can adequately describe the behaviour of brittle materials under complex stresses has led to a number of investigations involving tests on a variety of materials which include concrete, rock, cast-iron, ceramics, glass and graphite. The various classical theories discussed, for example by Timoshenko[55], - the maximum stress theory, the maximum strain theory, the maximum shear stress theory, the maximum strain energy theory, the maximum strain energy of distortion theory, the maximum octahedral shear stress theory - which were developed chiefly to explain the behaviour of ductile materials under load, have been found to be unsatisfactory when applied to brittle materials. Consequently, the search for a suitable failure criterion for brittle materials continues.

The research into the behaviour of brittle materials under stress may be broadly categorised into two levels. At the "phenomenological" or "strength" level, the investigation is principally concerned with the strength performance of the test material under varying stress combinations. A number of investigations have been carried out in this field, but of late it is realised that a satisfactory failure criterion is more likely to come out of a more fundamental study of the material. Therefore, an increasing amount of work on the behaviour of brittle materials is now being done at the "structural" or "fracture mechanics" level.

In the past, it was the hope that there would exist a single criterion which could/

which could describe the failure of brittle materials under all states of applied stresses. A survey of recent literature tends to indicate that it is probable that more than one criterion will be necessary, since it is recognised that there are two basic modes of failure in a brittle material, viz. separation or cleavage fracture (tensile failure) and sliding or friction fracture (shear failure).

The two available failure criteria which best describe the behaviour of brittle materials under stress are:-

(1) Coulomb's shear failure theory

(2) Griffith's flaw theory.

Each of these will be discussed in greater detail in a later section. It is interesting to note that the first of these theories is at the phenomenological level and the other is at the structural level.

As explained in Section 1.4, only two particular states of combined stresses are of interest in this thesis and these are:-

(1) the biaxial compression-tension strength

(2) the triaxial compression strength.

2.2 COULOMB'S SHEAR FAILURE THEORY

Coulomb[15] introduced the simplest and most useful criterion for shear failure in materials. In this criterion, the shear stress causing failure across a plane is linearly related to the normal stress acting on the plane, given by the equation

$$\tau = s_o + \mu\sigma \qquad \text{.....(2.1)}$$

where

τ = shear stress

σ = normal stress

s_o = shear strength of the material at zero normal stress

μ = coefficient of internal friction of the material.

Shear failure occurs in the material when

$$\tau - \mu\sigma > s_o \qquad \text{.....(2.2)}$$

In a two dimensional case, the normal and shear stresses across a plane in terms of their principal stresses, see Fig. 2.1, are:-

$$\sigma = \tfrac{1}{2}(\sigma_1 + \sigma_3) + \tfrac{1}{2}(\sigma_1 - \sigma_3)\cos 2\beta \qquad \text{.....(2.3)}$$

$$\tau = -\tfrac{1}{2}(\sigma_1 - \sigma_3)\sin 2\beta \qquad \text{.....(2.4)}$$

where

σ_1 = major principal stress

σ_3 = minor principal stress

β = inclination of the normal to the plane to the major principal stress.

Using equations (2.3) and (2.4),

$$\tau - \mu\sigma = \tfrac{1}{2}(\sigma_1 - \sigma_3)\left[\sin 2\beta - \mu\cos 2\beta\right] - \tfrac{1}{2}\mu(\sigma_1 + \sigma_3) \qquad \text{.....(2.5)}$$

which is maximum when

$$\tan 2\beta = -1/\mu \qquad \text{.....(2.6)}$$

and its maximum value is

$$\tau - \mu\sigma = \tfrac{1}{2}(\sigma_1 - \sigma_3)(\mu^2 + 1)^{\frac{1}{2}} - \tfrac{1}{2}\mu(\sigma_1 + \sigma_3) \qquad \text{.....(2.7)}$$

Therefore, Coulomb's criterion, from equations (2.2) and (2.7) is

$$\sigma_1\left[(\mu^2 + 1)^{\frac{1}{2}} - \mu\right] - \sigma_3\left[(\mu^2 + 1)^{\frac{1}{2}} + \mu\right] \geq 2s_o \qquad \text{.....(2.8)}$$

This is a linear equation denoted by the line pq in Fig. 2.2. The intercept/

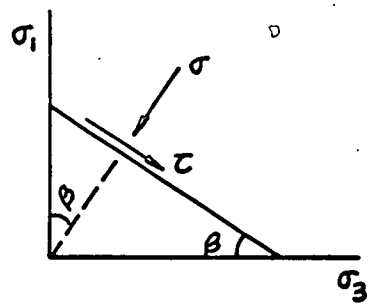

Fig 2.1 STRESSES ACTING ON A PLANE

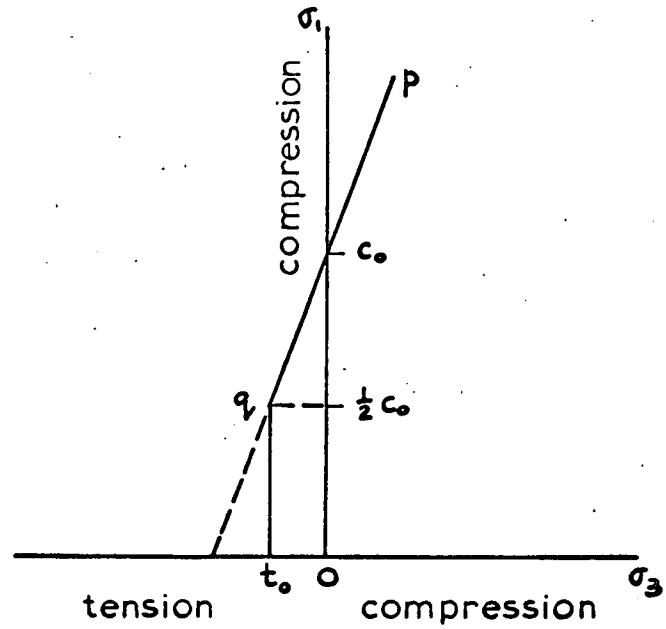

Fig 2.2 COULOMB'S CRITERION

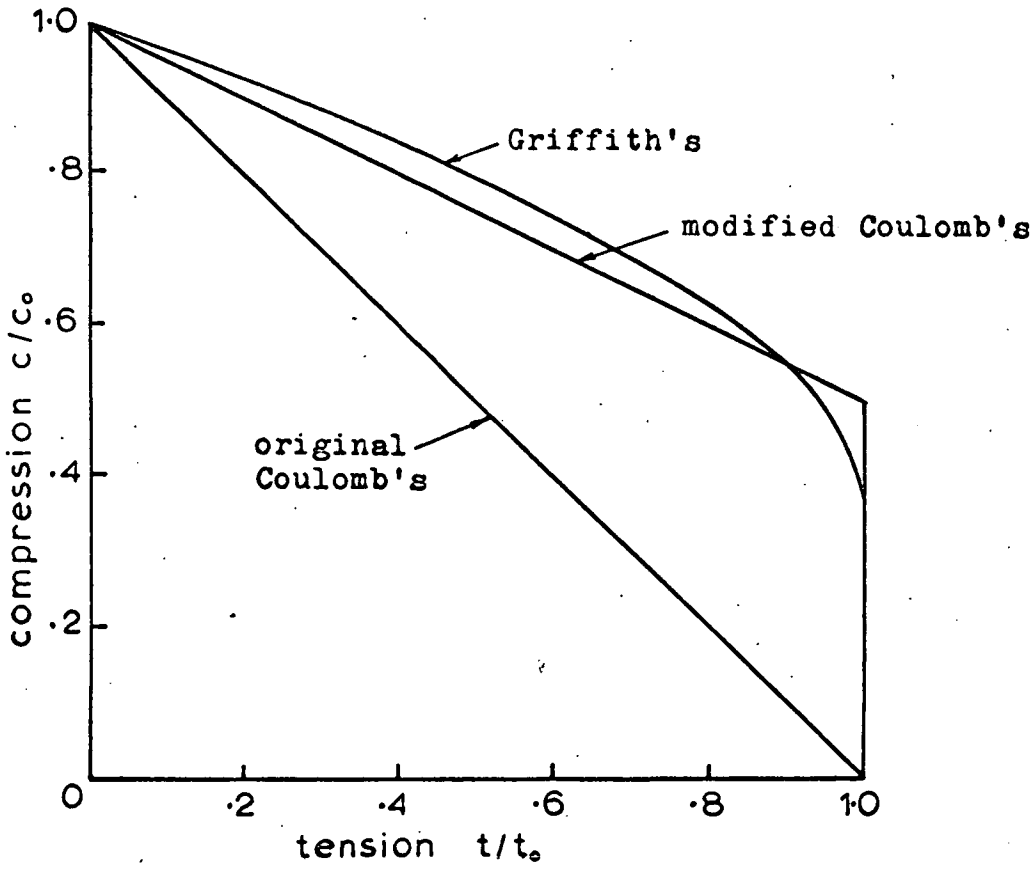

Fig 2.3 COULOMB & GRIFFITH CRITERIA FOR BIAXIAL COMPRESSION-TENSION

intercept c_o which is the uniaxial compressive strength is given by

$$c_o = 2s_o\left[(\mu^2 + 1)^{\frac{1}{2}} + \mu\right] \qquad \text{.....(2.9)}$$

Rearranging equations (2.8) and (2.9) and eliminating s_o, the resulting equation becomes

$$\frac{\sigma_1}{c_o} = \frac{\sigma_3}{c_o}\left[\frac{(\mu^2 + 1)^{\frac{1}{2}} + \mu}{(\mu^2 + 1)^{\frac{1}{2}} - \mu}\right] + 1 \qquad \text{.....(2.10)}$$

Coulomb's criterion may not be extended completely into the tensile range, since the physical conditions require the normal stress σ to be positive. The limit of applicability of the criterion so long as σ is positive, from equation (2.3), is

$$\sigma = \tfrac{1}{2}(\sigma_1 + \sigma_3) + \tfrac{1}{2}(\sigma_1 - \sigma_3)\cos 2\beta > 0 \text{.....(2.11)}$$

Substituting for β given in equation (2.6), equation (2.11) becomes

$$\sigma_1\left[(\mu^2 + 1)^{\frac{1}{2}} - \mu\right] + \sigma_3\left[(\mu^2 + 1) + \mu\right] > 0 \text{.....(2.12)}$$

and this combined with equation (2.8) requires

$$\sigma_1 > s_o\left[(\mu^2 + 1)^{\frac{1}{2}} + \mu\right] = \tfrac{1}{2}c_o \qquad \text{.....(2.13)}$$

The point q in Fig. 2.2 marks the limit of Coulomb's criterion. For $\sigma_1 < \frac{1}{2}c_o$, the failure criterion is defined by what is known as a "tension cut-off" given by the equation

$$\sigma_3 = -t_o \qquad \text{.....(2.14)}$$

where

t_o is the tensile strength of the material.

Both the original and the modified Coulomb criteria for the biaxial compression-tension quadrant are indicated in Fig. 2.3 on a dimensionless form.

Paul/

Paul[45] made a similar modification to the Coulomb criterion in the compression-tension zone. In his analysis, it is assumed that the brittle material will fail in shear where the shear stress reaches the critical value s_o, or in tension where the tensile stress reaches the critical value t_o, whichever occurs first. This leads to the criterion

$$\text{for } \sigma_1 > c_o\left[1 - \frac{c_o t_o}{4s_o^2}\right]\sigma_1\left[(\mu^2+1)^{\frac{1}{2}} - \mu\right] - \sigma_3\left[(\mu^2+1)^{\frac{1}{2}} + \mu\right] = 2s_o \quad \ldots\ldots\ldots\ldots(2.15)$$

and

$$\text{for } \sigma_1 < c_o\left[1 - \frac{c_o t_o}{4s_o^2}\right], \sigma_3 = -t_o \quad \ldots\ldots\ldots\ldots(2.16)$$

The important conclusions to be drawn from Coulomb's analysis are:-

(1) The principal stress relationship is linear,

(2) The intermediate principal stress σ_2 does not affect failure, and the fracture plane passes through the direction of the intermediate principal stress.

Mohr's hypothesis[38] is a generalised form of the Coulomb shear criterion, in which the normal stress σ and the shear stress τ across the failure plane are related by a function involving the characteristic of the material,

$$\tau = f(\sigma) \quad \ldots\ldots\ldots\ldots(2.17)$$

The relationship is not defined by an explicit formula, but is to be obtained experimentally as the envelope of the Mohr circles corresponding to failure under a variety of conditions.

2.3 GRIFFITH'S FLAW THEORY

In order to explain the cause for the low tensile strength of brittle materials, in particular of glass, when compared with the theoretical strength calculated from intermolecular forces, Griffith[23] postulated the existence/

the existence of minute flaws in these materials, the presence of which greatly affected the fracture strength in tension. His theory is based on the assumption that fracture initiates at these cracks as a result of very high tensile stress concentrations which are induced at the crack tip when the material is loaded.

Griffith assumed that a crack could be regarded as a very flat two-dimensional ellipse. The tangential stress on the boundary of the elliptical crack in a loaded material, as shown in Fig. 2.4, is given in an analysis by Inglis[29] as:-

$$\sigma_b = \frac{\sigma_y\left[m(m+2)\cos^2\alpha - \sin^2\alpha\right] + \sigma_x\left[(1+2m)\sin^2\alpha - m^2\cos\alpha\right] - \tau_{xy}\left[2(1+m^2)\sin\alpha\cos\alpha\right]}{m^2\cos^2\alpha + \sin^2\alpha} \quad \ldots\ldots\ldots\ldots\ldots\ldots (2.18)$$

where

σ_b = tangential stress on the boundary of the elliptical flaw

m = b/a, ratio of semi-minor to semi-major axis of the ellipse

α = eccentric angle of ellipse

σ_x, σ_y = normal stresses in material surrounding the elliptical flaw

τ_{xy} = shear stress in material surrounding the elliptical flaw

with the sign convention that compression is positive.

In a very flat ellipse, the maximum tensile stress will occur near the tip of the elliptical flaw, i.e. $\alpha \longrightarrow 0$. Neglecting terms of second order or higher which appear in the numerator in equation (2.18), the expression simplifies to

$$\sigma_b = \frac{2(\sigma_y \cdot m - \tau_{xy} \cdot \alpha)}{m^2 + \alpha^2} \quad \ldots\ldots\ldots\ldots\ldots\ldots (2.19)$$

It is noted from this simplification that the stress σ_x which lies parallel to the major axis of the ellipse has a negligible influence on the/

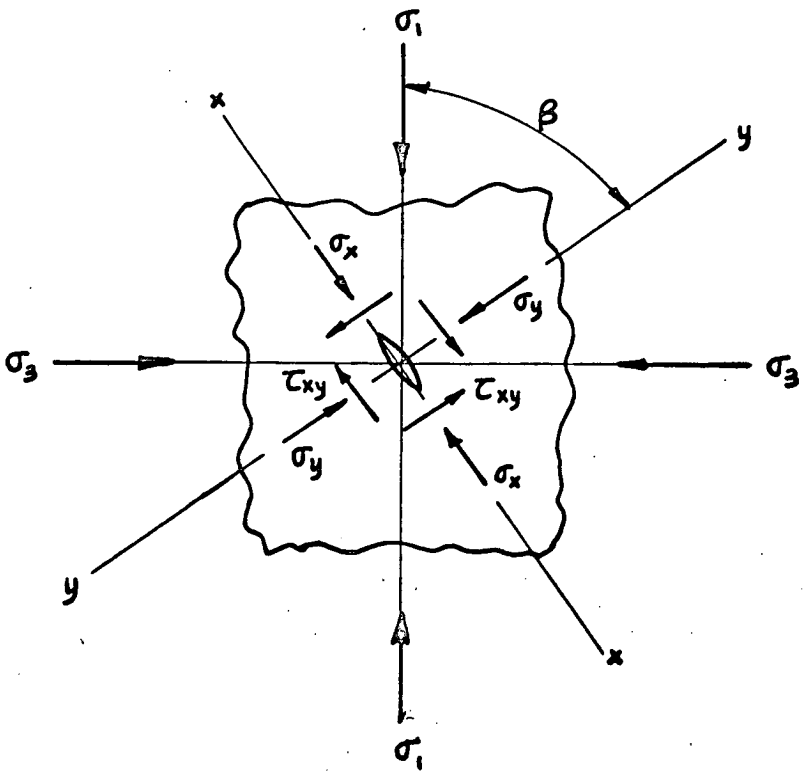

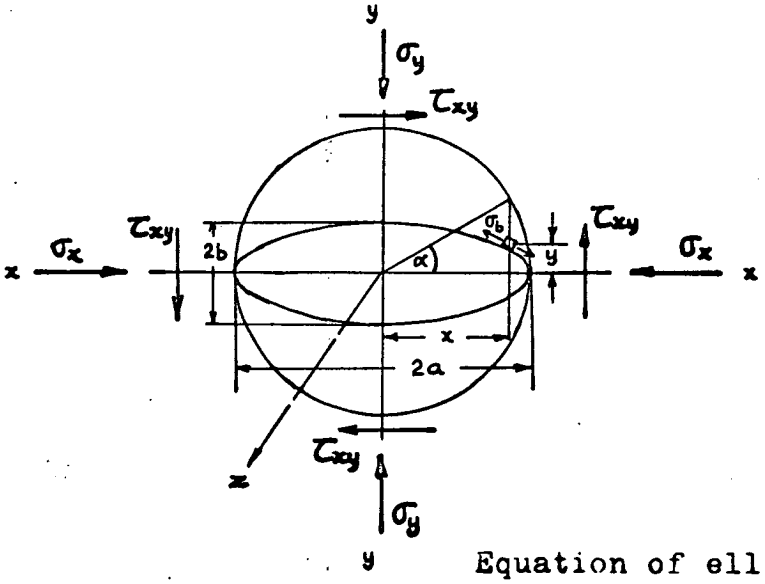

Equation of ellipse:

$$x = a.\cos\alpha$$
$$y = b.\sin\alpha$$

where α = eccentric angle
$m = b/a$

Fig 2.4 STRESSES ACTING ON MATERIAL SURROUNDING A TWO-DIMENSIONAL ELLIPTICAL FLAW

on the boundary stress near the tip of the flaw. On similar ground, the influence of the intermediate stress σ_z can be ignored. The maximum tangential stress on the boundary of the elliptical flaw is given when

$$\frac{d\sigma_b}{d\alpha} = 0$$

Differentiating equation (2.19) and eliminating α, the following expression is obtained:-

$$\sigma_b.m = \sigma_y - (\sigma_y^2 + \tau_{xy}^2)^{\frac{1}{2}} \qquad \text{.....(2.20)}$$

In terms of the principal stresses whose relationships to the normal and shear stresses are

$$\left.\begin{aligned} \sigma_x &= \sigma_1 \sin^2\beta + \sigma_3 \cos^2\beta \\ \sigma_y &= \sigma_1 \cos^2\beta + \sigma_3 \sin^2\beta \\ \tau_{xy} &= -\tfrac{1}{2}(\sigma_1 - \sigma_3)\sin 2\beta \end{aligned}\right] \qquad \text{.....(2.21)}$$

where

σ_1, σ_3 = principal stresses, $\sigma_1 > \sigma_3$

β = angle between the direction of the major principal stress σ_1 and the y-axis,

equation (2.20) becomes

$$\sigma_b.m = \left[\sigma_1 \cos^2\beta + \sigma_3 \sin^2\beta\right] - \left[\sigma_1^2 \cos^2\beta + \sigma_3^2 \sin^2\beta\right]^{\frac{1}{2}} \qquad \text{.....(2.22)}$$

The orientation β of the stresses σ_1, σ_3 which makes σ_b a maximum is given by differentiating equation (2.22)

$$m\frac{d\sigma_b}{d\beta} = \left[2\sigma_3 - 2\sigma_1 + \frac{\sigma_1^2 - \sigma_3^2}{(\sigma_1^2 \cos^2\beta + \sigma_3^2 \sin^2\beta)^{\frac{1}{2}}}\right] \sin\beta \cos\beta \qquad \text{.....(2.23)}$$

This is zero if $\beta = 0$, $\beta = \frac{1}{2}\pi$, or

$$\cos 2\beta = -\tfrac{1}{2}(\sigma_1 - \sigma_3)/(\sigma_1 + \sigma_3) \qquad \text{.....(2.24)}$$

The inclined position exists only if $|\cos 2\beta| < 1$, which requires

$$(\sigma_1 + 3\sigma_3) > 0 \qquad \text{.....(2.25)}$$

Using equation (2.24) in equation (2.22) gives

$$\sigma_{b.m} = -(\sigma_1 - \sigma_3)^2/4(\sigma_1 + \sigma_3) \qquad \text{.....(2.26)}$$

For $(\sigma_1 + 3\sigma_3) < 0$, i.e. σ_3 must be negative, the greatest tensile stress in the crack surface occurs when $\beta = \frac{\pi}{2}$ and has the value from equation (2.22)

$$\sigma_{b.m} = 2\sigma_3 \qquad \text{.....(2.27)}$$

It is now assumed that failure takes place when this maximum tensile stress in the crack reaches some value characteristic of the material. If t_o is the uniaxial tensile strength, so that $\sigma_3 = -t_o$, then

$$\sigma_{b.m} = -2t_o \qquad \text{.....(2.28)}$$

Combining equation (2.26) and (2.28) gives

$$(\sigma_1 - \sigma_3)^2 - 8t_o(\sigma_1 + \sigma_3) = 0, \text{ if } (\sigma_1 + 3\sigma_3) > 0 \qquad \text{.....(2.29)}$$

which with

$$\sigma_3 = -t_o, \quad \text{if } (\sigma_1 + 3\sigma_3) < 0 \qquad \text{.....(2.30)}$$

constitutes the Griffith criterion for failure.

It may be seen from equation (2.29) by putting $\sigma_3 = 0$, that Griffith's material has a compressive strength c_o equal to $8t_o$. The biaxial compression-tension relationship is indicated in Fig. 2.3.

Equation (2.29) may be rewritten for the compression range in terms of c_o as

$$\frac{\sigma_1}{c_o} = \tfrac{1}{2} + \frac{\sigma_3}{c_o} + \sqrt{\frac{2\sigma_3}{c_o} + \tfrac{1}{4}} \qquad \text{.....(2.31)}$$

It is worthwhile noting that the following assumptions have been implied in the above analysis:-

(1) Failure is caused by fracture initiation of a single crack. Adjacent flaws do not interact and local variations in material properties are ignored.

(2) The analysis is treated two dimensionally, and the influence of stress in the third direction is insignificant.

McClintok & Walsh[36] and Brace[4] modified Griffith's theory by assuming that in compression Griffith's cracks close and a frictional force develops across the crack surface. In this event, failure occurs when

$$\frac{\sigma_1}{c_o} = \left[\frac{(1+\mu^2)^{\frac{1}{2}}+\mu}{(1+\mu^2)^{\frac{1}{2}}-\mu}\right]\frac{\sigma_3}{c_o} + 1 \qquad \text{.....(2.32)}$$

with

$$\frac{c_o}{t_o} = 4\left[(1+\mu^2)^{\frac{1}{2}}+\mu\right] \qquad \text{.....(2.33)}$$

where

μ is the coefficient of internal friction.

Equation (2.32) is linear and identical to Coulomb's failure criterion gives by equation (2.10) in section 2.2. The original and the modified Griffith criteria in the compression range are shown in Fig. 2.5. Murrell[41] extended Griffith's criterion to three dimensions and the resulting paraboloid of revolution whose axis is the line $\sigma_1 = \sigma_2 = \sigma_3$ has the equation

$$(\sigma_1-\sigma_2)^2+(\sigma_2-\sigma_3)^2+(\sigma_3-\sigma_1)^2 = 24t_o(\sigma_1+\sigma_2+\sigma_3) \qquad \text{.....(2.34)}$$

It follows from equation (2.34) that the uniaxial compressive strength c_o is

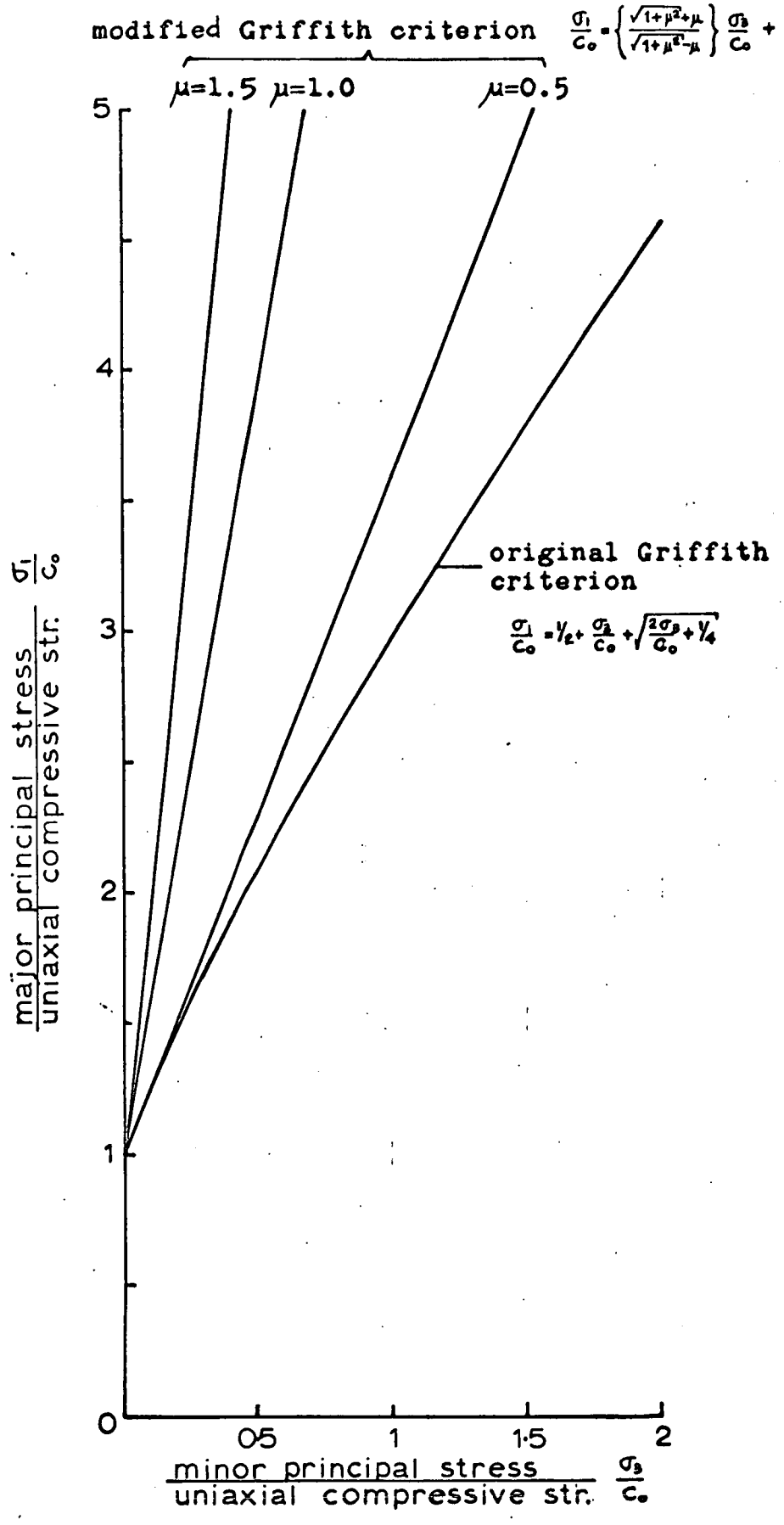

Fig 2.5 GRIFFITH CRITERION FOR TRIAXIAL COMPRESSION

$$c_o = 12\, t_o \qquad \text{.....(2.35)}$$

which is an improvement over the low value of $8t_o$ derived from the plane theory.

Murrell's three dimensional criterion, unlike the plane Griffith's or Coulomb's criterion, predicts an influence of the intermediate principal stress. This criterion, however, is purely a geometrical extension of the plane criterion and is not derived from a fundamental analysis. It does not account for the closure of cracks in compression.

2.4 BIAXIAL COMPRESSION-TENSION STRENGTH

Various testing methods have been employed to determine the biaxial compression-tension failure envelopes of brittle materials. These are listed below, and the merits and limitations of each of these methods is discussed:

(1) Direct Tension and Compression

(2) Hollow Cylinders: Hoop Tension and Axial Compression

(3) Hollow Cylinders: Torsion and Axial Compression

(4) Flexural Tension and Compression

(5) Plate Test

(6) Indirect Tensile Splitting Test

1. Direct Tension and Compression

This method involves the application of a direct tensile and a compressive stress in perpendicular directions on a test specimen. Two main difficulties arise from this test arrangement. The first is that it is often difficult to achieve a truly uniform tensile stress in the specimen under direct tension. The other is the problem of the platen restraint on the specimen subject to a compressive load.

In his/

In his experiments on concrete and mortar, Vile[60] used a dog-bone shape specimen shown in Fig. 2.6 on which a tensile force was applied with the aid of special grips devised by Ward[61]. Compression in the perpendicular direction is applied through a pair of cubes of similar material as the test specimen with the view to eliminate the presence of platen restraint.

Kupfer et al.[34] avoided the problem of platen restraint by introducing Hilsdorf brush platens made up of closely-packed flexible steel bristles to load on concrete square plate specimens. For the tensile stress, the ends of the filaments were glued to the concrete faces of the specimen. The flexibility of the brush platen permitted free movement of the concrete faces in contact with the load platens.

Notwithstanding the difficulties stated above, this test method has the distinct advantage in providing a homogenous stress field, and the unknown effect of stress gradient on failure is therefore absent.

2. Hollow Cylinders: Hoop Tension and Axial Compression

In this method, a hollow cylinder is subjected to an internal pressure producing a circumferential or hoop tension in the wall of the cylinder, and in addition, an axial compression is applied along its length.

Provided a specimen of sufficient length to diameter ratio is selected, the influence of the compression platen restraint on the stress field in the test cylinder is insignificant. The disadvantage associated with this method of compression-tension test is that the stress field is not strictly biaxial. There exists a radial compression of magnitude varying from the value of the/

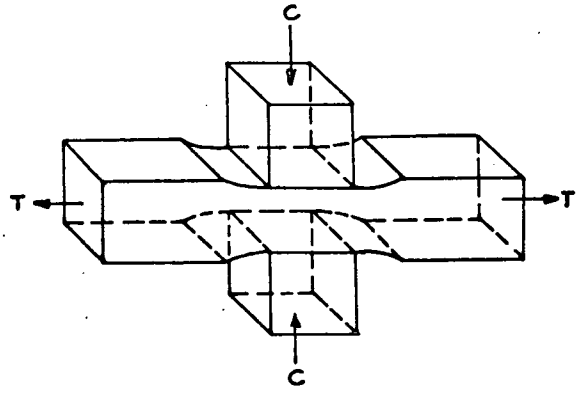

Fig 2.6 USE OF CONCRETE CUBES TO APPLY COMPRESSIVE STRESSES TO TENSION SPECIMEN (after VILE)

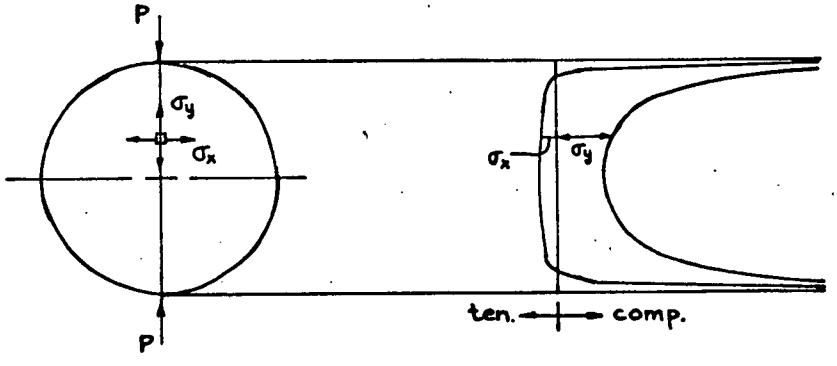

Fig 2.7 CYLINDER SPLITTING TEST: STRESS DISTRIBUTION

of the internal pressure acting on the inside face of the cylinder to zero on the external face. Since failure is normally assumed to initiate at the inner face of the cylinder under this system of stresses, the presence of the radial compression may be material. Moreover, the stresses created are not homogenous throughout the cylinder wall and a stress gradient exists. However, these effects are usually minimised by using cylinders of very thin walls for the tests.

This method was used by McHendry and Karni[37] and by Tsuboi and Suenaga[57] in their biaxial compression-tension tests on concrete. In order to determine the influence of the intermediate stress on failure, Campbell-Allen[12] tested hollow cylinders under combinations of internal and external pressures, together with an axial compression. The biaxial compression-tension failure of cast-iron was investigated by Grassi and Cornet[22], Coffin[13], Cornet and Grassi[14] using hollow thin-walled tubes. Similar tests were carried out on graphite tubes by Ely[18] and on polycrystalline alumina ceramics by Broutman and Cornish[8].

3. Hollow Cylinders: Torsion and Axial Compression

A state of biaxial compression-tension stresses exists when shear stresses, produced by twisting a hollow cylinder, are combined with an axial compression. One of the principal stresses will be tensile when an element is acted upon by shear stresses.

A number of investigators have employed this method of strength test on concrete, probably because this particular combination of shear and compressive stresses are commonly found in loaded reinforced concrete members, and therefore, the problem is of relevant interest. These included Bresler and Pister[6], Tsuboi and Suenaga[57]/

and Suenaga[57], Reeves[47], Isenberg[30], and Goode and Helmy[21]. However, a serious objection to the choice of this method for the determination of the biaxial compression-tension strength of inelastic materials, such as concrete, is that the computation of the values of the failure stresses derived from an elastic analysis will not be altogether correct. Isenberg[30] found that the biaxial envelope derived from stresses at discontinuity (i.e. proportional limit on the stress-strain curve, see Newman[43]) differs considerably from that derived at failure, see Fig. 2.12.

4. Flexural Tension and Compression

In this method of biaxial compression-tension test, a rectangular beam specimen is subjected to bending which provides a longitudinal tensile stress, and an axial compression is applied to the specimen in a direction normal to the plane of bending.

The only recorded experiment using this technique is that of Smith[52]. The principal objection to this method of biaxial testing is that the tensile strength from flexure test is calculated on the assumption of a linear relationship between stress and strain. Blakey and Beresford[3] have pointed out that the tensile stress distribution is not linear but parabolic. Furthermore, the maximum tensile stress in bending is confined to only the extreme fibre of the cross-section of the beam, and therefore, the assumption that failure is initiated at this point in the beam when the tensile stress reaches a critical value may not apply.

It is therefore understandable that this method of biaxial compression-tension test is not favoured by other researchers.

5. Plate Test

By loading transversely on an opposite pair of corners of a rhombic plate/

plate supported on the two remaining corners, a state of biaxial compression-tension stresses is created which is maximum at the centre of the plate. By varying the ratio of the major to minor diagonal of the rhombic plate, different combinations of compression-tension stresses may be obtained.

This test method suffers the same disadvantages as those described in Method (4) "Flexural Tension and Compression" and is therefore not an attractive method to choose.

6. Indirect Tensile Splitting Test

In a cylinder splitting test, the state of stress along the loaded diameter in the specimen is biaxial compression-tension, as shown in Fig. 2.7, An examination of the stress distribution reveals that the lateral stress σ_x is tensile and uniformly distributed over nearly the whole length of the loaded diameter, while the vertical stress σ_y is compressive and increases to infinity at the loaded points. Thus, different ratios of compression-tension stresses exist along the loaded diameter of the specimen.

In his method of determining the biaxial compression-tension failure envelope for concrete, Desayi[17] assumed that at failure, the cylinder splits wholly and concurrently across the length of the loaded diameter, and therefore, it follows that the varying compression-tension stress ratios along the loaded diameter would define the biaxial failure envelope. In other words, the biaxial compression-tension failure envelope may be derived from a single cylinder splitting test.

Unfortunately, Desayi's assumption that failure in a cylinder splitting test takes place concurrently over the whole length of the loaded diameter is unacceptable. It is more likely that, under uniform/

under uniform lateral tensile stresses, failure will initiate where the ratio of compression-tension stresses is maximum. Using Brisbane's[7] analysis of stresses in an elliptical specimen in a splitting test, Krishnaswamy[33] in an attempt to define the biaxial compression-tension relationship carried out experiments on elliptic-shaped concrete specimens of varying aspect ratios. He assumed that failure occurred at the centre of the specimens, and obtained different compression-tension strength ratios from the various specimens.

It is difficult to justify that failure initiated at the centre of the ellipse, and for this reason Krishnaswamy's approach to the problem is of limited use.

Of the six test methods for the determination of the biaxial compression-tension strength presented above, only the first two methods may be considered reliable enough to be used. The criticisms against the remaining four methods are sufficiently serious to discount them. The biaxial compression-tension test results extracted from some of the publications are presented, where possible, on a dimensionless plot in Fig. 2.8. The number assigned to each curve is referenced in Table 2.1 which lists the source from which the data have been taken. Other results not so convenient to do so, such as those of Tsuboi and Suenaga[57] and Broutman and Cornish[8] in Figs. 2.9 and 2.10 respectively, or which are to be singled out for comment, are given separately.

It is seen that almost all of the failure envelopes obtained fall within the region bounded by the theoretical curves of Coulomb's original criterion and Griffith's criterion, see Fig. 2.3, although the applicability of the test data from some of these experiments is questionable.

TABLE 2.1 - BIAXIAL COMPRESSION-TENSION TEST DATA

Graph No.	Author & Ref. No.	Test Method	Test Material
1	Smith (52) (1953)	flexural tension & compression	concrete
2	Cornet & Grassi (14) (1955)	hollow cylinder: hoop tension & axial compression	cast-iron
3	McHendry & Karni (37) (1958)	hollow cylinder: hoop tension & axial compression	concrete
4	Bresler & Pister (6) (1958)	hollow cylinder: torsion and axial compression	concrete
5	Campbell-Allen (12) (1962)	hollow cylinder: hoop tension & axial compression	mortar
6	Ely (18) (1965)	hollow cylinder: hoop tension & axial compression	graphite
7	Desayi (17) (1969)	indirect tension	concrete
8	Krishnaswamy (33) (1969)	indirect tension	concrete
9	Kupfer et al. (34) (1969)	direct tension & compression	concrete
10	Tsuboi & Suenaga (57) (1960)	hollow cylinder: hoop tension & axial compression and torsion & axial compression	concrete
11	Broutman & Cornish (8) (1965)	hollow cylinder: hoop tension & axial compression	polycrystalline alumina
12	Vile (60) (1965)	direct tension & compression	concrete & mortar
13	Isenberg (30) (1966)	hollow cylinder: torsion and axial compression	concrete

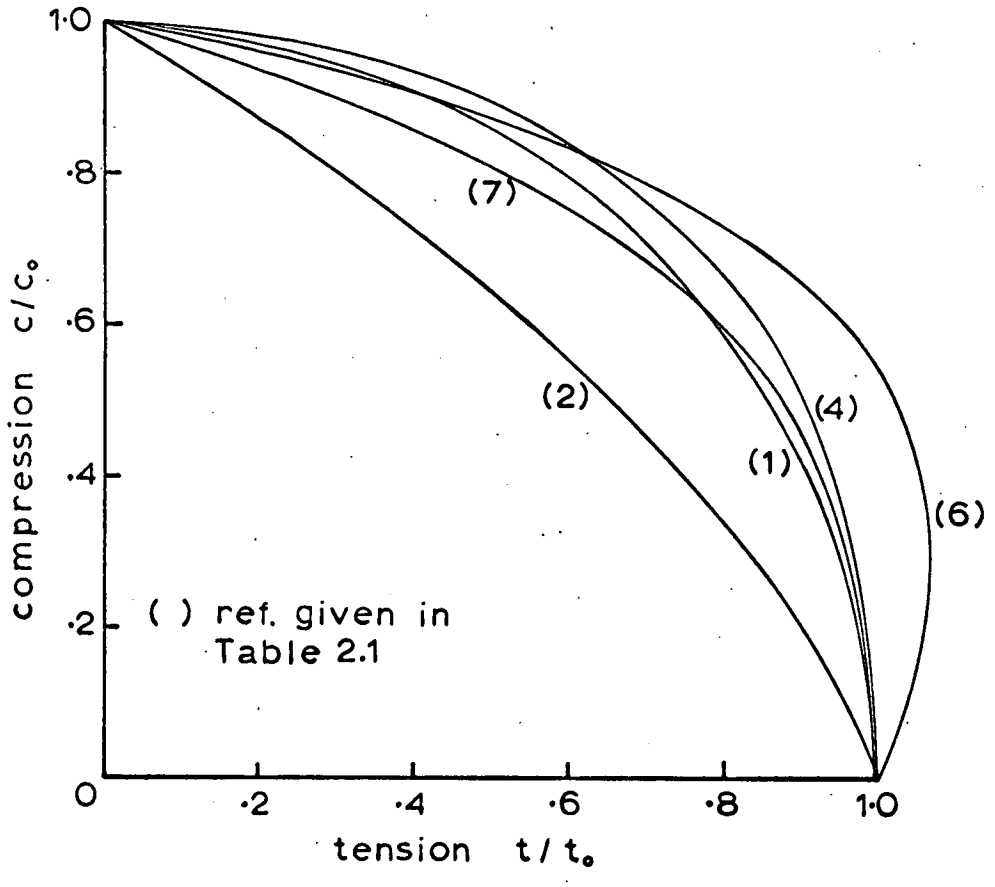

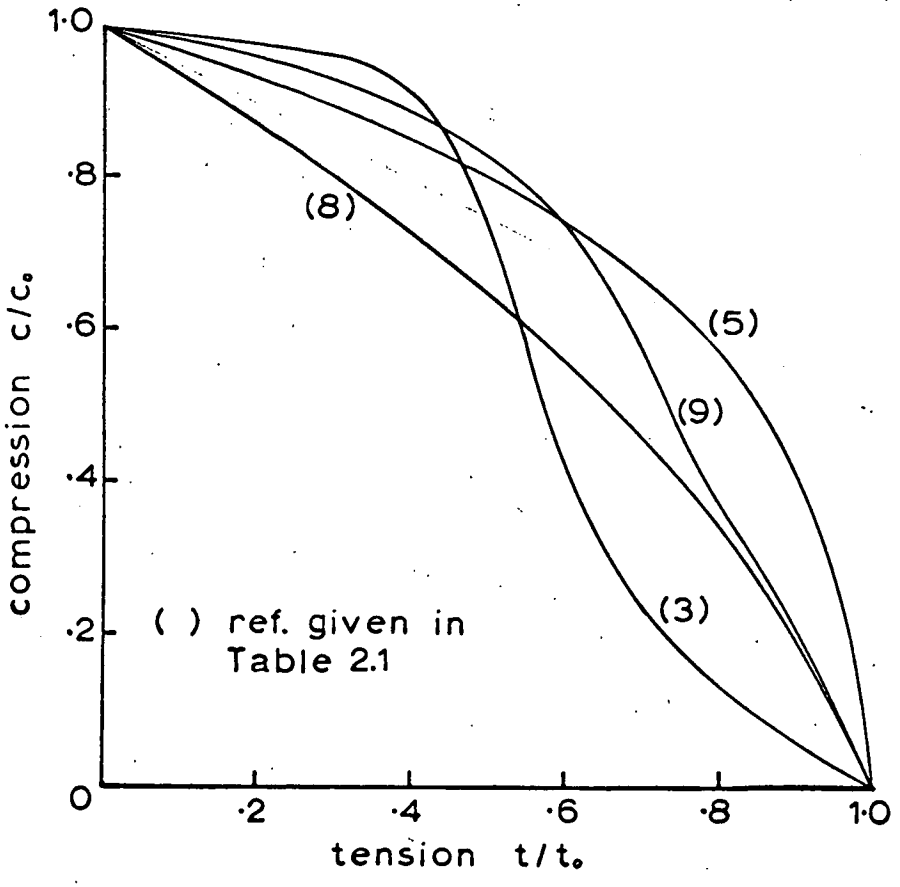

Fig 2.8 BIAXIAL COMPRESSION-TENSION FAILURE ENVELOPES

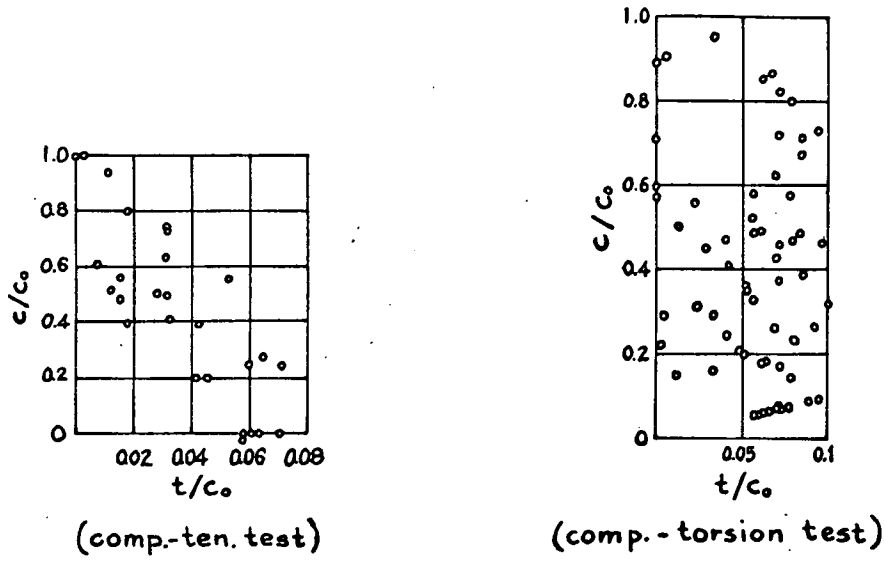

Fig 2.9 TSUBOI & SUENAGA'S BIAXIAL COMPRESSION-TENSION TEST DATA FOR CONCRETE

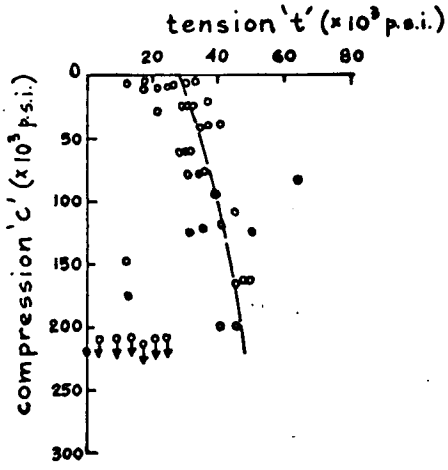

Fig 2.10 BROUTMAN & CORNISH'S BIAXIAL COMPRESSION-TENSION TEST DATA FOR ALUMINA CERAMICS

Of considerable interest are the results of Vile[60] in Fig. 2.11 and of Isenberg[30] in Fig. 2.12. Vile obtained differing biaxial failure envelopes, the profile of which appears to be affected by the volume fraction, V_f, of the coarse aggregates in the concrete mix. For mortar mixes where $V_f = 0$, there exists a concavity in the biaxial curve. Similarly, it is significant to note that the biaxial envelopes given by Isenberg at discontinuity and at failure stresses are essentially different. At discontinuity, the biaxial curve is distinctly concave. The validity of the biaxial curve at failure stresses derived from the method of torsion and compression test, as discussed earlier, is suspect.

The significance of the observations on Vile's and Isenberg's test data will be discussed in greater detail in Chapter 4.

2.5 TRIAXIAL COMPRESSION STRENGTH

The term "triaxial compression" has now been chosen to describe three dimensional compression with equal minor principal stresses, i.e.

$$\sigma_1 > \sigma_2 = \sigma_3$$

where

σ_1 = major principal stress

σ_2, σ_3 = minor principal stresses

In the general case where the principal stresses are of unequal magnitude, i.e. $\sigma_1 > \sigma_2 > \sigma_3$, the term "polyaxial compression" is used. The particular state of triaxial compression is of interest in this thesis.

Unlike the case for biaxial compression-tension strength where a wide choice of test methods is available, the test for triaxial compression is inevitably conducted in a hydraulic cell because in this arrangement it is easy to produce the required stresses. A

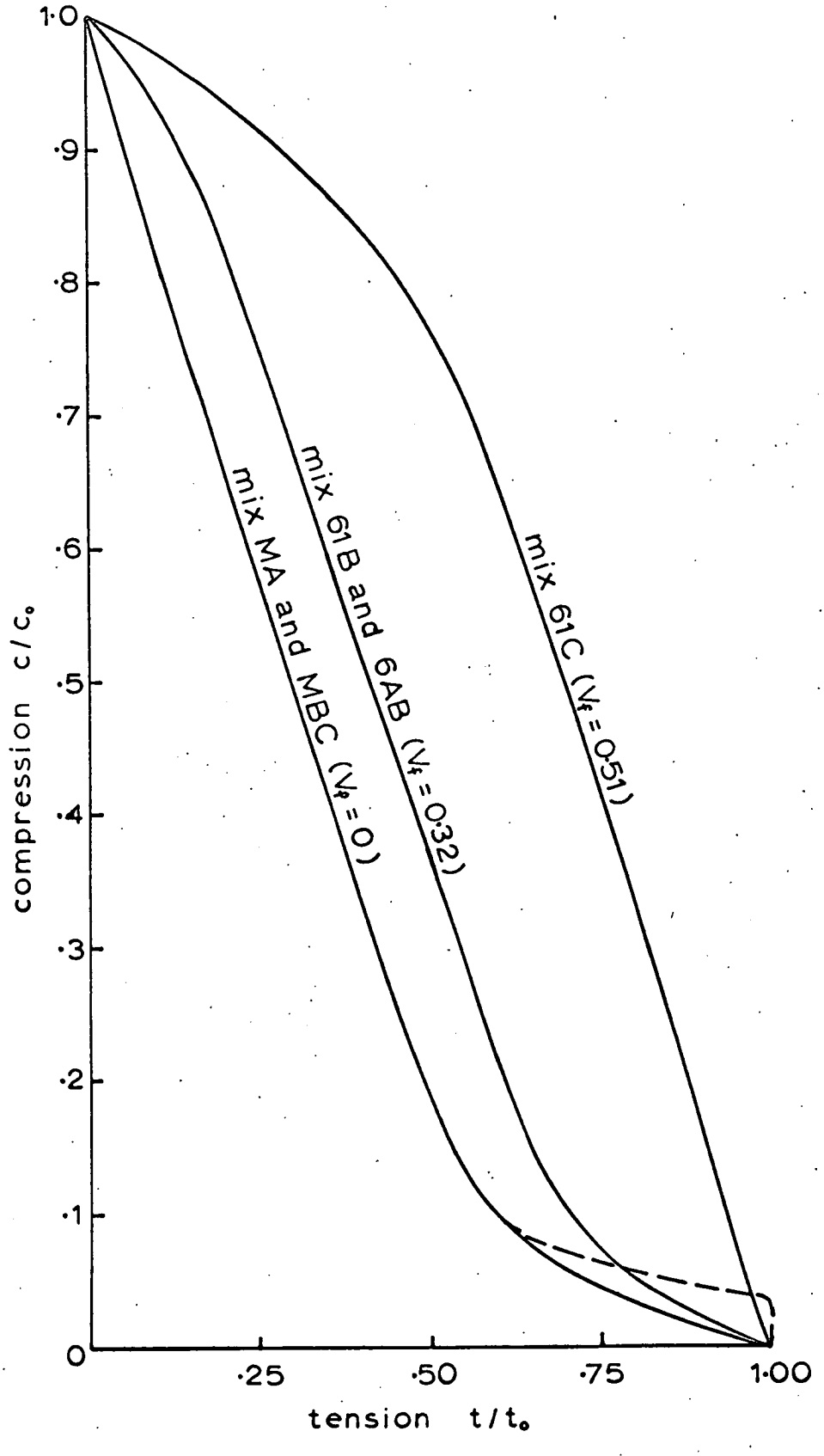

Fig 2.11 VILE'S BIAXIAL COMPRESSION-TENSION TEST DATA FOR CONCRETE & MORTAR

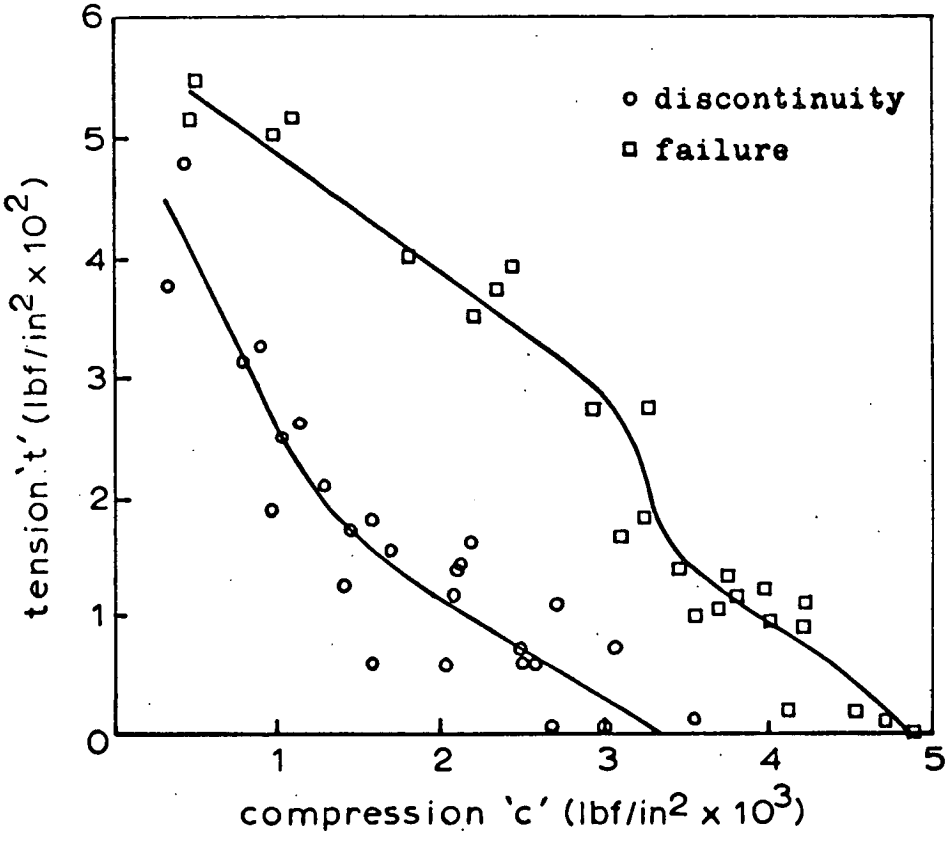

Fig 2.12 ISENBERG'S BIAXIAL COMPRESSION-TENSION TEST DATA FOR CONCRETE

cylindrical specimen placed in a pressure chamber is subjected first to a fluid pressure and then loaded axially to failure.

Where it is proposed to investigate into the influence of the intermediate principal stress σ_2 on failure, the triaxial cell will not be a suitable apparatus and other test arrangements are therefore necessary. Three dimensional compression on cubes, and use of hollow cylinders subject to internal and external pressure combined with axial compression are alternative test methods for polyaxial compression.

Numerous triaxial compression tests have been carried out mainly on concrete and rocks, since Karman's[32] experiments on marble in 1911. A comprehensive reference to works on triaxial compression on rocks may be found in Hoek's[27] report. Some published results on the triaxial compression of concrete and mortar are given in Fig. 2.13 where the number designated to each curve may be referred to Table 2.2 which lists the sources from which the data have been extracted. Also indicated in Fig. 2.13 are the curves corresponding to the original and the modified Griffith criteria.

It is evident from an examination of Fig. 2.13 that the principal stress relationship for concrete and mortar is not linear, as predicted by the modified Griffith criterion (which it is recalled is identical with the Coulomb criterion). The experimental curves suggest that the coefficient of internal friction μ may not be constant but perhaps reduces with increasing compression. Although parabolic, the original Griffith criterion gives strength values well below the experimental results.

A comparison between the failure envelopes for concrete and those for mortar shows that the increase in ultimate strength of concrete with increasing confining pressure is higher than that for mortar.

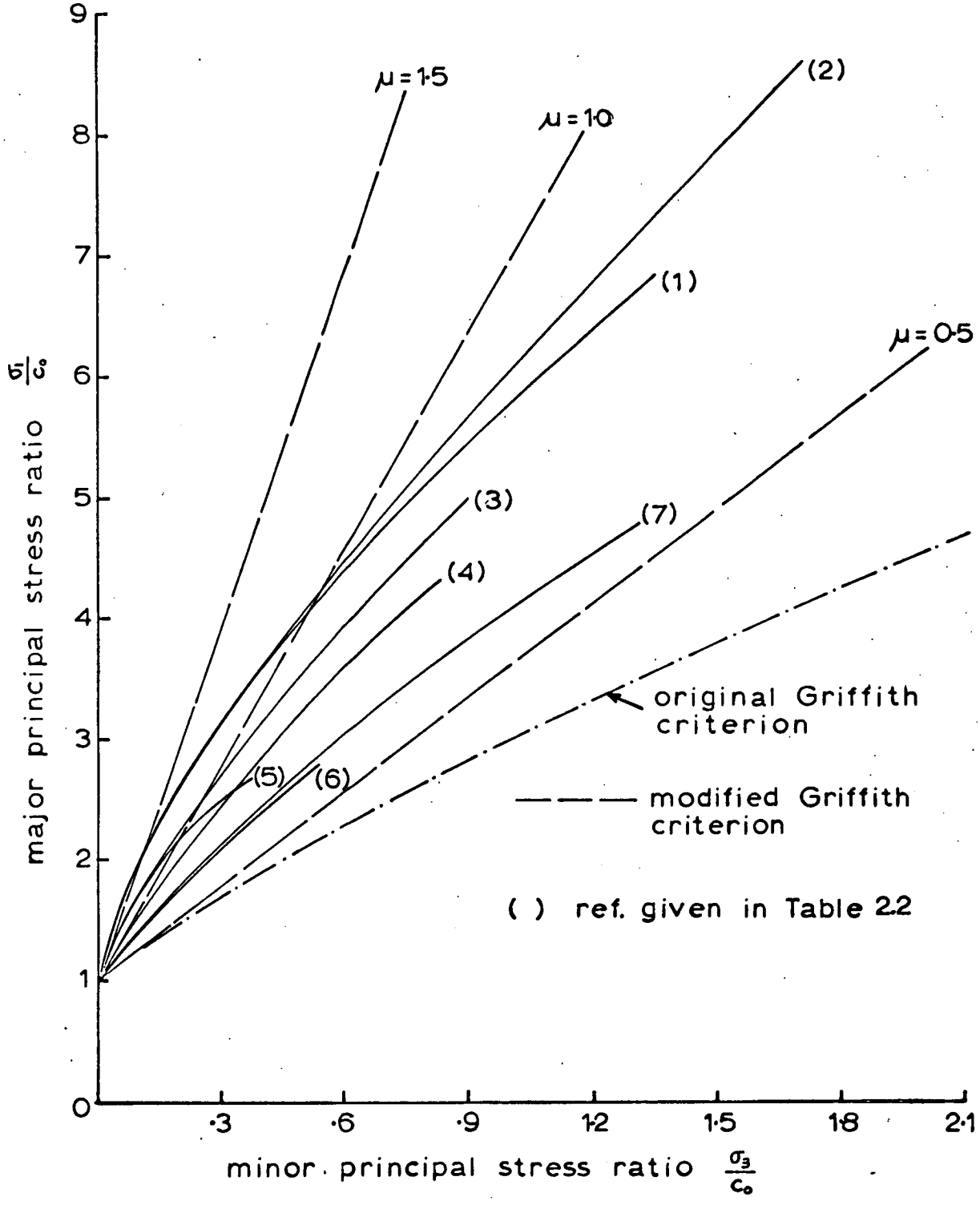

Fig 2.13 TRIAXIAL COMPRESSION STRENGTH OF CONCRETE & MORTAR

TABLE 2.2 - TRIAXIAL COMPRESSION OF CONCRETE & MORTAR

Graph No.	Author & Ref. No.	Material & Mix	Uniaxial compressive Strength c_o (approx.) lbf/in^2
1	Balmer (2) (1949)	1:2.86:4.47 concrete	3500
2	Akroyd (1) (1961)	1:3.42:5.59 concrete	1650
3	Gardner (20) (1969)	concrete (mix not given)	3900
4	Hobbs (26) (1971)	1:3.9 concrete	4350 - 6500
5	U.S.B.R. (58) (1954)	1:2 mortar & neat cement	10000
6	Smith & Brown (51) (1941)	1:2 & 1:3 mortar	4500
7	Campbell-Allen (12) (1962)	1:2.64 mortar	4600

2.6 SUMMARY

1. The two failure criteria which best describe the behaviour of brittle materials under complex stresses are

   (a) Coulomb's shear failure theory

   (b) Griffith's flaw theory.

2. Coulomb's theory predicts a straight line relationship between the major and minor principal stresses at failure, given by the equation

$$\frac{\sigma_1}{c_o} = \frac{\sigma_3}{c_o}\left[\frac{(\mu^2+1)^{\frac{1}{2}}+\mu}{(\mu^2+1)^{\frac{1}{2}}-\mu}\right]+1 \qquad \text{.....(2.10)}$$

   where

   σ_1 = major principal stress

   σ_3 = minor principal stress

   c_o = uniaxial compression strength

   μ = coefficient of internal friction

   It is necessary to modify the criterion for part of the biaxial compression-tension region near the uniaxial tensile strength axis by a tension cut-off defined by the equation

$$\sigma_3 = -t_o \qquad \text{.....(2.14)}$$

   where

   t_o = uniaxial tensile strength.

3. Griffith's flaw theory produces a parabolic strength relationship between the principal stresses, given by the equation for the compression quadrant:

$$\frac{\sigma_1}{c_o} = \tfrac{1}{2} + \frac{\sigma_3}{c_o} + \sqrt{\frac{2\sigma_3}{c_o} + \tfrac{1}{4}} \qquad \text{.....(2.31)}$$

In the/

In the compression-tension quadrant, the criterion consists of two parts defined by the equations:

for $(\sigma_1 + 3\sigma_3) > 0$,

$$(\sigma_1 - \sigma_3)^2 - 8t_o(\sigma_1 + \sigma_3) = 0 \quad \text{.....(2.29)}$$

for $(\sigma_1 + 3\sigma_3) < 0$,

$$\sigma_3 = -t_o \quad \text{.....(2.30)}$$

where

t_o = tensile strength.

Griffith's material has a uniaxial compression strength c_o equal to $8t_o$.

4. The original Griffith criterion given in (3) above is modified to account for the closing of cracks in compression, and the resulting criterion is identical with the Coulomb criterion.

5. Two particular states of combined stresses are of interest in this thesis, and they are:-

   (a) biaxial compression-tension

   (b) triaxial compression.

6. Of the various test methods available for the determination of the biaxial compression-tension strength of brittle materials, the two most favourable methods are:-

   (a) direct tension and compression

   (b) hollow cylinders: hoop tension and axial compression.

7. Triaxial compression tests in which the minor principal stresses are equal are most conveniently carried out in a hydraulic cell where the cylindrical specimen is subjected first to a confining fluid pressure and then loaded axially to failure.

8./

8. The principal stress relationship for concrete and mortar obtained from experiments is not linear as predicted by the modified Griffith or Coulomb criterion.

9. The increase in ultimate strength of concrete with increasing confining pressure is higher than that for mortar.

CHAPTER 3 - BIAXIAL COMPRESSION-TENSION STRENGTH TESTS ON ONE-THIRD SCALE MODEL BRICKS

3.1 INTRODUCTION

It was pointed out in Chapter 1 that the state of stress in a brick element within a brickwork panel under vertical compression is a combination of vertical compression and bi-lateral tension. The bi-lateral tension is the result of the differential lateral strain between the mortar and the brick element; the mortar joint tends to expand laterally more than the brick and in so doing imparts a tensile stress to the brick.

In order to be able to develop the proposed failure theory for brickwork in compression as described in Section 1.3, it is necessary to investigate the behaviour of brick under a state of compression-tension-tension stresses. However, since it was not possible to devise a testing method which could generate a state of compression-tension-tension stresses in brick, the study was confined with regret to a biaxial state of compression-tension stresses. Even so, brick being a non-castable material, the choice of testing methods which can produce the desired stress field is very limited.

In this chapter, an experimental investigation carried out to determine the biaxial compression-tension strength relationship for brick is described, using the method of direct tension and compression on one-third scale model bricks of various strengths. Some compression and tension strength tests were also carried out.

Two series of one-third scale model bricks were used in these tests. The bricks in the first series were designated as types A, B, C and D whose B.S. crushing strengths were 3224, 4549, 9336 and 13448 lbf/in^2 (22.33,/

(22.23, 31.36, 64.37, 92.72 MN/m^2) respectively. The second series of bricks, which were to supplement the first series, were designated as types K, L, M and N, and their B.S. crushing strengths were 2944, 9135, 10620 and 15448 lbf/in^2 (20.30, 62.98, 73.22, 106.51 MN/m^2) respectively.

3.2 COMPRESSION STRENGTH

The physical dimensions, B.S. crushing strengths and water absorption properties of the one-third scale model bricks, types A, B, C and D, are listed in Tables 3.1 and 3.2. The B.S. crushing strengths, in both soaked and dry conditions, for types K, L, M and N are listed in Table 3.3. Soaked bricks were kept in water for at least 24 hours, and dry bricks were dried in an oven at 110 degrees Centigrade for 1 day.

From Table 3.3, it is noted that for the B.S. crushing strength test, bricks tested in a dry condition yielded higher strengths than those tested soaked.

Compression tests were also carried out on soaked bricks, types A (B.S. 3224 lbf/in^2) and D (B.S. 13448 lbf/in^2), tested on end with different capping material in an attempt to establish a test condition which would give strength values representing the uniaxial compression strength which is the compression strength of a material free from the influence of the loading platens in a compression test, and is therefore an intrinsic property of that material.

A brick tested on end had a height:width and a height:thickness ratio of 2.1 and 3.0 respectively. For each brick strength, the test results for four end conditions - three using different capping materials and one without - are given in Table 3.4.

Except for tests where 1/8 in./

TABLE 3.1 -DIMENSIONS OF ONE-THIRD SCALE MODEL BRICKS, TYPES A, B, C, D.

	Type A (BS 3224 lbf/in^2)			Type B (BS 4549 lbf/in^2)		
	Dimensions (ins)			Dimensions (ins)		
	Length	Width	Thickness	Length	Width	Thickness
Mean Value	3.09	1.47	1.03	3.03	1.45	0.99
Range						
Max.	3.13	1.49	1.04	3.05	1.45	0.99
Min.	3.06	1.46	1.02	3.00	1.44	0.98
Coefft.of var. (%)	<1.0	<1.0	<1.0	<1.0	<1.0	<1.0
No. of specimens	10	10	10	10	10	10
	Type C (BS 9336 lbf/in^2)			Type D (BS 13448 lbf/in^2)		
	Dimensions (ins)			Dimensions (ins)		
	Length	Width	Thickness	Length	Width	Thickness
Mean value	3.04	1.44	1.00	2.99	1.41	0.98
Range						
Max.	3.07	1.45	1.01	3.02	1.42	0.99
Min.	3.00	1.44	1.00	2.96	1.41	0.97
Coefft. of var. (%)	<1.0	<1.0	<1.0	<1.0	<1.0	<1.0
No. of specimens	10	10	10	10	10	10

1 in = 2.54 cm

TABLE 3.2 - B.S. CRUSHING STRENGTH (SOAKED) & WATER ABSORPTION OF ONE-THIRD SCALE MODEL BRICKS, TYPES, A, B, C, D.

Brick type	A	B	C	D
Mean value (lbf/in^2)	3224	4549	9336	13448
Range (lbf/in^2) Max. Min.	 4047 2548	 5051 4184	 10156 8929	 14319 12149
Coefft. of var.(%)	15.3	7.3	4.0	5.2
No. of specimens	20	10	10	10
Water absorption(%)	12.0	11.2	11.5	9.3

TABLE 3.3 - B.S. CRUSHING STRENGTHS (SOAKED & DRY) OF ONE-THIRD SCALE MODEL BRICKS, TYPE K, L, M, N.

	Brick type	K	L	M	N
SOAKED	Mean value(lbf/in^2)	2944	9135	10620	15448
	Range (lbf/in^2) Max. Min.	 3526 2447	 9935 8575	 11677 9373	 16027 13684
	Coefft. of var.(%)	12.8	5.7	7.3	4.7
	No. of specimens	10	10	10	10
DRY	Mean value (lbf/in^2)	4498	10706	12389	16407
	Range (lbf/in^2) Max. Min.	 5631 3448	 12433 9298	 14086 9108	 17401 16162
	Coefft. of var.(%)	14.5	9.6	13.7	4.4
	No. of specimens	10	10	10	10

$1\ lbf/in^2 = 6.8948 \times 10^{-3}\ MN/m^2$

TABLE 3.4 - EFFECT OF DIFFERENT CAPPING MATERIAL ON THE COMPRESSION STRENGTH OF ONE-THIRD SCALE MODEL BRICKS TESTED ON END (SOAKED)

BS crushing strength (lbf/in^2)	3224 (Type A)			
Capping material	nil	1/8 in plywood	1/16 in ptfe	MGA pad
Mean value (lbf/in^2)	2580	2409	2089	2747
Range (lbf/in^2) Max. Min.	3595 1228	2811 2042	2500 1553	3802 1775
Coefft. of var. (%)	30.0	11.1	16.7	25.2
No. of specimens	10	10	10	10
BS crushing strength (lbf/in^2)	13448 (Type D)			
Capping material	nil	1/8 in plywood	1/16 in ptfe	MGA pad
Mean value (lbf/in^2)	10103	11633	4855	9832
Range (lbf/in^2) Max. Min.	12353 8624	12644 10375	5398 4150	11737 7716
Coefft. of var. (%)	12.2	6.0	8.9	15.8
No. of specimens	10	10	6	10

$$1\ lbf/in^2 = 6.8948 \times 10^{-3}\ MN/m^2$$

Except for tests where 1/8 in (3.18 mm) thick plywood was used as a capping material, the ends of every specimen were cut parallel with the aid of a rock-cutting machine to a tolerance not exceeding 0.003 in (0.076 mm).

The MGA pad was a frictionless sandwich layer consisting of a Melinex polyester film, gauge 100, and a hardened aluminium foil 0.001 in (0.025 mm) thick, with a thin layer of Molyslip grease in between (see Hughes & Bahramian[28]). In use, the aluminium face of the MGA pad was placed towards the brick specimen.

The effect of the 1/8 in (3.18 mm) plywood on the crushing strength, though not apparent for the low-strength brick, was significant for the BS 13448 lbf/in^2 brick. The heavy indentation of the brick into the plywood served as a lateral restraint on the brick which resulted in an increased compression strength.

The 1/16 in (1.59 mm) thick p.t.f.e. (polytetrafluoroethylene) sheet yielded particularly under high pressure and induced premature tensile splitting failure in the brick which explains the very low figure of 4855 lbf/in^2 (33.47 MN/m^2) obtained for brick type D.

There was little difference in strength between the bricks tested with MGA pads and those without any capping material. The usefulness of the MGA pads was not apparent perhaps because the influence of the end restraint in a test specimen of height:width ratio of the order of 2.1 to 3.0 was not serious. However, the compression strength of brick tests on end using MGA pads had been taken to represent the uniaxial compression strength of the brick.

The uniaxial compression strength of brick types C (BS 4549 lbf/in^2) and D (BS 9336 lbf/in^2) were also determined using soaked bricks, and the results are seen in Table 3.5.

TABLE 3.5 - UNIAXIAL COMPRESSION STRENGTH (SOAKED) OF ONE-THIRD SCALE MODEL BRICKS, TYPES A, B, C, D.

Brick type	A	B	C	D
Mean value (lbf/in^2)	2747	3981	6847	9832
Range (lbf/in^2)				
Max.	3802	4603	8353	11737
Min.	1775	3729	4729	7716
Coefft. of var. (%)	25.2	6.3	14.9	15.8
No. of specimens	10	10	10	10

TABLE 3.6 - UNIAXIAL COMPRESSION STRENGTHS (SOAKED & DRY) OF ONE-THIRD SCALE MODEL BRICKS, TYPE K, L, M, N.

	Brick type	K	L	M	N
SOAKED	Mean value (lbf/in^2)	2974	7465	7299	12265
	Range (lbf/in^2)				
	Max.	3457	8208	9833	13900
	Min.	2483	6388	6003	11467
	Coefft. of var. (%)	9.7	8.0	20.5	6.3
	No. of specimens	10	10	10	10
DRY	Mean value (lbf/in^2)	4576	8954	9109	13132
	Range (lbf/in^2)				
	Max.	5515	10326	11572	14600
	Min.	3834	7778	7492	11633
	Coefft. of var. (%)	13.5	9.5	18.5	7.2
	No. of specimens	10	10	10	10

$$1\ lbf/in^2 = 6.8948 \times 10^{-3}\ MN/m^2$$

Subsequently, it was decided to test the second series of bricks, types K, L, M and N, for their uniaxial compression strengths in both soaked and dry conditions, and the values are given in Table 3.6. Note that, as in the case of the B.S. crushing strength, the dry strengths for uniaxial compression were also higher than the soaked values.

Fig. 3.1 shows the relationship between the soaked and the dry uniaxial compression strengths for brick types K, L, M and N. The values of the dry uniaxial compression strengths for brick types A, B, C and D, not determined experimentally but which are required for the establishment of the proposed failure theory, interpolated from Fig. 3.1, are approximately 4600, 5700, 8300 and 11000 lbf/in^2 (31.72, 39.30, 57.23, 75,84 MN/m^2) respectively.

All compression tests were carried out in an Avery compression machine, and the rate of loading was 2000 lbf/in^2/min (13.79 MN/m^2/min).

A comparison between the B.S. crushing and the uniaxial compression strengths shows that for a low strength brick, below B.S. 5000 lbf/in^2 (34.47 MN/m^2), the B.S. crushing strength was near enough the uniaxial compression strength. However, for a stronger brick, due to the heavy indentation of the brick into the plywood under load which served as a lateral restraint on the brick, the B.S. crushing strength was significantly higher than its uniaxial compression strength.

This is, of course, an observation pertaining to one-third scale model bricks where the influence of the 1/8 in. (3.18 mm) thick plywood on the brick strength in a B.S. crushing test is great. It may be expected that in the case of a full size brick, the influence of the plywood on the brick strength will be less.

More important, however, is the influence of the pore water pressure on the compression strength of soaked bricks, about which more will be said later.

Hilsdorf's brush platens have been/

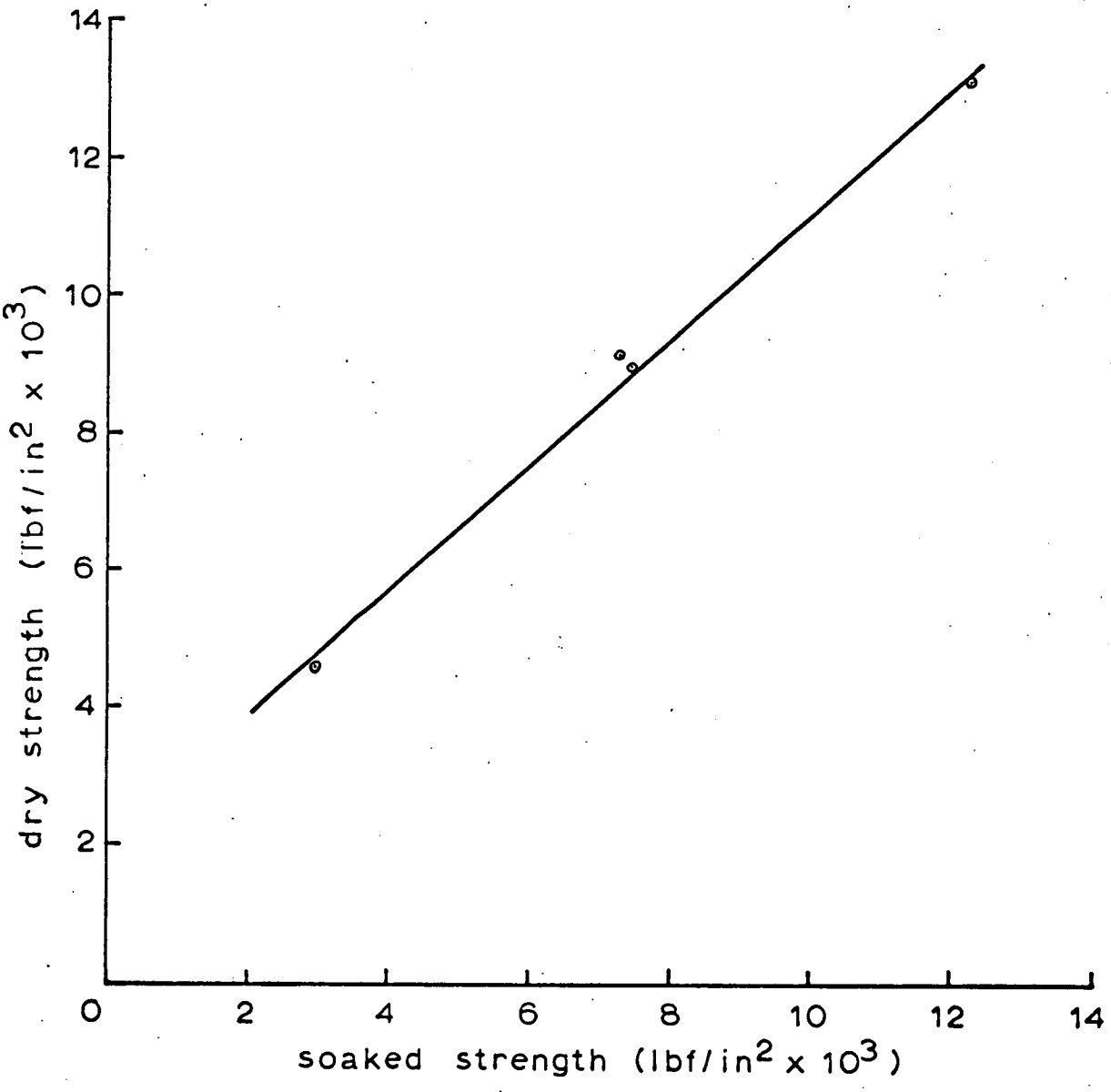

Fig 3.1 Uniaxial Compression Strength of Brick Types K, L, M, N

Hilsdorf's brush platens have been used in compression tests to determine the uniaxial compression strength of brick (see Thomas & O'Leary[54]) in which it was assumed that the flexible steel brushes would not restrain the lateral expansion of the ends of the brick specimen under a compressive load, and thereby eliminate the problem of platen influence on the compression strength of brick. The indiscriminate use of such brush platens can result in premature tensile splitting in the test specimen if the flexibility of the brushes under load exceeds the lateral strain in the test specimen. The low ratios of the compression strength using Hilsdorf's brushes to the B.S. compression strength of brick reported by Thomas & O'Leary[54] may be on this account.

3.3 TENSILE STRENGTH

The direct briquet tensile test and the indirect Brazilian splitting test were employed to determine the strength of one-third scale model bricks on both dry and soaked specimens.

In the direct briquet tensile test, specimens of cross-section 1 in square x 3 in long (2.54 x 7.62 cm) cut from the one-third scale model bricks on a rock-cutting machine were used. The ends of these specimens were capped with an Araldite-sand mix to a shape similar to that of the standard cement mortar specimen, in timber moulds, leaving a clear central section of about $1\frac{1}{4}$ in (3.18 cm) length, see Fig. 3.2. The purpose of the $1\frac{1}{4}$ in clear section was to accomodate a 1 in (2.54 cm) square compression-loaded area required in the biaxial compression-tension test to be described in a later section.

These specimens were then tested to failure in a Hounsfield tensometer which may be seen laid horizontally in Fig. 3.14. The tensile load in a Hounsfield tensometer was applied by turning a screw-jack which pulled the specimen/

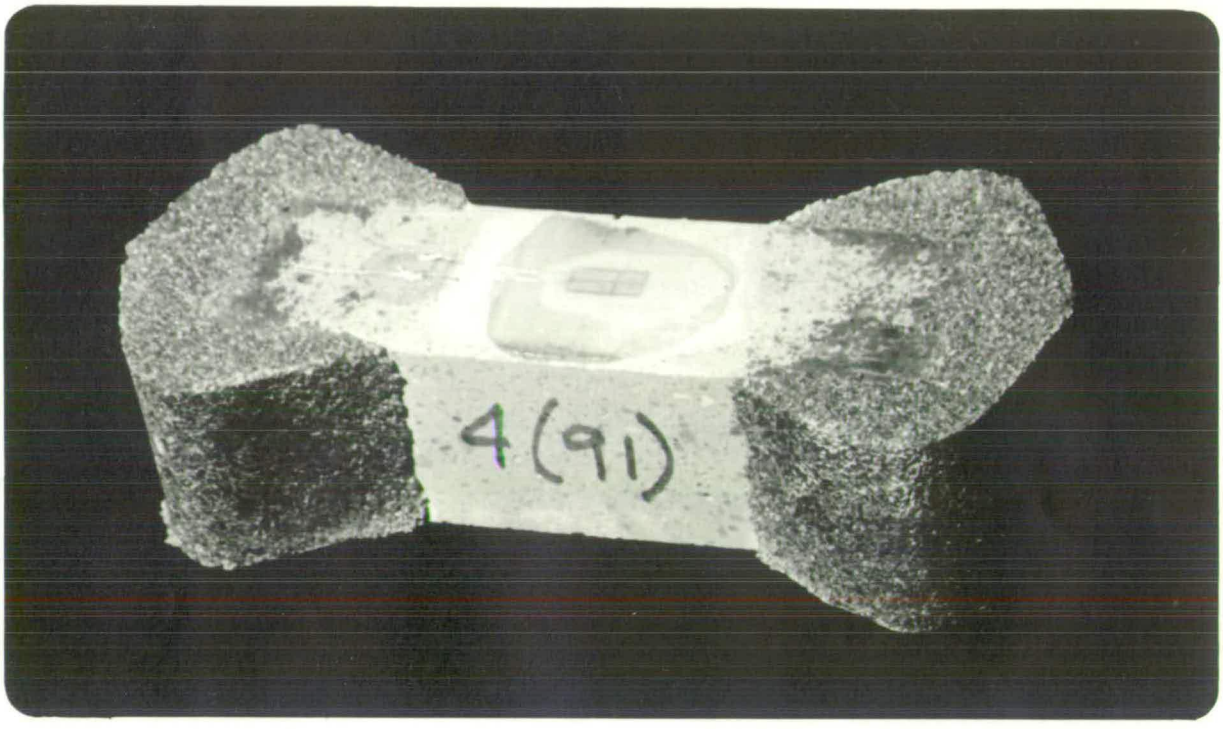

Fig 3.2 A BRICK BRIQUET SPECIMEN

the specimen apart. The reaction to the applied load deflected a standard leaf-spring whose deflection actuated a mercury column. The applied load was read off a load scale adjacent to the mercury column whose movement had been calibrated against the particular leaf-spring in use. The rate of loading was principally determined by the ease with which the mercury reading could be traced, which may be taken to be between 200 to 800 lbf/in^2/min (1.38 to 5.52 MN/m^2/min) for these tests.

The briquet-shaped grips used for pulling the test specimen were lined with a sheet of hard rubber in order to spread the applied load, and thereby reduce the stress concentration, at the points of contact with the test specimen.

After some preliminary trials, the following Araldite-sand mix was found to be suitable:-

Araldite CY 219	100 gms
Hardener HY 219	50 gms
Accelerator DY 219	6 gms
Leighton-Buzzard sand 25/52	600 gms

An Araldite-sand mix that was too dry would not bond well with the brick specimen. On the other hand, a wet mix on setting would be too soft and would yield under pressure at the grips.

The timber moulds, one of which is seen in Fig. 3.3, thoroughly waxed before casting, were stripped after 24 hours, and the specimens could be tested 2 days or more after casting.

In the indirect Brazilian splitting test, knife-edge loads were applied on the opposite faces of the one-third scale model bricks along its length, see Fig. 3.4. The faces of each brick had previously been polished flat in order to achieve a uniform knife-edge loading.

Provision/

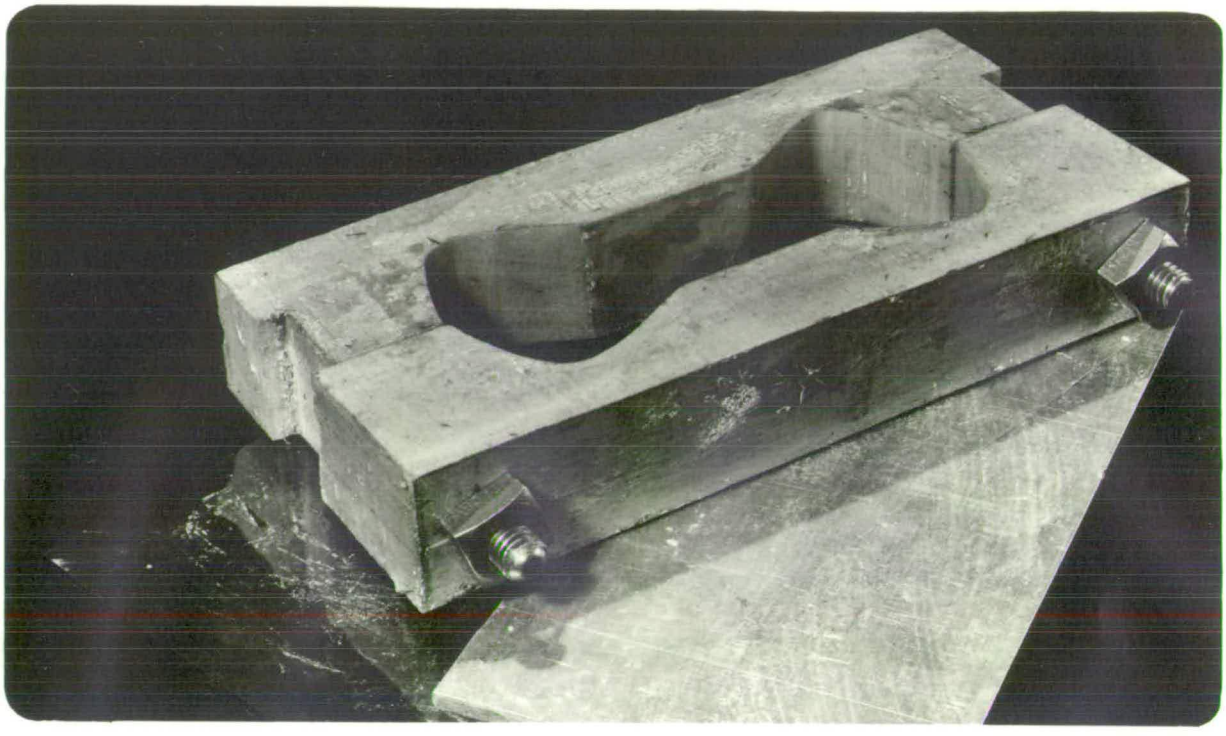

Fig 3.3 A TIMBER MOULD FOR BRIQUET SPECIMEN

Fig 3.4 DEVICE FOR TENSILE SPLITTING TEST

Provision was also made through the incorporation of guide plates adjacent to the knife-edge platens to ensure that the knife-edge loads act in line.

A 6-ton (59.78 kN) hand-operated jack exerted the load reacting against a self-straining steel frame. The applied load was registered on a proving ring.

Since in this arrangement of the Brazilian splitting test the cross-section of the specimen was not circular (for which the standard formula $t_o = 2P/\pi Dl$ applies, where t_o = tensile strength, P = knife-edge load, D = diameter of specimen, and l = length of specimen), a finite element analysis of the stress distribution within a rectangular section whose width:depth ratio L/D = 1.4 in this case, was made, the details of which are plotted in Fig. 3.5. The lateral tensile stress distribution was not altogether uniform throughout the depth of the specimen. Nevertheless, an average k-value of 0.60 in the expression $t_o = kP/Dl$ had been assumed in the calculation of the tensile splitting strengths.

Results of the tensile tests on the first series of one-third scale model bricks, types A, B, C and D, from both the direct briquet test and the indirect splitting test are listed in Table 3.7. There was a strength difference between the dry and the soaked specimens, particularly for high strength bricks. The existence of a pore water pressure in the soaked brick was the cause for the increased strength. However, unlike the compression test specimens, the soaked strengths for the tensile specimens were higher than those tested dry. The reason for this is discussed in a later section dealing with the influence of the pore water pressure on brick strength.

Further/

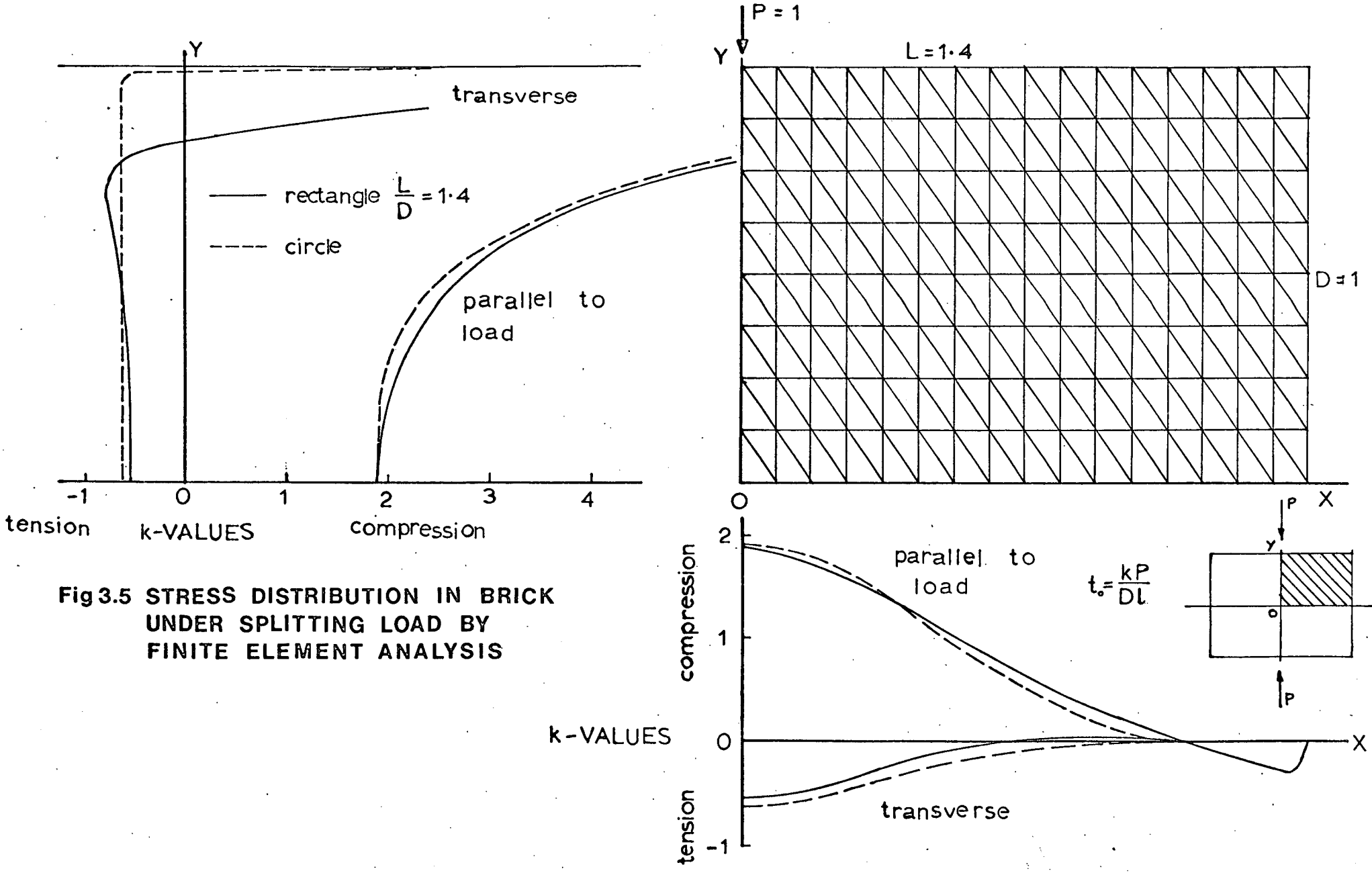

Fig 3.5 STRESS DISTRIBUTION IN BRICK UNDER SPLITTING LOAD BY FINITE ELEMENT ANALYSIS

TABLE 3.7 - DIRECT & INDIRECT TENSILE STRENGTHS OF ONE-THIRD SCALE MODEL BRICKS, TYPES A, B, C, D.

Brick type	A		B		
Tensile test	Direct briquet	Indirect splitting	Direct briquet		Indirect splitting
Specimen condition	Soaked	Soaked	Dry	Soaked	Dry
Mean value (lbf/in^2)	192	198	273	287	238
Range (lbf/in^2) Max. Min.	 242 139	 251 117	 376 184	 342 216	 258 216
Coefft. of var. (%)	16.6	24.5	22.9	14.2	5.9
No. of specimens	12	10	11	10	10

Brick type	C			D		
Tensile test	Direct briquet		Indirect splitting	Direct briquet		Indirect splitting
Specimen condition	Dry	Soaked	Soaked	Dry	Soaked	Soaked
Mean value (lbf/in^2)	489	577	615	686	877	800
Range (lbf/in^2) Max. Min.	 639 410	 629 526	 702 529	 813 531	 1011 735	 966 701
Coefft. of var. (%)	15.2	5.9	9.6	13.8	10.2	11.6
No. of specimens	10	10	10	10	10	10

$$1\ lbf/in^2 = 6.8948 \times 10^{-3}\ MN/m^2$$

Further direct briquet tensile tests were carried out on the second series of one-third scale model bricks, types K, L, M and N. Specimens in a dry state only had been tested. The results are presented in Table 3.8. The coefficient of variation in tensile strength for brick types L and M were rather high.

It may be helpful for easy reference to summarise, at this stage, the results of the various strength tests obtained so far, and this is done in Table 3.9.

The indirect splitting tensile strengths compared favourably with those obtained from the direct briquet test. However, it must be remembered that the Brazilian splitting test is in itself a biaxial compression-tension test, for in addition to the lateral tensile stress, there exists a compressive stress in the direction parallel to the knife-edge load. Not only is there a biaxial state of stress in the Brazilian splitting test, the ratio of the compressive to tensile stresses is not constant but varies along the depth of the specimen.

Nevertheless, in consideration of the relative ease with which the indirect splitting test may be performed when compared with the direct tensile test, the splitting test may be adopted for routine testing for the tensile strength of brick. A problem exists, however, in testing perforated bricks.

The Brazilian splitting test was also carried out elsewhere[40],[54] with the knife-edge load applied across the width of the brick. In this arrangement, the cross-section of the specimen is very rectangular and the resulting lateral tensile stress distribution with depth is far from uniform. In this event, it is doubtful whether the tensile strength of brick may be derived from the indirect tensile splitting formula, however modified.

TABLE 3.8 - DIRECT TENSILE STRENGTH (DRY) OF ONE-THIRD SCALE MODEL BRICKS, TYPES K, L, M, N.

Brick type	K	L	M	N
Mean value (lbf/in^2)	226	437	401	908
Range (lbf/in^2)				
Max.	273	708	935	1042
Min.	173	260	266	674
Coefft. of var. (%)	15.5	35.8	49.7	11.2
No. of specimens	10	10	10	10

TABLE 3.9 - STRENGTH PROPERTIES OF ONE-THIRD SCALE MODEL BRICKS.

lbf/in^2

Brick type	A	B	C	D
B.S. crushing (soaked)	3224	4549	9336	13448
Uniaxial compression (soaked)	2747	3981	6847	9832
Uniaxial compression (dry)	(4600)	(5700)	(8300)	(11000)
Tensile direct (soaked)	192	287	577	877
Tensile direct (dry)	-	273	489	686
Tensile indirect (soaked)	198	-	615	800
Tensile indirect (dry)	-	238	-	-
Brick type	**K**	**L**	**M**	**N**
B.S. crushing (soaked)	2944	9135	10620	15448
B.S. crushing (dry)	4498	10706	12389	16407
Uniaxial compression (soaked)	2974	7465	7299	12265
Uniaxial compression (dry)	4576	8954	9109	13132
Tensile direct (dry)	226	437	401	908

$1\ lbf/in^2 = 6.8948 \times 10^{-3}\ MN/m^2$.

A plot is made in Fig. 3.6 of the dry tensile strength against the dry uniaxial compression strength of brick. An additional point on the graph taken from the tests on clay pipes of very high strength, described in Chapter 4, provides a useful confirmation of the trend of the curve towards the region of high strength. The relationship indicates clearly that the tensile to compression strength ratio is not constant but varies with the strength of brick. For low strength bricks, the tensile strength is about 1/16 the uniaxial compression strength, and this ratio increases to about 1/12 for high strength bricks. This evidence is contrary to the results obtained by Sinha[49] from tests on one-sixth scale model bricks where the tensile to compression strength ratio was found to decrease with increasing brick strength, see Table 3.10 and Fig. 3.8.

It is believed that the tensile to compression strength ratio could rise with increased brick strength. This is because a poorly-fired low strength brick contains a higher proportion of flaws and fissures, leading to a low ratio of tensile to compression strength, the compression strength being less affected in this regard than the tensile strength which is sensitive to the presence of flaws and fissures. Paul[45] in his tests on cast-iron also obtained an increased tensile to compression strength ratio with increasing strength of cast-iron, see Fig. 3.7.

Fig. 3.8 shows the relationship between the B.S. crushing strength and the dry tensile strength of brick derived from these tests, as well as other test data extracted from published works whose references are enumerated in Table 3.10. Except for the results of Thomas & O'Leary[54] where the values were for dry strength, it is not known/

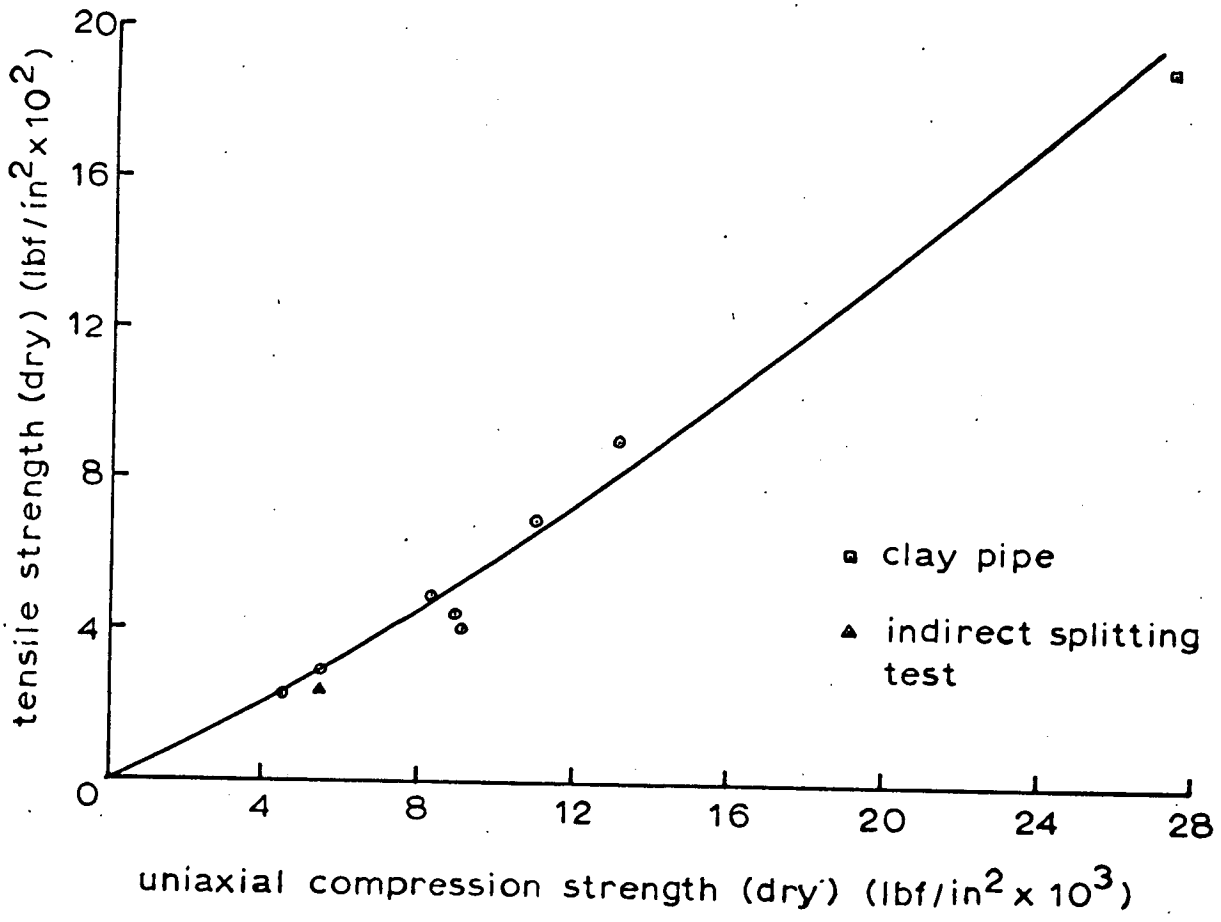

Fig 3.6 Tension & Compression Strengths for Brick

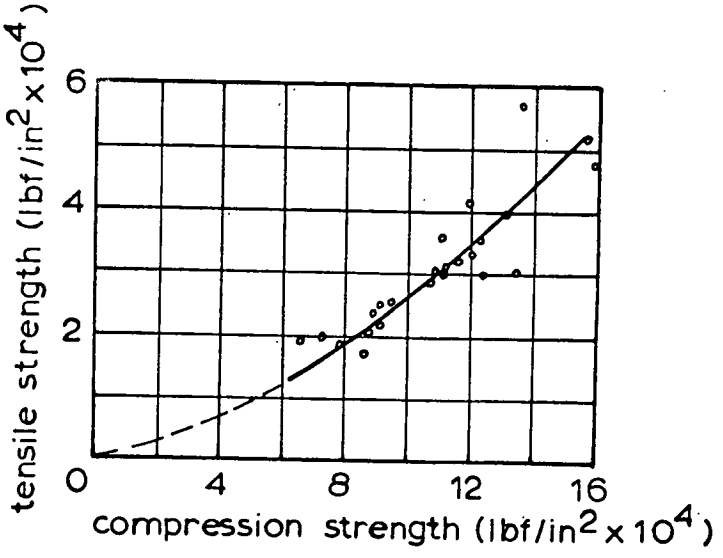

Fig 3.7 Tension & Compression Strengths for Grey Cast Iron (after Paul)

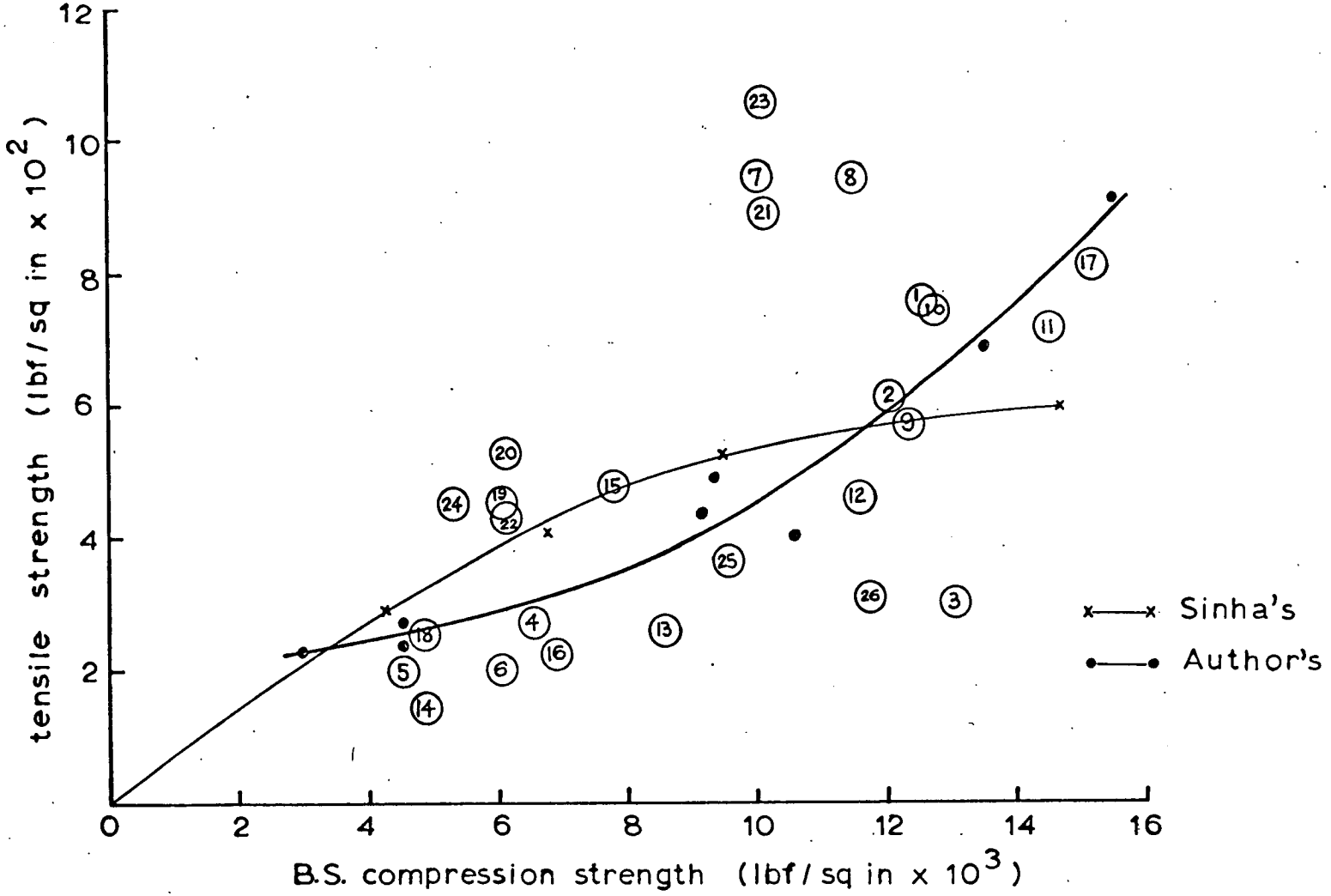

Fig 3.8 Relationship between B.S. Compression & Tensile Strengths of Brick

TABLE 3.10 - B.S. CRUSHING STRENGTH & TENSILE STRENGTH OF BRICK - PUBLISHED RESULTS.

Reference	Tensile test method	Brick size	Brick type	B.S. comp. strength (lbf/in^2)	Tensile strength (lbf/in^2)	No. of specimens	Graph point No.
Morsy (unpublished results, 1968)	Scissor device	Full size	Solid	12500	756	6	1
				12000	610	6	2
				13000	302	6	3
				6500	272	6	4
				4500	200	6	5
				6000	201	6	6
			Perf.	9980	945	6	7
				11460	940	6	8
				12300	568	6	9
				12710	745	6	10
				14460	715	6	11
				11540	457	6	12
				8550	261	6	13
				4870	142	6	14
				7750	478	8	15
				6860	227	8	16
				15120	807	8	17
Morsy[40]	Indirect splitting	One-third scale	Solid	4854	253	11	18
		One-sixth scale	Solid	6040	453	10	19
Thomas & O'Leary (54)	Indirect splitting	Full size	Solid	6100	527	10	20
			Perf.	10093	886	10	21
		$1\frac{3}{4}$in dia cores	Solid	6100	430	10	22
			Perf.	10093	1059	10	23
Hilsdorf (34)	Indirect splitting	Full size	Solid	5300*	450	-	24
Francis (19)	Indirect splitting	Full size	Solid	9530	364	6	25
			Perf.	11740	310	6	26
Sinha[49]	Direct briquet	One-sixth scale	Solid	4227	294	10	x
				6738	408	10	x
				9434	524	10	x
				14651	598	10	x

* In accordance with German specification DIN 105

Note: For perforated bricks, both compression and tensile strengths are based on net cross-sectional area of brick.

not known whether the tensile strength given in these references were also for dry strength. In the case of perforated bricks, the net cross-sectional area of the brick had been used in the calculation of both the compression and the tensile strengths. The curve in Fig. 3.8 is not expected to pass through the origin since the BS compression strength is affected by the existence of a pore water pressure in the soaked bricks.

Strain measurements with 3 mm resistance wire polyester gauges TML-PL3 were recorded on brick specimens of types A, B, C and D in the direct briquet test, three specimens for each brick strength. A strain gauge may be seen mounted on a briquet specimen in Fig. 3.2. The stress-strain curves are shown in Figs. 3.9 to 3.12. The ultimate strain does not appear to depend upon the tensile strength, the values ranging from 150 to 300 micro-units approximately. The elastic modulus taken over 80% of the ultimate strength is plotted against the tensile strength in Fig. 3.13. Notwithstanding a rather wide scatter of values, the elastic modulus-tensile strength relationship may be represented by the simple equation

$$E_t = 0.0046 t_o \times 10^6 \qquad \text{.....(3.1)}$$

where

E_t is the elastic modulus in tension and t_o the tensile strength.

In view of the low value of the ultimate tensile strain for brick, it will be extremely difficult to measure experimentally with sufficient accuracy the lateral strain distribution within a brick element in axially-loaded brickwork. Strain measurements at the surfaces of bricks in brickwork, made by Hilsdorf[25], using mechanical gauges over a 2 in. gauge length, the results of which led him to introduce a/

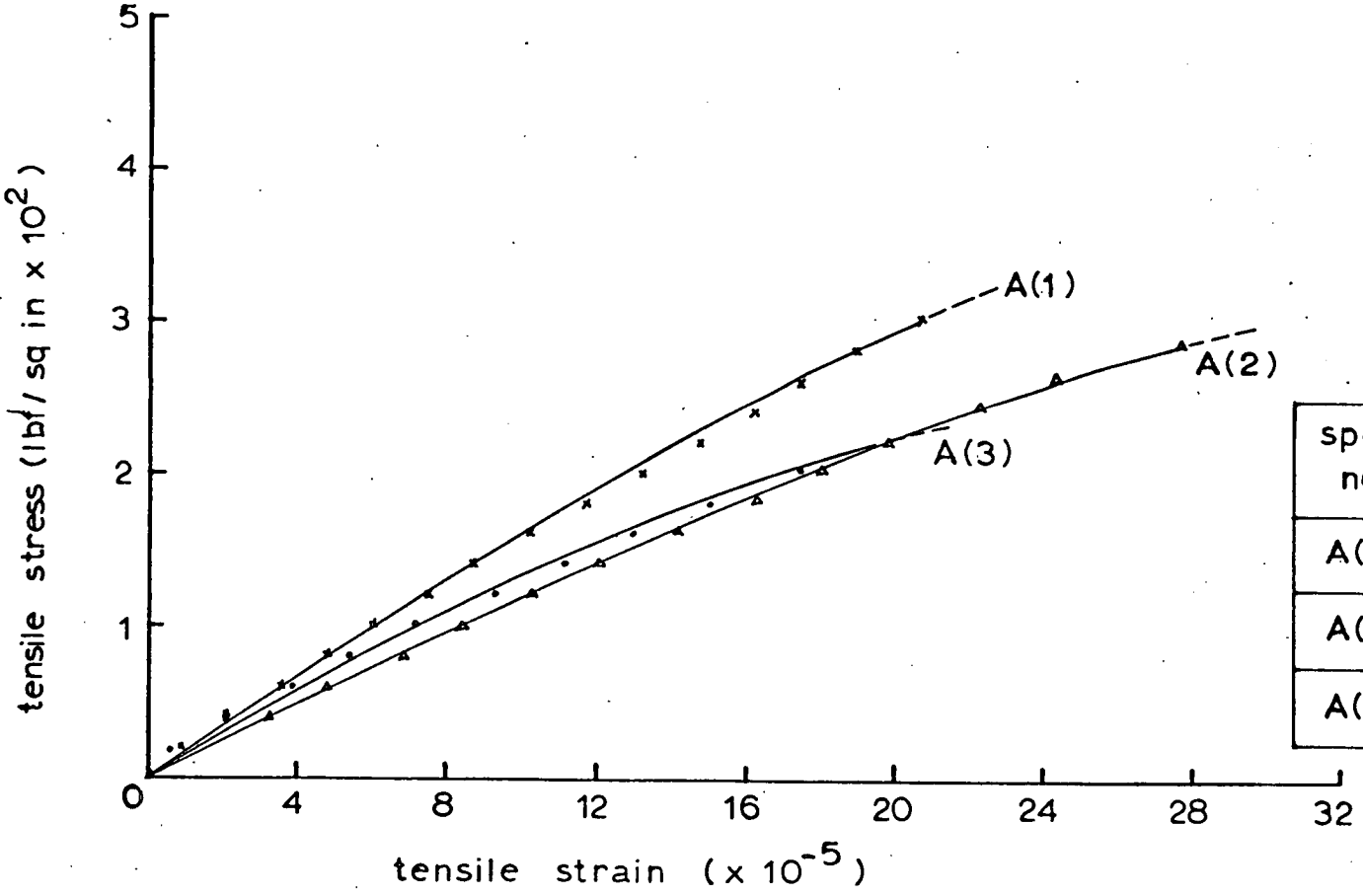

spec no.	tensile strength	elastic modulus x 10^6
A(1)	323	1·54
A(2)	301	1·12
A(3)	237	1·28

Fig 3.9 STRESS-STRAIN CURVE IN TENSION FOR B.S. 3224 psi BRICK

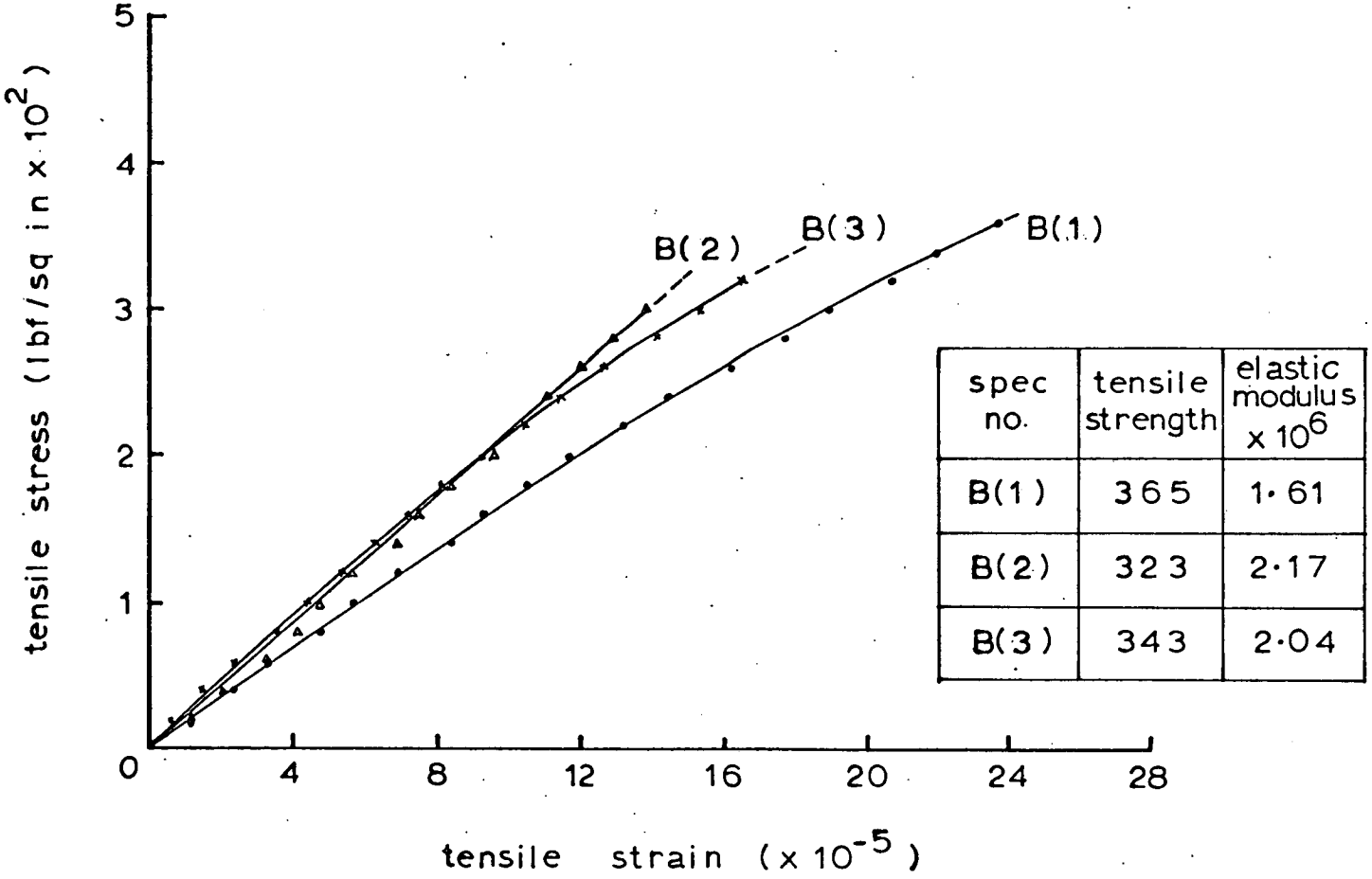

spec no.	tensile strength	elastic modulus x 10^6
B(1)	365	1·61
B(2)	323	2·17
B(3)	343	2·04

Fig 3.10 STRESS - STRAIN CURVE IN TENSION FOR B.S. 4549 psi BRICK

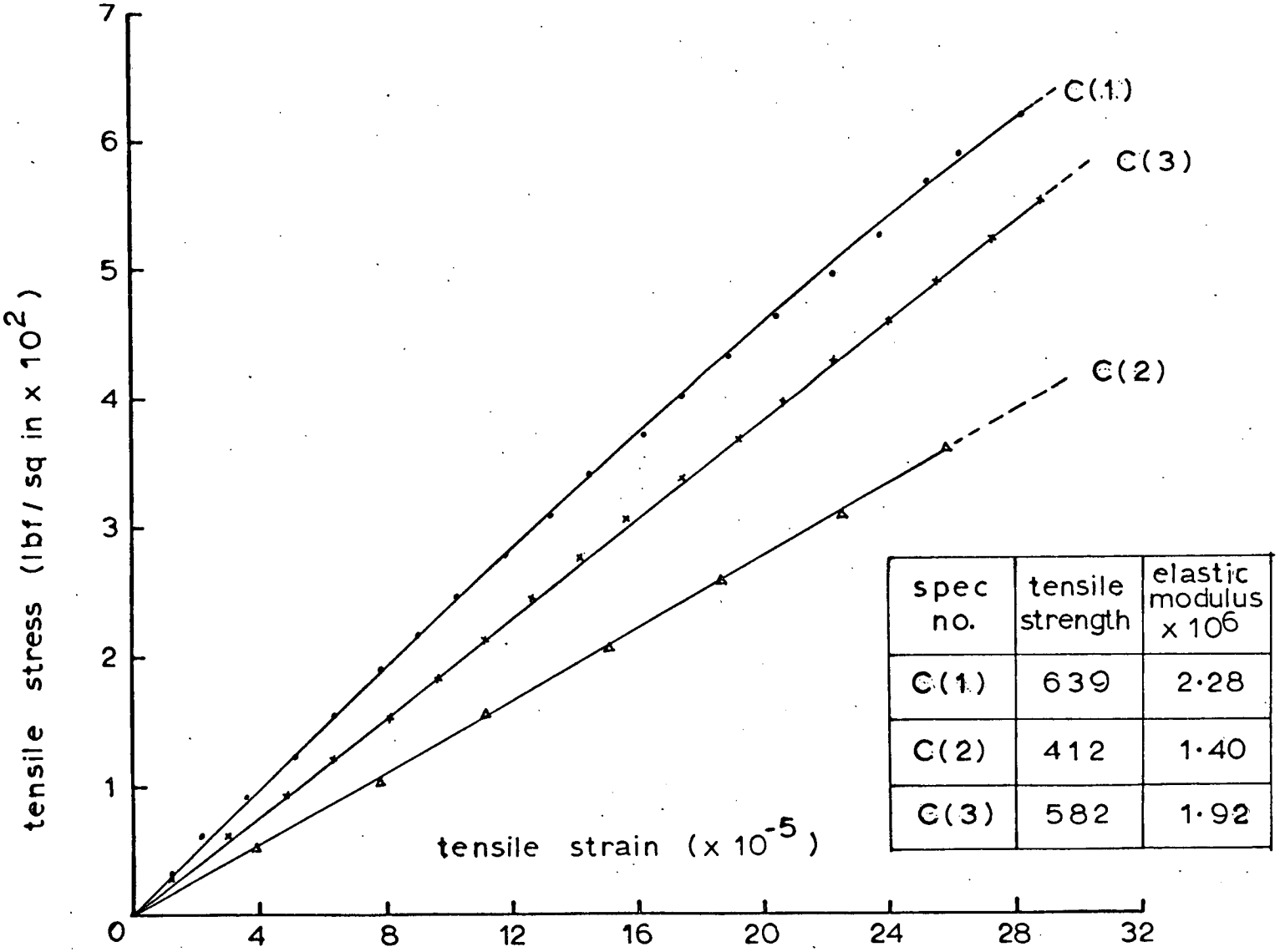

spec no.	tensile strength	elastic modulus x 10^6
C(1)	639	2·28
C(2)	412	1·40
C(3)	582	1·92

Fig 3.11 STRESS – STRAIN CURVE IN TENSION FOR B.S. 9336 psi BRICK

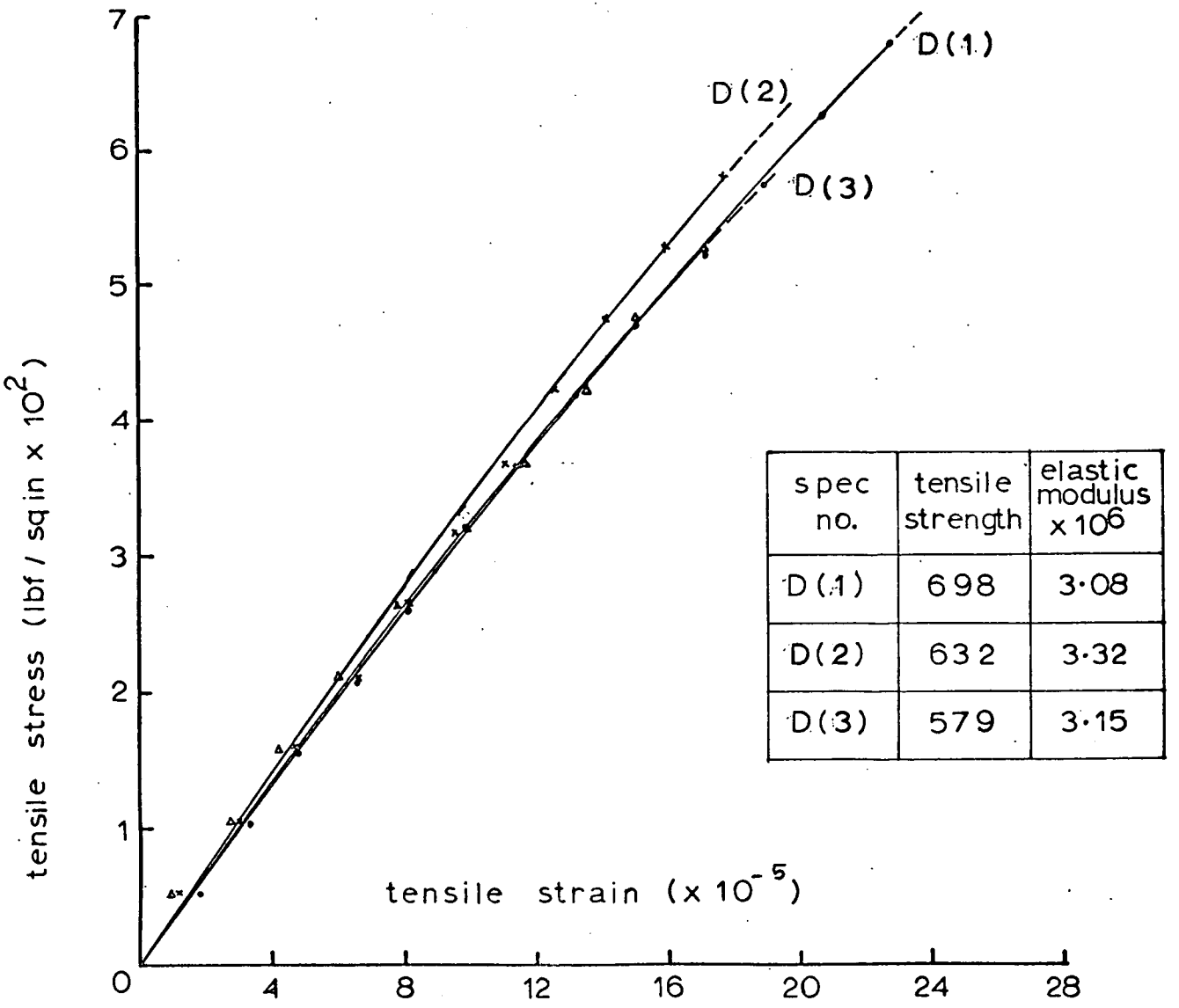

spec no.	tensile strength	elastic modulus x 10^6
D(1)	698	3·08
D(2)	632	3·32
D(3)	579	3·15

Fig 3.12 STRESS - STRAIN CURVE IN TENSION FOR B.S. 13448 psi BRICK

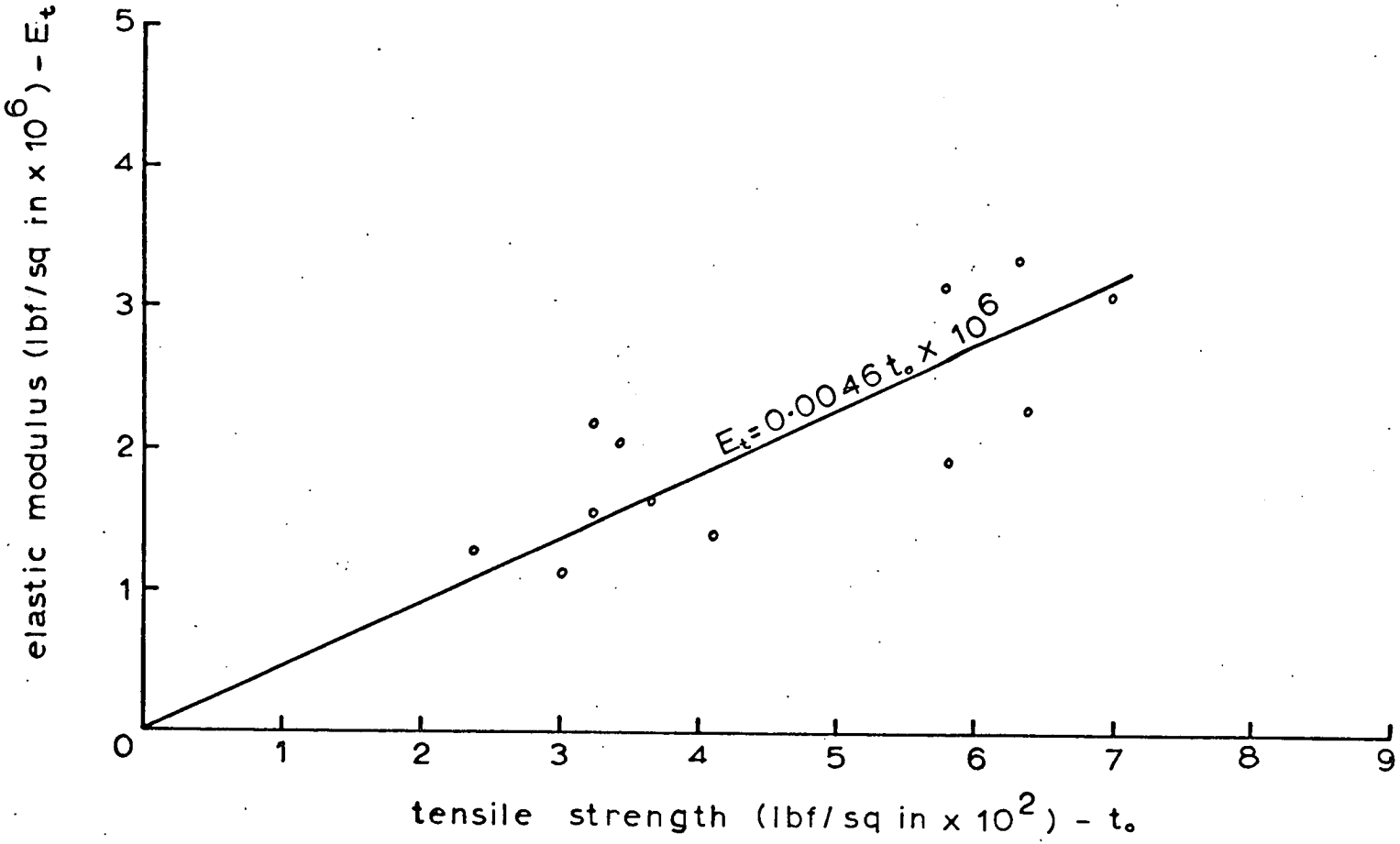

Fig 3.13 ELASTIC MODULUS - TENSILE STRENGTH RELATIONSHIP

introduce a "nonuniformity coefficient" to account for the observed stress variation in brick, must therefore be received with caution.

3.4 PORE WATER PRESSURE IN SOAKED BRICKS

It was observed in the earlier sections that there existed a significant strength difference between the dry and the soaked specimen. This was attributed to the presence of a pore water pressure in the soaked brick. The experimental data for the dry and the soaked specimens for the various strength tests are set out in Table 3.11 for easy reference.

In the compression tests, the BS crushing and the uniaxial compression, the strength values of soaked bricks were lower than those of dry bricks. However, the reverse was true for the tensile strength of bricks where the soaked strengths were higher then the dry strengths.

Whether the pore water pressure in a soaked specimen under load is positive (i.e. compressed), thus resulting in a reduced strength of brick as in the compression tests, or is negative (i.e. in suction) leading to an increased strength of brick as in the tensile test, depends upon the resulting volume of voids in a brick specimen under load. In a compression test where the effect is to reduce the volume of voids in the specimen, the pore water pressure in the soaked specimen is positive. Conversely, the increase in the volume of voids in a tensile test leads to a negative pore water pressure in a soaked specimen.

Further examination of Table 3.11 shows that in the compression tests, the influence of pore water pressure decreases with increasing brick strength. The reverse is the case for the tensile test where the influence of pore water pressure increases with higher brick strength.

TABLE 3.11 - EFFECT OF PORE WATER PRESSURE ON BRICK STRENGTH

B.S. CRUSHING STRENGTH

Brick type	K	L	M	N
Soaked (lbf/in^2)	2944	9135	10620	15448
Dry (lbf/in^2)	4498	10706	12389	16407
Pore water pressure (%)	34.5	14.7	14.3	5.8

UNIAXIAL COMPRESSION STRENGTH

Brick type	K	L	M	N
Soaked (lbf/in^2)	2974	7465	7299	12265
Dry (lbf/in^2)	4576	8954	9109	13132
Pore water pressure (%)	35.0	16.6	19.9	6.6

TENSILE STRENGTH (DIRECT BRIQUET)

Brick type	B	C	D
Soaked (lbf/in^2)	287	577	877
Dry (lbf/in^2)	273	489	686
Pore water pressure (%)	5.1	18.0	27.8

$1\ lbf/in^2 = 6.8948 \times 10^{-3} MN/m^2$

The reason for this trend of behaviour is not apparent. Perhaps further investigation need be carried out in this area before an explanation is forthcoming.

In addition to the water absorption property of brick, the influence of pore water pressure on the strength of brick depends on the rate of loading of the test specimen, as the rate of loading determines the extent of pore water pressure dissipation in the soaked brick.

Earlier investigators gave little or no consideration to the influence of pore water pressure on brick strength, although it had been reported that a soaked brick could cause a drop in compression strength. Recently, in experiments on the tensile strength of brick, Thomas & O'Leary[54] observed an increase in tensile strength of wet bricks.

3.5 BIAXIAL COMPRESSION-TENSION STRENGTH

In the biaxial compression-tension strength test, in addition to being pulled apart horizontally on the Hounsfield tensometer, the briquet specimen was compressed in a vertical direction on a 1 in. square (2.54 cm) polished brick surface through a pair of steel platens, see Fig. 3.14. The vertical compression was exerted by a 6-ton (59.78 kN) hand-operated jack reacting against a self-straining steel frame.

In order to minimize the friction between the compression-loading platen and the specimen surface, the steel platens were mirror-finished and MGA pads were used in all tests.

An earlier attempt to use a pair of brick plates in place of the steel platens, in the hope of eliminating the differential lateral strain between the loading platens and the test specimen, was unsuccessful/

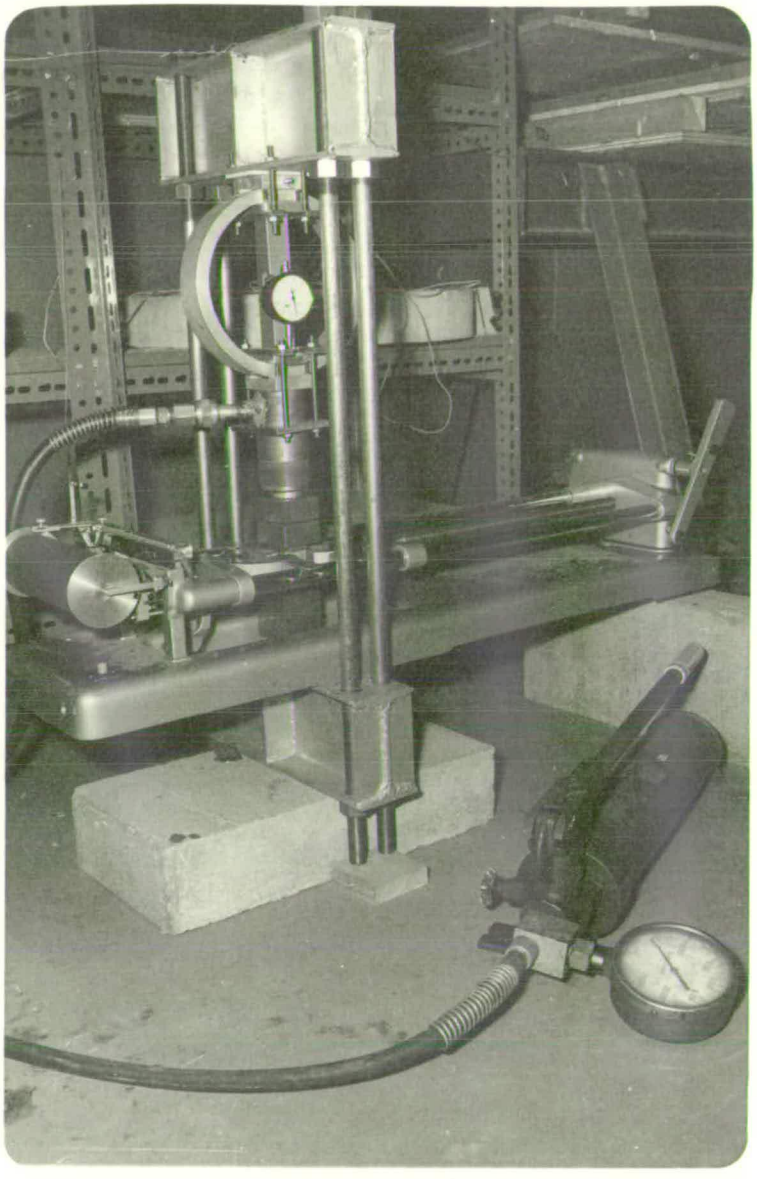

Fig 3.14 DEVICE FOR BIAXIAL COMPRESSION-TENSION TEST

successful as it was difficult to achieve a uniform distribution of the compressive load.

On account of the presence of friction between the loading platen and the test specimen, it was preferable to apply the tensile stress first, followed by the compression to failure. In most specimens, during the application of the compression load, the tensile reading changed slightly. However, no attempt was made to adjust the tensile load to its original value during the compression loading to failure.

Bricks of three strength levels, viz. BS crushing strengths 4549, 9338 and 13448 lbf/in^2 (31.36, 64.38 and 92.72 MN/m^2) were selected for the biaxial compression-tension tests, and all specimens were tested in a dry condition. For each brick strength, the specimens were tested under varying combinations of compression-tension stresses. The test results are set out in Tables 3.12A to 3.12C, and plotted in Fig. 3.15, and are presented in a dimensionless form in Fig. 3.16. Each point on the graph is an average of at least six specimens.

In nearly all specimens, failure occurred across a plane at the edge of the compression loaded area, suggesting that the influence of the platen restraint was not altogether eliminated. Under pure compression, some specimens of the high strength bricks fractured along the edge of the compression loaded area at a load slightly below their ultimate crushing. For the purpose of determining the compression-tension failure envelope, it was more appropriate to register these loads for uniaxial compression, since failure under compression-tension combinations occurred also along the edge of the compression loaded area.

Most of/

TABLE 3.12A - BIAXIAL COMPRESSION-TENSION STRENGTH TESTS ON 1/3 SCALE MODEL BRICKS (B.S. CRUSHING STRENGTH 4549 lbf/in^2)

Compressive Stress (lbf/in^2)	Tensile Stress (lbf/in^2)	Compressive Stress (lbf/in^2)	Tensile Stress (lbf/in^2)	Compressive Stress (lbf/in^2)	Tensile Stress (lbf/in^2)
0	344	167 *	184	668	219
0	354	167	242	590	224
0	303	167	237	169	222
0	184	165	185	126	222
0	210	169	302	802	207
0	376	164	198	596	219
0	253				
0	253	167	224	492	219
0	245				
0	250	* compression applied			
0	227	first			
ave 0	273				
1002	201	919	153	1351	88
935	201	917	149	2191	90
827	201	543	153	2004	97
944	197	1157	150	1687	96
1075	195	971	153	1670	101
777	197	767	158	1837	91
926	199	879	153	1790	94
3100	47	3720	15	5229	0
2456	50	2756	21	6179	0
1599	62	4134	18	4131	0
1704	63	2480	17	3006	0
1363	63	3111	15	3810	0
1670	61	3846	18	4960	0
2324	66			4259	0
2884	58	3341	17	2922	0
				3766	0
2138	59			4251	0

1lbf/in^2 = 6.8948 x 10^{-3}MN/m^2

TABLE 3.12B - BIAXIAL COMPRESSION-TENSION STRENGTH TESTS ON 1/3 SCALE MODEL BRICKS (B.S. CRUSHING STRENGTH 9336 lbf/in^2)

Compressive Stress (lbf/in^2)	Tensile Stress (lbf/in^2)	Compressive Stress (lbf/in^2)	Tensile Stress (lbf/in^2)	Compressive Stress (lbf/in^2)	Tensile Stress (lbf/in^2)
0	515	1064	420	1606	265
0	459	409	420	1135	285
0	410	414	418	1702	265
0	515	752	423	1555	285
0	443	334	428	1670	270
0	474	334	428	2292	270
0	443	—	—	—	—
0	639	551	423	1660	273
0	412	—	—	—	—
0	582				
—	—				
ave 0	489				
—	—				
2918	208	3018	153	3356	98
2742	205	2392	149	3766	92
2863	186	2716	145	2386	91
3183	173	3029	140	3029	98
2027	220	3405	129	2865	91
2513	205	3234	135	3183	97
—	—	—	—	2839	98
2708	200	2966	142	3173	101
—	—	—	—	—	—
				3075	96
				—	—
3507	52	4509	15	5837	0
5344	36	5787	15	6485	0
4634	41	5398	12	6161	0
5126	44	5678	14	6242	0
3720	46	4994	16	6263	0
3340	51	5837	13	5620	0
—	—	—	—	—	—
4279	45	5367	14	6101	0
—	—	—	—	—	—

TABLE 3.12C - BIAXIAL COMPRESSION-TENSION STRENGTH TESTS ON 1/3 SCALE MODEL BRICKS (B.S. CRUSHING STRENGTH 13448 lbf/in^2)

	Compressive Stress (lbf/in^2)	Tensile Stress (lbf/in^2)	Compressive Stress (lbf/in^2)	Tensile Stress (lbf/in^2)	Compressive Stress (lbf/in^2)	Tensile Stress (lbf/in^2)
	0	660	2024	463	2213	359
	0	646	1336	490	2338	344
	0	698	1503	500	2646	345
	0	579	1514	470	2171	344
	0	632	1760	490	2235	347
	0	716	827	505	2756	354
	0	531				
	0	802	1494	486	2393	349
	0	813				
	0	781				
ave	0	686				
	3173	266	3799	191	6597	88
	3340	266	3968	165	4634	86
	3591	255	4601	159	6161	76
	3431	253	4639	147	5094	83
	2881	271	4340	191	4499	83
	3438	260	4892	179	6179	86
	3309	262	4373	172	5527	84
	5511	31	8267	0		
	8186	31	6263	0		
	4864	35	7682	0		
	7682	34	9102	0		
	7181	37	6764	0		
	4676	35	7441	0		
	6350	34	7564	0		

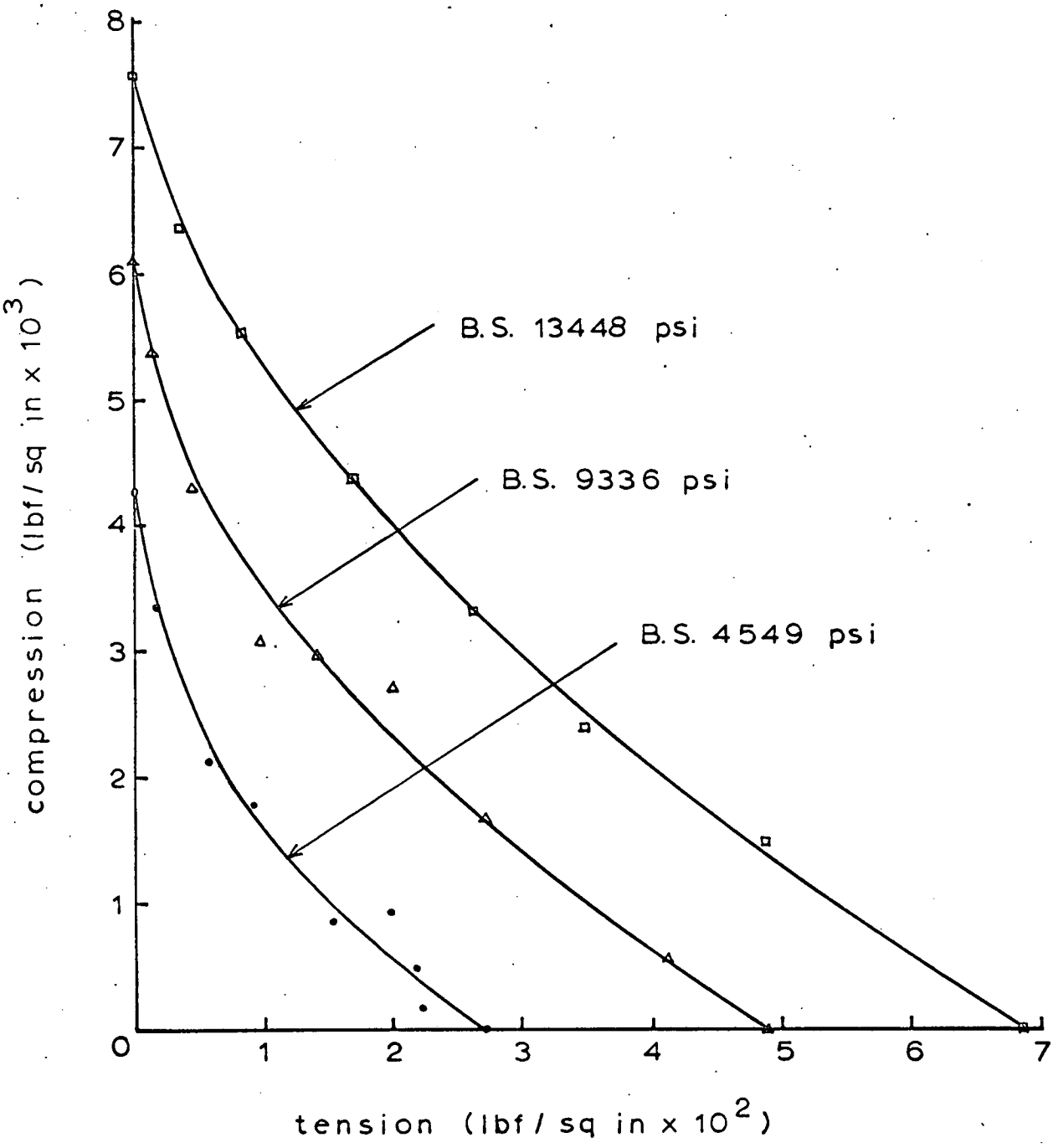

Fig 3.15 BIAXIAL COMPRESSION - TENSION FAILURE ENVELOPE FOR 1/3 SCALE MODEL BRICKS

Coulomb : $c/c_o + t/t_o = 1$
(original)

Griffith : (a) for $(c - 3t) < 0$

$$t = t_o$$

(b) for $(c - 3t) > 0$

$$(t + c)^2 + 8t_o(t - c) = 0$$

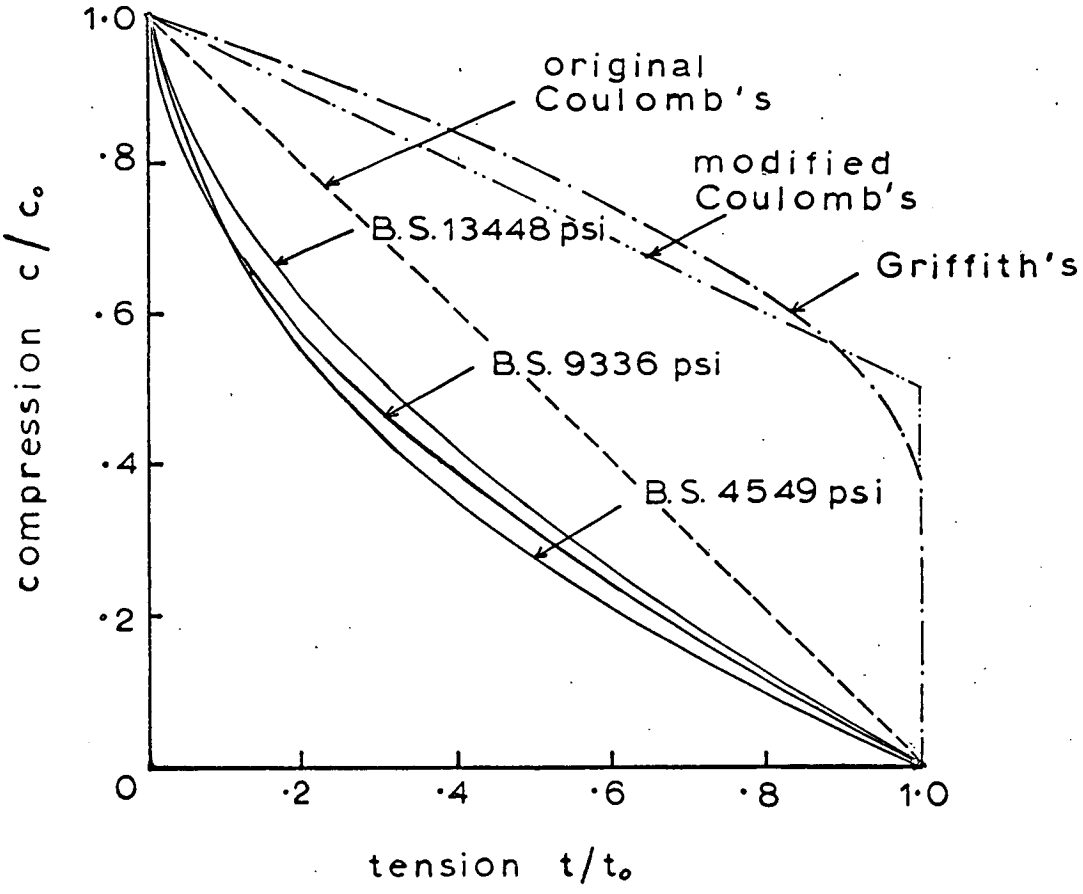

Fig 3.16 BIAXIAL COMPRESSION - TENSION FAILURE ENVELOPE FOR BRICK - DIMENSIONLESS PLOT

Most of the failure planes under biaxial compression-tension were single cleavage fractures except for specimens tested very near the uniaxial compression where sometimes the fracture planes were multi-cleavage.

The theoretical curves of Coulomb and Griffith are shown in Fig. 3.16. The failure envelopes for brick obtained experimentally are concave, and indicate a more significant effect of the interaction of compression-tension than those presented by the theoretical curves. The biaxial compression-tension failure envelope may be represented by the equation:

$$\left(\frac{c}{c_o}\right) = 1 - \left(\frac{t}{t_o}\right)^{0.5456} \qquad \text{.....(3.2)}$$

where

c = compressive stress in brick

c_o = uniaxial compression strength of brick

t = tensile stress in brick

t_o = tensile strength of brick.

3.6 SUMMARY

1. A significant strength difference exists between bricks tested soaked and those tested dry, and this is attributed to the presence of a pore water pressure in the soaked brick under load.
2. In the compression tests, the soaked strength of brick is less than its dry strength, but the reverse is the case for specimens tested in tension where the soaked strength is greater than the dry strength. A compressed specimen creates a positive pore water pressure which leads to a reduction in compression strength, while a negative pore water pressure exists in a specimen under tensile load, causing an increase in tensile strength.

3. The compression strength of brick tested on end using MGA pads as a capping material may be taken to represent the uniaxial compression strength of the brick.

4. The effect of the 1/8 in (3.18 mm) plywood as a capping material for the one-third scale model bricks in the BS crushing test is to increase significantly its crushing strength for the high strength brick, although the effect is not apparent for the low strength brick.

5. Results from the indirect Brazilian splitting tests where the knife-edge loads were applied along the length of the brick specimen, compare favourably with those obtained from the direct briquet test.

6. The relationship between the dry tensile strength and the dry uniaxial compression strength indicates that the tensile to compression strength ratio is not constant but varies from 1/16 for low strength bricks to 1/12 for high strength bricks.

7. The ultimate tensile strain is apparently unrelated to the tensile strength of brick. The ultimate strain ranges from 150 to 300 micro-units.

8. The elastic modulus (E_t) of brick in tension is approximately given by the expression:

$$E_t = 0.0046 t_o \times 10^6 \qquad \text{.....(3.1)}$$

where

t_o is the tensile strength.

9. The failure envelope for brick in biaxial compression-tension is concave. This means that the interaction between compression and tension stresses is more significant than those given by the Coulomb's or Griffith's curves.

The failure envelope is defined by the equation:

$$\left(\frac{c}{c_o}\right) = 1 - \left(\frac{t}{t_o}\right)^{0.5456} \qquad \text{.....(3.2)}$$

where

c = compressive stress in brick

c_o = uniaxial compression strength of brick

t = tensile stress in brick

t_o = tensile strength of brick.

CHAPTER 4 - BIAXIAL COMPRESSION-TENSION STRENGTH TESTS ON CLAY PIPES

4.1 INTRODUCTION

In Chapter 3, an attempt to define the failure envelope for brick under biaxial compression-tension was carried out using the method of direct tension and compression on one-third scale model bricks. The failure envelope obtained was significantly different from those predicted by the various theories. In consequence, it was considered necessary to determine the compression-tension strength relationship by an alternative method of testing.

This chapter describes compression-tension strength tests on clay pipes which were subjected to an internal pressure, thereby creating a circumferential (or hoop) tension in the wall of the pipe, and in addition, an axial compression was applied to the pipe in the direction of its length.

There are two main advantages in this method of testing over the method using direct tension and compression. The first is that the influence of the load platen on the stress field in the test specimen is of no importance provided a pipe of sufficient length to diameter ratio is selected. The other is that, in this arrangement, it is possible to mount resistance gauges on the clay pipe for strain measurement.

However, this method suffers the disadvantage that the stress field created in the pipe is, in fact, three dimensional, with a radial compression of the value of the internal pressure acting on the inside face of the pipe wall reducing to zero on the external face. Secondly, because the clay pipes used were not thin-walled, the circumferential/

circumferential tension in the pipe was not uniform but varied along its thickness. However, it may be seen later in Section 4.3 that this radial compression is small in value and its influence on the biaxial compression-tension strength of the clay pipes is not significant.

4.2 MATERIAL AND TEST APPARATUS

An attempt to obtain purpose-made pipes of brick material for these tests was unsuccessful, and consequently, commercially available unglazed clay pipes were used. These pipes were manufactured in accordance with BS 65 & 540[9], and were of very high strength.

The nominal dimensions of the pipes were 6 ins internal diameter x 12 ins length x $\frac{3}{4}$ ins wall thickness (15.24 cm x 30.48 cm x 1.90 cm). The actual dimensions are 5.87 ins internal diameter x $11\frac{1}{2}$ ins length x 0.70 ins wall thickness.

Preliminary tests indicated that a fair proportion of the pipes delivered were faulty. The "hammer test" was applied to sort out the pipes. Only those which registered a clear ring sound when struck with a hammer were selected for the tests, and these were assumed to be in good condition. On some of the rejected pipes, hairline cracks could be seen running usually along the length of the pipes.

The selected pipes, about 60 in number, were sent to a masonry works to have the uneven ends trimmed off in order to attain plane ends with a satisfactory degree of parallelism.

The internal pressure in the pipe was exerted hydraulically by means of a rubber bag, as shown in Fig. 4.1. The rubber bag was designed with two inward-turned teats which fitted on to two brass nipples attached to/

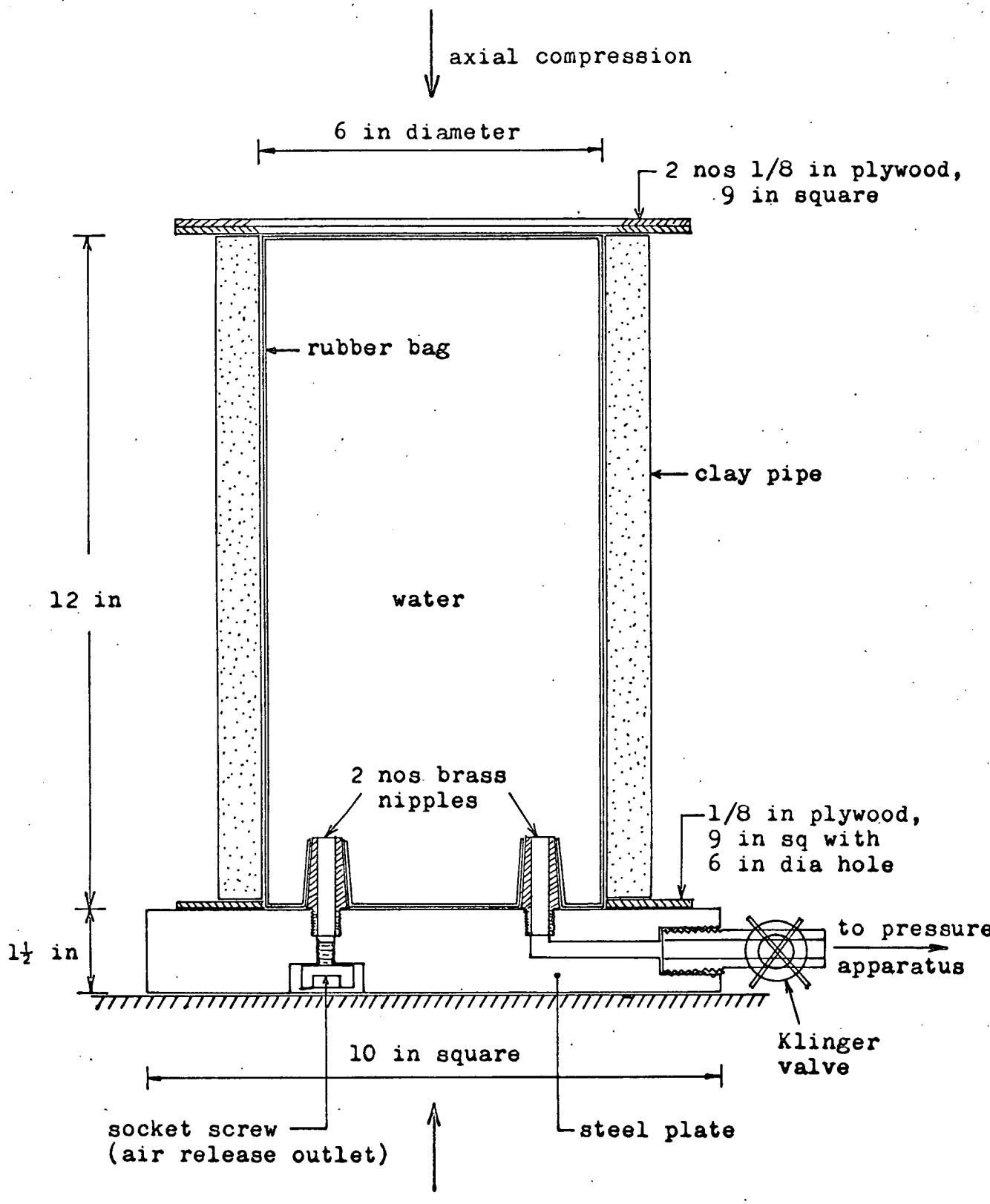

Fig 4.1 Apparatus for Clay Pipe Test

attached to a steel base plate. This type of connection where the brass nipples intruded into the rubber bag allowed the internal water pressure to act upon the nipples, and thus successfully prevented any leakage of fluid at this point.

One of the two outlets was connected to a pressure apparatus, seen on the left in Fig. 4.2. Details of this pressure apparatus are given in Section 5.3 in the next chapter. The other outlet was used initially to de-air the rubber bag and subsequently sealed off. A completely de-aired rubber bag, not only ensures greater sensitivity of pressure readings to volume changes, but also minimises the chances of bursting the rubber bag when failure occurs in the pipe since a slight increase in volume causes a rapid drop in pressure.

In order to ensure a more uniform axial compression, 1/8 in (3.18 mm) thick plywood pieces were inserted at the top and bottom ends of the clay pipe under test. The bottom plywood had a 6 ins diameter hole to accommodate the rubber bag. Axial loading was carried out in a 250-ton (2491 kN) Denison compression machine equipped with a spherical seating at the top loading platen, see Fig. 4.2.

On five of these pipes, resistance wire polyester gauges, 500 ohms, were mounted in both axial and lateral directions, on opposite external faces of each pipe. These were tested under different combinations of compression-tension stresses.

4.3 STRESS DISTRIBUTION IN PIPE UNDER INTERNAL PRESSURE

In an elastic analysis, the stress distribution in the wall of a thick cylinder pipe subjected to an internal pressure is given by Timoshenko & Goodier[56] as:-

$$\sigma_r = \frac{a^2 p}{b^2 - a^2}\left[1 - \frac{b^2}{r^2}\right] = k_r p \qquad \text{.....(4.1)}$$

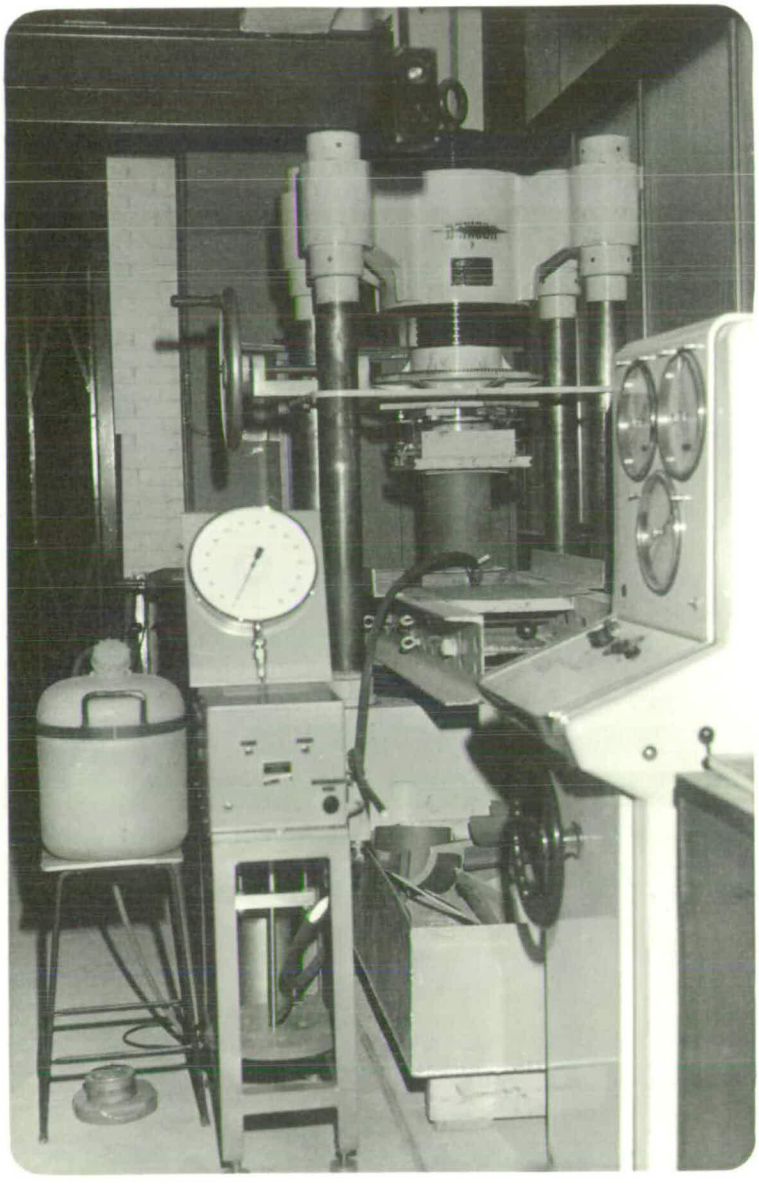

Fig 4.2 APPARATUS FOR BIAXIAL COMPRESSION-TENSION TEST ON CLAY PIPES

$$\sigma_\theta = \frac{a^2 p}{b^2 - a^2}\left[1 + \frac{b^2}{r^2}\right] = k_\theta\, p \qquad \text{.....(4.2)}$$

where

σ_r = radial stress in pipe

σ_θ = circumferential stress in pipe

p = internal pressure

a = internal radius of pipe

b = external radius of pipe

r = radius at any point in pipe

For the dimensions of the pipe used in these tests, the stress distribution in the pipe is illustrated in Fig. 4.3. The maximum circumferential tension occurs at the inner face of the pipe and is 4.746 times the internal pressure. This circumferential tension reduces to 3.746 times the internal pressure at the outer face. Stress-strain curves show the pipes to be very brittle, and therefore it may be assumed that failure is initiated at the inner face of the pipe when the circumferential tension reaches its tensile strength.

In addition to the presence of a circumferential tension in the pipe, there exists a radial compression which varies from a maximum value equal to the internal pressure at the inner face of the pipe to zero value at the outer face. Therefore, in this test arrangement, the stresses generated in the pipe is not strictly biaxial compression-tension, but have an additional radial compression. However, for the given geometry of the pipe cross-section, the magnitude of the radial compressive stress is small in relation to the circumferential tension, and ought not to affect seriously the biaxial compression-tension failure envelope.

4.4/

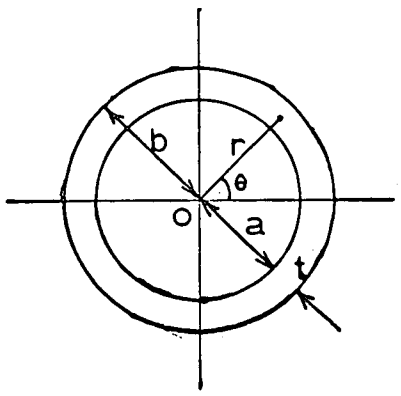

$$\sigma_r = \frac{a^2 p}{b^2 - a^2}\left(1 - \frac{b^2}{r^2}\right) = k_r p$$

$$\sigma_\theta = \frac{a^2 p}{b^2 - a^2}\left(1 + \frac{b^2}{r^2}\right) = k_\theta p$$

$a = 2.975$ in

$b = 3.675$ in

$t = 0.700$ in

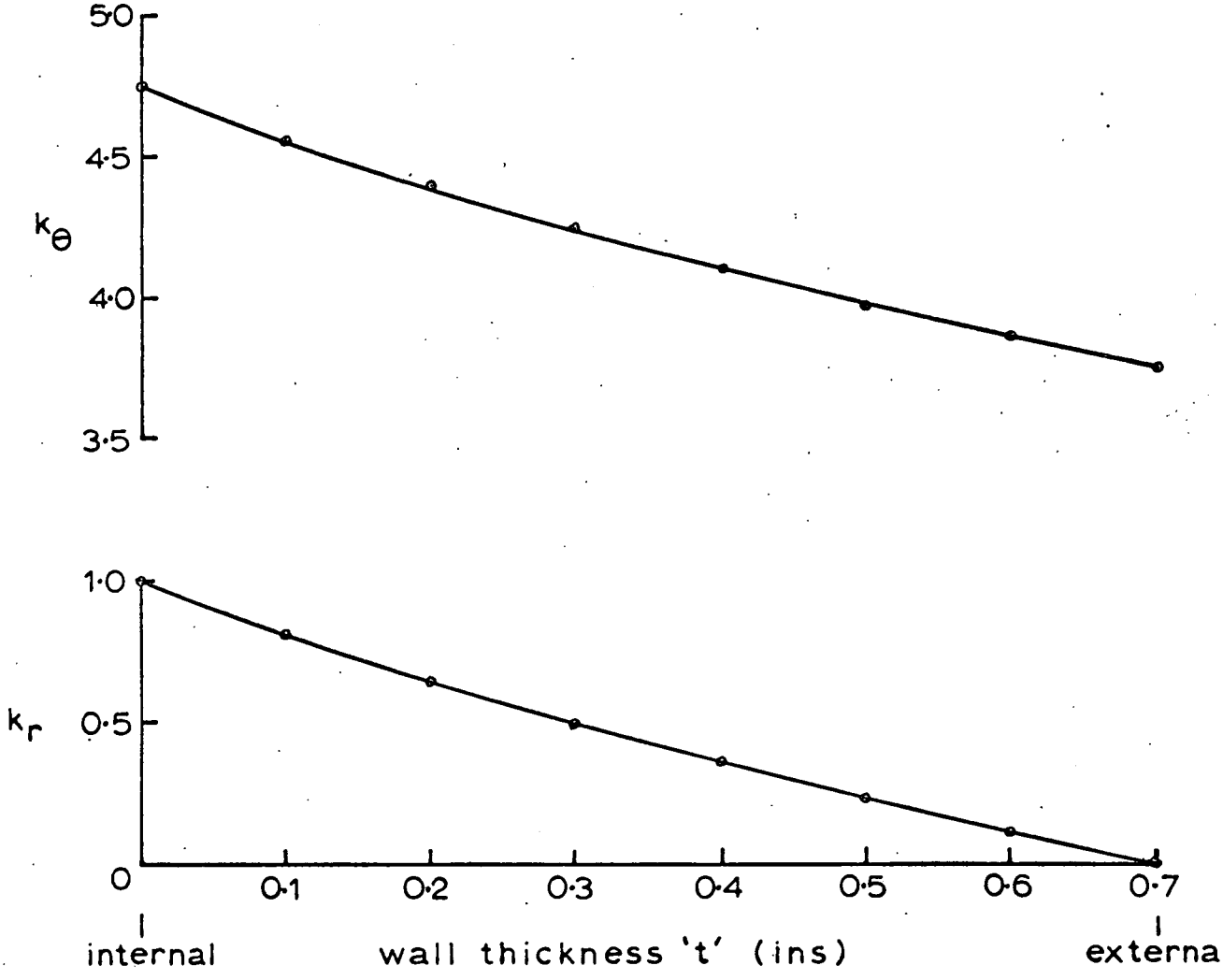

Fig 4.3 Stress Distribution in Pipe under Internal Pressure

4.4 BIAXIAL COMPRESSION-TENSION TESTS

It was found on loading specimens under pure compression that vertical cracking occurred in the pipe at a load considerably below its ultimate. The load at first cracking varied between 60 to 85% of the ultimate. This suggests either the axial load was not uniformly distributed in spite of the provision of the plywood packing, or perhaps, the strength property of the pipe was not homogenous throughout. The possibility of the plywood causing premature tensile splitting was unlikely, since the heavy indentation of the pipe into the plywood served as a lateral restraint on the pipe, and also because the vertical cracks appear wider at the mid-section of the pipe than at the ends.

At any rate, for the purpose of ascertaining the compression-tension failure envelope, it is appropriate to use the values of the compressive stress at first cracking, since failure under compression-tension combinations is also determined through vertical cracking in the test pipe.

At ultimate load, the clay pipe failed explosively into small fragments.

In the biaxial test, axial compression was first applied to the specimen, followed by the application of internal pressure to failure, except for the graph point nearest the pure compression in Fig. 4.6. It was undssirable to apply the circumferential tension first because subsequent application of the axial loading caused a rapid increase in internal pressure which was consequently difficult to maintain at a particular level. For the graph point nearest the pure compression, in order to avoid the possibility of a premature explosive failure in axial compression, which could injure the rubber bag, the required internal pressure/

internal pressure was first applied followed by axial compression to failure. In this way, failure through vertical cracking always occurred before complete fracture.

Under all combinations of compression-tension stresses, failure occurred through simple vertical cracking along the pipe length, as indicated typically in Fig. 4.4. However, in the case of pure tension, the crack formation might have different configuration such as that shown in Fig. 4.5.

Table 4.1 and Fig. 4.6 show the results of 51 pipes tested under various combinations of compression-tension stresses. Each point on the graph is an average of at least six specimens.

The results have also been plotted in a dimensionless form in Fig. 4.7 which includes, for comparison, the theoretical curves of Coulomb and Griffith, and the failure envelope obtained experimentally from tests on model bricks.

Strain measurements, recorded on a Westland data logger, a description of which may be found in Kalita's[31] thesis, were carried out on five specimens - one in pure compression, one in pure tension, and the remaining three under various combinations of compression-tension stresses. The stress-strain curves are presented in Fig. 4.8, and the failure stresses given in Table 4.2. In the biaxial tests, axial compression was applied first, followed by internal pressure to failure.

From Fig. 4.8, it appears that the ultimate lateral strain in the pipe is independent of the combination of compression-tension stresses, and ranges between 200 to 300 micro-units. The elastic modulus in tension and in compression is about the same and equals 7.5×10^6 lbf/in^2 (5.17×10^4 MN/m^2).

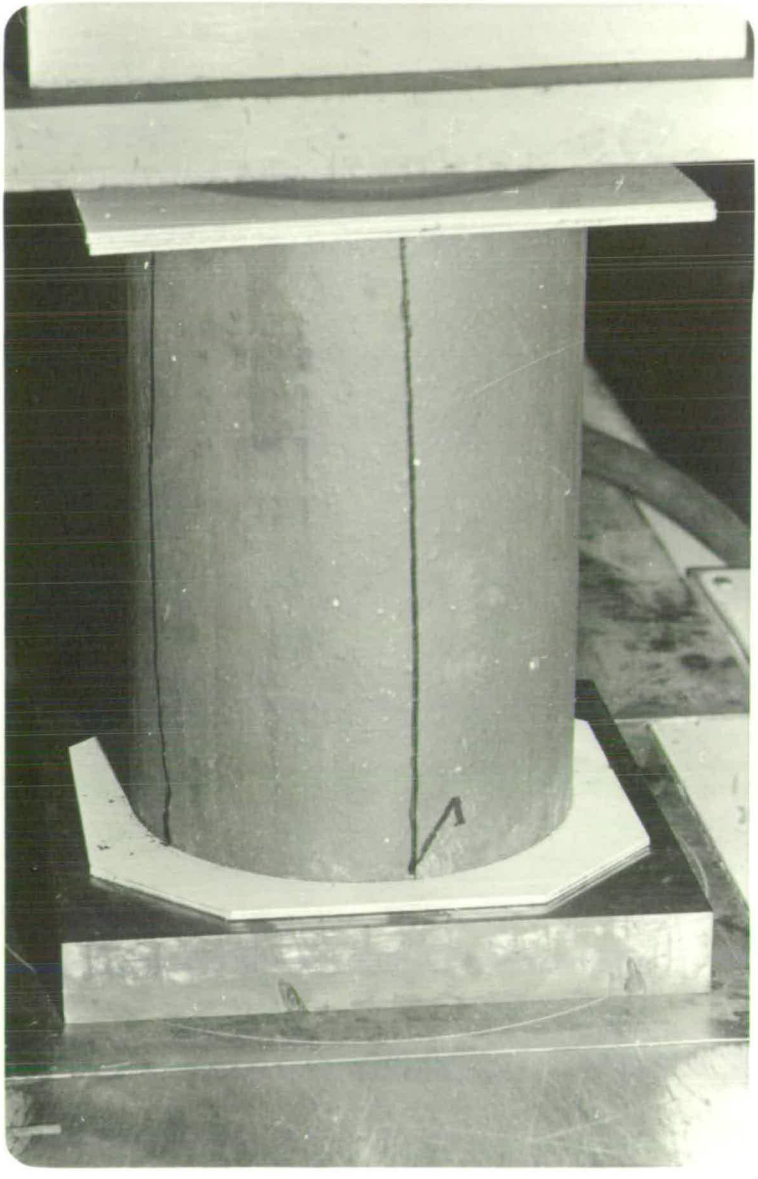

Fig 4.4 TYPICAL CRACK FORMATION IN CLAY PIPE UNDER BIAXIAL COMPRESSION-TENSION

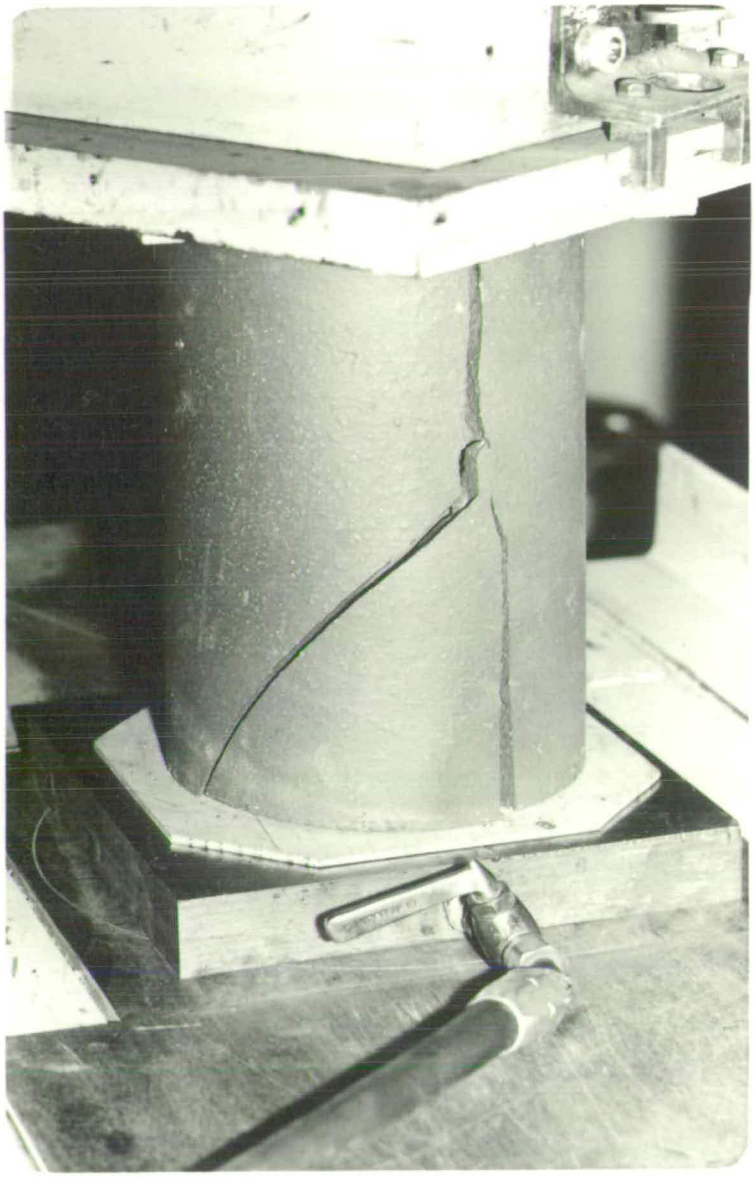

Fig 4.5 CRACK FORMATION IN CLAY PIPE UNDER PURE TENSION

TABLE 4.1 - BIAXIAL COMPRESSION-TENSION STRENGTH TESTS ON CLAY PIPES

Compressive Stress (lbf/in^2)	Tensile Stress (lbf/in^2)	Compressive Stress (lbf/in^2)	Tensile Stress (lbf/in^2)
0	1851	1724	1523
0	1946	1539	1993
0	1898	1691	1609
0	2088	1586	1875
0	1860	1633	1756
0	1566	1530	2017
0	1989		
0	1946	1617	1796
mean = 0	1893		
4108	1376	5857	873
3934	1818	6031	432
3893	1922	6018	465
4425	574	5816	978
4398	641	6020	460
4426	570	5928	693
4130	1319		
		5945	650
mean = 4188	1174		
9085	551	12182	560
9029	693	12343	152
9104	503	12175	579
8939	930	12293	280
8950	892	12173	584
9156	370	12265	351
mean= 9044	657	12238	418

		1st. crack		ultimate
23181	190*	11628	19225	0
4576	190	21705	28527	0
11553	190	13333	21395	0
20700	190	24806	34574	0
17755	190	21705	27907	0
16359	190	28217	32558	0
mean= 15687	190	20232	27364	0

* circumferential tension applied first

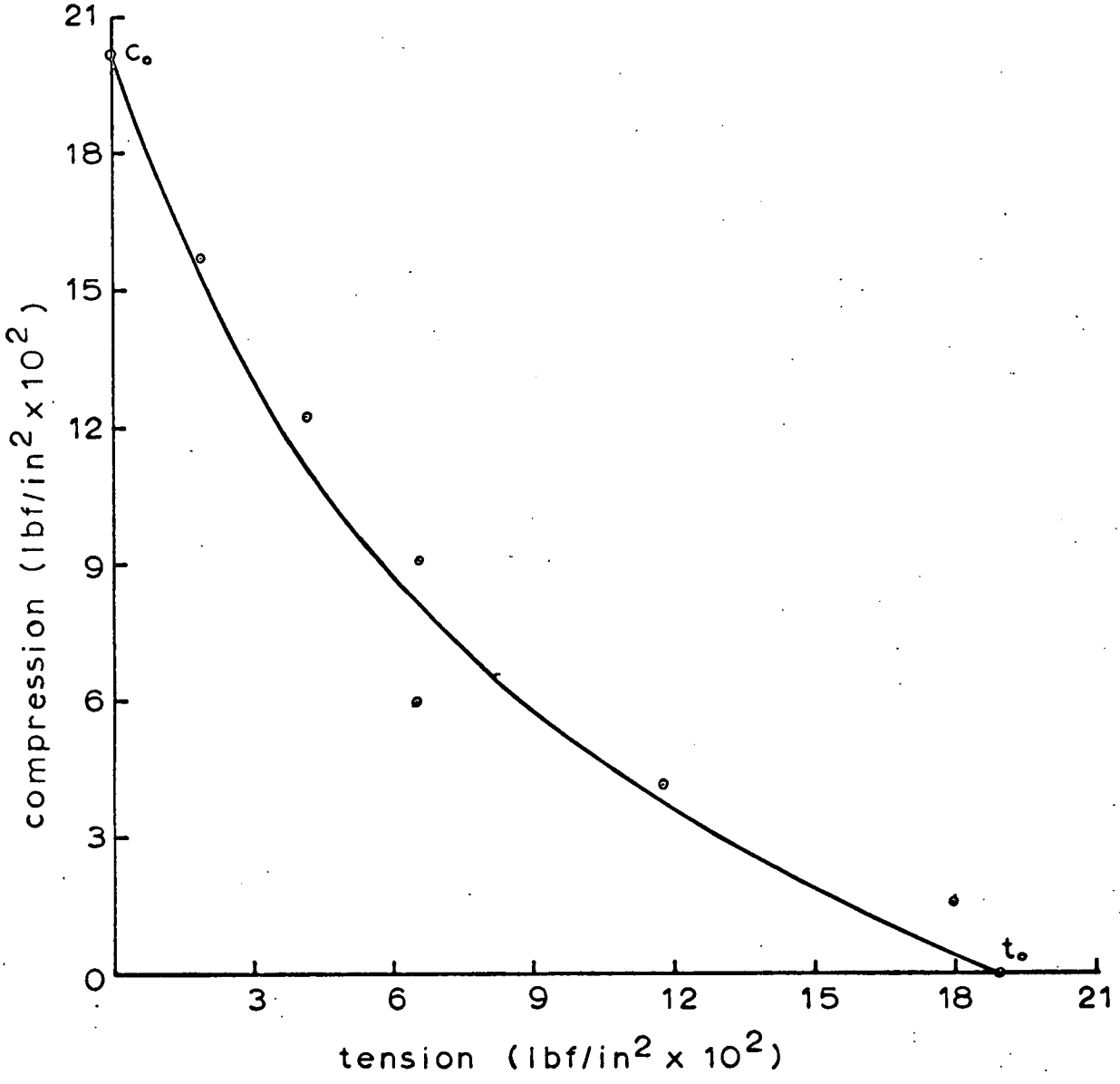

Fig 4.6 Biaxial Compression – Tension Failure Envelope for Clay Pipes

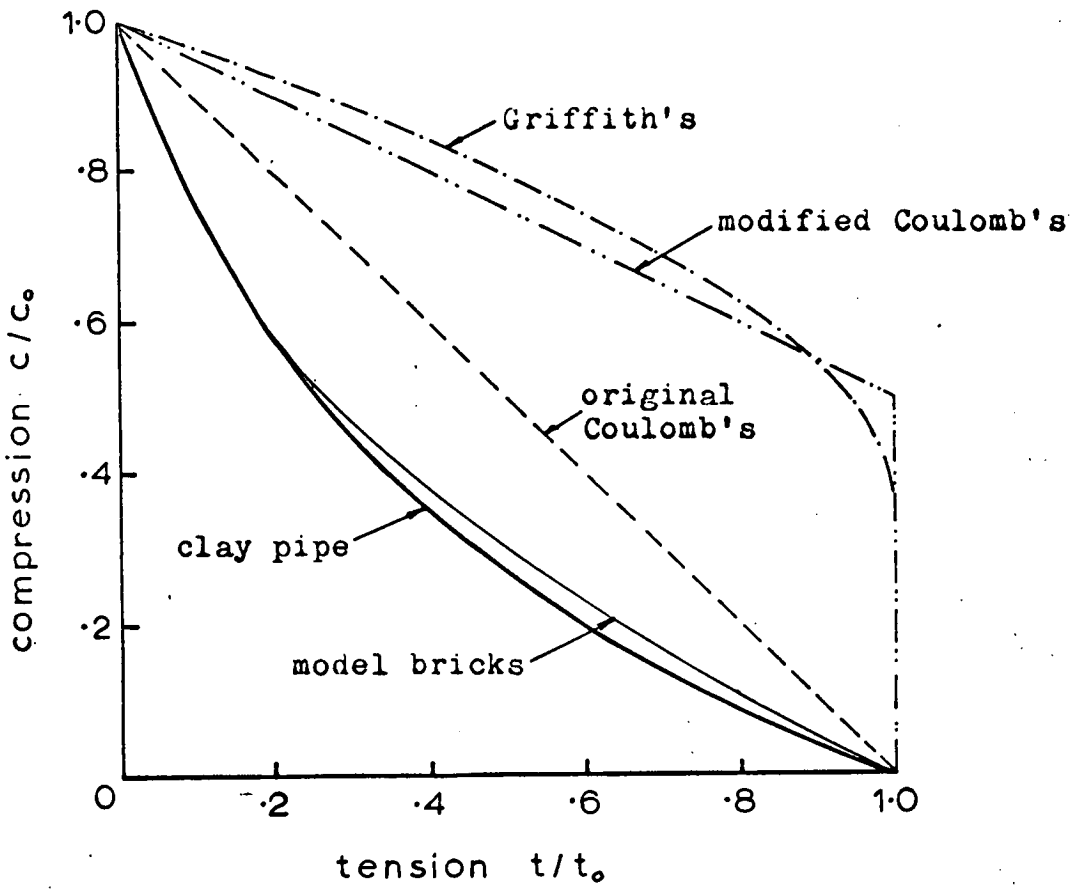

Fig 4.7 Biaxial Compression – Tension Failure Envelopes

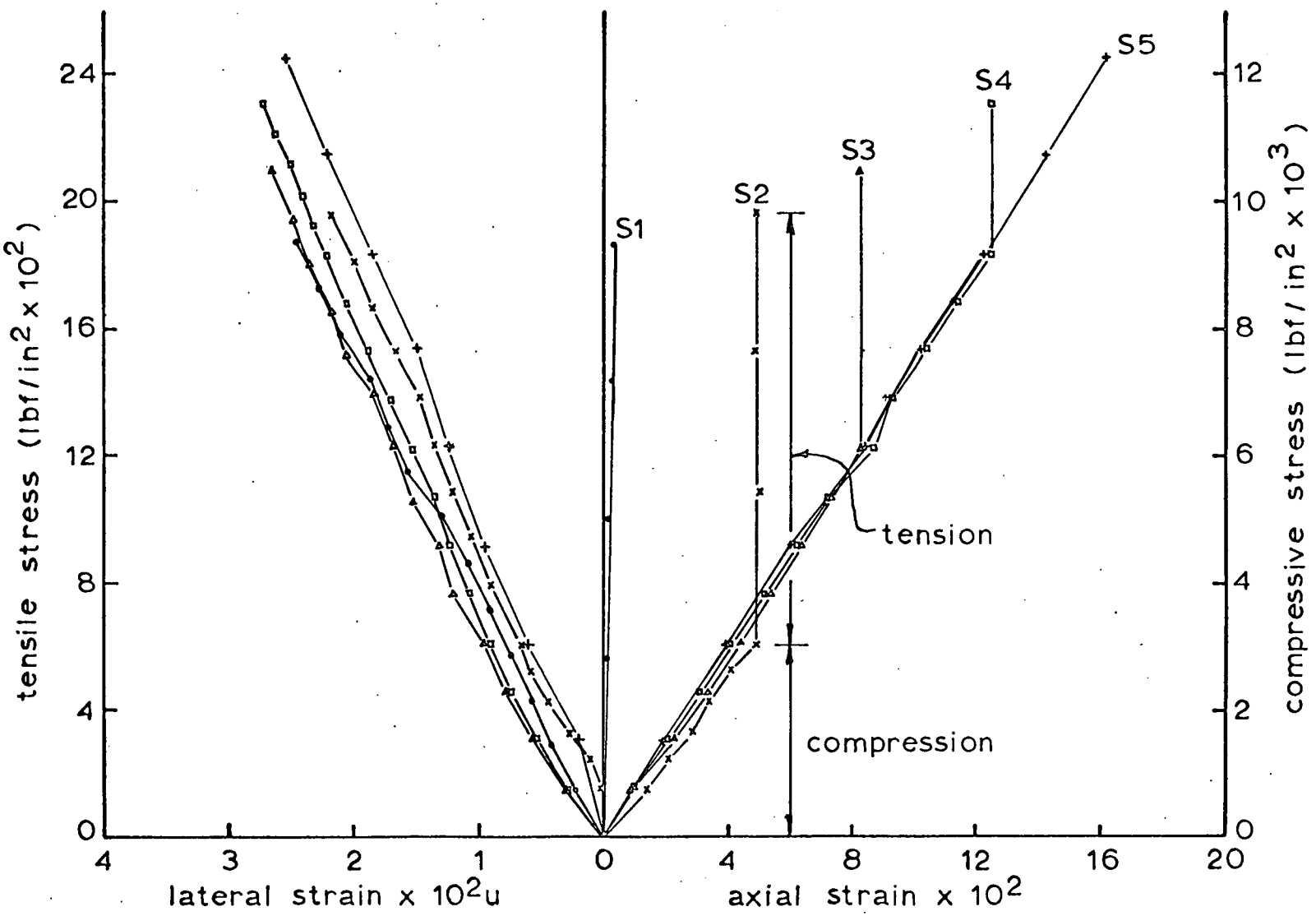

Fig 4.8 Stress – Strain Curves for Clay Pipes in Biaxial Compression – Tension.

TABLE 4.2 - BIAXIAL COMPRESSION-TENSION ON CLAY PIPES WITH STRAIN GAUGES

Specimen No.		Compressive Stress (lbf/in^2)	Tensile Stress (lbf/in^2)
S1		0	1921
S2		2780	1489
S3		5757	1009
S4		8976	538
S5	first crack	13171	0
	ultimate	19297	

4.5 DISCUSSION OF TEST RESULTS

Although the test results in Table 4.1 reflect a wide variation in the strength of the pipes, the general trend of the biaxial compression-tension failure envelope, seen in Fig. 4.6, is unmistakably concave. This means that the compression strength of the pipe is severely reduced by the presence of a perpendicular tensile stress, and vice versa.

It is evident that the experimental failure envelopes for brick and clay pipe, shown in Fig. 4.7, differ considerably from those predicted by the theories. An adequate explanation for this difference cannot be expected to emerge from simple tests, such as these, carried out at a phenomenological level. Nonetheless, an examination of the assumptions made in Griffith's theory and a comparison with the observed physical and strength properties of brick material may suggest some differences which can be reflected in the failure envelopes.

In his analysis, Griffith assumed the existence of very minute elliptic-shaped cracks of atomic magnitude. The flaws which are present in brick material are probably larger. Griffith's criterion is established from the behaviour of an isolated crack remote from the influence of adjacent cracks, an assumption probably not valid in a real ceramic material with numerous flaws.

The ratio of the compression to tensile strength of Griffith's material is 8, while statistics on brick strength show a figure of 12, increasing to 16 for weak bricks. The reduced tensile strength in a brittle material with a high compression to tensile strength ratio must indicate a more critical system of flaws present in the material, and therefore, it is reasonable to believe that in a biaxial state of compression-tension, the interaction of the stresses in such a material could be more severe.

It is recalled that Vile[60] in his biaxial compression-tension tests on concrete and mortar obtained differing shapes of the failure envelopes depending upon the volume fraction of coarse aggregates in the concrete mixes (see Fig. 2.11). A concavity in the failure envelope exists for mortar with no coarse aggregates. The change in profile of the biaxial failure envelopes with varying percentage of coarse aggregates may be explained by reference to the role of stone aggregates in the concrete matrix. It has been established in the study of microcracking of concrete that the stones in the mix function as crack-arresters during the phase of major microcracking in the concrete under load, past the point of discontinuity. In the light of this concept, it is not surprising to expect an increased biaxial strength of concrete with increasing percentage of coarse aggregates in the mix. This corresponds to a higher convexity in the profile of the biaxial failure envelope.

It is also recalled that Isenberg's[30] biaxial compression-tension curve for concrete for stresses at discontinuity is concave (see Fig. 2.12). It is known that at stresses below the point of discontinuity, major micro-cracking does not take place in the concrete and so the contribution of the coarse aggregates as crack-arresters is absent. Thus, Isenberg's biaxial curve for concrete for stresses at discontinuity is not incompatible with Vile's results for mortar.

Therefore, evidence seen in Vile's and Isenberg's test data lends support to the probability that the profile of the biaxial compression-tension failure envelope for a more homogenous mortar- and brick-like material may be concave.

4.6 SUMMARY

1. The failure envelope under biaxial compression-tension determined for the clay pipe is concave in shape, indicating a severe interaction between compression-tension stresses.

2. This failure envelope is remarkably similar to that obtained from tests on model scale bricks, but differs radically from the theoretical curves of Coulomb and Griffith.

3. The physical and strength properties of brick material do not conform totally with the assumptions made in Griffith's flaw theory, and perhaps these differences contribute to the variation in the biaxial compression-tension failure envelopes between theory and experiment.

4. Evidence observed from test data on biaxial compression-tension strength of concrete and mortar supports the probability that the failure envelope under these stresses for mortar- and brick-like materials is concave in shape.

5. The ultimate lateral strain in the pipe is unrelated to the combination of compression-tension stresses applied, and ranges between 200 to 300 micro-units.

CHAPTER 5 - TRIAXIAL COMPRESSION OF BRICKWORK MORTAR

5.1 INTRODUCTION

The state of stress existing in a horizontal mortar joint of a brickwork panel in compression is one of triaxial compression, comprising a vertical compression and a pair of equal lateral compression. The bilateral compression is on account of the differential lateral strain between the mortar joint and the brick element, the mortar joint tending to expand laterally more than the brick which in turn exerts a compressive restraint on the mortar.

For the development of the proposed failure criterion for brickwork in compression, it is necessary to determine the behaviour of brickwork mortar in a state of triaxial compression in which the second and third principal stresses are equal.

This chapter describes the experimental work carried out on the triaxial compression of brickwork mortar, using a standard high pressure triaxial apparatus.

5.2 MATERIALS AND SPECIMEN PREPARATION

Standard mortar mixes 1:$\frac{1}{4}$:3 and 1:1:6 of consistency 10-11 mm determined by the dropping ball method in accordance with BS 4551[11] were selected for the triaxial tests. These mortar consistencies corresponded to water-cement ratios of 0.64 and 1.29 for 1:$\frac{1}{4}$:3 and 1:1:6 mixes respectively. The cement used was rapid-hardening Ferrocrete and the fine sand was Leighton-Buzzard No. 19 of grading 25/52. The choice of Leighton-Buzzard sand would result in a higher mortar strength than if ordinary building sand was used. However, the variation in strength of mortars made with the standard laboratory sand would be smaller, and for this reason it was decided to use the Leighton-Buzzard sand in mortars for these tests.

Specimens, 1½ in diameter x 4 in length (3.8 x 10.2 cm), were cast in steel moulds shown in Fig. 5.1, six specimens per casting. The mortar was hand-tamped in three layers with a ½ in diameter (12.7 mm) rod. For each mortar mix a total of eighteen specimens in six sets of three specimens per set were put aside for the triaxial tests. Each set of specimens was tested at a particular cell pressure.

Specimens, demoulded 24 hours after casting, were immersed in water at 20 degrees Centigrade for the next 13 days and afterwards dried in an oven at 110 degrees Centigrade for one day. During the period of curing in water, the top end of the specimen was trimmed flat and parallel to its bottom end with the aid of a rock-cutting machine.

For axial and lateral strain measurements, two 120-ohm resistance wire polyester gauges TML-PC 10, each consisting of a pair of perpendicular 10 mm gauges, were mounted diametrically on every mortar specimen. The limiting strain for these gauges is 2% in compression and 1.5% in tension.

In mounting the strain gauges, the affected area on the specimen was first sandpapered lightly to remove any loose particles, and then thoroughly cleaned with acetone. A thin coat of precoating adhesive, recommended by the suppliers of the strain gauges, was then applied. After setting, the precoating adhesive was sandpapered to a smooth finish and cleaned with acetone. It was then ready to receive the strain gauge. In fixing the strain gauges over the curved surface of the specimen, it was necessary to hold down the gauges with insulation tape until the cement had set.

5.3 TRIAXIAL EQUIPMENT

The triaxial cell used was of standard manufacture, see Fig. 5.2, but with the chamber height specially extended to accommodate a 1½ in diameter x 4 in length (3.8 x 10.2 cm) specimen, 1 in longer than

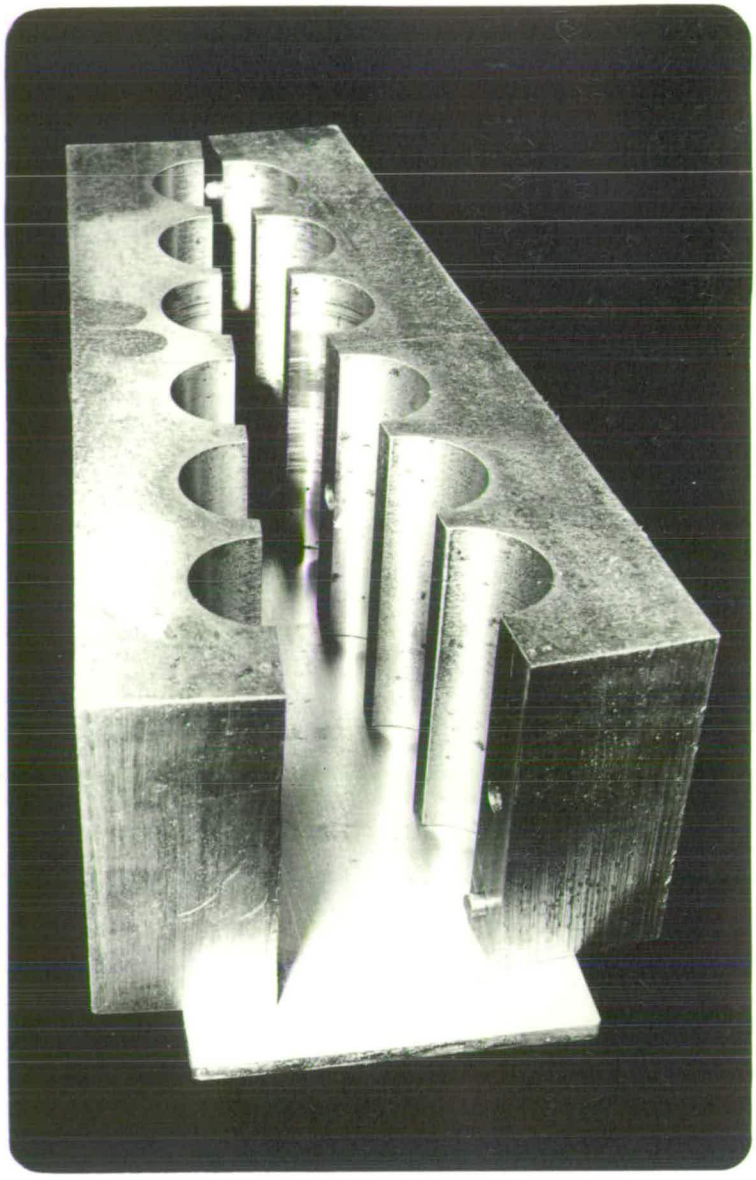

Fig 5.1 STEEL MOULDS FOR MORTAR SPECIMENS
$1\frac{1}{2}$ ins DIAMETER x 4 ins LENGTH

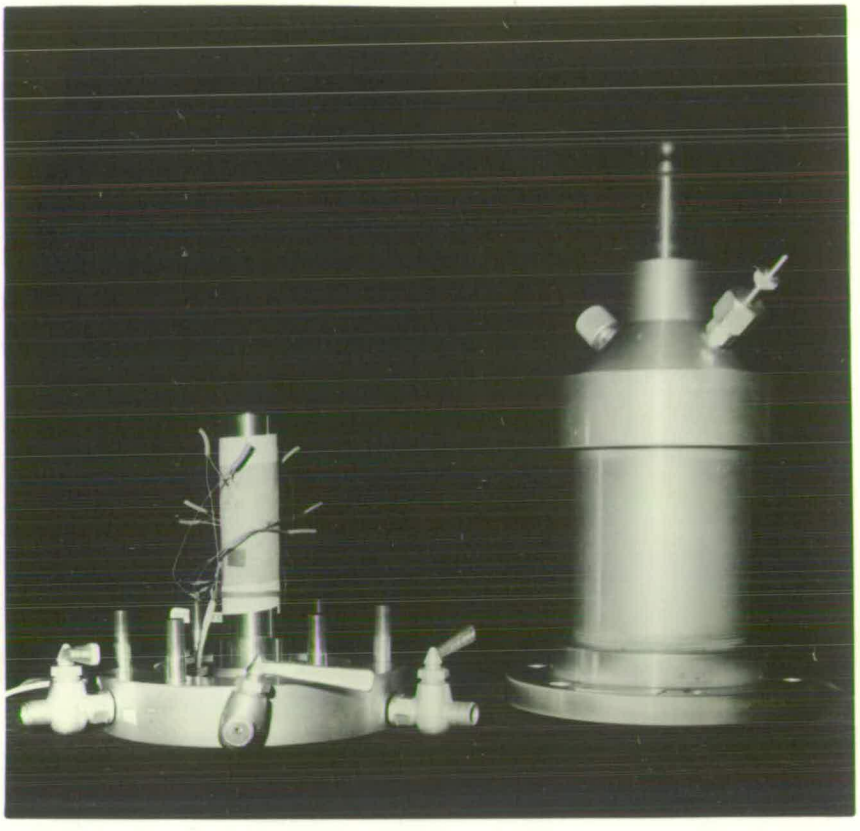

Fig 5.2 TRIAXIAL CELL

the standard 3 in length specimen. A longer specimen was decided upon in order to eliminate any influence of the end loading plates upon the stress field in the central portion of the specimen where resistance gauges were mounted.

The essential features of the high pressure traixial cell were similar to those of an ordinary triaxial cell for soil tests. In this particular model, there were no windows to the pressure cell, and the test specimen could not be inspected once it was enclosed. The specimen was mounted on the central pedestal, then capped with a steel platen specially designed with a cone seating to receive the loading ram through which the axial load was applied.

A new inlet, drilled through the base of the triaxial cell, allowed a nine-strand wire cable about 5 mm diameter to be threaded through into the chamber. A total of eight strands was required to feed the two resistance gauges mounted on each test specimen. A gland fitted with a rubber O-ring prevented any leakage of cell fluid. The gap between the core cable and the nine wires was sealed with a PVC solvent cement, and it was also necessary to seal off the opening in each of the individual wires.

The triaxial cell was rated to withstand a cell pressure of up to 1500 lbf/in^2 (10.34 MN/m^2), the cell pressure being exerted hydraulically by a pressure apparatus shown on the left in Fig. 5.6. The pressure apparatus had two functions: the first was to apply a high pressure to the cell, and the second was to maintain the cell pressure constant during the test. A diagrammatic layout of the constant pressure apparatus is given in Fig. 5.3.

The maintenance of a particular cell pressure was made possible with the provision in the pressure system of a balancing load cylinder to which was attached a hanger weight. A drop in cell pressure caused the lowering/

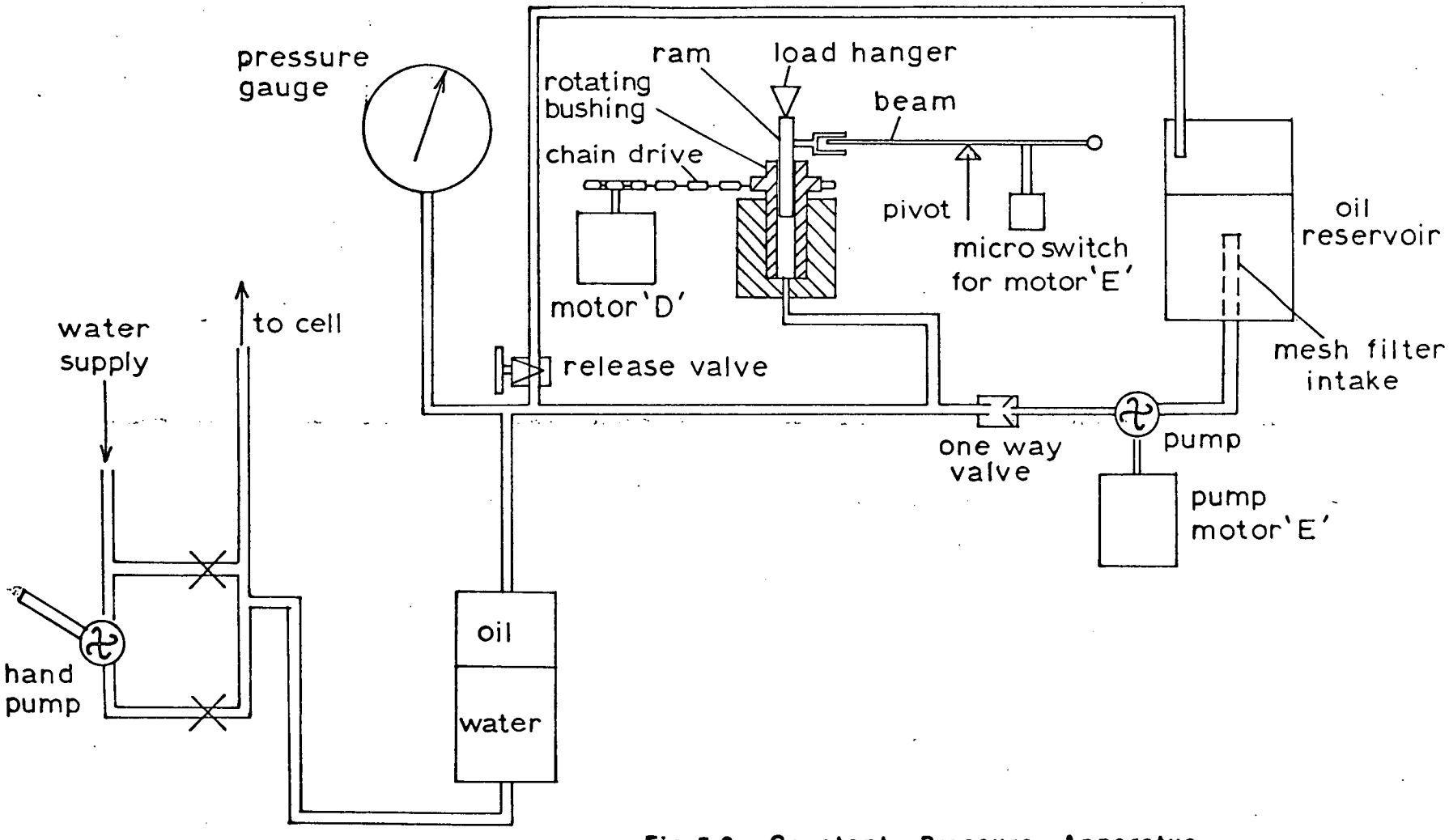

Fig 5.3 Constant Pressure Apparatus

the lowering of the balancing cylinder ram which in turn activated a pump motor through a microswitch. The pumping action raised the cell pressure to the designated value which when exceeded lifted the balancing cylinder ram and operated the microswitch that cut off the pump motor.

In a test there were four effects that could alter the pressure in the system:

(a) change in the volume of the test specimen,

(b) entry of the loading ram into the cell,

(c) expansion of the system with the pressure,

(d) unavoidable leakage as around the loading ram.

Usually, the combined effect of these was to reduce the pressure in the triaxial cell.

5.4 PRELIMINARY TESTS

5.4.1 Cube Strength and Water Absorption

The comparative strengths for the 1:$\frac{1}{4}$:3 and the 1:1:6 mortar mixes between 2.78 in (7 cm) cubes and $1\frac{1}{2}$ in diameter (3.8 cm) cylinders are shown in Table 5.1. The cubes were cast in accordance with the BS 4551[11].

The cube strength was much greater than the corresponding cylinder strength, and was in fact about 1.4 times higher for both mixes. This difference in strength is mainly due to the fact that the cubes were vibrated while the cylinders were hand-tamped. The vibration of wet mixes, such as a brickwork mortar, produces a compacted specimen of much reduced water-cement ratio, as was borne out by a visual comparison between a cube and a cylinder during casting. Also, the strength difference between the cube and the cylinder is due to the greater restraining influence of the loading platens on a cube than on a cylinder of height-diameter ratio of 2.66.

TABLE 5.1 - MORTAR CUBE & CYLINDER STRENGTHS

Mortar	2.78 in cube soaked 14-day	$1\frac{1}{2}$ in cylinder soaked 14-day	$1\frac{1}{2}$ in cylinder soaked 28-day	$1\frac{1}{2}$ in cylinder air-cured 14-day
	stress (lbf/in^2)	stress (lbf/in^2)	stress (lbf/in^2)	stress (lbf/in^2)
1:$\frac{1}{4}$:3	4957	3334	3664	1553
	4957	3372	3613	1559
	4919	3473	3435	1648
	4928	3283	3524	1540
	4957	3347	3486	1597
	4977	3347	3309	1597
mean =	4949	3359	3505	1582
1:1:6	986	767	659	364
	1041	743	735	374
	1052	729	754	450
	1043	672	800	394
	1038	726	723	332
	1038	710	711	368
mean =	1033	724	730	380

1 lbf/in^2 = 6.8948×10^{-3} MN/m^2

Negligible difference exists in the cylinder strengths between the 14-day and the 28-day specimens. Therefore, the testing of specimens spread over a period of days as was necessary in the triaxial series ought not to cause any significant variation in strength between specimens on account of their age difference.

Cylinder specimens air-cured for 14 days showed a drastic reduction in strength, about half the value of those water-cured. The actual strength of mortar joints in brickwork will generally be between these values, depending upon the water absorption of the bricks and how well the mortar is cured.

Table 5.2 lists the percentage water absorption for both mortar mixes as well as the moisture content in air-dried samples at 14 days. Since the degree of saturation in mortar joints of brickwork after 14 days is relatively low, it may be assumed that the presence of pore water pressure, if any, in mortar joints of loaded brickwork is of no consequence. Accordingly, the triaxial tests were carried out on dry specimens.

5.4.2 Waterproofing of Test Specimens

After extensive trials in search of a suitable means of sealing the test specimen against the ingress of cell fluid, including the use of rubber membrane, silicone and other synthetic rubbers, polyurethane, etc., it was found that a specimen painted with one coat of Araldite CY 219 (an epoxy resin) and two thin coats of TML strain-gauge waterproofing adhesive PS (an unsaturated polyester resin with an inorganic filler) was sufficiently waterproof. The use of Araldite by itself had not been successful as the mix contained minute air bubbles which were not easily expelled. However, an initial coat of the low-viscosity epoxy resin was beneficial in that it readily filled the numerous surface pores of the mortar specimen.

TABLE 5.2 - WATER ABSORPTION OF MORTAR

Mortar	absorption soaked 24 hrs. (%)	moisture content air-cured 14 days (%)
1:$\frac{1}{4}$:3	11.7 11.9 11.9 11.7 11.7 11.5	5.9 5.3 5.8 5.8 5.7 5.7
mean =	11.7	5.7
1:1:6	15.1 15.3 15.1 15.0 14.5 14.8	2.9 2.9 2.9 2.6 2.6 2.9
mean =	15.0	2.8

The test criterion for a successful water-proofing was to subject a coated specimen to a 1500 lbf/in^2 (10.34 MN/m^2) cell pressure for 30 minutes, which was roughly the duration of a triaxial test, without any fluid absorption. Six specimens were pressurized in this manner which at the termination of the test registered an increase in weight of less than 0.5 gms. A coated specimen (right) and an uncoated specimen with strain gauges mounted (left) are shown in Fig. 5.4.

5.4.3 Electrical Insulation

Originally, water was used as the cell fluid. Great care was taken to secure the necessary degree of electrical insulation which for these resistance gauges required a minimum of 100 megaohms. In spite of very meticulous preparation, this degree of insulation was unattainable. Consequently, the use of water as the cell fluid was abandoned in favour of a non-conducting low-viscosity oil, Tellus 15, a Shell product. The switch to oil as the cell fluid not only enabled the required insulation to be attained but also avoided the need to achieve watertight connections in the electrical wires.

5.4.4 Resistance Instability

Unstable strain readings occurred at first, the cause of which was traced to the use of stranded wire within the triaxial cell. The cell fluid under immense pressure forced its way among the filaments in each wire causing fluctuations in resistance. A change to solid-core wires within the cell for as long a length as was practicable eliminated this problem.

5.4.5 Effect of Cell Pressure on Resistance Gauges

To investigate the effect of cell pressure on the resistance gauges, a 1½ in diameter x 4 in length (3.8 x 10.2 cm) mild steel specimen on to which a pair of resistance gauges were mounted was subjected to various cell/

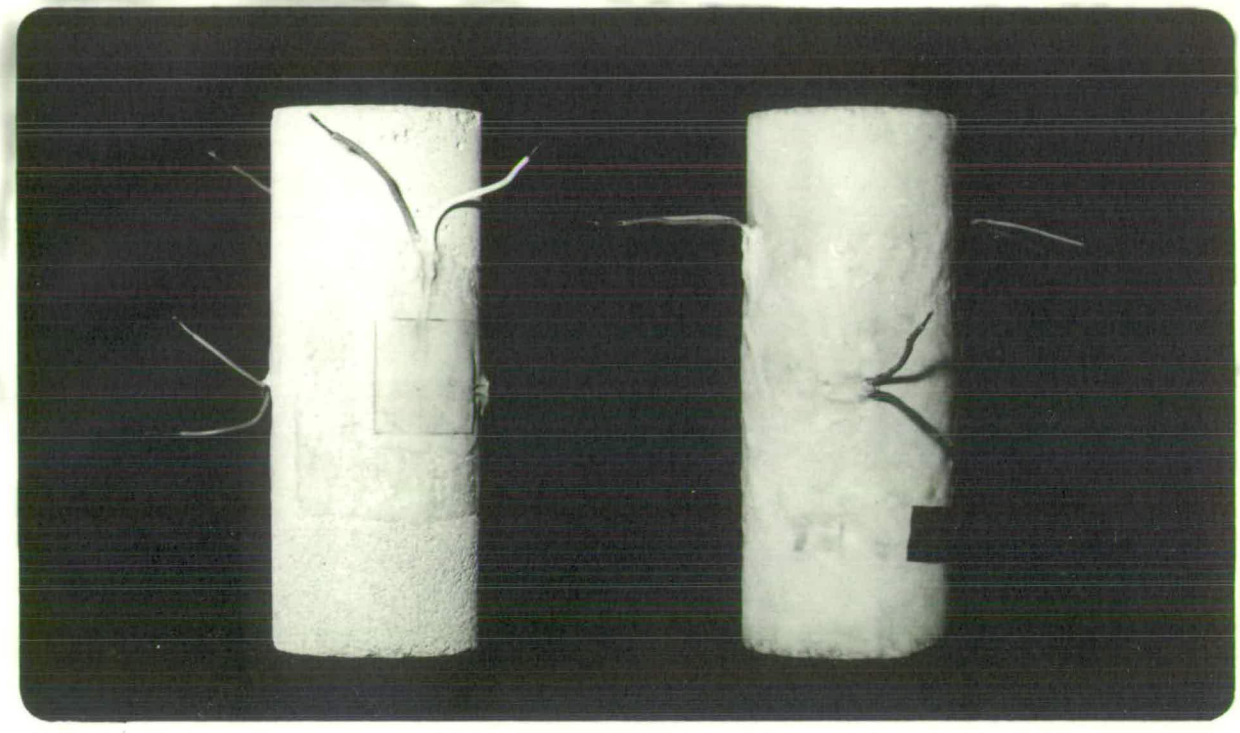

Fig 5.4 MORTAR SPECIMENS - COATED (right) & UNCOATED (left) WITH STRAIN GAUGES

various cell pressures. The compressive strain in the steel specimen under a given cell pressure could be computed if values of its elastic modulus and Poisson's ratio were known. The elastic modulus and the Poisson's ratio for mild steel had been taken to be 30×10^6 lbf/in^2 (20.68×10^4 MN/m^2) and 0.26 respectively. Deducting the amount of compressive strain in the steel specimen, the change in strain in the resistance gauges with varying cell pressure was determined, see Fig. 5.5.

It may be seen that the effect of cell pressure upon the resistance gauges is minimal. At a cell pressure of 1500 lbf/in^2 (10.34 MN/m^2) the change in strain is less than 10 micro-units. It is interesting to note, however, that the cell pressure induced a tensile strain in the vertical gauges but a compressive strain in the horizontal gauges. The strain in the horizontal gauges was compressive because these gauges were mounted on a curved surface of the specimen.

5.5 TRIAXIAL TESTS

In the triaxial tests, for each mortar mix there were six sets, each set comprising three specimens. The six sets of specimens were tested at cell pressures of 0, 282, 590, 896, 1206 and 1510 lbf/in^2 (0, 1.94, 4.07, 6.18, 8.31 and 10.41 MN/m^2). Except for the set of specimens tested at zero cell pressure where waterproofing was not required, the other specimens were waterproofed as described earlier. The 1:$\frac{1}{4}$:3 series were designated by letters A, B, C and the 1:1:6 by D, E, F, and numbered from 1 to 6.

The triaxial cell was filled with oil with the aid of a hand-pump. Axial loading to failure was carried out in an Avery compression machine. Strain measurements were recorded on a Westland data logger which printed out direct strain readings. A fuller description of the Westland/

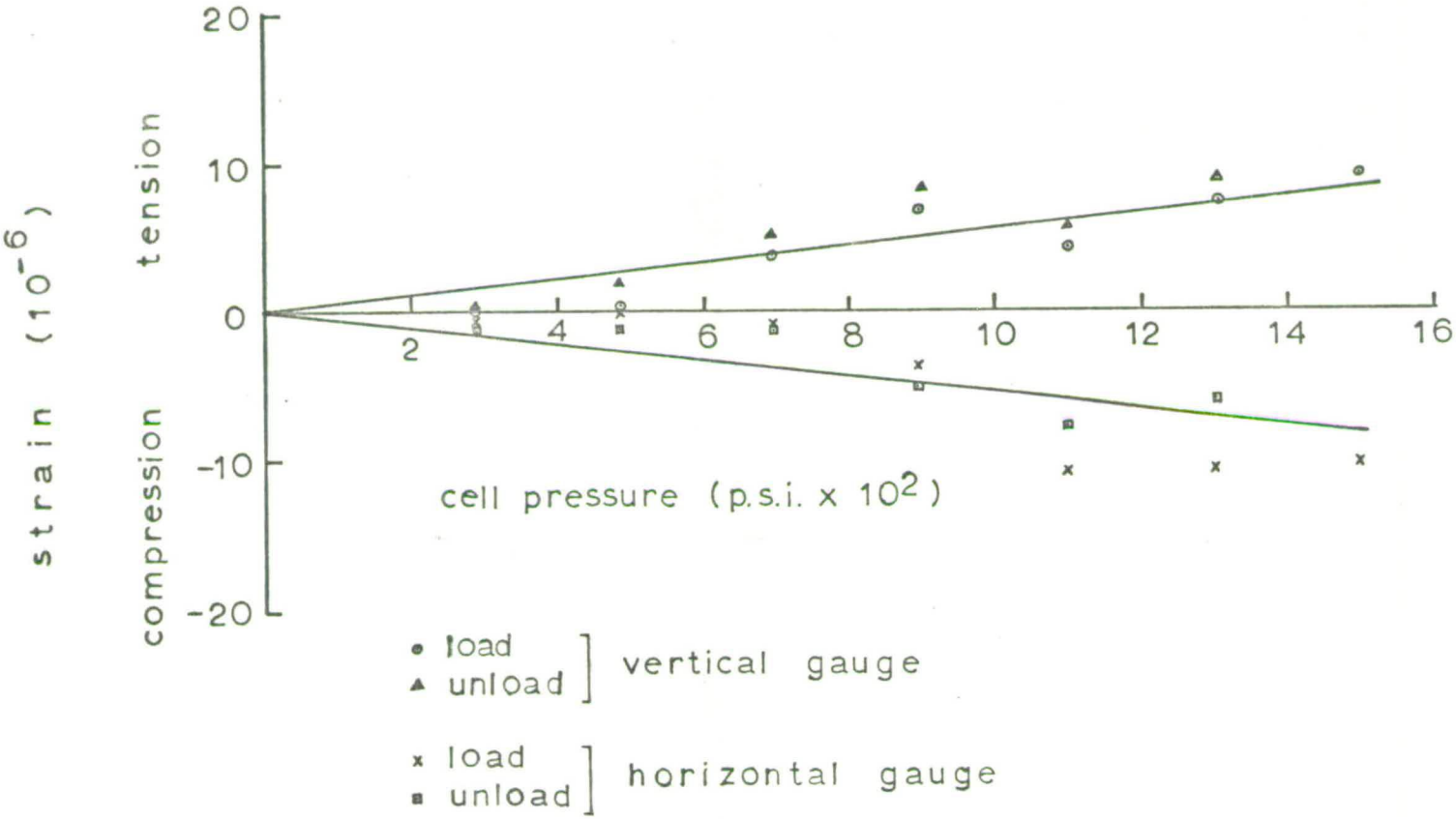

Fig 5.5 EFFECT OF CELL PRESSURE ON STRAIN GAUGE

the Westland data logger and its use may be found in reference (31). The complete set-up for the triaxial test is shown in Fig. 5.6.

All specimens behaved satisfactorily during the test except for two specimens A4 and F6. In specimen A4, one of the resistance gauges was defective. A leakage in the waterproofing of specimen F6 was suspected, for during the test there was a continuing tendency for the cell pressure to drop due to the absorption of fluid into the specimen.

Although the axial load was applied in incremental steps in order to allow strain readings to be taken, the rate of loading may be approximated at between 200 to 2000 lbf/in^2 per minute (1.38 to 13.79 $MN/m^2/min$).

The stress-strain curves for each cell pressure for both mixes are illustrated in Figs. 5.7 to 5.20. The principal-stress relationship is presented in Tables 5.3 and 5.4 and in Fig. 5.21, and on a dimensionless plot in Fig. 5.22. The corresponding Mohr circles are seen in Figs. 5.23 and 5.24.

Fig. 5.25 records the volumetric contraction of the specimen on application of the cell pressure. The influence of lateral pressure on the initial elastic modulus and Poisson's ratio of mortar is given in Fig. 5.26.

Figs. 5.27 and 5.28 show the crack formations in failed specimens tested at various cell pressuees. These same specimens were later dismantled into parts to reveal more clearly the internal fractures which are seen in Figs. 5.29 and 5.30. In general, the shearing surface was inclined at 60 to 70 degrees to the horizontal, corresponding to an angle of shearing resistance of 30 to 50 degrees. Whereas the failure surface for the unconfined specimen was a reasonably clean fracture, considerable crushing occurred/

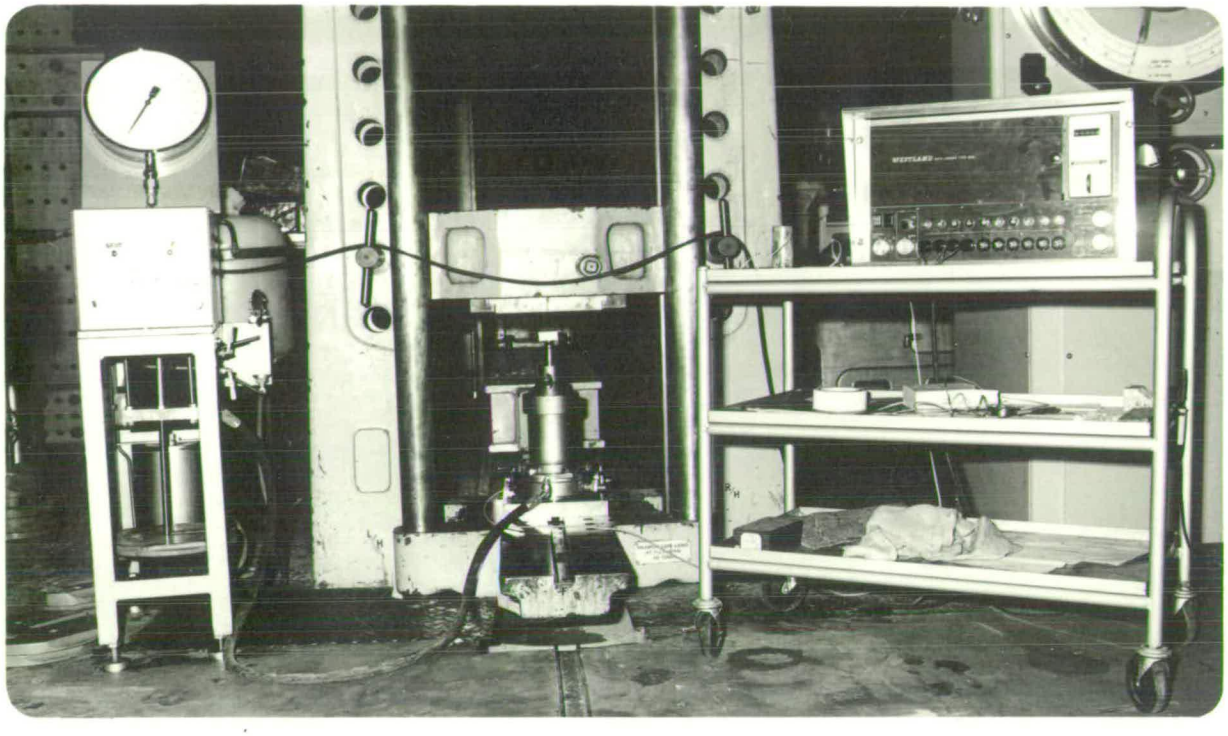

Fig 5.6 COMPLETE SET-UP FOR TRIAXIAL TEST

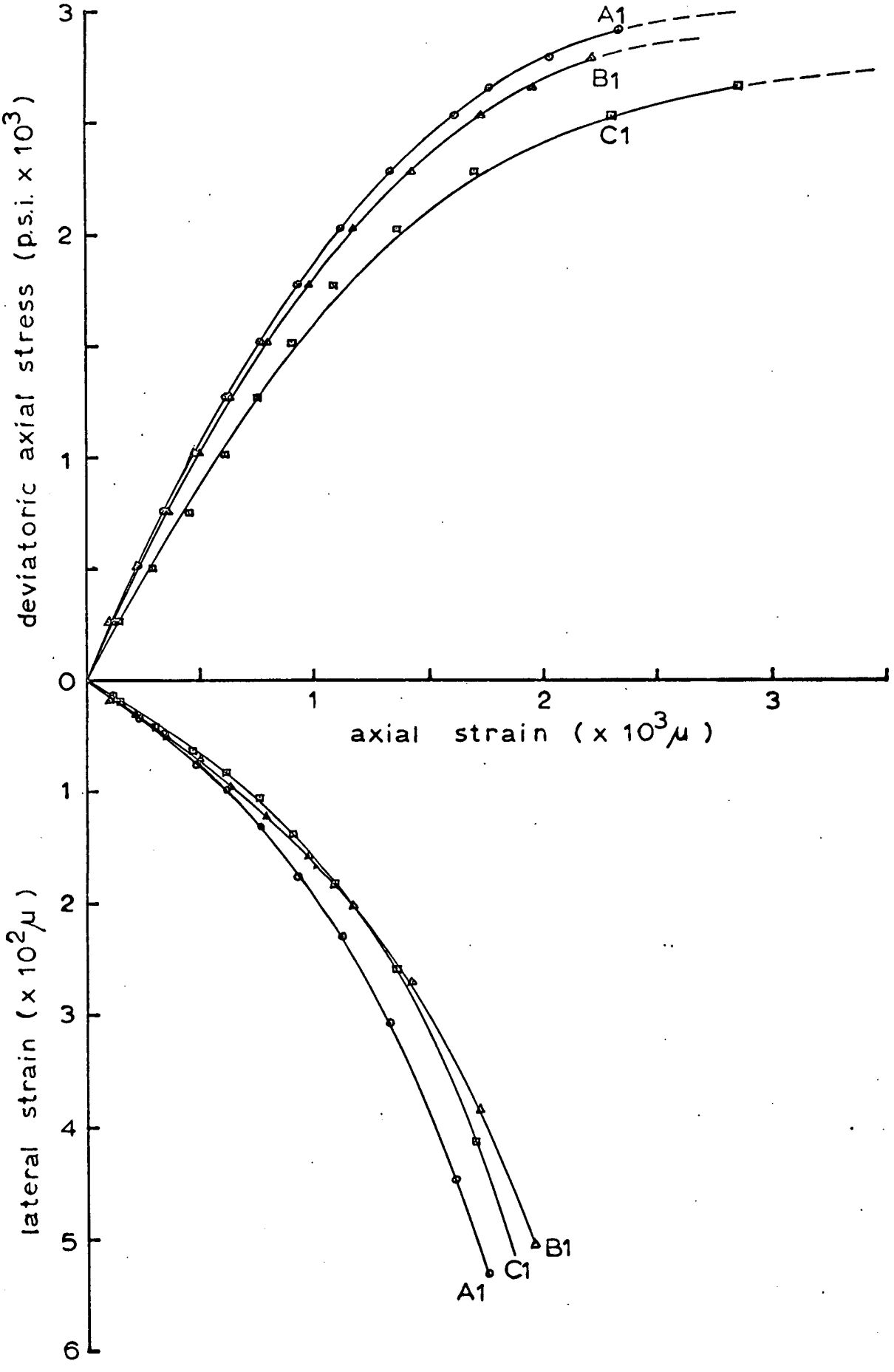

Fig 5.7 STRESS – STRAIN CURVES FOR 1:1/4:3 MORTAR. LATERAL PRESSURE = 0 p.s.i.

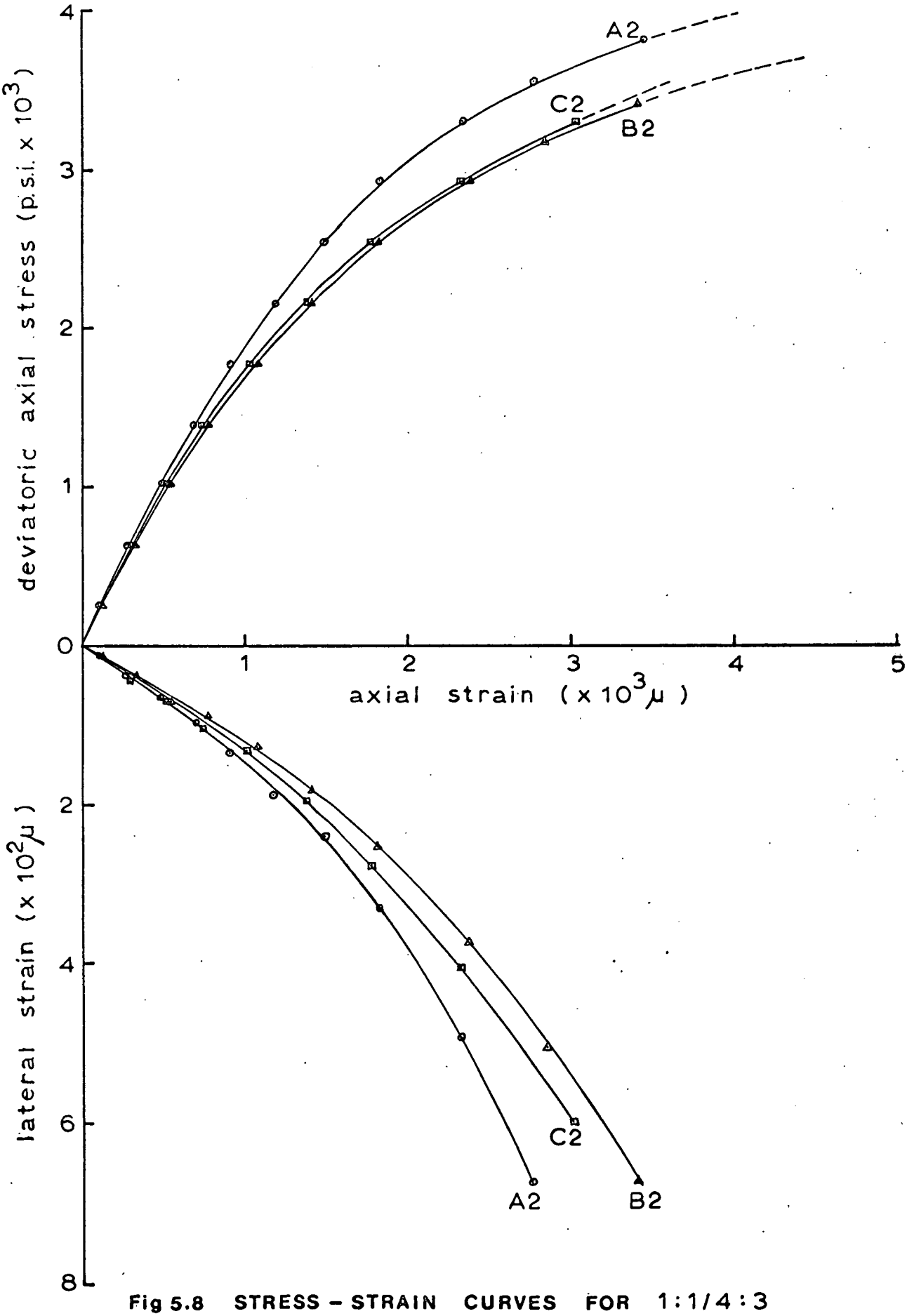

Fig 5.8 STRESS – STRAIN CURVES FOR 1:1/4:3 MORTAR. LATERAL PRESSURE = 282 p.s.i.

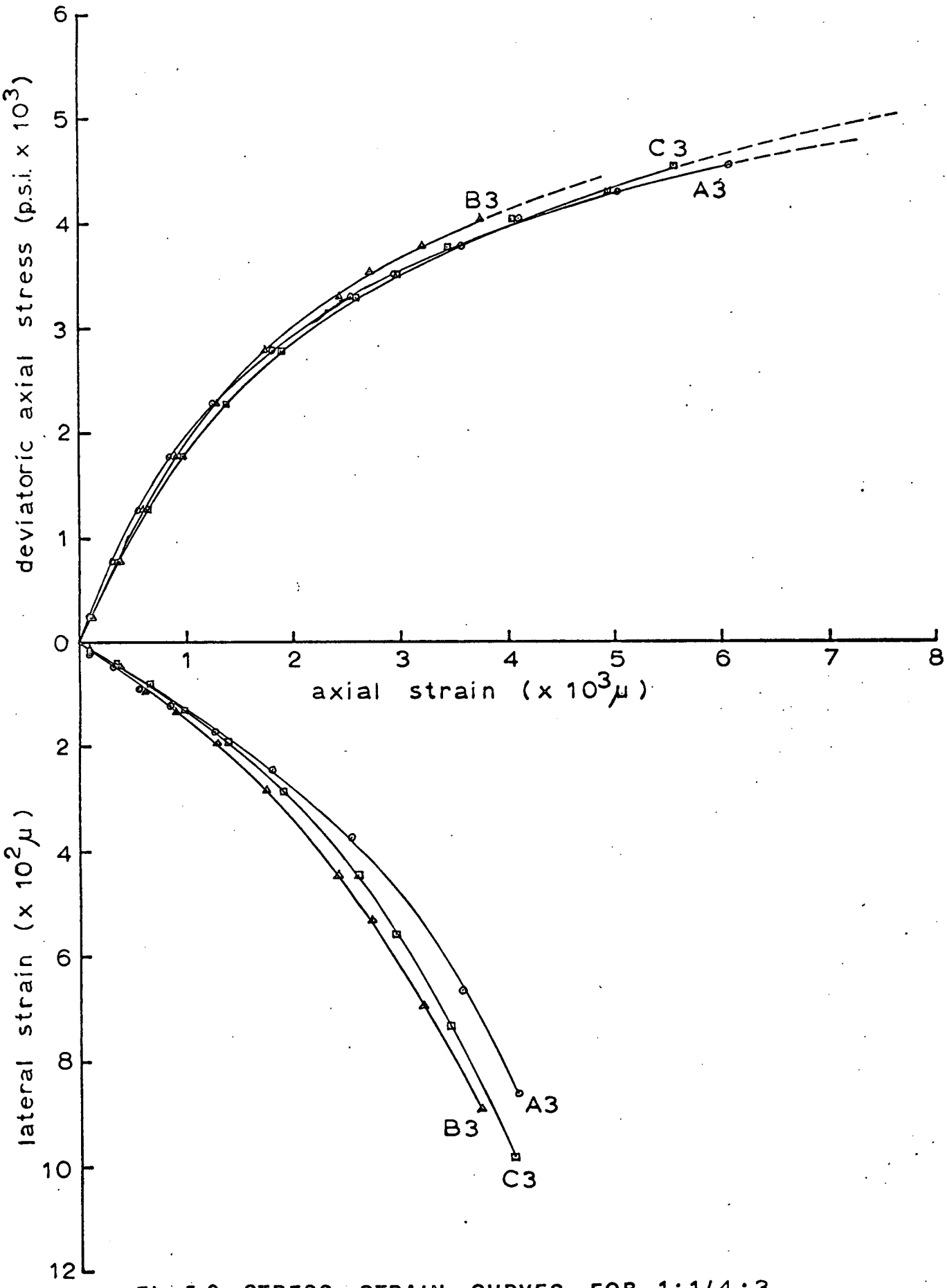

Fig 5.9 STRESS-STRAIN CURVES FOR 1:1/4:3 MORTAR. LATERAL PRESSURE = 590 p.s.i.

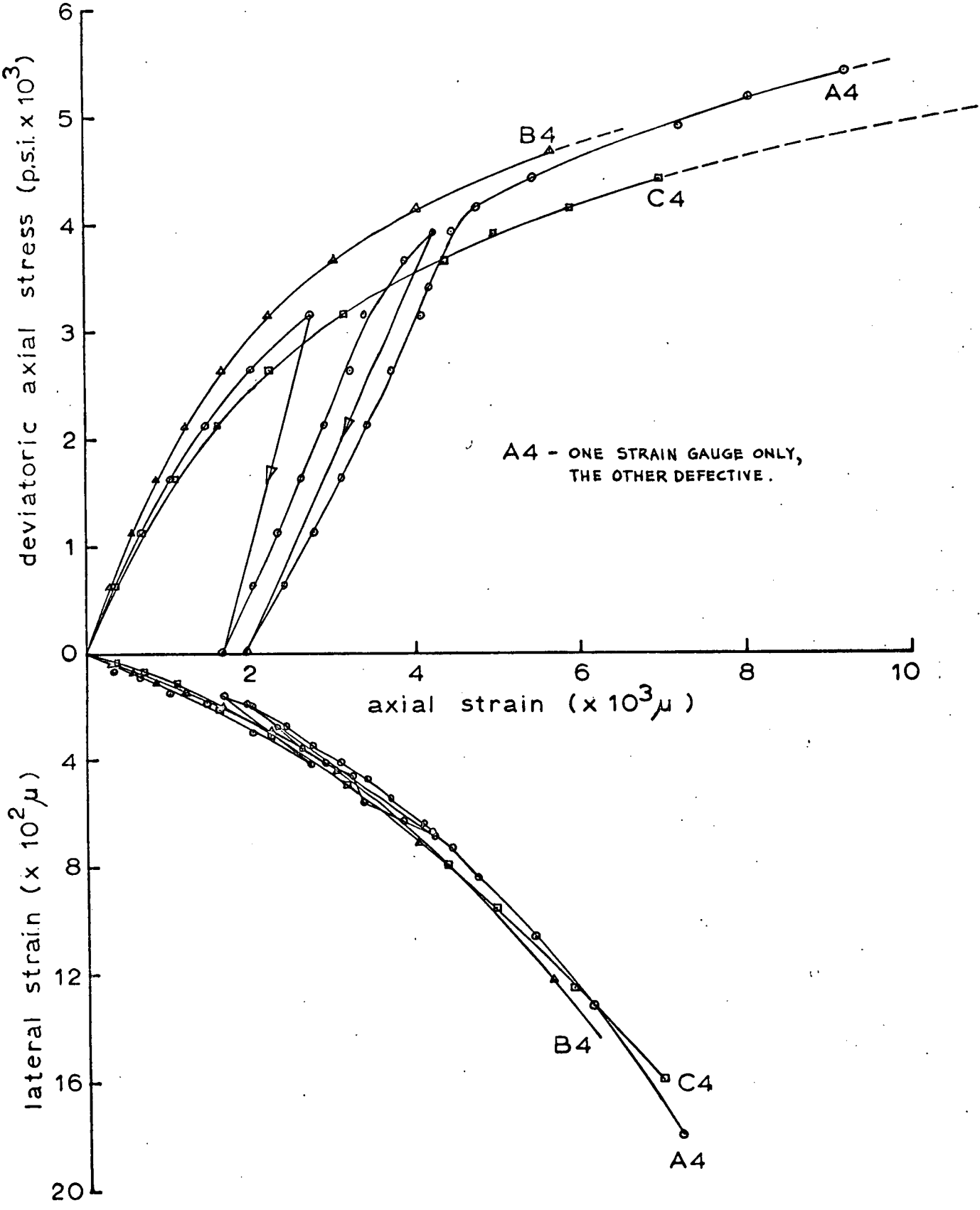

Fig 5.10 STRESS – STRAIN CURVES FOR 1 : 1/4 : 3 MORTAR. LATERAL PRESSURE = 896 p.s.i.

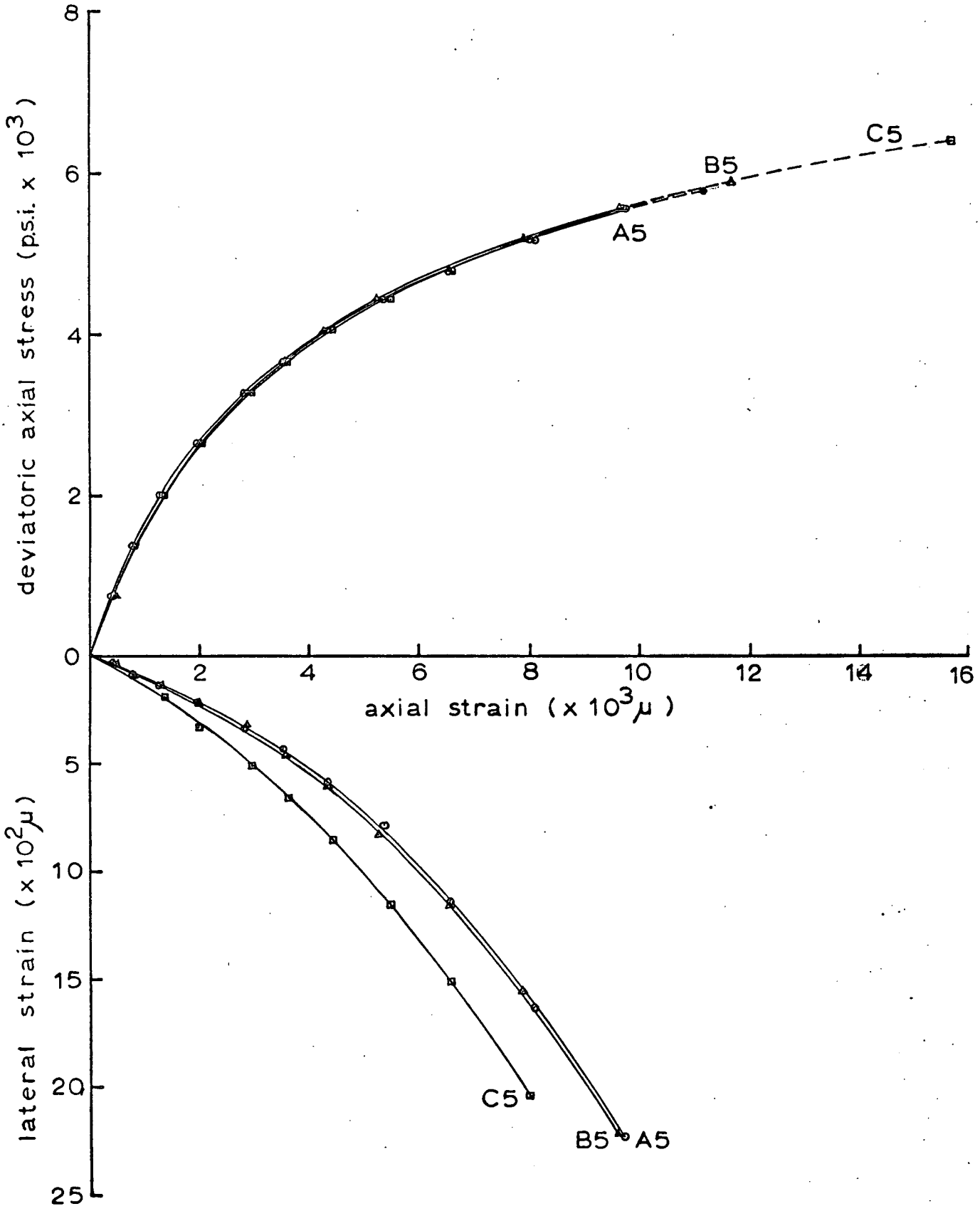

Fig 5.11 STRESS – STRAIN CURVES FOR 1 : 1/4 : 3 MORTAR. LATERAL PRESSURE = 1206 p.s.i.

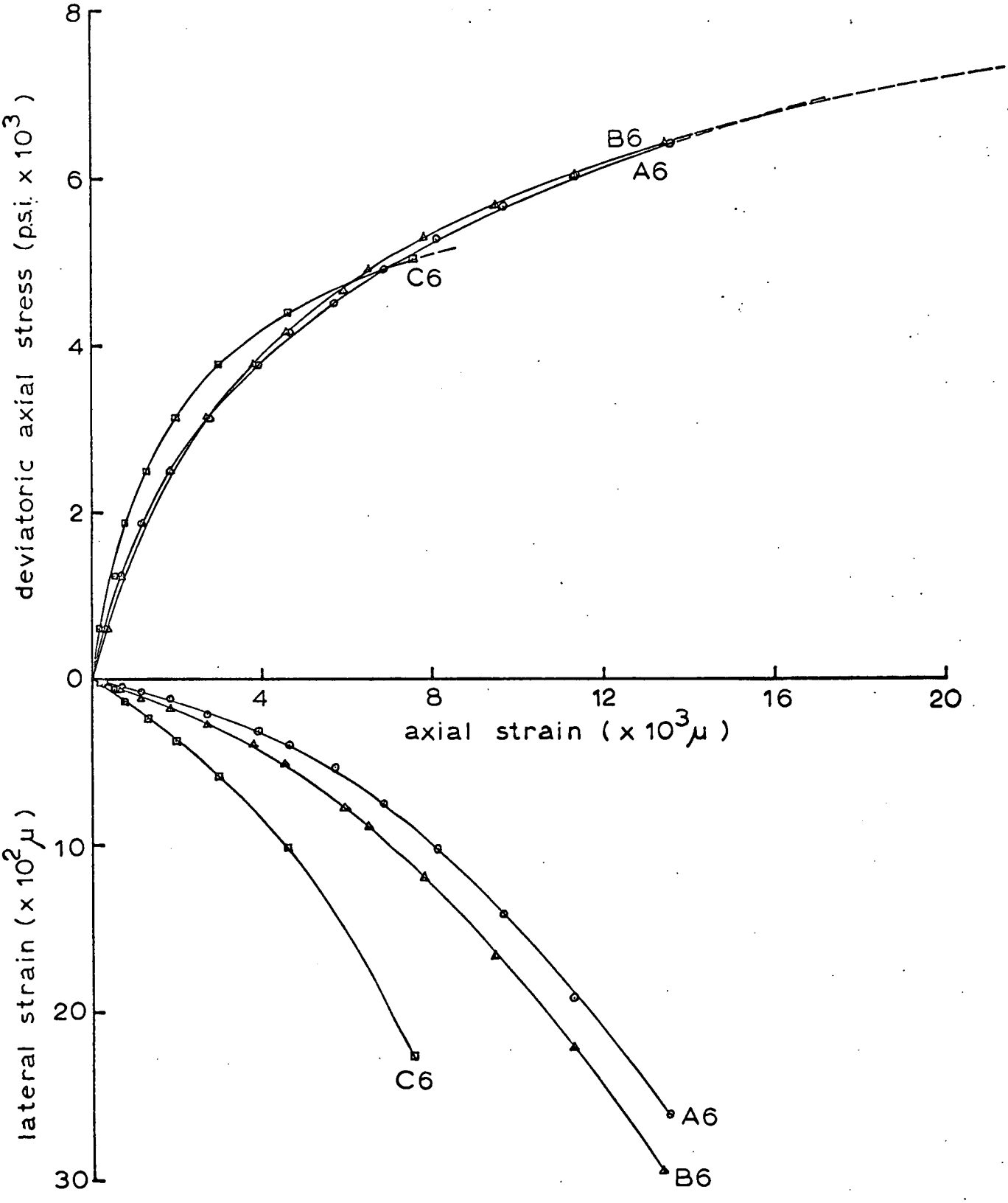

Fig 5.12 STRESS - STRAIN CURVES FOR 1 : 1/4 : 3 MORTAR. LATERAL PRESSURE = 1510 p.s.i.

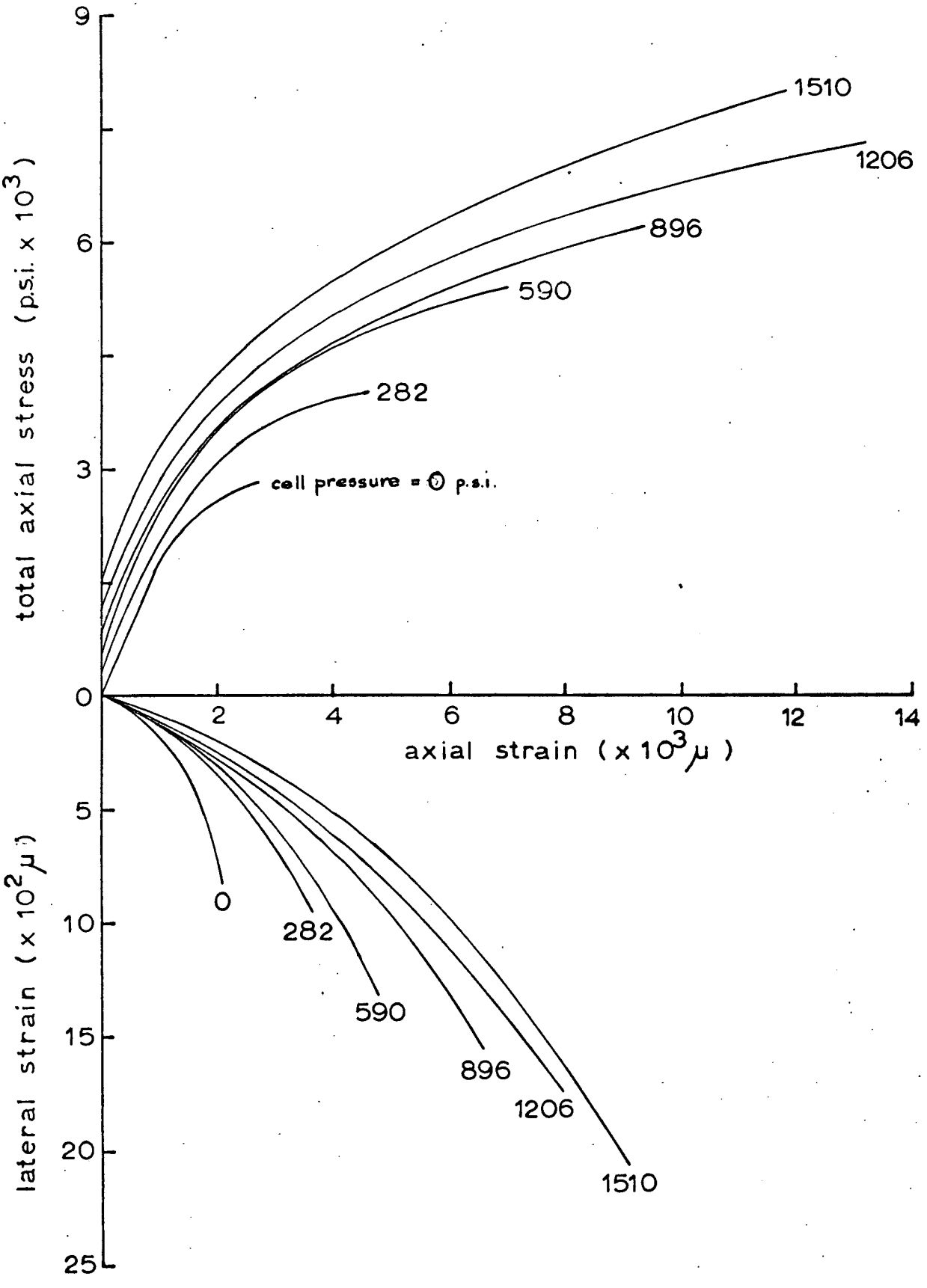

Fig 5.13 STRESS – STRAIN CURVES FOR 1:1/4:3 MORTAR

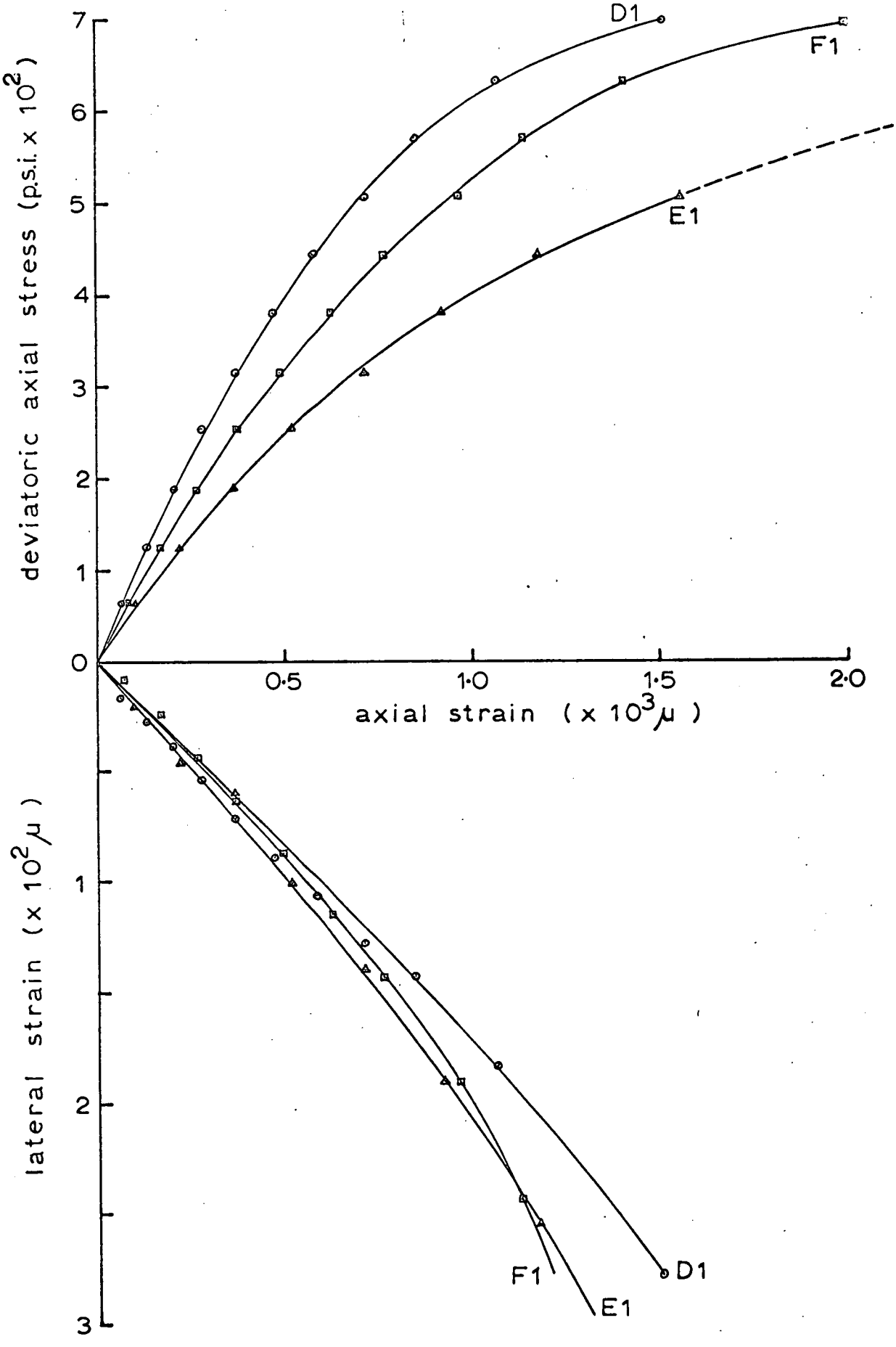

Fig 5.14 STRESS – STRAIN CURVES FOR 1:1:6 MORTAR. LATERAL PRESSURE = 0 p.s.i.

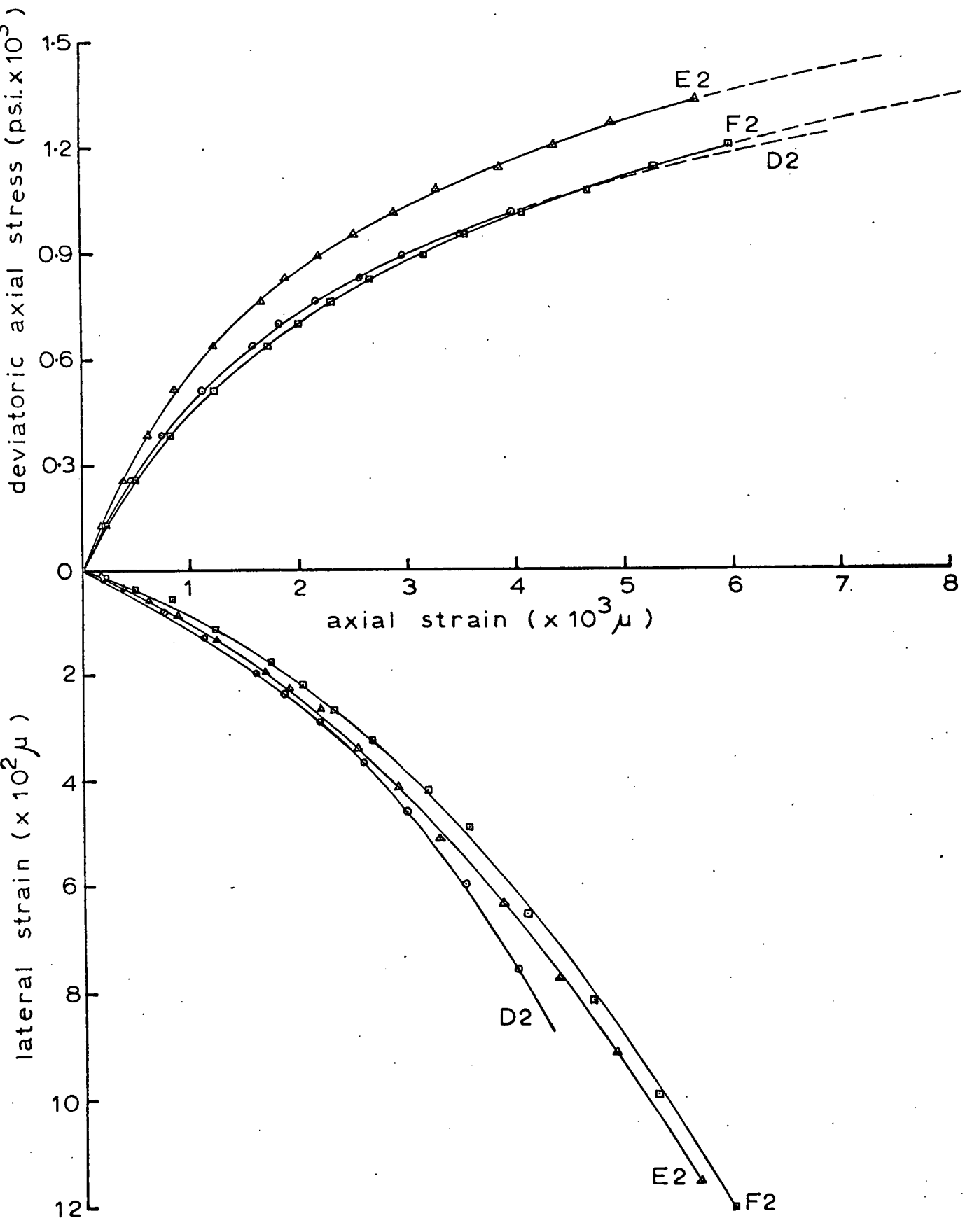

Fig 5.15 STRESS – STRAIN CURVES FOR 1:1:6 MORTAR. LATERAL PRESSURE = 282 p.s.i.

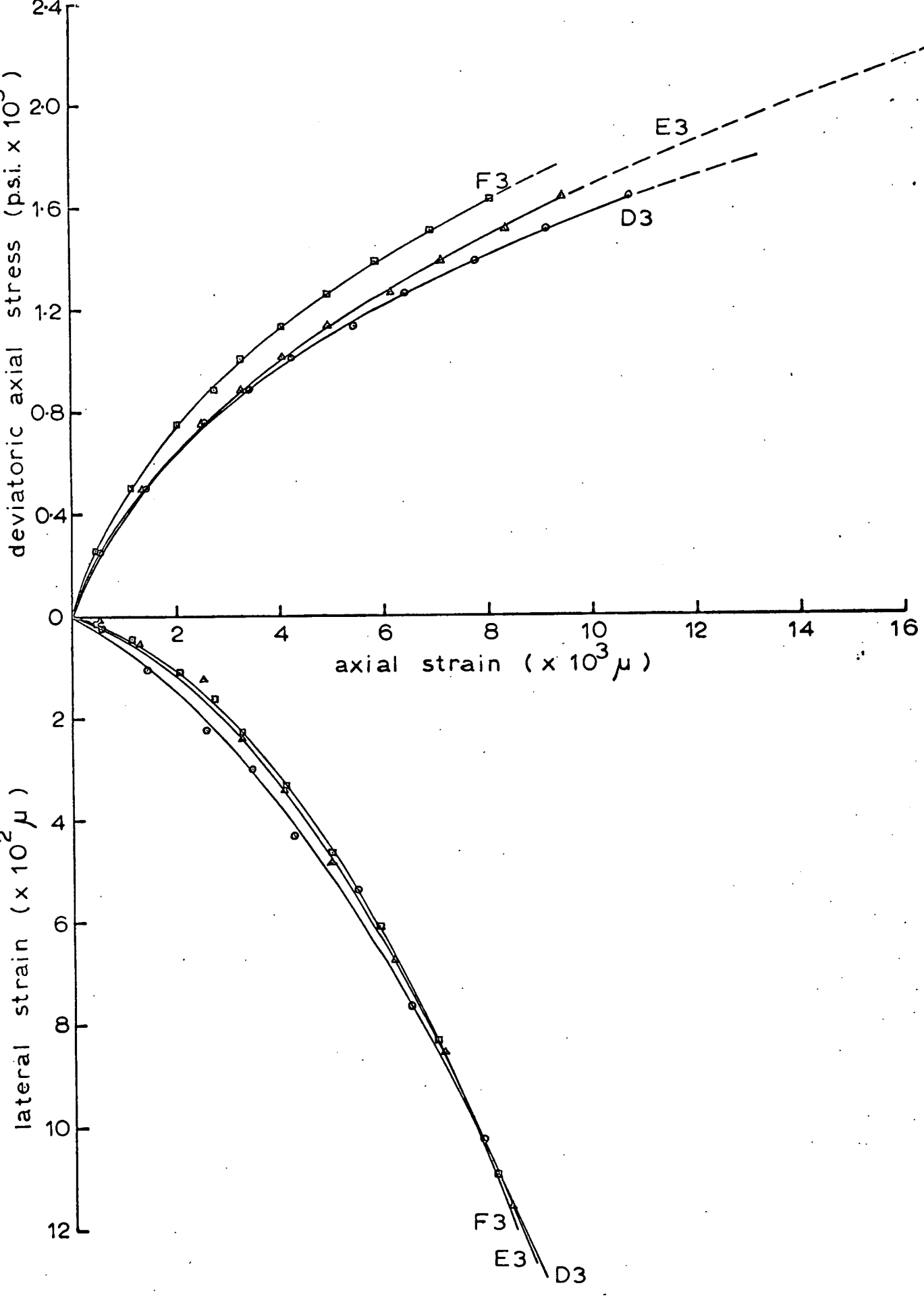

Fig 5.16 STRESS - STRAIN CURVES FOR 1 : 1 : 6 MORTAR. LATERAL PRESSURE = 590 p.s.i.

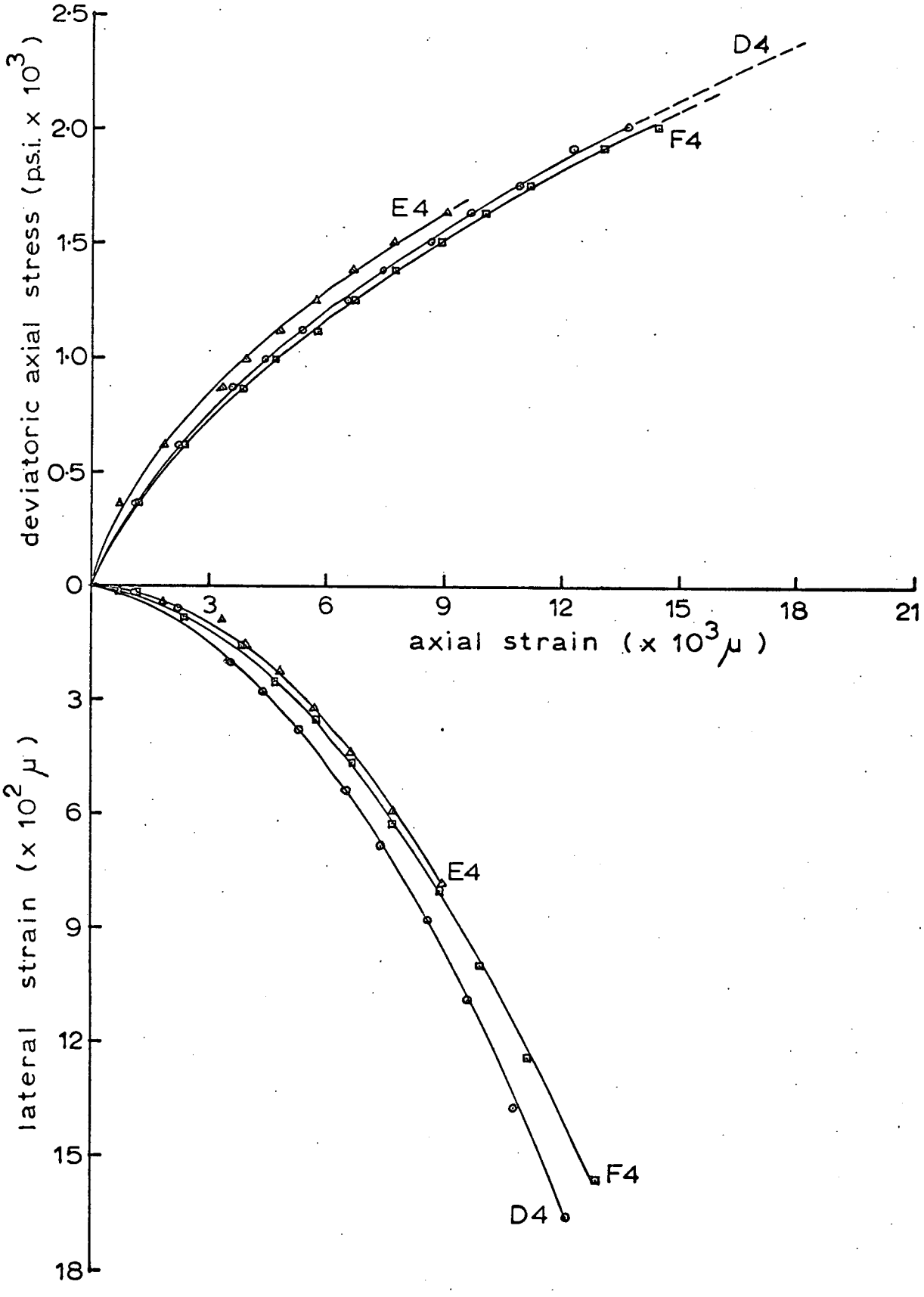

Fig 5.17 STRESS – STRAIN CURVES FOR 1:1:6 MORTAR. LATERAL PRESSURE = 896 p.s.i.

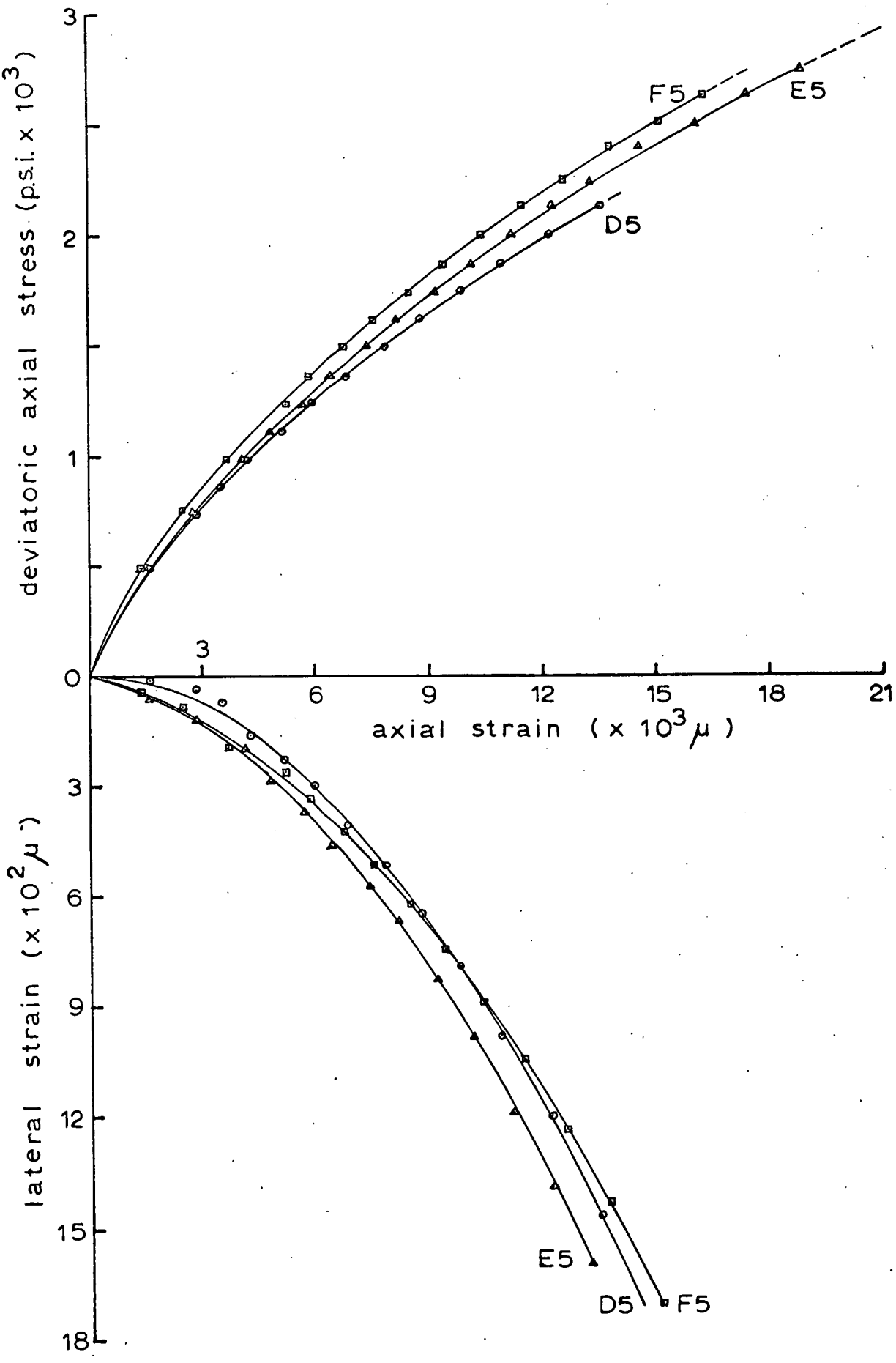

Fig 5.18 STRESS - STRAIN CURVES FOR 1:1:6 MORTAR. LATERAL PRESSURE = 1206 p.s.i.

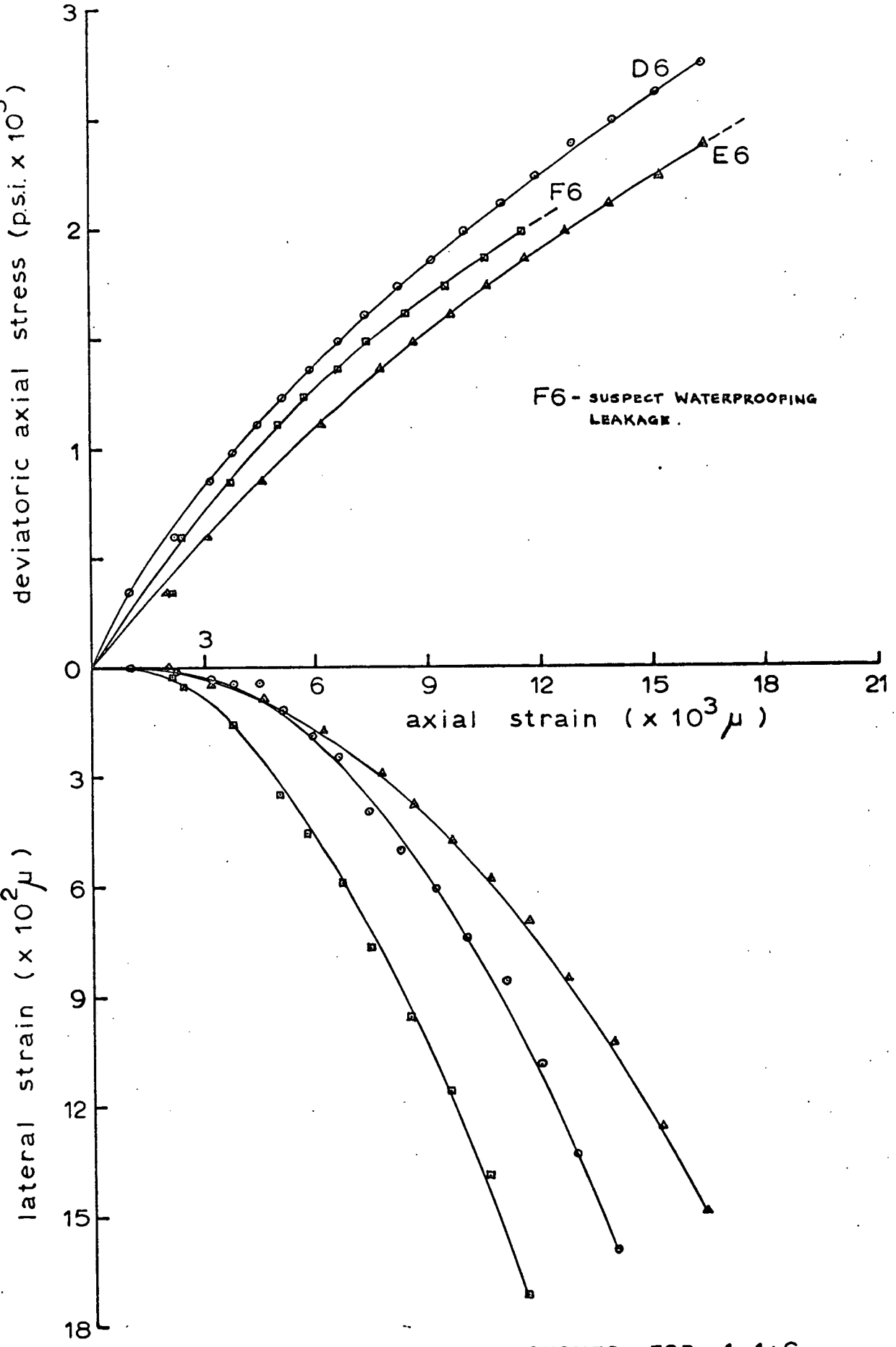

Fig 5.19 STRESS – STRAIN CURVES FOR 1:1:6 MORTAR. LATERAL PRESSURE = 1510 p.s.i.

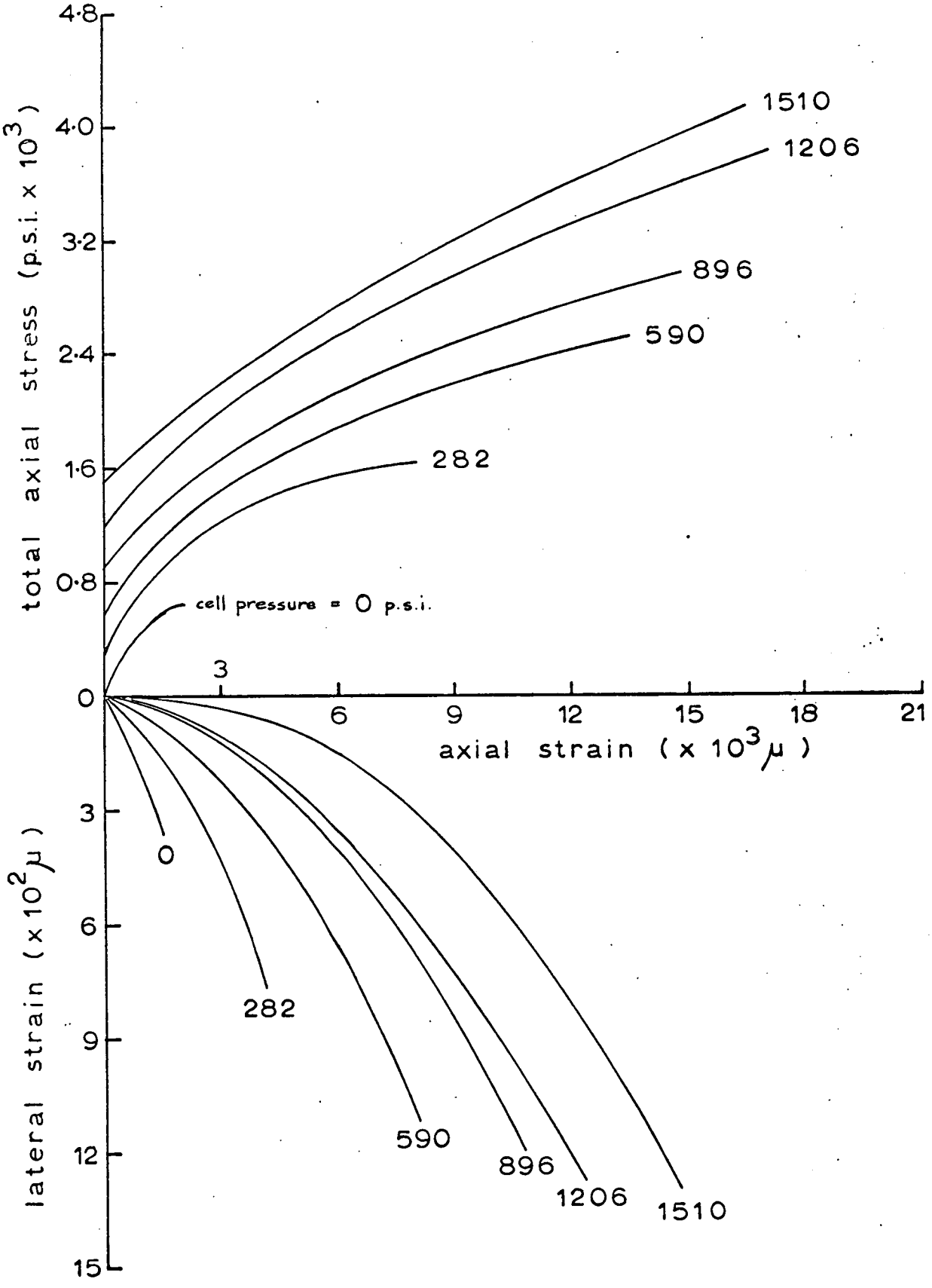

Fig 5.20 STRESS – STRAIN CURVES FOR 1:1:6 MORTAR

TABLE 5.3 - PRINCIPAL STRESS RELATIONSHIP FOR 1:$\frac{1}{4}$:3 MORTAR

cell pressure		axial stress	
σ_3 lbf/in^2	$\frac{\sigma_3}{\sigma_o}$	σ_1 lbf/in^2	$\frac{\sigma_1}{\sigma_o}$
0	0	3004 2878 2738	1.000
		σ_o = 2873	
282	.098	4277 3998 3846	1.406
		4040	
590	.205	5411 5044 5891	1.897
		5449	
896	.312	6431 5784 6431	2.163
		6215	
1206	.420	7009 7135 7642	2.528
		7262	
1510	.526	8420 9054 6696	2.804
		8057	

TABLE 5.4 - PRINCIPAL STRESS RELATIONSHIP FOR 1:1:6 MORTAR

cell pressure		axial stress	
σ_3 lbf/in^2	$\frac{\sigma_3}{\sigma_o}$	σ_1 lbf/in^2	$\frac{\sigma_1}{\sigma_o}$
0	0	697 583 697 --- σ_o = 659	1.000
282	0.428	1526 1741 1678 --- 1648	2.501
590	0.895	2394 2838 2356 --- 2529	3.838
896	1.360	3287 2590 3071 --- 2983	4.526
1206	1.830	3396 4156 3966 --- 3839	5.826
1510	2.291	4275 4008 -- --- 4142	6.285

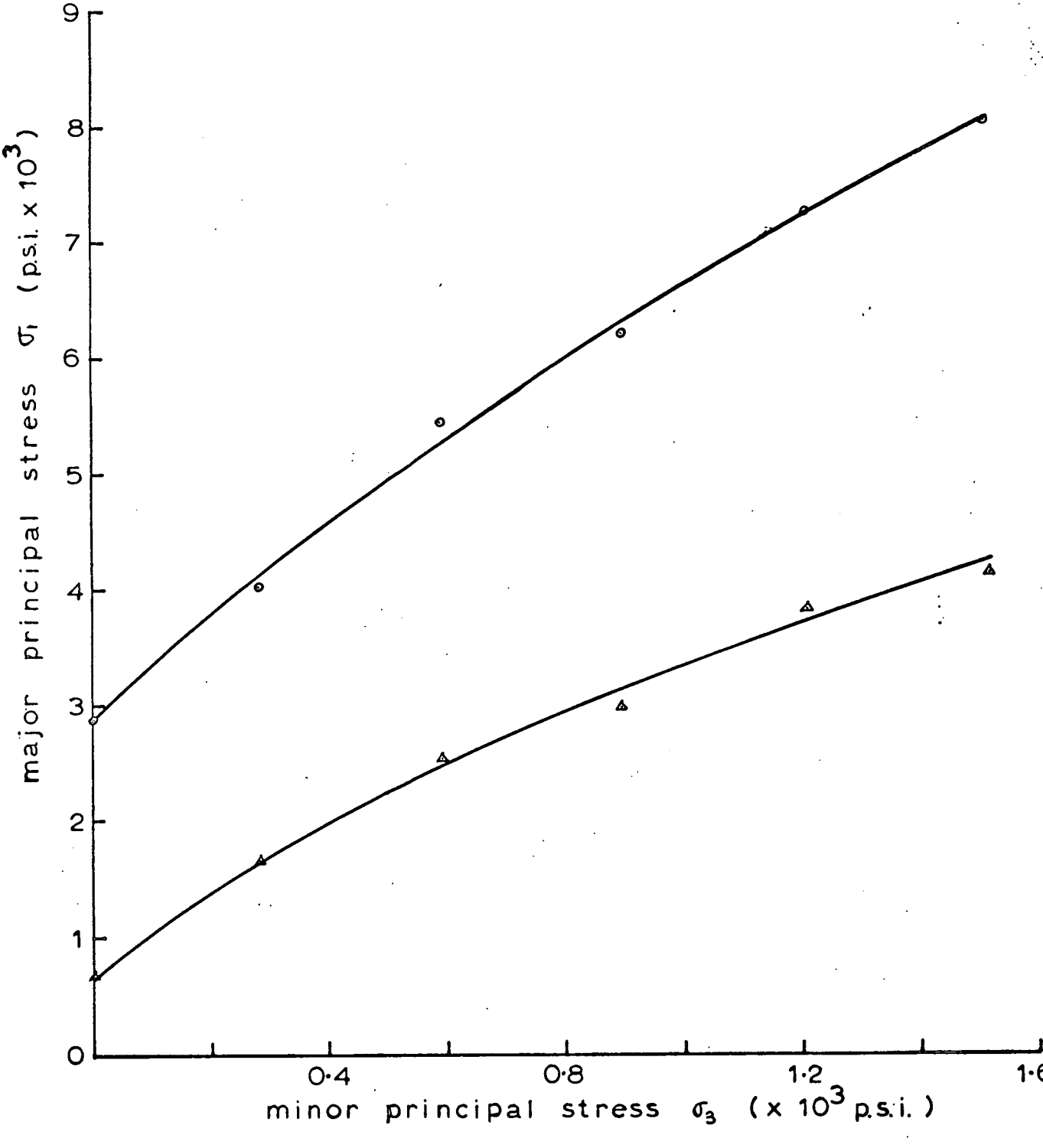

Fig 5.21 PRINCIPAL STRESS RELATIONSHIP

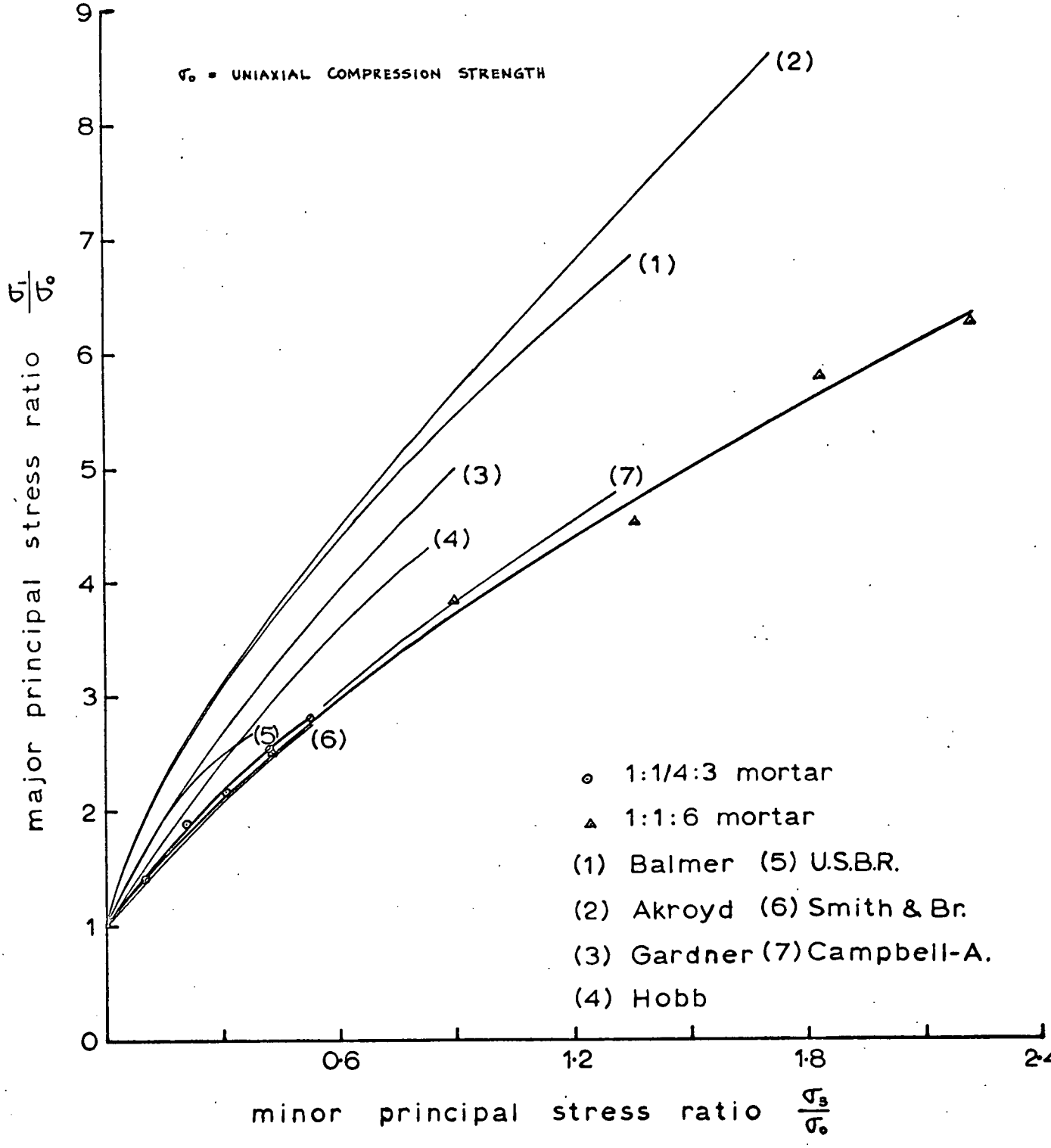

Fig 5.22 PRINCIPAL STRESS RELATIONSHIP – DIMENSIONLESS PLOT

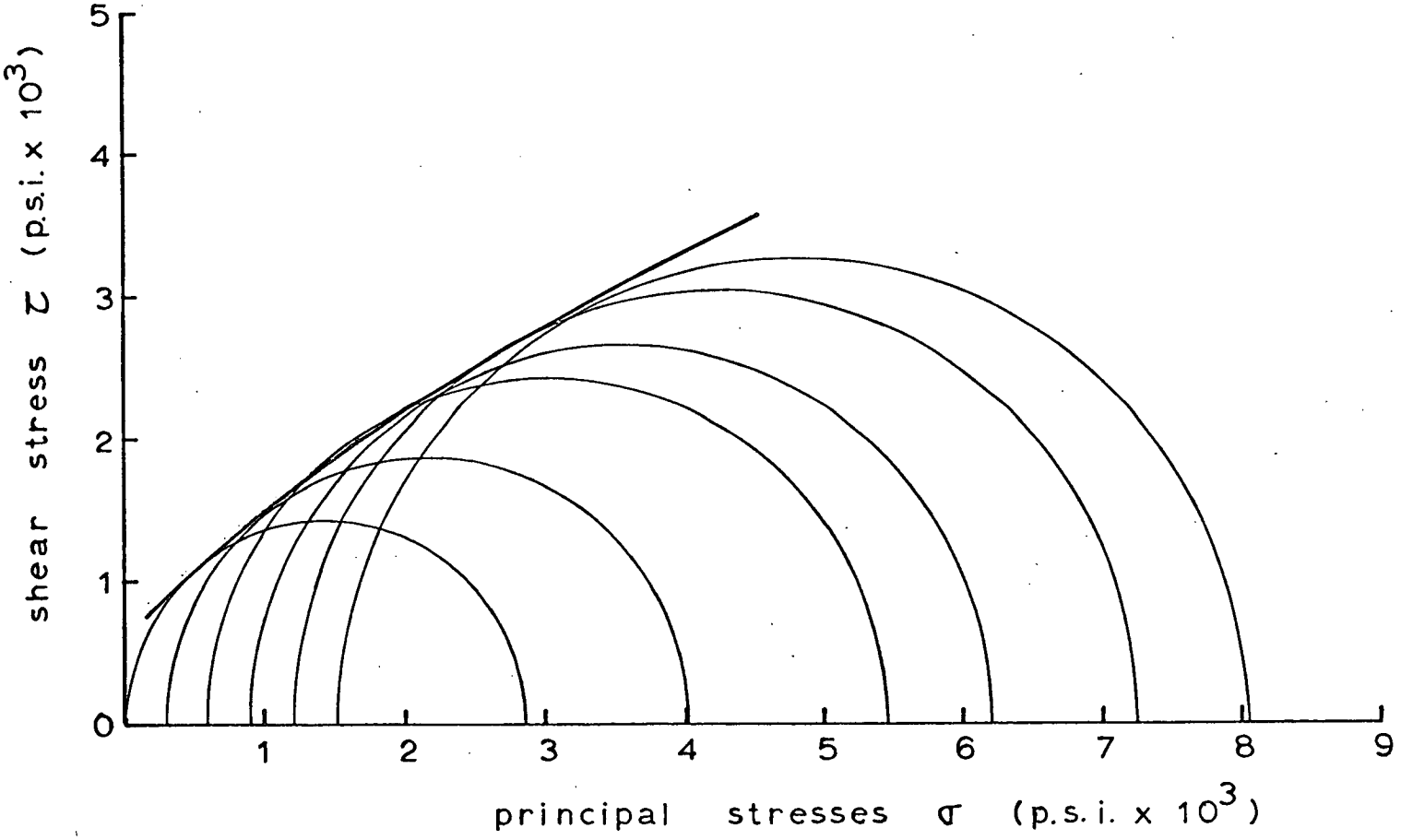

Fig 5.23 MOHR CIRCLES FOR 1 : 1/4 : 3 MORTAR

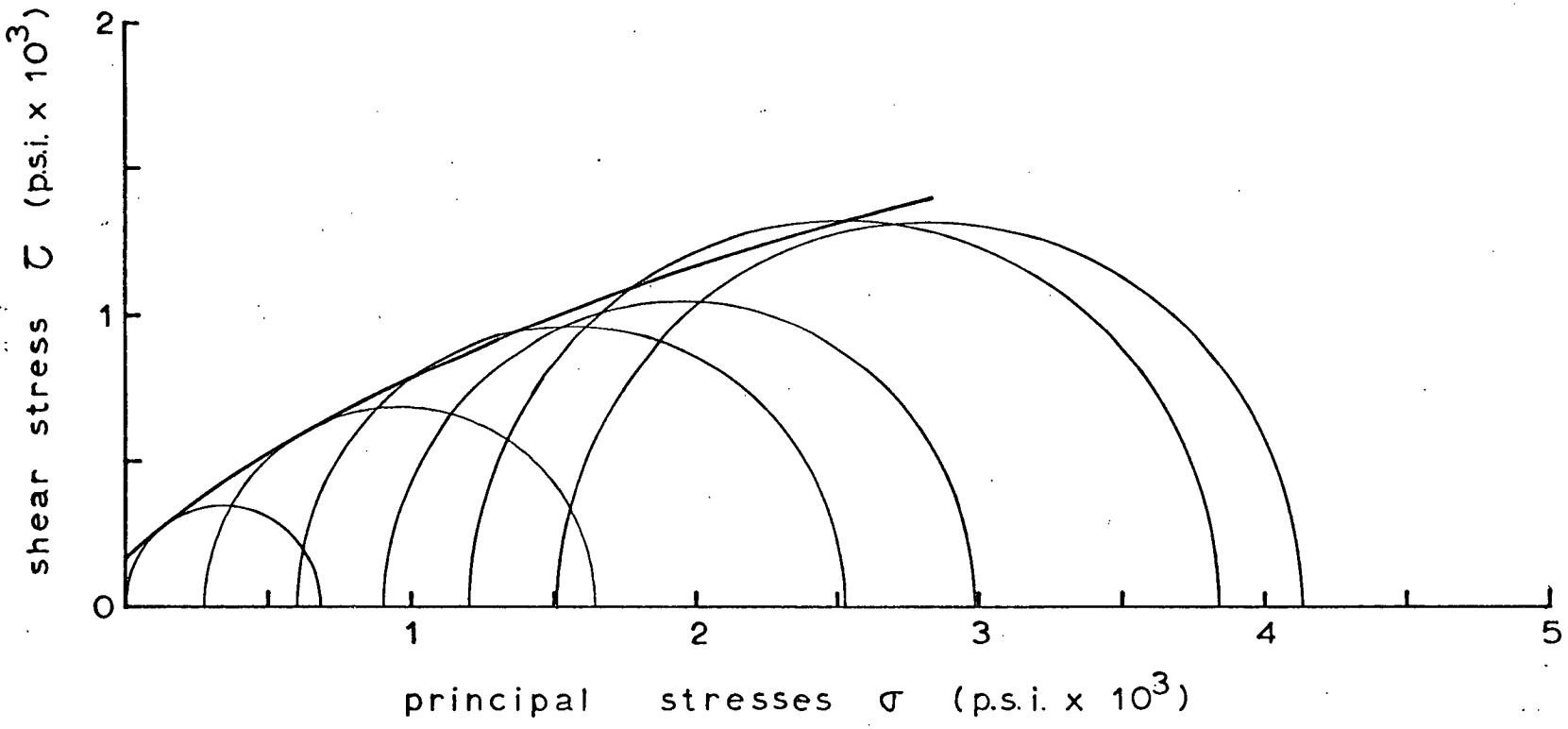

Fig 5.24 MOHR CIRCLES FOR 1:1:6 MORTAR

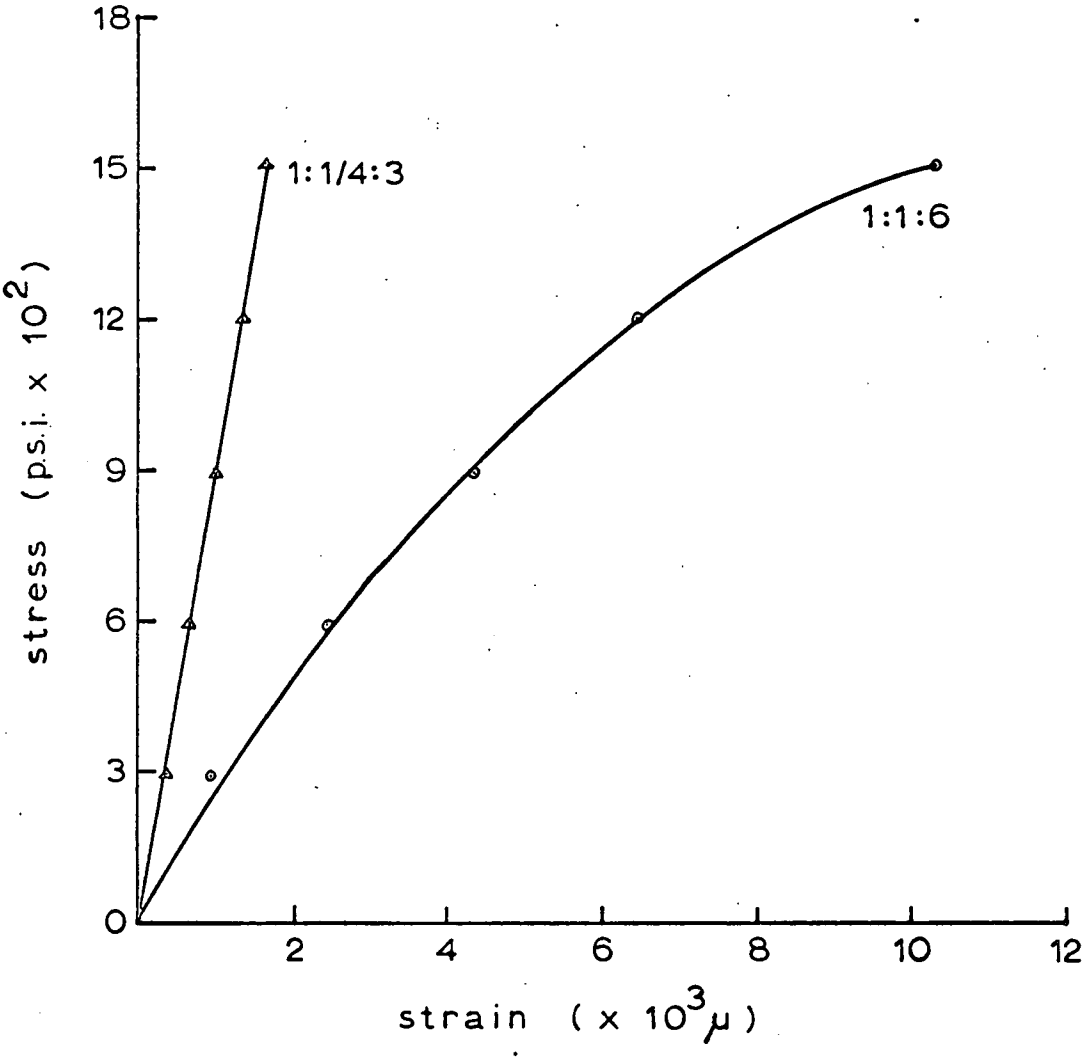

Fig 5.25 VOLUMETRIC STRESS – STRAIN RELATIONSHIP UNDER ALL – ROUND COMPRESSION

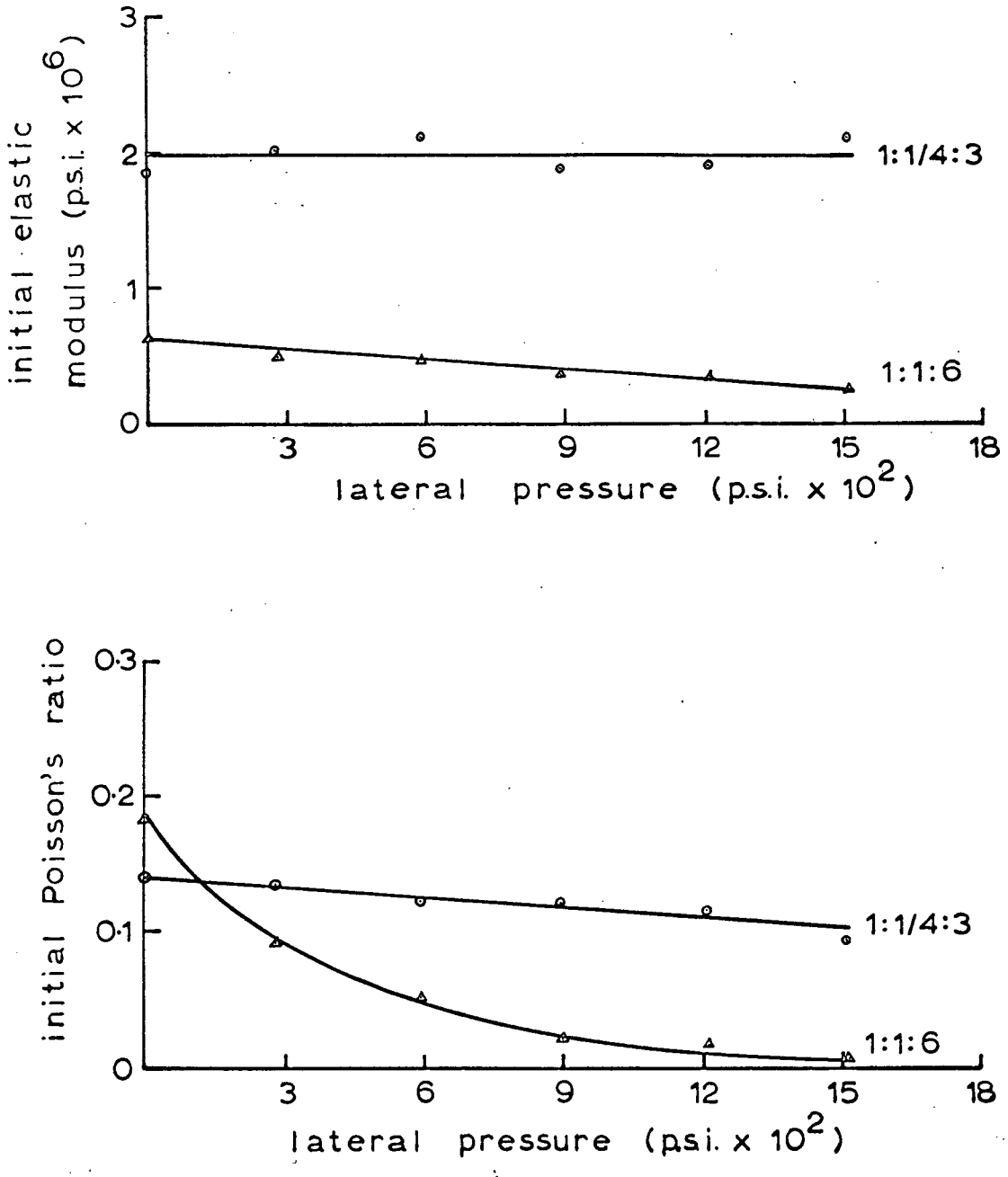

Fig 5.26 EFFECT OF LATERAL PRESSURE ON ELASTIC MODULUS & POISSON'S RATIO OF MORTAR

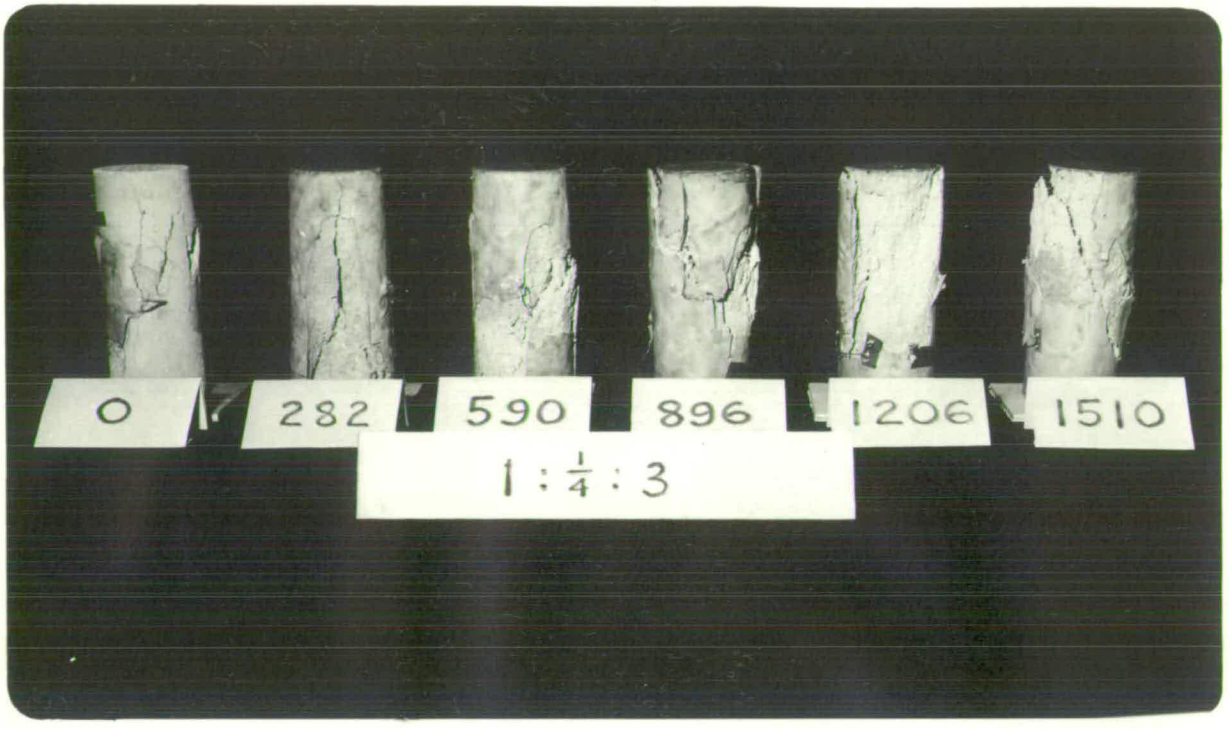

Fig 5.27 CRACK FORMATION IN 1:¼:3 MORTAR SPECIMENS

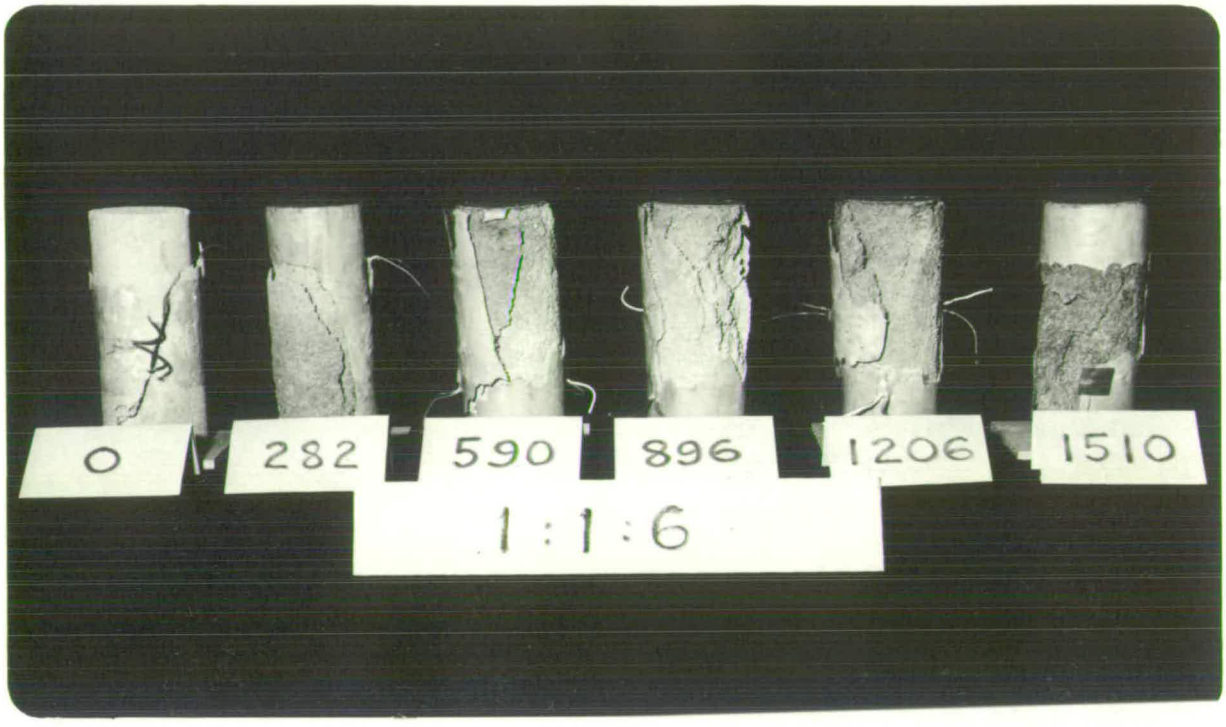

Fig 5.28 CRACK FORMATION IN 1:1:6 MORTAR SPECIMENS

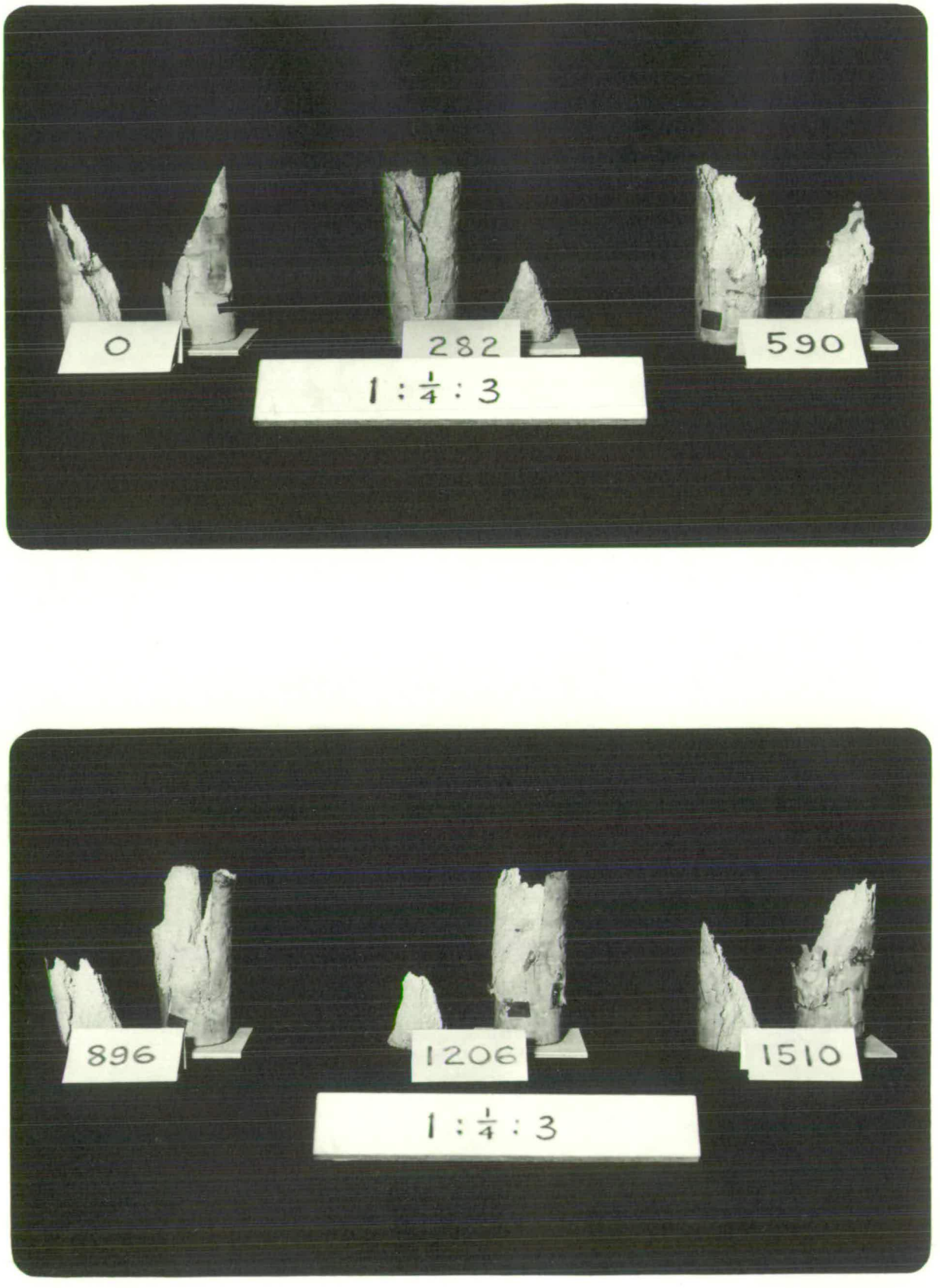

Fig 5.29 INTERNAL FRACTURE IN 1:¼:3 MORTAR SPECIMENS

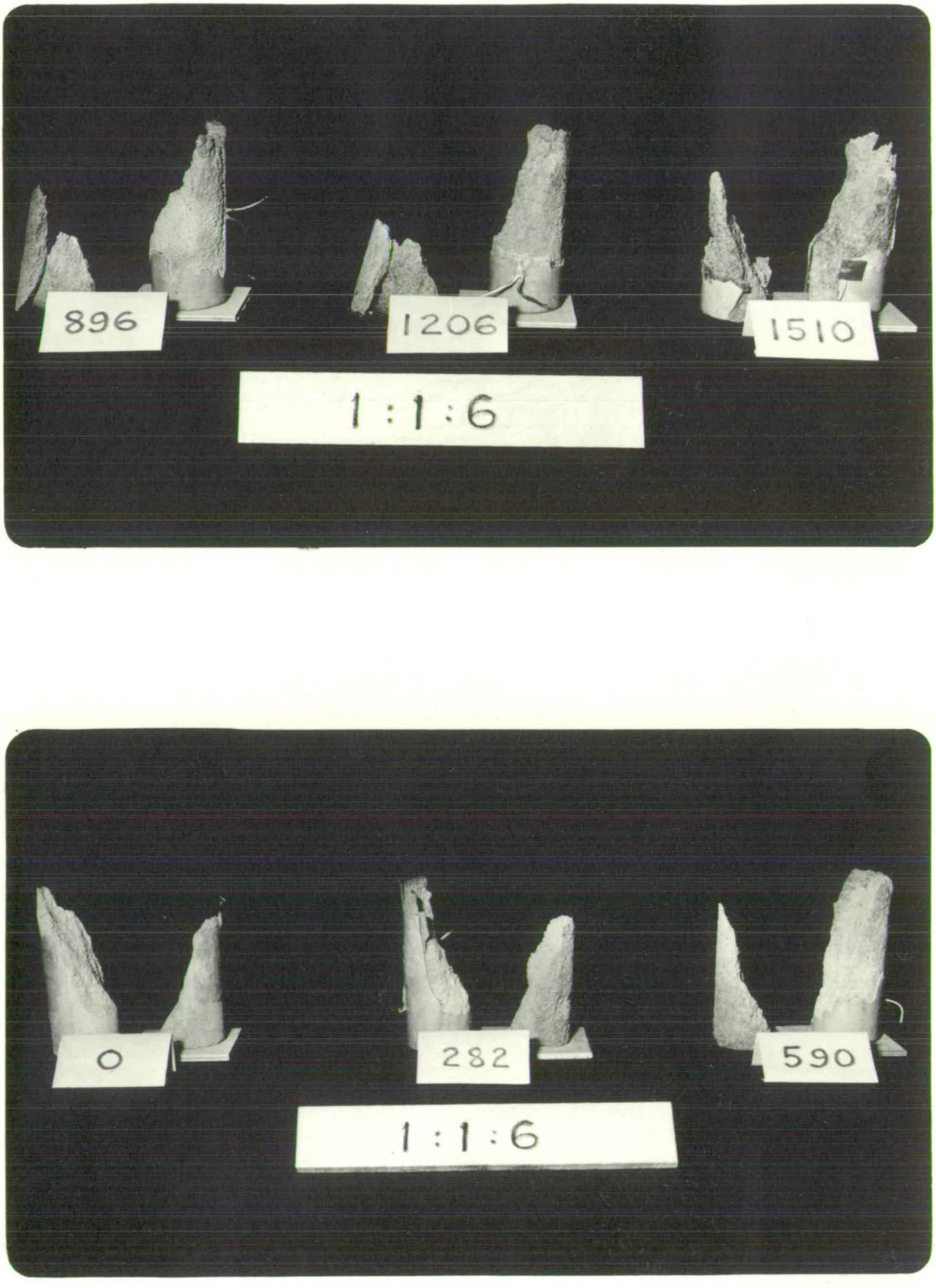

Fig 5.30 INTERNAL FRACTURE IN 1:1:6 MORTAR SPECIMENS

crushing occurred in the vicinity of the failure surface for highly confined specimens.

5.6 DISCUSSION OF RESULTS

The effect of a confining pressure on a brickwork mortar specimen in triaxial compression is to produce a higher ultimate strength and an increased ultimate strain.

The increase in ultimate strength of brickwork mortar with increasing lateral pressure agrees well with the test data of Smith & Brown[51] and Campbell-Allen[12] on cement mortar, as seen in Fig. 22. However, the increase is less than that obtained for concrete. The results of Balmer[2], Akroyd[1], Gardner[20] and Hobb[26] on the triaxial compression of concrete are also indicated in Fig. 5.22. Details of these mortar and concrete mixes may be found in Table 2.2.

The principal stress relationship for brickwork mortar is not linear for the range of lateral pressure tested, and with increasing lateral pressure, the principal stress curve shown in Fig. 5.22 on a dimensionless plot flattens slightly. The principal stress relationship may be defined by the expression:

$$\left(\frac{\sigma_1}{\sigma_o}\right) = 1 + 2.91 \left(\frac{\sigma_3}{\sigma_o}\right)^{0.805} \qquad \text{.....(5.1)}$$

where

σ_1 = major principal stress,

σ_3 = minor principal stress,

σ_o = uniaxial compressive strength.

Of considerable interest is the change in the shape of the stress-strain curve with increasing lateral pressure. The uniaxial compression stress-strain curve for the initial part up to its discontinuity point i.e. 40 to 60% of ultimate strength, is reasonably straight.

At/

At a stress beyond its discontinuity point, major microcracking - the result of bond failures at the aggregate-paste interfaces - takes place leading to increased strains corresponding to a flattening of the stress-strain curve towards ultimate failure.

However, as the confining pressure increases, the profile of the stress-strain curve alters. The curvature occurs in the initial portion of the curve which then approaches ultimate at a straight incline. The stress-strain curve for 1:1:6 mortar at 1510 lbf/in^2 (10.34 MN/m^2) cell pressure is remarkably linear up to ultimate. It is probable that the mechanics of deformation in mortar at high triaxial compression is principally one of inter-particle friction, for the high level of deformation of mortar would have largely destroyed the aggregate-mortar bond. Support for this view comes from an examination of the volumetric stress-strain relationship in Fig. 5.25 for the 1:1:6 mortar where the bulk modulus decreases at high confining pressure. This suggests a re-orientation of the structural matrix within the mortar at high confining pressure, involving a breakdown of the aggregate-mortar bond, resulting in a much larger volumetric strain increase.

Furthermore, a visual examination of failed specimens shows that whereas the failure surface for the unconfined specimen was one of clean fracture, considerable crushing occurred in the region of the fracture plane for highly confined specimens.

As the stress-strain curves for mortar in a state of triaxial compression is non-linear, the values of the elastic modulus and Poisson's ratio vary according to the level of the axial stress applied. Fig. 5.26 shows the extent to which the lateral pressure affects the initial Poisson's ratio. In the case of the 1:1:6 mortar where the ratio of lateral pressure to its uniaxial compression strength is/

strength is high, the reduction in the values of the elastic modulus and the Poisson's ratio is more significant. These characteristics are consistent with the large volumetric contraction obtained for the 1:1:6 mortar with increasing cell pressure.

5.7 SUMMARY

1. The 2.78 in (7 cm) cube strength for brickwork mortar cast in accordance with the BS 4551[11] is about 1.4 times higher than its uniaxial (cylinder) compressive strength.
2. Mortar specimens air-cured for 14 days showed a drastic reduction in strength, about half the value of those water-cured. The actual strength of mortar joints in brickwork will be between these values, depending upon the water absorption of the bricks and how well the mortar is cured.
3. The degree of saturation in mortar joints of brickwork after 14 days is low, and hence the presence of pore water pressure, if any, in mortar joints of loaded brickwork is of no consequence.
4. In order to attain the desired degree of electrical insulation for resistance gauges on test specimens under triaxial compression, it is necessary to use a non-conducting fluid, such as a thin oil, in the triaxial cell.
5. The effect of cell pressure up to 1500 lbf/in^2 (10.34 MN/m^2) on the resistance gauges mounted on test specimens in triaxial compression is minimal.
6. The increase in ultimate strength of brickwork mortar in triaxial compression with increasing confining pressure is much the same as that obtained for cement mortar but is less than that obtained for concrete. The principal-stress relationship is given by the expression:

$$\left(\frac{\sigma_1}{\sigma_o}\right) = 1 + 2.91\left(\frac{\sigma_3}{\sigma_o}\right)^{0.805} \qquad \text{.....(5.1)}$$

where

σ_1 = major principal stress

σ_3 = minor principal stress

σ_o = uniaxial compression strength.

7. An all-round confining pressure on mortar in excess of its uniaxial compression strength causes a dislocation of the structural matrix of the mortar as revealed by a decrease in bulk modulus with increasing lateral pressure.

8. The deformation characteristics of mortar under a state of high triaxial compression depend largely on the action of interparticle friction.

CHAPTER 6 - LATERAL STRESS DISTRIBUTION WITHIN BRICK AND MORTAR ELEMENTS IN BRICKWORK PRISM UNDER AXIAL COMPRESSION

6.1 FINITE ELEMENT ANALYSIS

It was stated in Section 1.3 that the stress distribution along the brick-mortar interface and within the brick and mortar elements in a brickwork prism subject to axial compression is presently not clear. In this chapter, an attempt will be made to define these stresses by theory using the method of finite element analysis for which a computer programme exists in the Department of Civil Engineering, University of Edinburgh for the case of plane stress and plane strain problems.

It is doubtful whether it is feasible to undertake experimental work on this problem since it will be very difficult to measure strains with sufficient accuracy in the brick and mortar elements.

6.1.1 The Philosophy of the Method

In the finite element method, the actual structure is divided into a finite number of small elements which are assumed to be connected only at the nodal points. The stresses acting along the edges of each of the elements are replaced by stress resultants which act at the nodal points. Application of the equations of equilibrium to the forces acting at the nodal points will lead to a number of simultaneous equations which can then be solved by the computer.

The accuracy of the finite element method depends upon how closely the actual structure is represented by the approximate structure consisting of these elements, and also upon the size of the elements selected.

6.1.2 An Outline of the Solution/

6.1.2 An Outline of the Solution

Only a very brief outline of the finite element solution is given here. Interested readers are referred to the work of Kalita[31] for details concerning this particular programme, and of Zienkiewicz and Cheung[63] for general information concerning the finite element method of analysis.

This finite element programme uses triangular elements. The strains within each of the elements are assumed constant.

The first step of the solution is to determine the stiffness matrix of each element, which is an expression for the nodal forces resulting from unit corner displacements. The procedure, in its order of solution, is as follows, where the subscript 'e' denotes an element:

1. Strain-Displacement Relationship

$$[\varepsilon]^e = [B]\,[\delta]^e \qquad \text{.....(6.1)}$$

where

$[\varepsilon]^e$ = strains in the element

$[B]$ = matrix which is a function of the co-ordinates of the nodal points of the element

$[\delta]^e$ = displacements of the nodal points

2. Stress-Strain Relationship

$$[\sigma]^e = [D]\,[\varepsilon]^e \qquad \text{.....(6.2)}$$

where

$[\sigma]^e$ = stresses in the element

$[D]$ = matrix which is a function of the elastic constants of the element material

3. Stress Resultants (Nodal Forces)-Stress Relationship

$$[F]^e = A[B^T][\sigma]^e \qquad \text{.....(6.3)}$$

where

$[F]^e$ = nodal forces in the element

A = area of the element

$[B^T]$ = transpose of the matrix $[B]$

4. Element Stiffness

$$[F]^e = [k][\delta]^e \qquad \text{.....(6.4)}$$

where

$[k]$ = stiffness matrix for the element

From equations (6.1), (6.2), (6.3) and (6.4)

$$\underset{6x6}{[k]} = A\underset{6x3}{[B^T]}\underset{3x3}{[D]}\underset{3x6}{[B]} \qquad \text{.....(6.5)}$$

For the case of plane stress or plane strain problems, the size of the various matrices are indicated in equation (6.5).

After the stiffness matrix for each of the elements is developed, the stiffness of the complete structure can be found by a systematic addition of stiffnesses of all the elements in the system. Therefore, for the complete structure,

$$[F] = [K][\delta] \qquad \text{.....(6.6)}$$

where

$[F]$ = forces at all nodal points

$[K]$ = stiffness matrix for the complete structure

$[\delta]$ = displacements for all nodal points

6.1.3 The Technique of Recycling

In any given finite element computer programme, there is a limit to the number of elements it can handle. (In this programme, the number of elements is restricted to 450.) In problems involving stress concentrations, the usual solution is to arrange an element mesh for the structure within/

structure within the permissible limit so that the element size approaching areas of high stress gradient is finer, but the resulting number of different sized elements will often entail considerable work in the data preparation. A better method is to employ the technique of recycling.

In this technique, the complete structure is first analysed containing as many elements as the programme allows. Then, a portion of the structure, for which a greater accuracy of results is required, is severed from the structure at a convenient location, and by assigning the appropriate displacement values along the severed boundary obtained from the previous analysis, the sub-structure is divided into further elements and reanalysed. This process can go on indefinitely until the desired accuracy is achieved.

It is evident that by skilful design in the layout of the element mesh so that it may be easily duplicated for subsequent analysis, the amount of effort spent on data preparation in a recycle is marginal. Moreover, the number of times of recycling is virtually unlimited, and it is on this score that the technique of recycling is indeed a powerful tool in finite element analysis.

6.2 ANALYSIS OF LATERAL STRESS DISTRIBUTION IN BRICKWORK PRISM

The method of finite element analysis will now be applied to determine the lateral stress distribution within the brick and mortar elements in a brickwork prism subject to axial compression. The analysis will be carried out for both the frontface and the endface sections of the brickwork prism for the condition of plane stress.

Fig. 6.1(a) and (b) show the front and the end faces of a brickwork prism axially loaded. A standard size brick measuring $8^{5}/_{8}$ in x $4^{1}/_{8}$ in x $2^{5}/_{8}$ in/

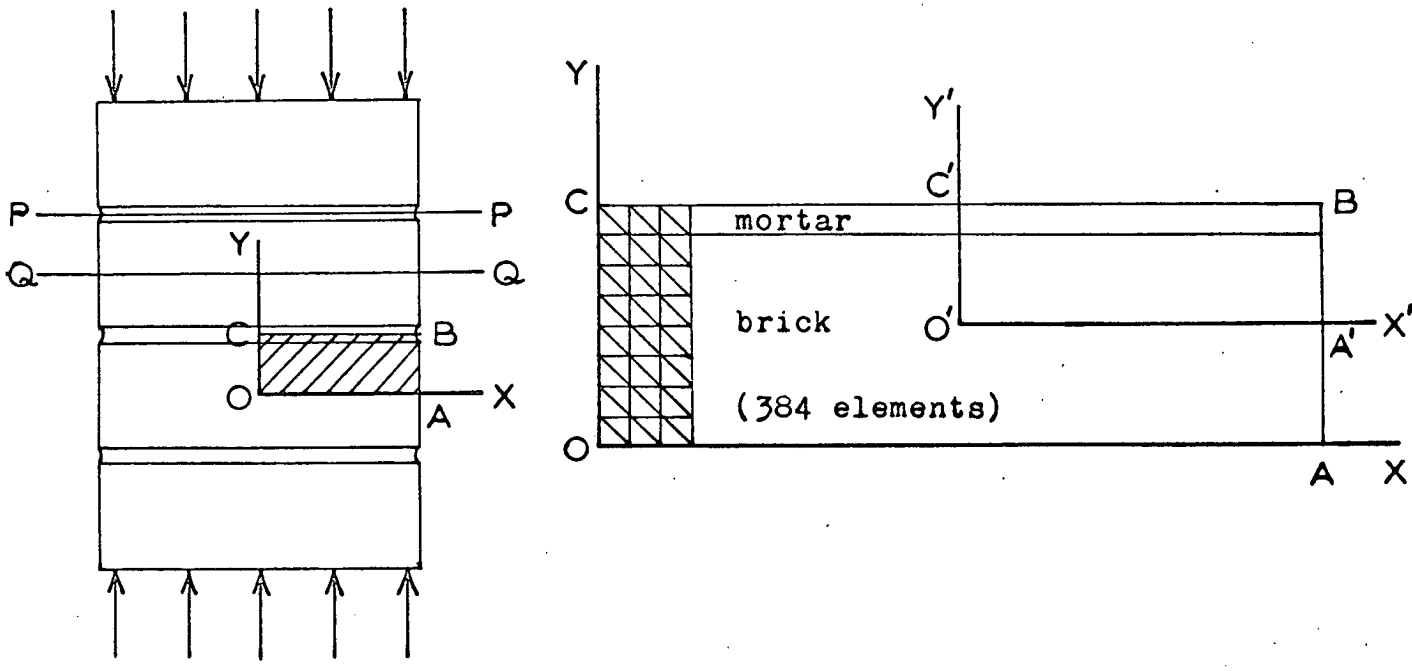

Fig 6.1(a) Brickwork Prism ; Front Face

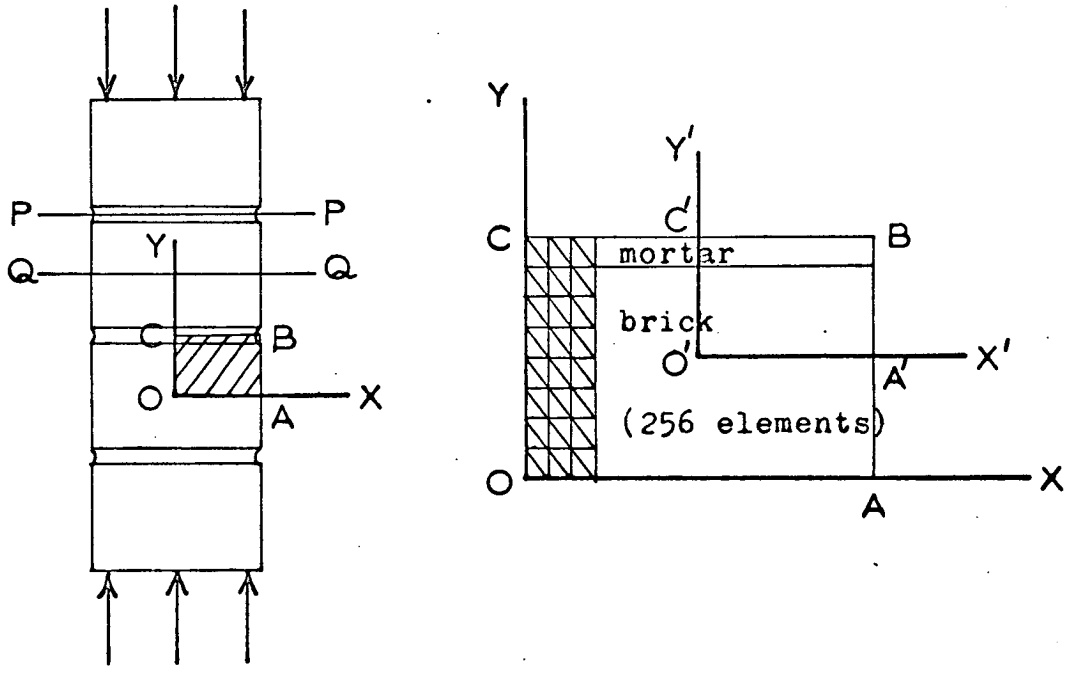

Fig 6.1(b) Brickwork Prism; End Face

x $2\frac{5}{8}$ in (21.9 cm x 10.5 cm x 6.7 cm) and a $\frac{3}{8}$ in (0.95 cm) thick mortar joint have been assumed. The ratio of brick to mortar thickness is thus seven.

In consideration of the compatibility in deformation, all horizontal planes such as planes PP and QQ which pass through the mid-depths of the mortar joint and the brick element respectively (except perhaps for the top and bottom bricks in contact with the rigid loading platens) remain plane and horizontal under the applied load.

On account of the symmetry of the problem, it is necessary to analyse only a section of the brickwork, OABC, shaded in Fig. 6.1(a) and (b) which forms a quarter each of the mortar joint and the brick. The displacement in the X-direction for all points in the structure along the OY axis, and the displacement in the Y-direction for all points in the structure along the OX axis are always zero.

The division into finite elements, 384 elements for the front face and 256 elements for the end face, are also indicated in Fig. 6.1(a) and (b).

In the analysis, an arbitrary but small uniform vertical compressive displacement is given to the plane CB in the brickwork structure OABC. This is equivalent to applying a vertical compression on the structure with the additional provision that the plane CB remains plane and horizontal under load.

Arbitrary values for the elastic properties of brick and mortar have been assumed, since the purpose of the analysis is not concerned with determining absolute values of stresses. For the record, the values of the elastic properties used in the analysis are:

elastic modulus of brick = 1.0×10^6 lbf/in^2 (6.895×10^3 MN/m^2)

Poisson's ratio of brick = 0.1

elastic/

elastic modulus of mortar = 0.1×10^6 lbf/in^2

Poisson's ratio of mortar = 0.1

A stress concentration is found to exist at the brick-mortar interface near the edge AB. Therefore, in order to attain a satisfactory degree of accuracy of results in that region, the technique of recycling has been applied to the top right quarter of the structure, designated by the section O'A'BC' in Fig. 6.1(a) and (b), using the same mesh layout as for section OABC.

The results of the analysis for both faces of the brickwork prism are illustrated in Figs. 6.2 and 6.3, in which the magnitude of the lateral stresses are given in terms of the ratios of the actual stress to the average stress which would exist if the lateral stresses are uniformly distributed throughout the depth of brick. The vertical compressive stresses are not shown.

The significant points to note from the analysis are:

1. The stress distribution along the brick-mortar interface is not uniform as is commonly believed, but is sharply concentrated at the edges of the interface, producing large lateral tensile stresses in the brick near the edges.
2. The lateral tensile stresses in the brick on the end-face section, where the width/depth ratio is smaller, are higher in value in this region and more concentrated than those on the front-face section of the brick.

Ogunlesi[44] in a somewhat analogous experiment in photoelasticity obtained similar results. In his experiment, which is an attempt to simulate thermal stress transfer in plates, two rectangular Araldite strips were stuck to a third piece which was held in tension, one on each of its sides, see Fig. 6.4(a). After the bond had set, the tension in the middle/

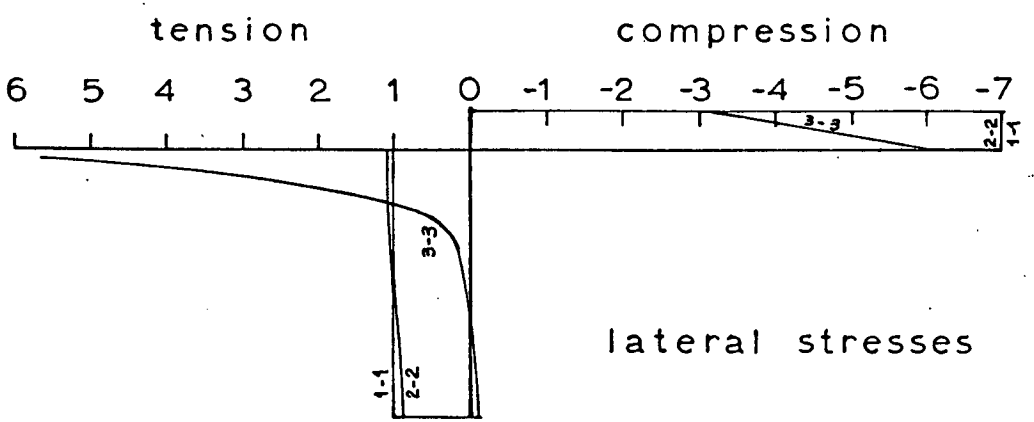

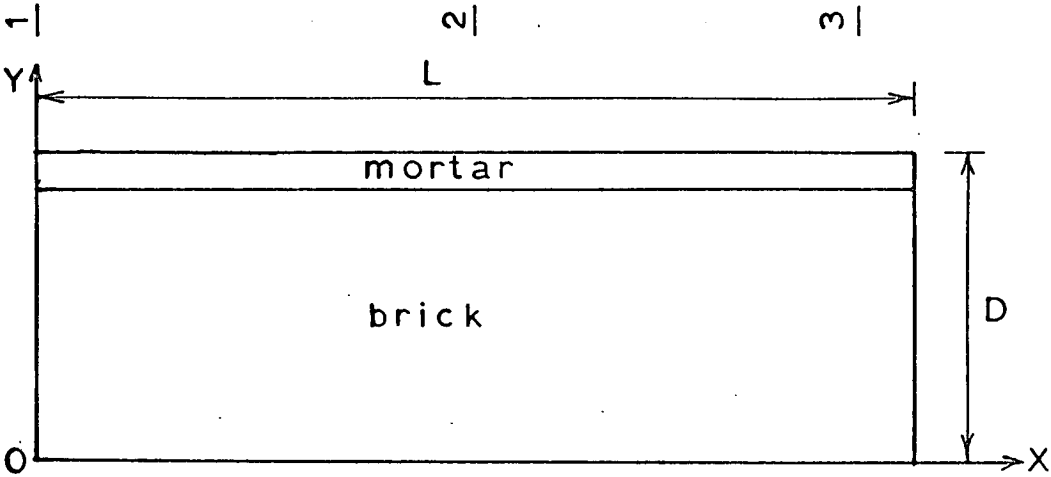

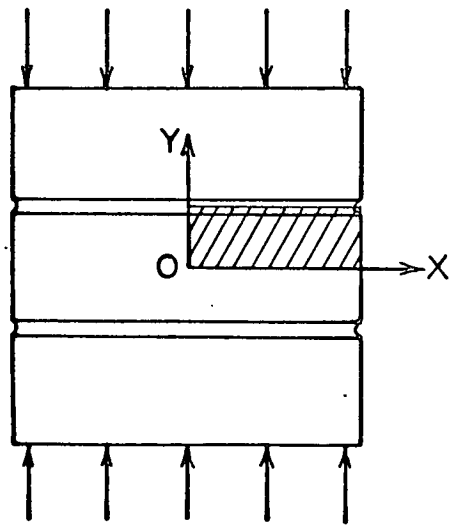

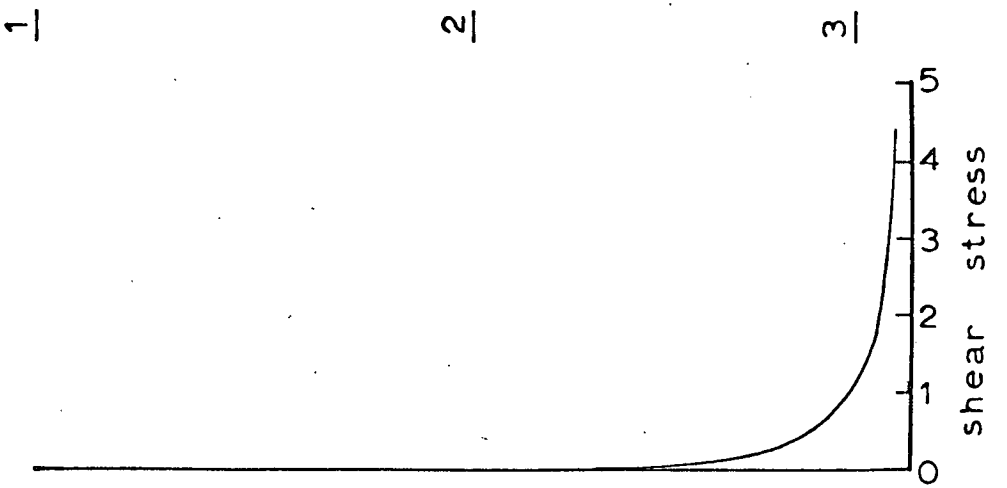

shear stress along mortar-brick interface

Fig 6.2 Stress Distribution in Brickwork under Compression. L/D = 2·9

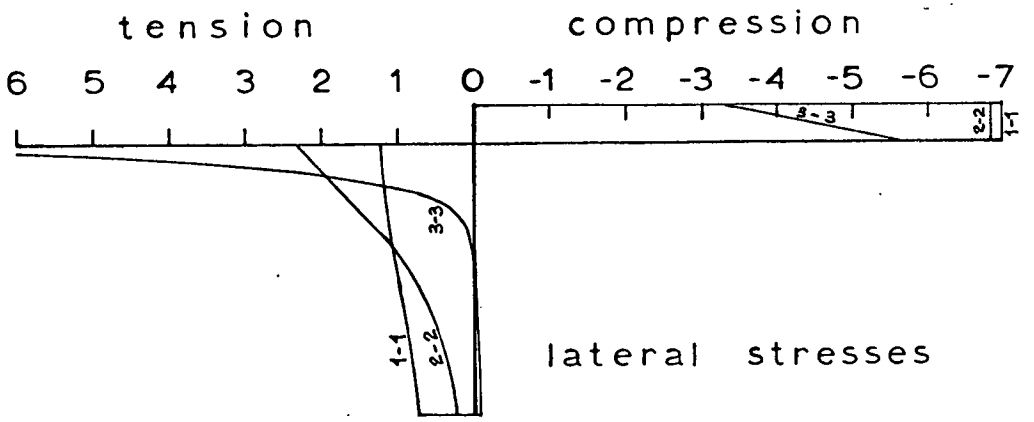

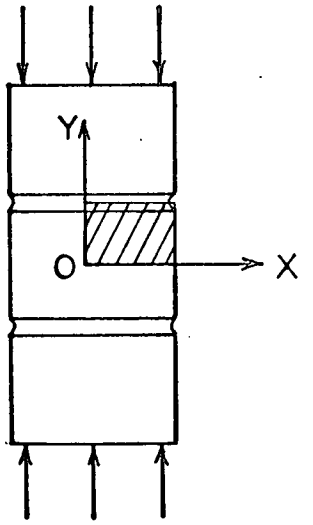

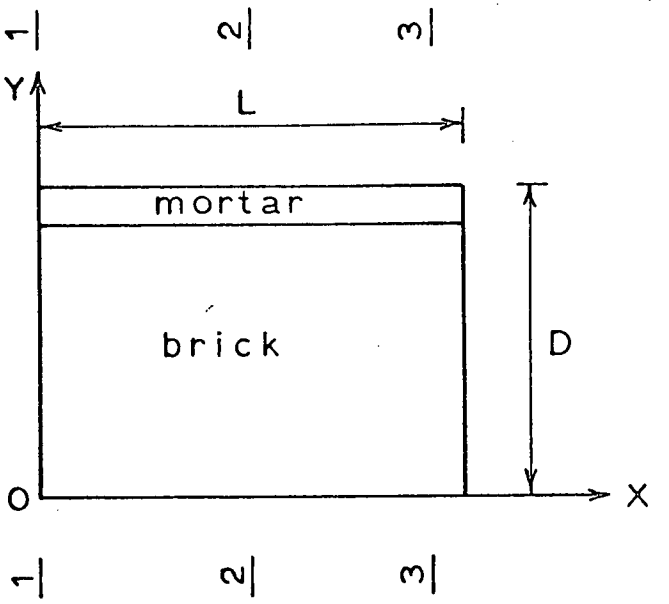

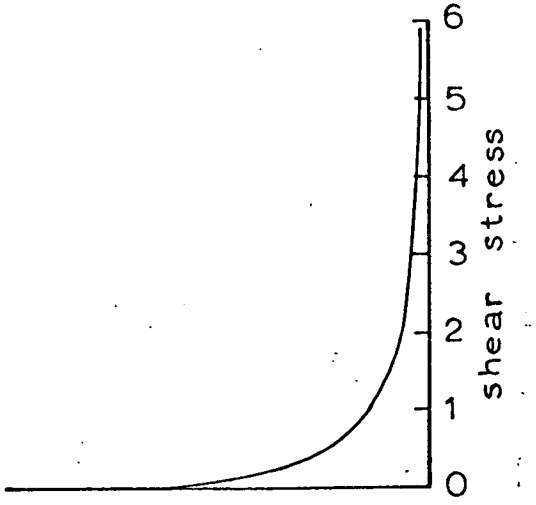

shear stress along mortar-brick interface

Fig 6.3 Stress Distribution in Brickwork under Compression. L/D = 1·4

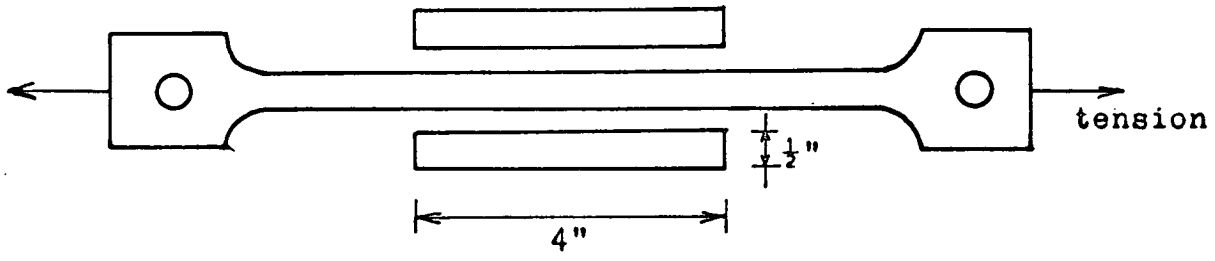

(a) Araldite Specimens, 1/3 in thick

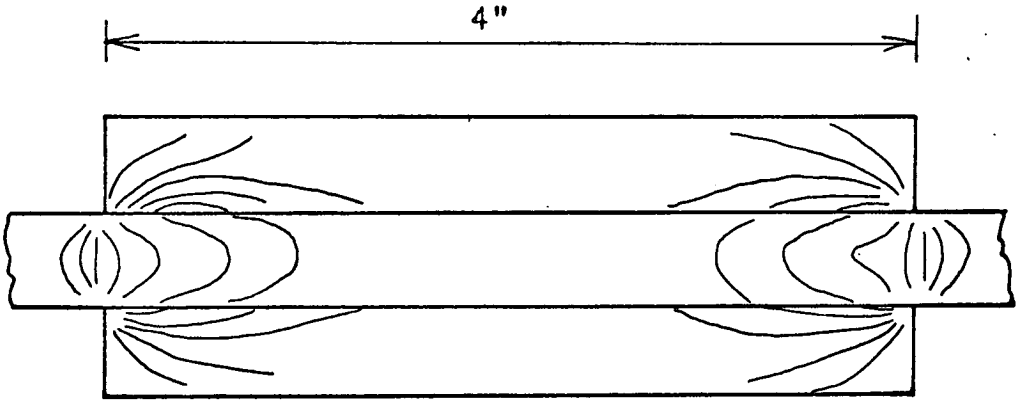

(b) Photoelastic Stress Fringes

Fig 6.4 Photoelastic Analysis of Stress Transfer in Plates (by Ogunlesi)

tension in the middle piece was released. The resulting stress distributions in the specimens in terms of stress fringes may be seen in Fig. 6.4(b). Stress concentration occurs at the edges of the interfaces.

6.3 SIGNIFICANCE OF THE THEORETICAL RESULTS

The theoretical results suggest that the initial tensile crack in a brickwork prism loaded axially to failure is likely to be along a plane at the edge of the end face in the direction of the brick length. This is found to be true in compression tests on numerous brickwork prisms without exception. Examples of failure in brickwork prisms are shown in Fig. 6.5. This mode of failure, which is indeed a tensile failure, has often been described as spalling failure in brickwork.

However, in practice there will probably be considerable stress redistribution approaching failure since these materials, especially mortar, are inelastic near ultimate stress. It is not possible to determine the actual stress distribution at failure. However, it was observed in the crushing tests on brickwork prisms that the stress at which spalling occurred in the majority of cases was very close to the ultimate strength of the prism, suggesting a more or less uniform stress condition at failure.

Tensile cracking which is usually observed in planes passing through the vertical mortar joints in an axially loaded brick wall has led to the erroneous belief that the stresses causing failure occur along the mid-length section of the brick. The tensile cracking of the brick at its mid-length is solely due to the existence of stress concentration in the brick in that region created by the presence of the mortar perpends. These cracks occur at a stress considerably below the ultimate strength of brickwork.

6.4 SUMMARY

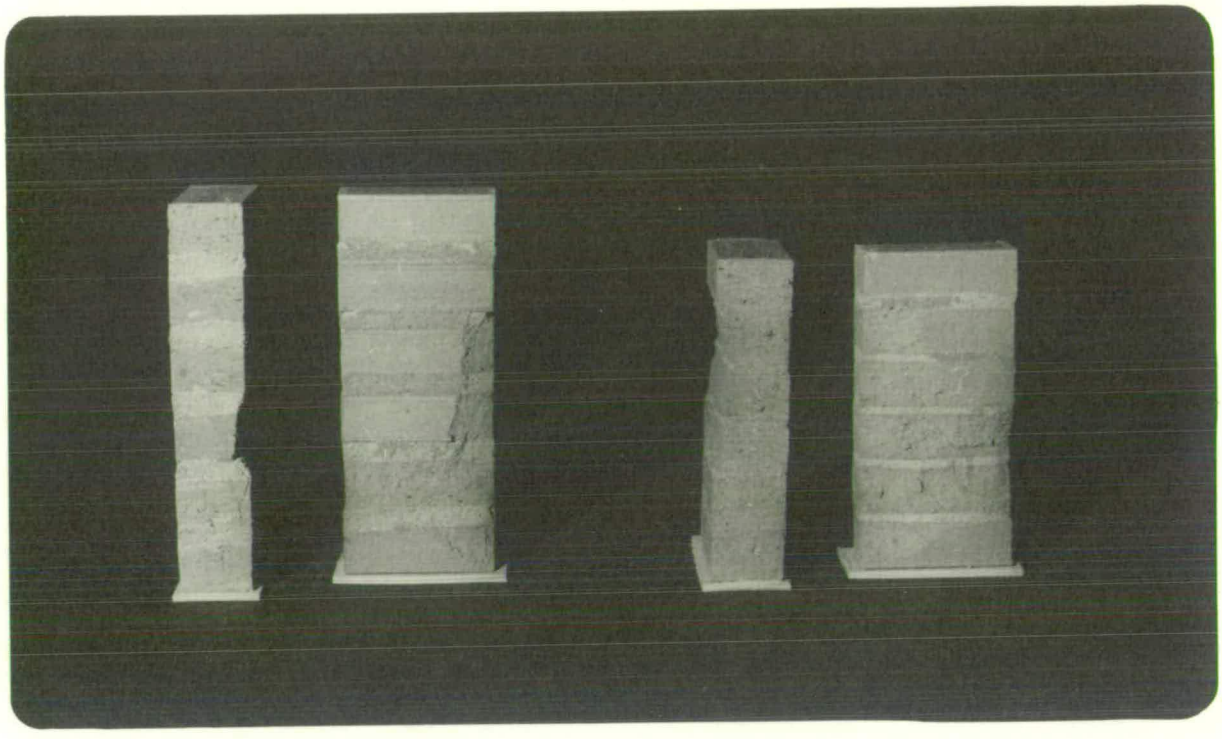

Fig 6.5 FAILURE MODE IN BRICKWORK PRISMS UNDER AXIAL COMPRESSION

6.4 SUMMARY

1. Finite element analysis for plane stress condition is applied to determine the lateral stress distribution within the brick and the mortar elements in a brickwork prism subject to axial compression, on both the front-face and end-face sections.
2. The technique of recycling is employed to achieve a higher degree of accuracy of results in regions where stress concentration exists.
3. The theoretical analysis reveals the existence of a stress concentration at the edge of the brick-mortar interface, causing high stress gradients in brick and mortar in that region.
4. The end-face section of the axially loaded brickwork prism, where the width/depth ratio of brick is lower, contains higher values of lateral stresses in the region of the stress concentration than the front-face section, and consequently theory suggests that the initial tensile cracking in the brickwork prism will occur along a plane at the edge of the end face in the direction of the brick length.
5. Experimental observation of the location of the initial tensile cracking in numerous crushing tests on brickwork prisms confirms the theoretical prediction.
6. In practice, a considerable stress redistribution will take place prior to failure on account of the inelastic behaviour of brick and mortar.

CHAPTER 7 - A FAILURE CRITERION FOR BRICKWORK IN AXIAL COMPRESSION

7.1 INTRODUCTION

The existing failure theories describing the compressive strength of brickwork, which have been derived largely or wholly on the assumption of an elastic behaviour in brick and mortar, have not been able to account for the compressive strength of brickwork in quantitative terms. These failure theories are useful only in so far as they offer a qualitative concept of the mechanics of failure in axially-loaded brickwork.

As an alternative to the elastic theory, a "strength" approach towards the development of a failure criterion for brickwork in compression is presented in this chapter. In this analysis, the brickwork compressive strength is determined by the interaction of the strength properties of brick and mortar in their particular state of complex stresses that exist in axially-loaded brickwork.

The investigation has been confined to a study of the behaviour of axially-loaded stack-bonded brickwork prisms, as illustrated in Fig. 1.1(a), using solid bricks. This eliminates consideration of the influence of mortar perpends, perforations and frogs on brickwork compressive strength.

The state of stress in a brick element in an axially-loaded brickwork prism is a combination of a vertical compression and bi-lateral tension, and the corresponding state of stress in the horizontal mortar joint is one of triaxial compression, as indicated in Fig. 1.1(b) and 1.1(c) respectively. The bi-lateral stresses are the result of the different strain characteristics of the two materials. The establishment of the proposed failure criterion requires information concerning the behaviour of brick and mortar under these combined stresses.

The combined stresses for brick have been simplified to a biaxial state of compression-tension, since it was not possible to devise a testing method which could produce a state of compression-tension-tension stresses. The behaviour of brick material under biaxial compression-tension stresses have been investigated in Chapter 3 using the method of direct tension and compression on one-third scale model bricks. A second series of biaxial compression-tension strength tests was also carried out on clay pipes subject to internal pressure and axial compression, as described in Chapter 4.

A comprehensive study into the behaviour of brickwork mortar of 1:$\frac{1}{4}$:3 and 1:1:6 mixes in a state of triaxial compression with strain measurements was reported in Chapter 5.

The lateral stresses in axially-loaded brickwork, which is on account of the different strain properties of brick and mortar, act along the interfaces of the brick unit and the mortar joint. The distribution of these stresses have been analysed by the finite element method in Chapter 6.

All the necessary information required for the formulation of the proposed failure criterion for brickwork in compression have been ascertained, and it is now possible to develop the proposed criterion which is explained in the following section. Finally, the theory is tested against experimental results on the crushing strength of brickwork in the concluding part of this chapter.

7.2 DEVELOPMENT OF PROPOSED FAILURE THEORY

7.2.1 Graphical Solution

The development of stresses in a brick element in a brickwork prism subject to axial compression is illustrated in Fig. 1.2 which shows an assumed failure envelope for brick in biaxial compression-tension, since the/

since the lateral tensile stresses in the x- and z-directions, σ_x and σ_z, are equal. c_o and t_o are the compression and tensile strengths of brick respectively. Any state of stress to the right of this curve denotes failure.

As the vertical compression acting on the brickwork prism increases, the state of stress in the brick element proceeds along the dashed line OA in Fig. 1.2. Failure occurs within the brick element when the line OA intersects the failure envelope at A, and hence the compressive strength of the brickwork prism is given by the ordinate of the point A. The stress path taken by the line OA depends on the properties of the mortar joint under triaxial compression. For a weaker mortar whose lateral strain is greater under load, the stress path travels along the lower line OB in Fig. 1.2, where B denotes the state of stress within the brick element at failure. Similarly, the compressive strength of the brickwork prism is given by the ordinate of the point B.

It is not necessary in the establishment of the proposed failure theory to determine the stress paths OA and OB. The curves A'A and B'B in Fig. 1.2 which intersect the failure envelope for brick at points A and B, represent the state of triaxial compressive stresses in the horizontal mortar joint in an axially-loaded brickwork prism at failure. The determination of these curves is now discussed.

The principal stresses appearing in Fig. 5.21 are the axial and lateral compressions in terms of mortar stresses in axially-loaded brickwork. These are, however, ultimate stresses. It is uncertain whether, at the instant of brick failure in a brickwork prism under compression, the state of triaxial stresses in the mortar joint is at its ultimate.

The state of triaxial stresses in the mortar joint at brickwork failure may be determined from a consideration of the strain compatibility in the brick and mortar elements. The lateral strains in these elements along their common interface are equal, since no slip occurs between these elements. The variation in lateral strains in these elements across a vertical section is small and may be assumed as constant. Therefore, if the ultimate lateral strain in the brick at brickwork failure is known, the triaxial stresses in the mortar at this value of lateral strain may be ascertained from the stress-strain curves of mortar in triaxial compression.

Figs. 7.1 and 7.2 give the relationship between the total axial stress and the total lateral strain for both mortars in triaxial compression, derived from the stress-strain curves in Figs. 5.19 and 5.20, and the volumetric stress-strain relationship on application of the cell pressure in Fig. 5.25. The ultimate tensile strain for brickwork, as obtained in Section 3.3, varies from 150 to 300 micro-units, with a mean value of 225 micro-units. This ultimate tensile strain does not alter under combinations of compression-tension stresses, as observed in tests on clay pipes described in Section 4.4. Therefore, it is reasonable to assume that at brickwork crushing failure, the ultimate lateral tensile strain in brick is approximately 225 micro-units, and this is indicated in Figs. 7.1 and 7.2. The points of intersection of this line with the mortar curves give the values of the triaxial stresses for mortar at the instant of brick failure in axially-loaded brickwork, and these values of the triaxial stresses are plotted in Fig. 7.3, together with the corresponding curves for ultimate stress.

It may/

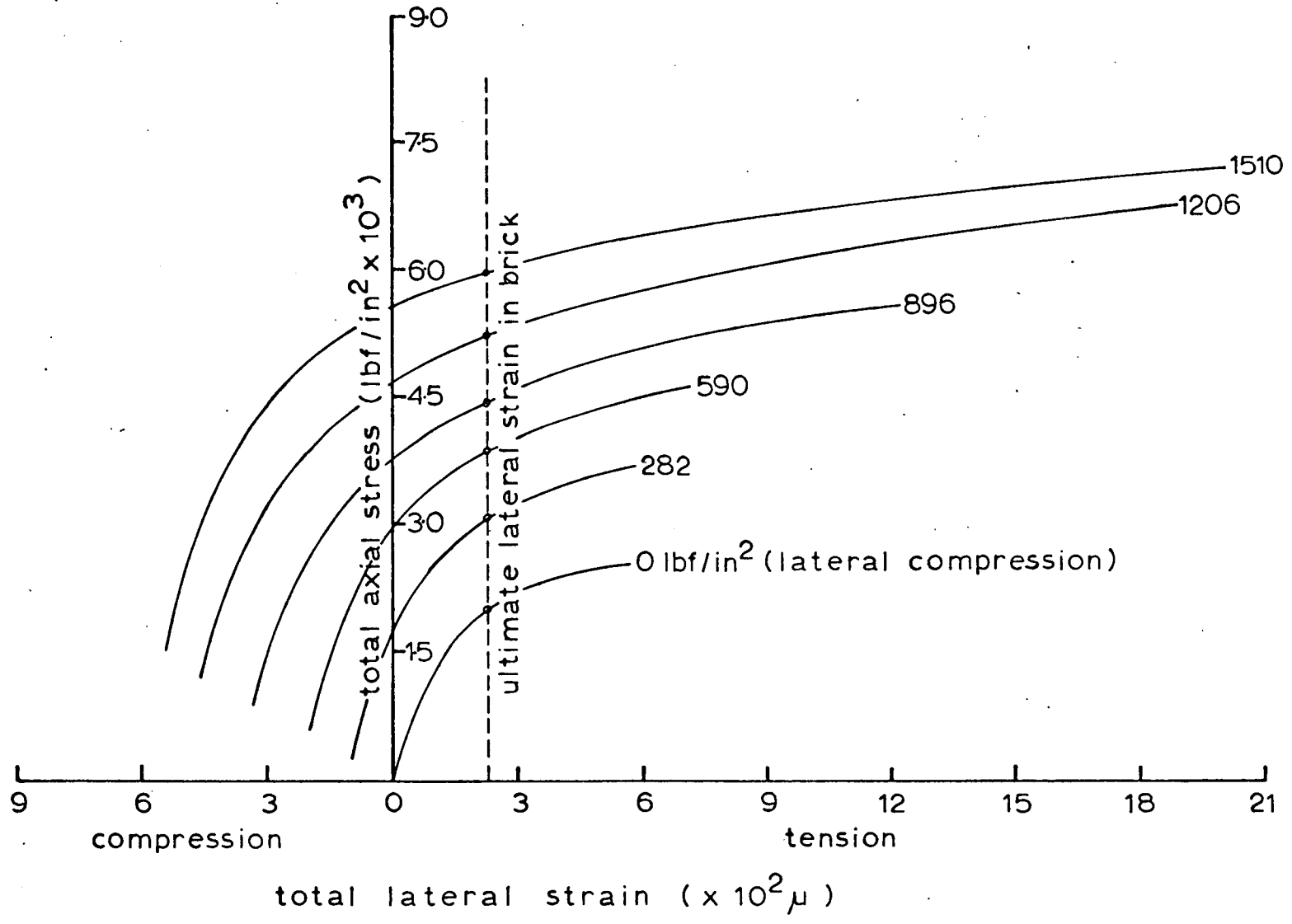

Fig 7.1 Axial Stress – Lateral Strain Relationship for 1:1/4:3 Mortar

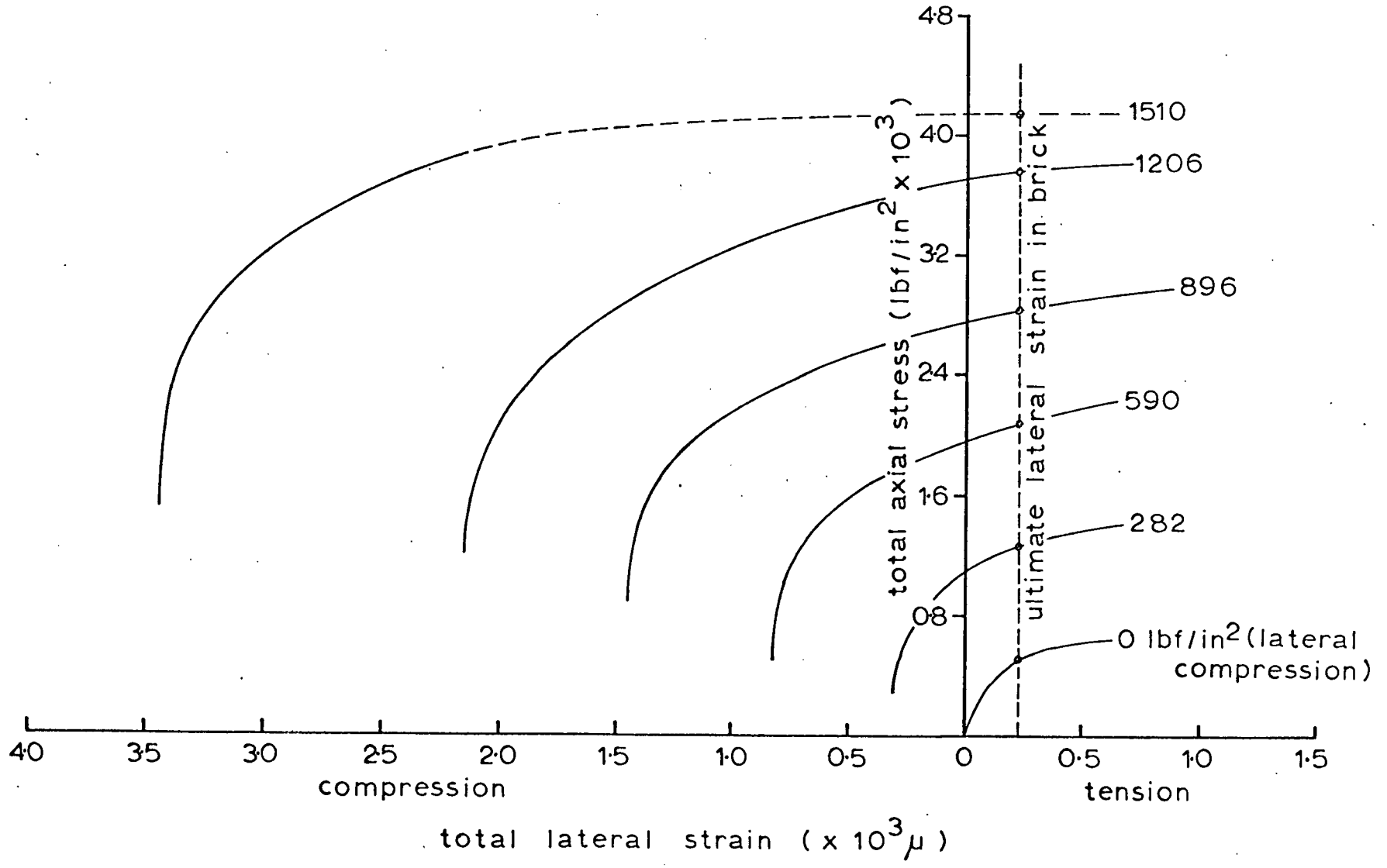

Fig 7.2 **Axial Stress – Lateral Strain Relationship for 1:1:6 Mortar**

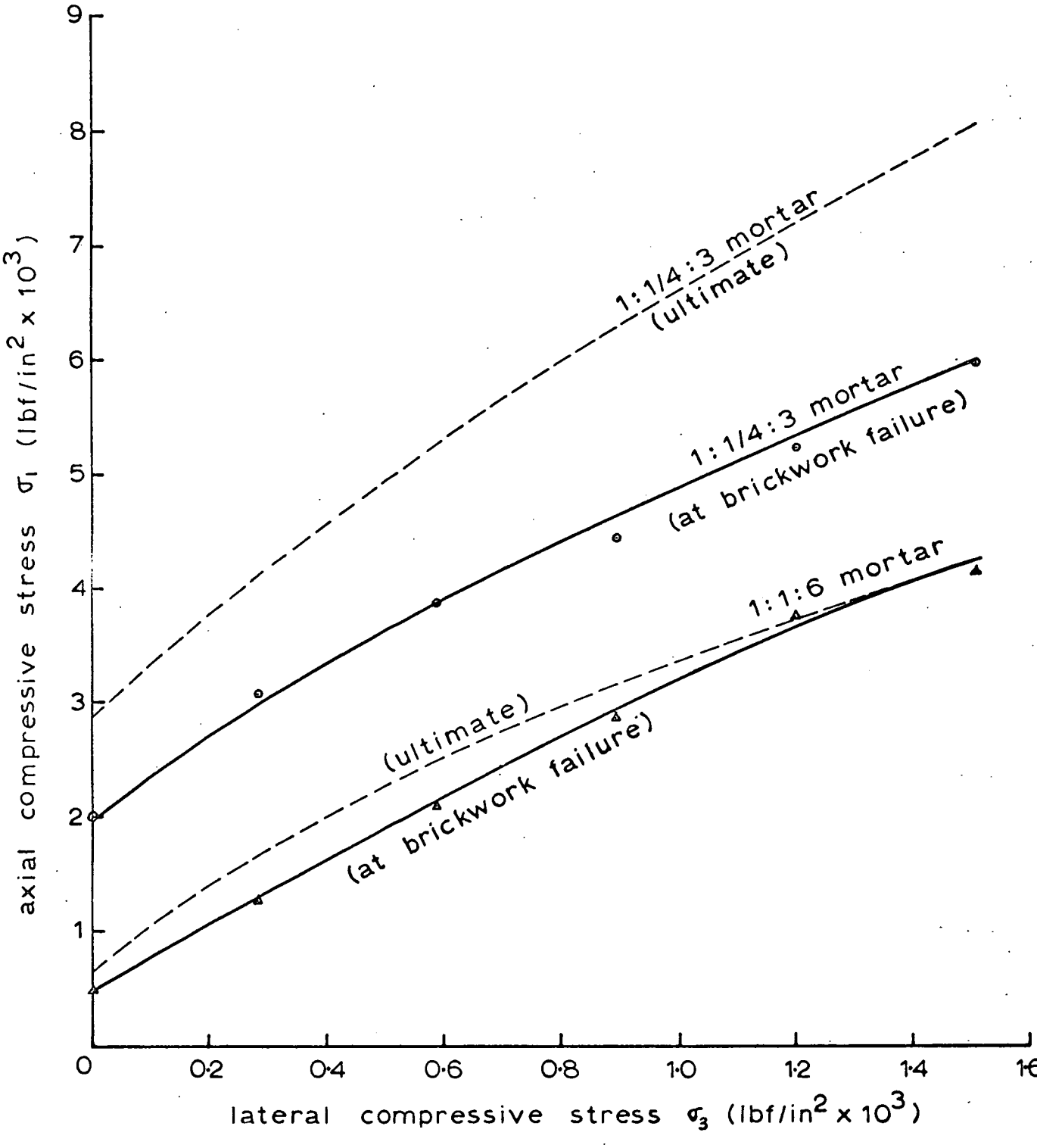

Fig 7.3 Triaxial Compressive Stresses for Mortar at Brickwork Failure

It may be seen from Fig. 7.3 that for the 1:$\frac{1}{4}$:3 mortar the state of triaxial stresses in the mortar at brickwork failure is considerably lower than the ultimate. Computation of the theoretical compressive strengths of brickwork using this curve produces values much lower than those obtained experimentally.

It would appear that the values of triaxial stresses in the horizontal mortar joint at brickwork failure determined from the stress-strain curves for mortar in triaxial compression does not yield satisfactory results for the compressive strength of brickwork. The reason is perhaps this: The mortar in a horizontal joint in brickwork is not laterally confined for the full depth of the joint, but is restrained by the bricks at the interfaces only, and it is probable that, as the compressive load is applied to the brickwork, substantial lateral yielding of the mortar takes place such that the state of triaxial stresses in the mortar is at its ultimate at the instant of brickwork failure. In this event, the determination of the brickwork compressive strength should involve the ultimate triaxial compressive strength of the mortar.

It was explained in Section 6.3 that on account of the inelastic behaviour of mortar, there would be considerable stress redistribution within the brick and mortar elements in axially-loaded brickwork approaching failure, and that a more or less uniform stress condition existed at failure. In this case, the following equation governs the equilibrium of horizontal forces in an axially-loaded brickwork prism:-

$$t_b = \frac{d_m}{d_b} \sigma_m = \alpha . \sigma_m \qquad \text{.....(7.1)}$$

where

t_b = lateral tensile stress in brick

m/

σ_m = lateral compressive stress in mortar

d_b = thickness of brick

d_m = thickness of mortar

α = thickness ratio.

The graphical solution for the compressive strength of the brickwork prism is achieved simply by superimposing the curve for the triaxial compression of mortar, suitably adjusted to account for the "thickness factor" given by equation (7.1), on to the biaxial compression-tension failure envelope for the brick. The ordinate of the point of intersection of these two curves represents the compressive strength of the brickwork prism.

Fig. 7.4 presents the graphical solution for the compressive strengths of brickwork prisms built with various strength bricks, two mortar mixes and for two thickness ratios. These theoretical values will be compared with the experimental results obtained from crushing tests on brickwork prisms later in Section 7.3.

7.2.2 Analytical Solution

The graphical method of solution serves to illustrate comprehensibly the basis of the proposed failure criterion for brickwork in compression. The solution may also be achieved analytically by assigning empirical equations to the failure envelopes.

The equation which best fits the experimental curve describing the biaxial compression-tension failure envelope for brick in Fig. 4.7 is given by a third degree polynomial:-

$$\frac{t}{t_o} = 0.9968 - 2.0264\left(\frac{c}{c_o}\right) + 1.2781\left(\frac{c}{c_o}\right)^2 - 0.2487\left(\frac{c}{c_o}\right)^3 \quad \text{.....(7.2)}$$

where

t = tensile stress in brick

t_o = tensile strength of brick

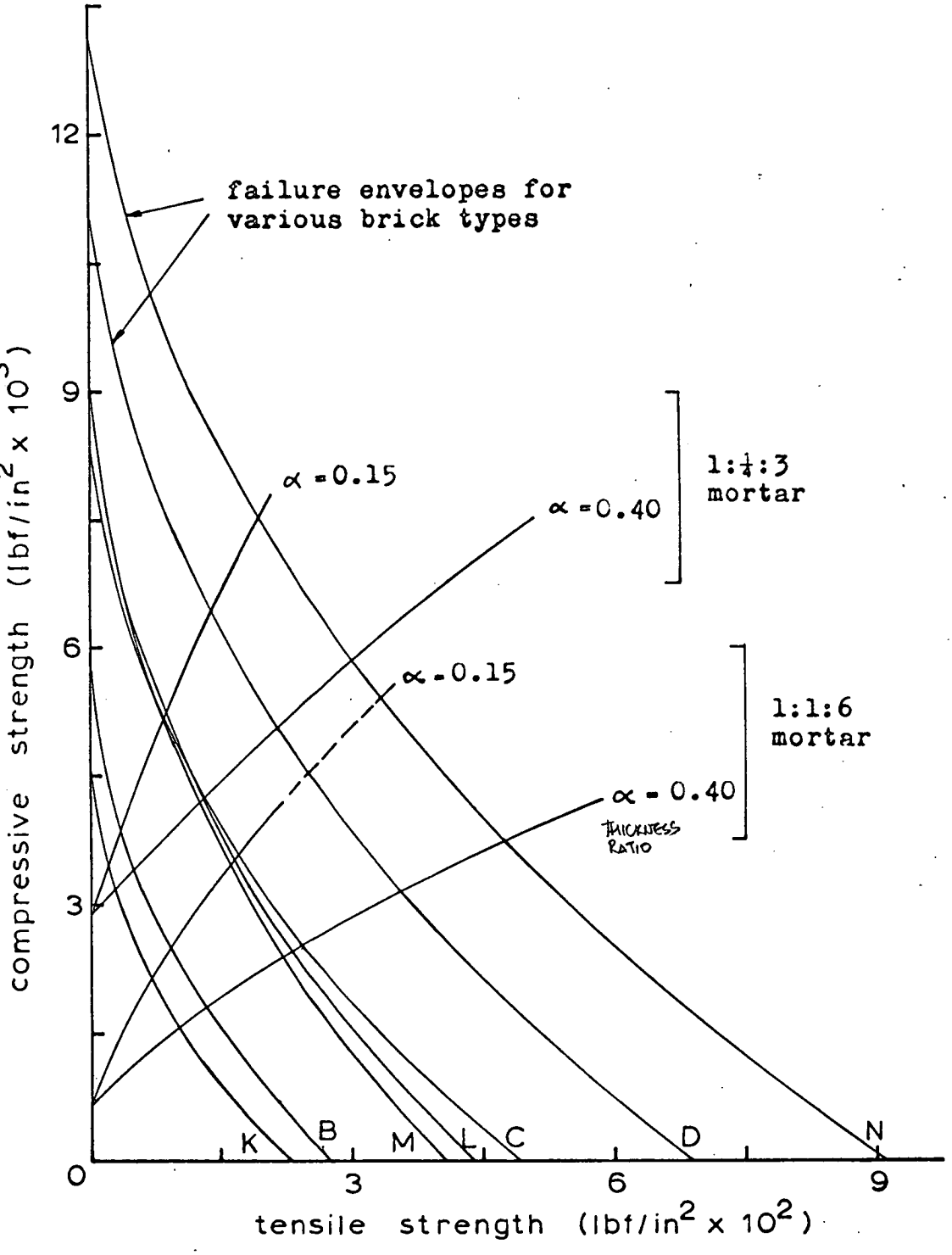

Fig 7.4 Graphical Solution for Brickwork Prism Compressive Strength

c = compressive stress in brick

c_o = uniaxial compressive strength of brick.

Similarly, the triaxial compression curve for brickwork mortar in Fig. 5.22 may be defined by the equation:-

$$\frac{\sigma_3}{\sigma_o} = -0.1620 + 0.1126\left(\frac{\sigma_1}{\sigma_o}\right) + 0.0529\left(\frac{\sigma_1}{\sigma_o}\right)^2 - 0.0018\left(\frac{\sigma_1}{\sigma_o}\right)^3 \quad \ldots\ldots\ldots\ldots\ldots(7.3)$$

where

σ_1 = axial compressive stress in mortar

σ_3 = lateral compressive stress in mortar

σ_o = uniaxial compression strength of mortar.

Equation (7.1) when rewritten in the appropriate symbols becomes:-

$$t = \alpha . \sigma_3 \quad \ldots\ldots\ldots\ldots\ldots(7.4)$$

The resulting equation from combining equations (7.2), (7.3) and (7.4) is:-

$$\left[0.9968\ t_o + 0.1620\alpha . \sigma_o\right] - \left[2.0264\ t_o\left(\frac{1}{c_o}\right) + 0.1126\alpha\right] x + \left[1.2781\ t_o\left(\frac{1}{c_o}\right)^2 - 0.0529\alpha .\left(\frac{1}{\sigma_o}\right)\right] x^2 - \left[0.2487\ t_o\left(\frac{1}{c_o}\right)^3 - 0.0018\alpha .\left(\frac{1}{\sigma_o}\right)^2\right] x^3 = 0 \quad \ldots\ldots\ldots\ldots\ldots(7.5)$$

where 'x' substitutes for 'c' and 'σ_1' (i.e. $x = c = \sigma_1$), and represents the compressive strength of the brickwork prism. Solution of equation (7.5) is readily carried out on the computer for various values of parameters t_o, c_o, σ_o and α. It is for this reason that a polynomial expression has been chosen to describe the experi mental envelopes.

7.3 BRICKWORK COMPRESSION STRENGTHS: THEORETICAL AND EXPERIMENTAL

In this section, a comparison of the brickwork compressive strength between theoretical predictions given by the failure theory described earlier and experimental results obtained from crushing tests on

brickwork prisms is made. The theory is also tested against data on the compressive strength of brickwork taken from selected publications. The extent of the influence of mortar joint thickness on brickwork strength is also discussed.

7.3.1 Brickwork Prism Crushing Tests

A number of brickwork prisms, six brick high, were built using one-third scale model bricks of various strengths and two mortar mixes 1:$\frac{1}{4}$:3 and 1:1:6 identical with those used for the triaxial compression tests on mortar. The mortar/brick thickness ratio for these prisms, designated by the symbol α , were 0.15 and 0.40.

The prisms were damped-cured for 13 days and afterwards dried in an oven at 110 degrees Centigrade for 1 day before testing. The drying was to eliminate the existence of a pore water pressure in wet brickwork.

Three specimens per set of brickwork prisms were made. The results of the crushing tests are given in Tables 7.1 and 7.2. The rate of loading was set at 2000 lbf/in^2/min (13.79 MN/m^2/min) for brickwork compressive strengths exceeding 3000 lbf/in^2 (20.68 MN/m^2) approximately, and at 1000 lbf/in^2/min for strengths below 3000 lbf/in^2.

Table 7.3 and Fig. 7.5 compare the experimental and theoretical results of the compressive strength of brickwork prisms. The narrowness of the 95% confidence limits in Fig. 7.5 implies an excellent correlation between the theoretical and the experimental values.

The theoretical relationship between brickwork compressive strength and brick compressive strength for varying mortar strengths for the case of mortar/brick thickness ratio of 1/7 is presented in Fig. 7.6. The relationship is virtually linear, and shows an increasing compressive strength difference in brickwork built with two different strength mortars/

TABLE 7.1. - COMPRESSION TESTS ON BRICKWORK PRISMS

Brick (1/3 scale) type			B	C	D
Brick strength (lbf/in^2)	BS crushing uniaxial compression tensile		4549 5700 273	9336 8300 489	13448 11000 686
Brickwork prism strength (lbf/in^2)	1:$\frac{1}{4}$:3 mortar	α = 0.15	3408 3556 3296	5274 4793 4762	6107 6357 6270
		mean =	3420	4943	6245
	1:1:6 mortar	α = 0.15	3235 3189 3332	4255 3566 3733	5049 4529 4475
		mean =	3252	3851	4684

$1\ lbf/in^2 = 6.8948 \times 10^{-3} MN/m^2$

TABLE 7.2 - COMPRESSION TESTS ON BRICKWORK PRISMS

Brick (1/3 scale) Type			K	L	M	N
Brick strength (lbf/in2)	BS crushing uniaxial compress. tensile		2944 4576 226	9135 8954 437	10620 9109 401	15448 13132 908
Brickwork prism strength (lbf/in^2)	1:$\frac{1}{4}$:3 mortar	α = 0.15	4305 4713 3633	5302 5967 5202	5036 5163 5269	7111 8027 8135
		mean=	4217	5490	5156	7758
		α = 0.40	2613 2396 2411	5154 4915 4872	4305 4713 3633	6416 6357 5549
		mean=	2473	4980	4217	6107
	1:1:6 mortar	α = 0.15	2219 2230 2188	4660 4798 4585	5115 4183 3919	5172 5851 5344
		mean=	2212	4681	4406	5455
		α = 0.40	1348 1001 1618	2348 1913 2380	2288 2182 2266	2785 2979 2489
		mean=	1322	2214	2245	2751

TABLE 7.3 - EXPERIMENTAL & THEORETICAL RESULTS OF COMPRESSIVE STRENGTH OF BRICKWORK PRISMS

Brick Type	Results	1:¼:3 mortar		1:1:6 mortar	
		α = 0.15	α = 0.40	α = 0.15	α = 0.40
		(lbf/in^2)	(lbf/in^2)	(lbf/in^2)	(lbf/in^2)
B	experimental	3420	-	3252	-
	graphical	3820	-	2480	-
	analytical	3886	-	2492	-
C	experimental	4943	-	3851	-
	graphical	5130	-	3570	-
	analytical	5129	-	3554	-
D	experimental	6245	-	4684	-
	graphical	6410	-	4510	-
	analytical	6353	-	4519	-
K	experimental	3469	2473	2212	1322
	graphical	3400	3150	2120	1560
	analytical	3452	3171	2134	1566
L	experimental	5490	4980	4681	2214
	graphical	5200	4220	3500	2440
	analytical	5204	4236	3533	2437
M	experimental	5156	4217	4406	2245
	graphical	5120	4180	3450	2400
	analytical	5152	4185	3450	2365
N	experimental	7758	6107	5455	2751
	graphical	7520	5850	5400	3720
	analytical	7429	5767	5404	3681

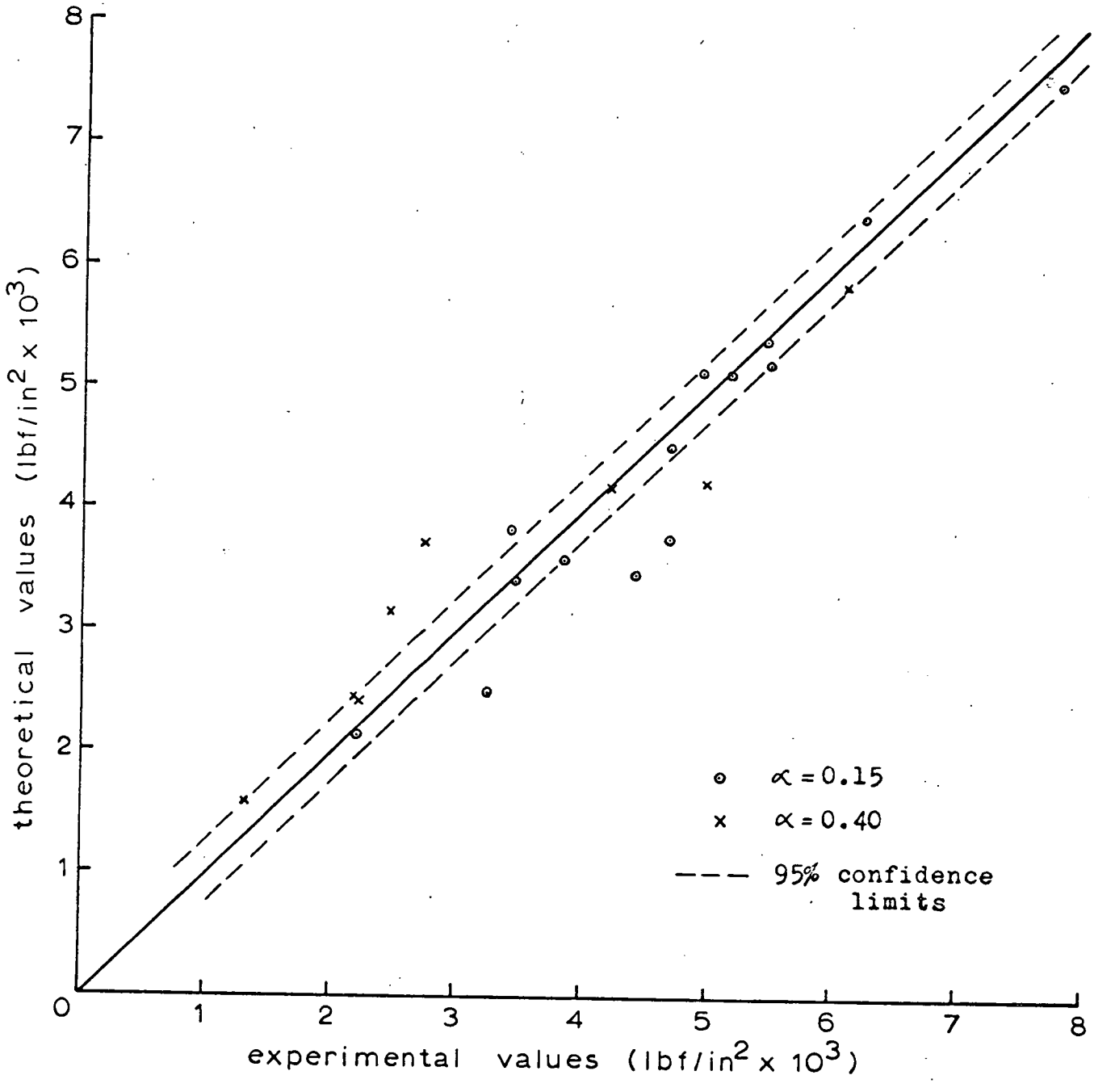

Fig 7.5 Brickwork Prism Compressive Strength

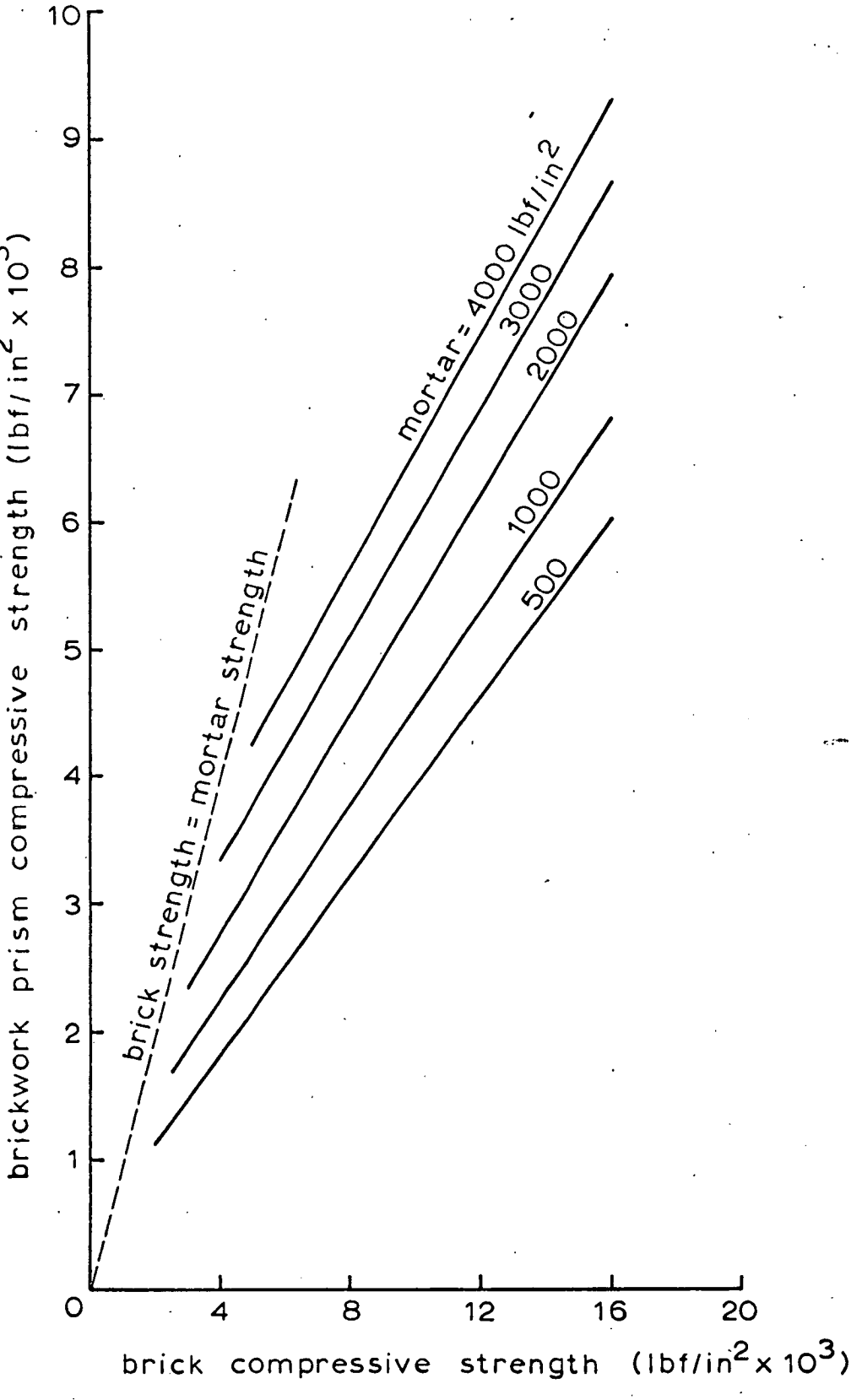

Fig 7.6 Theoretical Brickwork Prism Compressive Strength ($\alpha = 1/7$)

mortars as the brick strength increases. The dashed line in Fig. 7.6, which denotes equal brick and mortar compressive strengths, marks the limit of the validity of the failure criterion. In physical concept, this means that beyond this line where the mortar strength exceeds the brick strength, the deformation properties of these materials are such that the brick element in an axially-loaded brickwork will no longer be subjected to a bi-lateral tension, and hence the proposed failure theory does not apply. In computing the theoretical brickwork strength, the tensile strength of brick, given its compressive strength, is taken from Fig. 3.6.

The curves in Fig. 7.6 resemble those given by Thomas[53] in Fig. 7.7 which show the experimental relationship between the crushing strength of brickwalls and the BS compression strength of brick. The parameters in both cases being not identical, a comparison of values is not possible. Nonetheless, it is noted that brickwalls have lower compressive strengths than the corresponding brickwork prisms, causes for which have yet to be established.

The failure theory has been tested against experimental data extracted from two publications viz. SCPRF National Testing Program[42] and BCRA Special Publication No. 60[62], and these are shown in Figs. 7.8 and 7.9. These particular publications have been chosen because of their comprehensive and thorough investigations.

In the SCPRF tests on six brick high brickwork prisms, 3-hole bricks were used with perforations varying from 4.77 to 19.80%, with a mean of 14.25%. The average mortar cube strength for the $1:\frac{1}{2}:4\frac{1}{2}$ mix is 1513 lbf/in^2 (10.43 MN/m^2) and this has been adjusted by a factor of 1.25 in accordance with BS 1881[10] to give a uniaxial compression strength of/

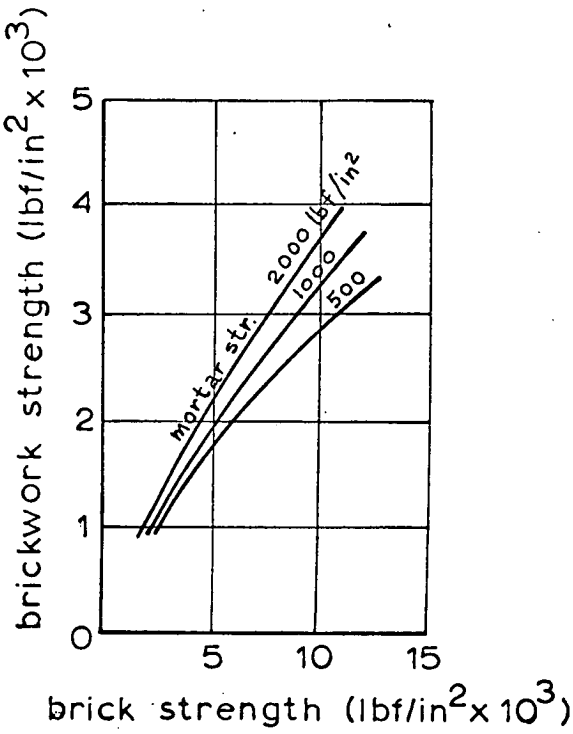

Fig 7.7 Crushing Strength of Brickwork Walls & Piers (after Thomas F.G.)

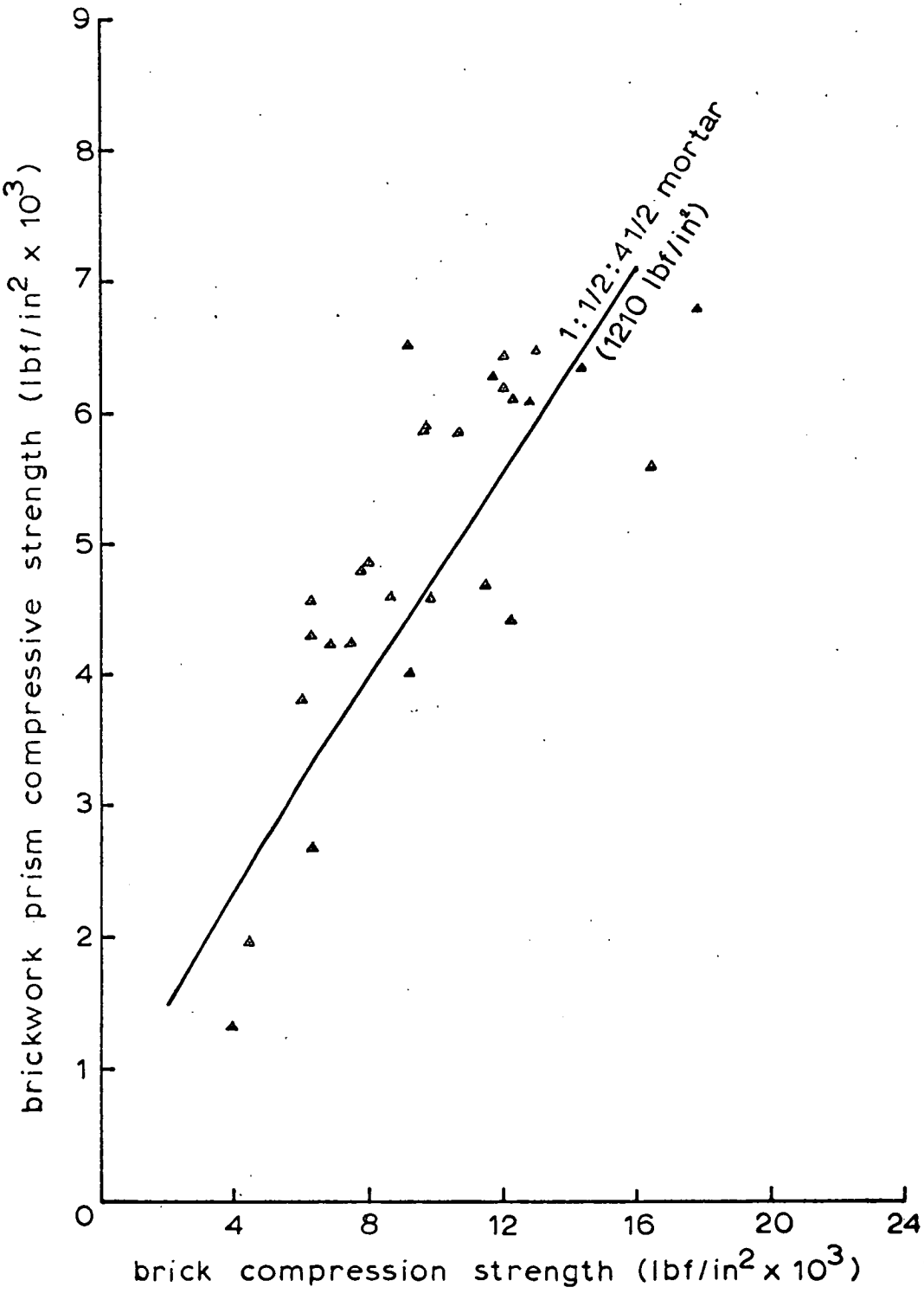

Fig 7.8 **Brickwork Prism Compressive Strength (SCPRF National Testing Program)**

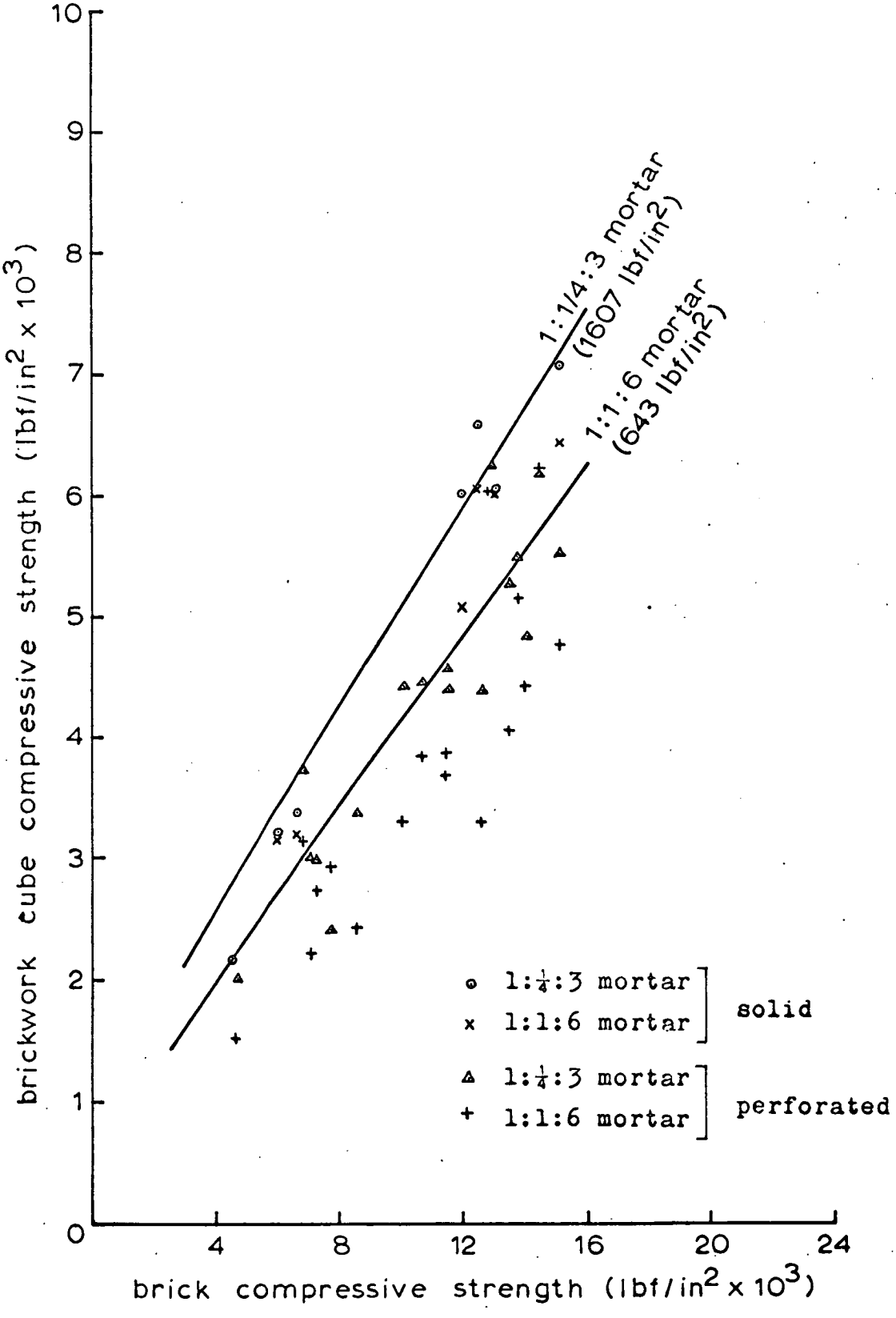

Fig 7.9 Brickwork Cube Compressive Strength (BCRA Special Publication No. 60)

strength of 1210 lbf/in^2 (8.34 MN/m^2). Details of the test results may be found in Appendix B.1.

The BCRA tests used both solid and perforated bricks in their brickwork cubes with two mortar mixes 1:$\frac{1}{4}$:3 and 1:1:6 whose average mortar cube strengths were 2009 and 804 lbf/in^2 (13.85 and 5.54 MN/m^2) respectively, which are modified to give the uniaxial compression strengths of 1607 and 643 lbf/in^2 (11.08 and 4.43 MN/m^2) respectively. As the percentage perforation for each type of brick is available, the strengths based on the net cross-sectional area of the perforated bricks and brickwork cubes are calculated. However, the brick strength is that of the BS crushing strength. The test results are given in Appendix B.2.

The theoretical curves compare reasonably well with the experimental results from these tests for solid bricks but rather less well in the case of the perforated bricks in the BCRA tests where the brickwork strengths are appreciably below the predicted theoretical values. It appears, therefore, that brick perforation is likely to have an influence on the brickwork compressive strength.

7.3.2 Effect of Mortar/Brick Thickness Ratio

The theoretical curves describing the influence of mortar/brick thickness ratio on brickwork compressive strength are given in Fig. 7.10 for various brick and mortar compressive strengths. The curve is sharply hyperbolic in the case where the brick-mortar strength difference is large.

The "thickness factor" is therefore a significant influence on the compressive strength of brickwork. For instance, an increase in brickwork strength up to 17% may be achieved by decreasing the mortar/brick thickness ratio from the present level of 1/7 (using imperial size brick with 3/8 in mortar joint) to a figure of 1/10.

In order to verify the influence of mortar/brick thickness ratio on the compressive/

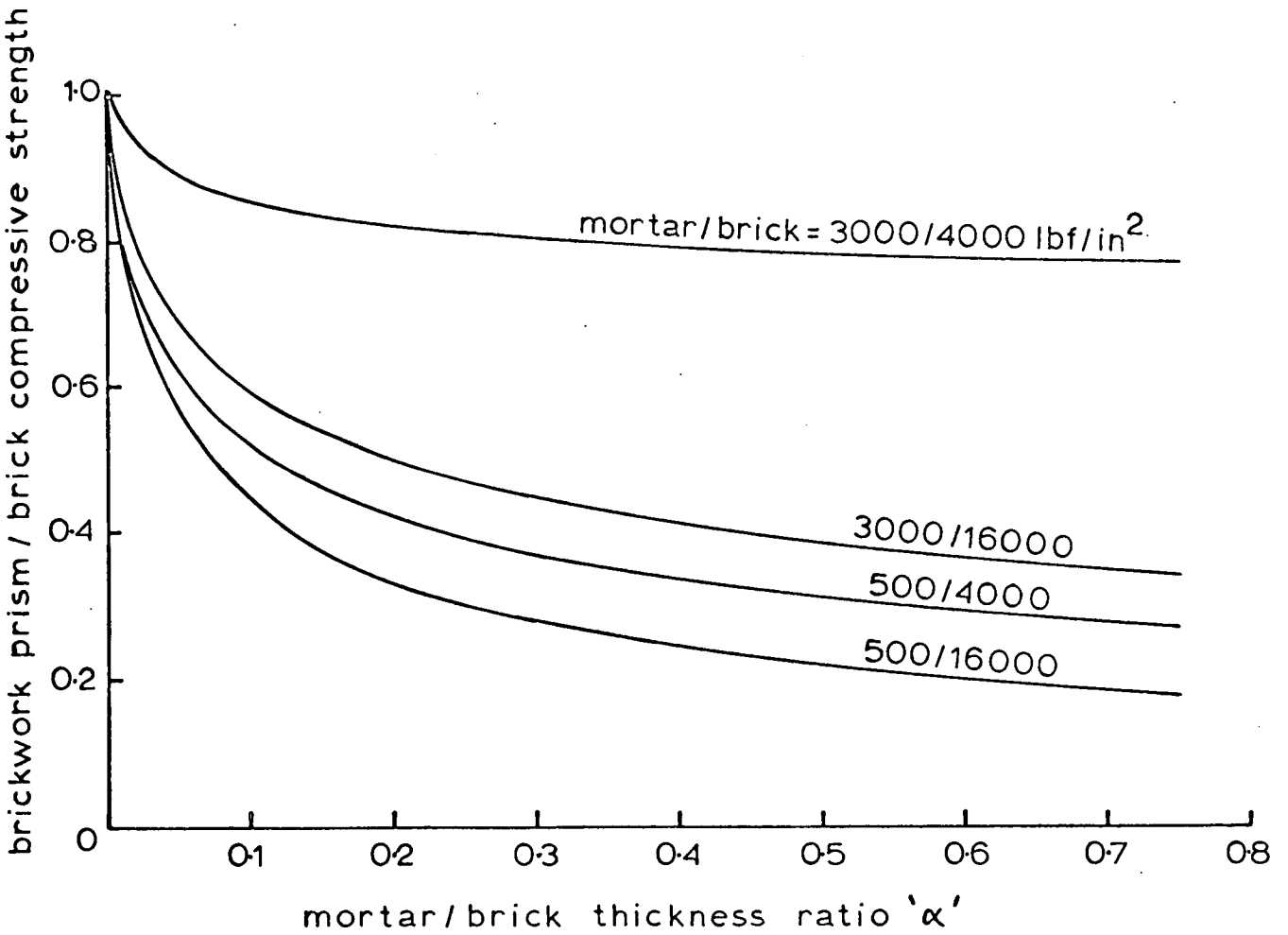

Fig 7.10 Effect of Mortar/Brick Thickness Ratio on Brickwork Compressive Strength

the compressive strength of brickwork given by theory, brickwork prisms, six brick high, were built with one-third scale model bricks, type 'N', with various mortar joint thickness. Practical considerations limit the thinnest joint attainable to about 0.07 in, giving a mortar/brick thickness ratio of, also, 0.07. In order to obtain a lower value of thickness ratio, a set of brickwork prism were built on edge, and in this way, a thickness ratio of 0.05 is obtained. The brickwork prisms on edge are five brick high so as to avoid possible effects of an increased slenderous ratio. The bricks used in prisms with thin joints are previously ground flat on a polishing machine.

The test results of these prisms are recorded in Table 7.4 and plotted in Fig. 7.11 against the corresponding theoretical curve. The experimental points fit reasonably well with the theoretical curve.

Fig. 7.11 also contains test data taken from published papers by SCPRF[42] and Francis et al.[19]. A correction factor of 1.25 has been applied to the compressive strength of these bricks which were tested flat for the platen restraint effect. The SCPRF data are values taken from a faired curve and are not actual prism compressive strengths obtained. The relevant test results from these papers are listed in Appendices B.1 and B.3. Although these test data do not conform closely to the theoretical curves, they underline nevertheless the significant influence of the mortar/brick thickness ratio on brickwork compressive strength.

7.4 SUMMARY

1. A failure theory describing the strength of axially-loaded brickwork has been developed which shows good correlation with experimental results obtained from crushing tests on brickwork prisms.
2. The theoretical values compare favourably also with test data extracted from published papers.

3./

TABLE 7.4 - EFFECT OF MORTAR/BRICK THICKNESS RATIO ON BRICKWORK PRISM COMPRESSIVE STRENGTH

Brick (1/3 scale) Type 'N'

B.S. compression strength = 15448 lbf/in^2

Uniaxial compression strength = 13132 lbf/in^2

Compressive strength of 1:$\frac{1}{4}$:3 mortar = 2873 lbf/in^2

Mortar/brick thickness ratio "α"	Brickwork prism compressive strength (lbf/in^2)	Brickwork/brick compressive strengths
0.05 *	8893 9844 9703 mean = 9480	0.7219
0.07	7434 7892 8469 mean = 7932	0.6040
0.15	7111 8027 8135 mean = 7758	0.5908
0.40	6416 6357 5549 mean = 6107	0.4650
0.69	4568 4331 5226 mean = 4708	0.3585

* Five-brick high prism built on edge

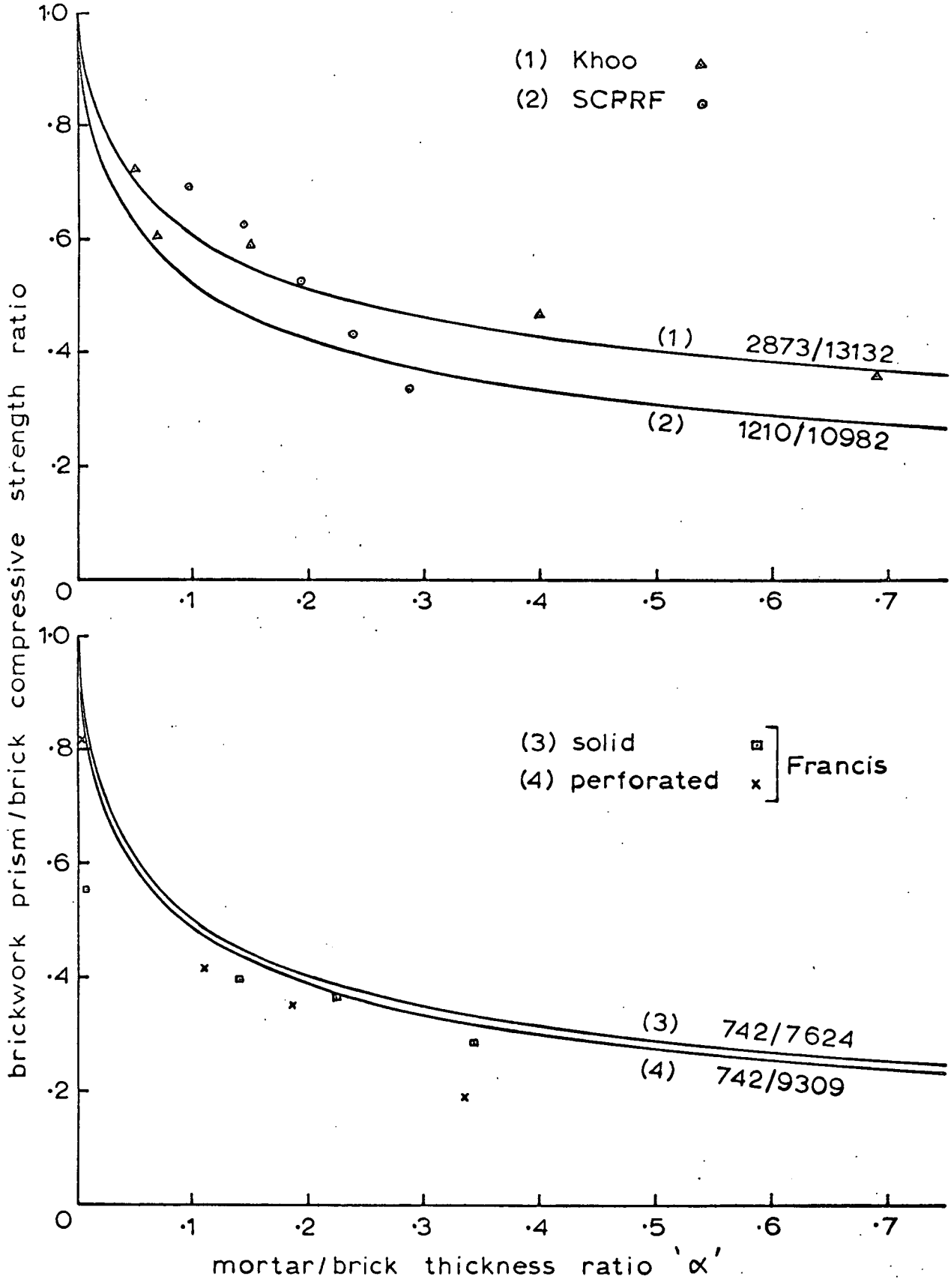

Fig 7.11 Effect of Mortar/Brick Thickness Ratio on Brickwork Compressive Strength; Comparison with Experimental Data

3. The relationship between brickwork compressive strength and brick compressive strength for a given mortar strength is almost linear.

4. The theoretical curve which represents the effect of mortar/brick thickness ratio on the compressive strength of brickwork is hyperbolic and is steepest where the strength difference between brick and mortar is the largest. An increase in brickwork strength up to 17% may be achieved by decreasing the mortar/brick thickness ratio from the present level of 1/7 to a value of 1/10.

5. The influence of mortar/brick thickness ratio on the compressive strength of brickwork given by theory has been verified by some experimental results obtained from crushing tests on brickwork prisms built with various mortar joint thicknesses.

CHAPTER 8 - GENERAL CONCLUSIONS & SUGGESTIONS FOR FURTHER RESEARCH

8.1 CONCLUSIONS

The following conclusions have been reached as a result of the investigations presented in this thesis:-

1. A failure criterion for brickwork under axial compression established from a "strength" approach has been sucessfully tested against experimental results obtained from crushing tests on brickwork prisms built with one-third scale model bricks. A favourable comparison of the brickwork compressive strength is also achieved between theoretical predictions given by the failure theory and experimental data taken from selected publications.
2. The relationship between brickwork compressive strength and brick compressive strength for a given mortar is almost linear.
3. The significant influence of the mortar/brick thickness ratio on the compressive strength of brickwork is reflected in their hyperbolic relationship which is steepest where the strength difference between brick and mortar is the largest.
4. The biaxial compression-tension failure envelope for brick obtained experimentally is concave in shape. Biaxial compression-tension strength tests on clay pipes also produced a concave relationship between the stresses. This means a severe interaction exists between the compression-tension stresses, which is more severe than those predicted by the theoretical curves of Coulomb and Griffith.
5. The increase in ultimate strength of brickwork mortar in triaxial compression/

compression with increasing confining pressure is much the same as that obtained for cement mortar but is less than that obtained for concrete. The principal-stress relationship is not linear and the principal-stress ratio reduces slightly with increasing lateral pressure.

6. A theoretical analysis by the finite element method into the lateral stress distribution in an axially-loaded brickwork prism reveals a stress concentration at the edges of the brick-mortar interface, causing high tensile stresses in brick in these regions which are more severe in an end-face section. Consequently, theory indicates that the mode of failure in an axially-loaded brickwork prism is through initial tensile cracking along a plane at the edge of the end-face section in the direction of the brick length. Experimental observation of the location of the initial tensile cracking in brick in numerous crushing tests on brickwork prisms confirms the theoretical prediction. This mode of failure has often been described as spalling failure in brickwork.

7. The strength of soaked bricks is affected by the presence of a pore water pressure whose effect is to reduce the compressive strength of brick and to increase its tensile strength.

8. The tensile to compressive strength ratio of brick increases from 1/16 for weak bricks to 1/12 for high strength bricks.

9. The ultimate tensile strain for brick varies between 150 to 300 micro-units regardless of strength, and remains unchanged under biaxial compression-tension stresses.

8.2 SUGGESTIONS FOR FUTURE RESEARCH

The failure criterion for the compressive strength of brickwork established in/

established in this thesis applies only to the simplest case of stack-bonded brickwork prism using solid bricks. A logical extension to the study carried out here is to determine the influence of other secondary parameters on brickwork compressive strength. In practical brickwork, these include the presence of vertical mortar joints, perforation and frogging in bricks, the slenderness ratio of brickwalls, and the influence of pore water pressure in wet brickwork. An investigation into the use and efficiency of horizontal reinforcement as a means of enhancing the compressive strength of brickwork may be worthwhile pursuing.

It is recalled that a simplification has been made in respect of the state of complex stresses in a brick element in axially-loaded brickwork from a compression-tension-tension to a biaxial compression-tension. It is hoped that some effort will be given to devise a test method which can produce the desired three dimensional stresses in brick.

For those delving in the field of fracture mechanics, the deviation of the biaxial compression-tension failure envelope obtained experimentally for ceramic material from the theoretical curves of Coulomb and Griffith should pose an interesting problem.

It may be necessary to look afresh into the deformation characteristics of concrete and mortar in triaxial compression under confining pressures in excess of their uniaxial compression strength. Experimental evidence indicates a re-orientation of the structural matrix of the cementitious material at high confining pressure involving a breakdown of the aggregate-mortar bond, resulting in a decreasing bulk modulus with increasing confining pressure.

REFERENCES

1. Akroyd, T.N.W. "CONCRETE UNDER TRIAXIAL STRESS" Mag. Conc. Res., Vol. 13(39), Nov. 1961.

2. Balmer G.G. "SHEARING STRENGTH OF CONCRETE UNDER HIGH TRIAXIAL STRESS - COMPUTATION OF MOHR'S ENVELOPE AS A CURVE" U.S. Bureau of Reclamation, Report No. SP23, Denver, 1949.

3. Blakey, F.A. & Beresford, F.D. "TENSILE STRAINS IN CONCRETE" Part 1, Report C2.2-1, Div. of Bldg. Res., Melbourne, 1953.

4. Brace, W.F. "AN EXTENSION OF GRIFFITH THEORY OF FRACTURE TO ROCKS" Journ. Geophys. Res., Vol. 65, 1960.

5. Bradshaw R.E. & Hendry A.W. "CRUSHING TESTS ON STOREY-HEIGHT WALLS 4½ IN. THICK: FURTHER RESULTS" B.C.R.A. Tech. Note NO. 105, June 1967.

6. Bresler B. & Pister K.S. "STRENGTH OF CONCRETE UNDER COMBINED STRESSES" Journ. A.C.I., Vol. 55, Sept. 1958.

7. Brisbane, J.J. "AXIAL LOADING OF AN ELLIPTICAL DISK" Journ. Appl. Mechs., Vol. 30, June 1963.

8. Broutman L.J. & Cornish R.H. "EFFECT OF POLYAXIAL STRESS STATES ON FAILURE STRENGTH OF ALUMINA CERAMICS" Journ. Amer. Ceramic Soc., Vol. 48, Oct. 1965.

9. B.S. 65 & 540 "CLAY DRAIN & SEWER PIPES" 1966.

10. B.S. 1881 "METHODS OF TESTING CONCRETE" Part 4 1970.

11. B.S. 4551 "METHODS OF TESTING MORTAR" 1969.

12. Campbell-Allen D. "STRENGTH OF CONCRETE UNDER COMBINED STRESSES" Constr. Review, Vol. 35 (4). April 1962.

13. Coffin L.F. "THE FLOW AND FRACTURE OF A BRITTLE MATERIAL" Journ. Appl. Mechs., Vol. 17, Trans. ASME, Vol. 72, 1950.

14. Cornet I. & Grassi R.C. "FRACTURE OF INNOCULATED IRON UNDER BIAXIAL STRESSES" Journ. Appl. Mechs., Vol. 22, June 1955.

15. Coulomb C.A. "SUR UNE APPLICATION DES REGLES DE MAXIMIS ET MINIMIS A QUELQUES PROBLEMES DE STATIQUE, RELATIFS A L'ARCHITECTURE" Memoires de Mathematique et de Physique, Academie Royal des Sciences, par divers Savans, Annee 1773, Paris 1776.

16. Davey N. & Thomas F.G. "THE STRUCTURAL USES OF BRICKWORK" Inst. of Civil Engrs., Structural & Bldg. Paper No. 24, 1950.

17. Dessayi P. "STRENGTH OF CONCRETE UNDER COMBINED COMPRESSION & TENSION; DETERMINATION OF INTERACTION CURVE AT FAILURE FROM CYLINDER SPLIT TEST" Materials & Structures, Vol. 2(9), May 1969.

18. Ely R.E. "STRENGTH OF GRAPHITE TUBE SPECIMENS UNDER COMBINED STRESSES" Journ. Amer. Ceramic Soc., Vol. 48, Oct. 1965.

19. Francis A.J., Horman C.B. & Jerrems L.E. "THE EFFECT OF JOINT THICKNESS AND OTHER FACTORS ON THE COMPRESSIVE STRENGTH OF BRICKWORK" Proc. 2nd Int. Brick Masonry Conf., April 1970.

20. Gardner N.J. "TRIAXIAL BEHAVIOUR OF CONCRETE". Journ. A.C.I., Vol. 66 (2), Feb. 1969.

21. Goode C.D. & Helmy M.A. "THE STRENGTH OF CONCRETE UNDER COMBINED SHEAR AND DIRECT STRESS" Mag. Conc. Res., Vol. 19 (59), June 1967.

22. Grassi R.C. & Cornet I. "FRACTURE OF GRAY CAST-IRON TUBES UNDER BIAXIAL STRESS" Journ. Appl. Mechs., Vol. 16, Trans. ASME, Vol. 71, 1949.

23. Griffith A.A. "THE PHENOMENA OF RUPTURE AND FLOW IN SOLIDS" Phil. Trans. Royal Soc., London, A221, 1921.

24. Haller P. "THE PHYSICS OF THE FIRED BRICK. PART ONE: STRENGTH PROPERTIES" Library Comm. 929, Bldg. Res. Stat., Garston, Jan. 1960. (Translated from the German by G.L. Cairns).

25. Hilsdorf, H.K. "AN INVESTIGATION INTO THE FAILURE MECHANISM OF BRICK MASONRY LOADED IN AXIAL COMPRESSION" Designing, Engineering/

25. Engineering and Constructing with Masonry Products. Edited by F.B. Johnson, Houston, Texas, Gulf Publishing, 1969.

26. Hobb D.W. "STRENGTH OF CONCRETE UNDER COMBINED STRESS" Cement & Conc. Res., Vol. 1, Jan. 1971.

27. Hoek E. "ROCK FRACTURE UNDER STATIC STRESS CONDITIONS" CSIR Report MEG 383, Pretoria, South Africa, 1965.

28. Hughes B.P. & Bahramian B. "CUBE TESTS AND THE UNIAXIAL COMPRESSIVE STRENGTH OF CONCRETE" Mag. Conc. Res., Vol. 17 (53), Dec. 1965.

29. Inglis C.E. "STRESSES IN A PLATE DUE TO THE PRESENCE OF CRACKS AND SHARP CORNERS" Trans. Inst. Naval Architects, London, Vol. 55, Part 1, 1913.

30. Isenberg J. "INELASTICITY & FRACTURE IN CONCRETE" Ph.D. Thesis, University of Cambridge, 1966.

31. Kalita U.C. "EXPERIMENTAL & THEORETICAL STUDIES OF THE STRUCTURAL BEHAVIOUR OF BRICKWORK CROSS-WALL SYSTEMS" Ph.D. Thesis, University of Edinburgh, 1970.

32. Karman Th. Von "FESTIGKEITSVERSUCHE UNTER ALLSEITIGEM DRUCK" Z. Ver. dt. Ing., 55, 1911.

33. Krishnaswamy K.T. "STRENGTH OF CONCRETE UNDER COMBINED TENSILE-COMPRESSIVE STRESSES" Materials & Structures, Vol. 2 (9), May 1969.

34. Kupfer H., Hilsdorf H.K. & Rusch H. "BEHAVIOUR OF CONCRETE UNDER BIAXIAL STRESS" Journ. A.C.I., Vol. 66, Aug. 1969.

35. Lenczner D. "SIMPLE THEORY OF FAILURE FOR BRICKWORK" Paper presented to 3rd Symp. Loadbearing Brickwork, Brit. Ceramic Soc., Nov. 1968.

36. McClintok F.A. & Walsh J. "FRICTION ON GRIFFITH CRACKS UNDER PRESSURE" Proc. 4th U.S. Nat. Cong. of Appl. Mechs., 1962.

37. McHendry D. & Karni J. "STRENGTH OF CONCRETE UNDER COMBINED TENSILE AND COMPRESSIVE STRESS" Journ. A.C.I., Vol. 54, April 1958.

38. Mohr O. "WELCHE UMSTANDE BEDINGEN DIE ELASTIZITATSGRANZE UND DEN BRUCH EINES MATERIALS?" Z. Ver. dt. Ing., Vol. 44, 1900.

39. Monk C.B. Jnr. " A HISTORICAL SURVEY AND ANALYSIS OF THE COMPRESSIVE STRENGTH OF BRICK MASONRY" Struct. Clay Products Res. Foundation, Research Report No. 12, Geneva, Illinois, July 1967.

40. Morsy E.H. "AN INVESTIGATION OF MORTAR PROPERTIES INFLUENCING BRICKWORK STRENGTH" Ph.D. Thesis, Univ. of Edinburgh, 1968.

41. Murrell S.A.F. "A CRITERION FOR BRITTLE FRACTURE OF ROCKS & CONCRETE UNDER TRIAXIAL STRESS AND THE EFFECT OF PORE PRESSURE ON THE CRITERION" Proc. 5th Rock Mechs. Symp., Univ. of Minnesota, in 'Rock

41. Mechanics' Edited by C. Fairhurst, Oxford, Pergamon, 1963.

42. National Testing Program "SMAIL SCALE SPECIMEN TESTING" Struct. Clay Products Res. Foundation, Prog. Report No. 1, Geneva, Illinois, Oct. 1964.

43. Newman K. "CRITERIA FOR THE BEHAVIOUR OF PLAIN CONCRETE UNDER COMPLEX STATES OF STRESS" Proc. Int. Conf. on the Structure of Concrete, London, Cement & Concrete Assoc, 1965.

44. Ogunlesi O. "THE ELASTIC ANALYSIS OF PLATES BY BIHARMONIC EIGENFUNCTIONS WITH SPECIAL REFERENCE TO THERMAL STRESSES" Ph.D. Thesis, Univ. of Liverpool, 1964.

45. Paul B. "A MODIFICATION OF THE COULOMB-MOHR THEORY OF FRACTURE" Journ. Appl. Mechs., Vol. 28 (2), June 1961.

46. Prasan S., Hendry A.W. & Bradshaw R.E. "CRUSHING TESTS ON STOREY-HEIGHT WALLS $4\frac{1}{2}$ in. THICK" Proc. Brit. Ceramic Soc. No. 4, July 1965.

47. Reeves J.S. "THE STRENGTH OF CONCRETE UNDER COMBINED DIRECT AND SHEAR STRESSES" Cement & Conc. Assoc. Tech. Report No. TRA/365, Nov. 1962.

48. Sinha B.P. "FURTHER CRUSHING TESTS ON MODEL STOREY-HEIGHT BRICK WALLS" Brit. Ceramic Res. Assoc. Tech. Note No. 130, August 1968.

49. Sinha B.P. "THE INFLUENCE OF NUMBERS OF COURSES AND THE EFFECT OF BRICK STRENGTH ON BRICKWORK STRENGTH" Brit. Ceramic Res. Assoc. Tech. Note No. 131, Aug. 1968.

50. Sinha B.P. & Hendry A.W. "SPLITTING FAILURE OF BRICKWORK AS A FUNCTION OF THE DEFORMATION PROPERTIES OF BRICKS AND MORTAR" Brit. Ceramic Res. Assoc. Tech. Note No. 86, May 1966.

51. Smith F.C. & Brown R.Q. "THE SHEARING STRENGTH OF CEMENT MORTAR" Univ. of Washington Engng. Expt. Stat. Bulletin No. 106, 1941.

52. Smith G.M. "FAILURE OF CONCRETE UNDER COMBINED TENSILE AND COMPRESSIVE STRESSES" Journ. A.C.I., Vol. 50, Oct. 1953.

53. Thomas F.G. "THE STRENGTH OF BRICKWORK" The Structural Engineer, Vol. 31, Feb. 1953.

54. Thomas K. & O'Leary, D.C. "TENSILE PROPERTIES OF BRICK" Proc. 2nd Int. Brick Masonry Conf., April 1970.

55. Timoshenko S. "STRENGTH OF MATERIALS, PART II: ADVANCED" Van Nostrand Reinhold Co., 1969.

56. Timoshenko S. & Goodier J.N. "THEORY OF ELASTICITY" McGraw-Hill Co., 1951.

57. Tsuboi Y. & Suenaga Y. "EXPERIMENTAL STUDY ON FAILURE OF PLAIN CONCRETE UNDER COMBINED STRESSES" Trans. Architectural Inst. of Japan No. 64, Feb. 1960.

58. U.S. Bureau of Reclamation — "TRIAXIAL STRENGTH TESTS OF NEAT CEMENT & MORTAR CYLINDERS" Conc. Lab. Report No. C-779, Nov. 1954.

59. Vile G.W.D. — "THE STRENGTH OF CONCRETE UNDER SHORT-TERM STATIC BIAXIAL STRESS" Proc. Symp. Int. Conf. on the Structure of Concrete, London, 1965.

60. Vile G.W.D. — "BEHAVIOUR OF CONCRETE UNDER SIMPLE AND COMBINED STRESSES" Ph.D. Thesis, Univ. of London, 1965.

61. Ward M.A. — THE TESTING OF CONCRETE MATERIALS BY PRECISELY CONTROLLED UNIAXIAL TENSION" Ph.D. Thesis, Univ. of London, 1964.

62. West H.W.H., Hodgkinson H.R. Davenport S.T.E. — "THE PERFORMANCE OF WALLS BUILT WITH & WITHOUT PERFORATIONS" Brit. Ceramic Res. Assoc. Special Publ. No. 60, 1968.

63. Zienkiewicz O.C. & Cheung Y.K. — "THE FINITE ELEMENT METHOD IN STRUCTURAL AND CONTINUUM MECHANICS" McGraw-Hill Co., 1967.

APPENDIX A

A.1 COMPUTER PROGRAM FOR SOLUTION OF POLYNOMIAL EQUATIONS - FORTRAN IV G LEVEL

```
      REAL MRCOM
      DIMENSION THICK(9),MRCOM(6),BKCOM(10),BKTEN(10),X(4),
     1RR(3), RI(3)
      READ(5,10) NTHK,NMORT,NBK
   10 FORMAT (3I4)
      DO 11 I=1,NTHK
   11 READ(5,12)THICK(I)
   12 FORMAT (F8.4)
      DO 13 I=1,NMORT
   13 READ(5,14) MRCOM(I)
   14 FORMAT (F8.1)
      DO 15 I=1,NBK
   15 READ(5,16) BKCOM(I),BKTEN(I)
   16 FORMAT (2F8.1)
      WRITE (6,17)
   17 FORMAT (3X, 'THICK.RATIO',6X,'MORTAR COMP',6X,'BRICK
     1COMP',6X,'BRICK TENSION'//8X,'ROOTS (REAL,IMAG)'//)
      DO 21 I=1,NTHK
      DO 21 J=1,NMORT
      DO 21 K=1,NBK
      X(1)= 0.9968*BKTEN(K)+0.1620*MRCOM(J)*THICK(I)
      X(2)=-2.0264*BKTEN(K)/BKCOM(K)-0.1126*THICK(I)
      X(3)= 1.2781*BKTEN(K)/(BKCOM(K)**2)-0.0529*THICK(I)/
     1MRCOM(J)
      X(4)=-0.2487*BKTEN(K)/(BKCOM(K)**3)+0.0018*THICK(I)/
     1(MRCOM(J)**2)
      CALL POLRT(X,W,3,RR,RI,IER)
      IF(IER.EQ.0) GOTO 19
```

```
      WRITE (6,18) IER
   18 FORMAT (2X,'POLRT FAILS,ERROR FLAG =',2X,12)
      GOTO 22
   19 WRITE(6,20) THICK(I),MRCOM(J),BKCOM(K),BKTEN(K),
     1X(1),X(2),X(3),X(4),RR(1),RI(1),RR(2),RI(2),RR(3),
     1RI(3)
   20 FORMAT (6X,F8.4,3(10X,F8.1)//4(3X,E10.4)//6(3X,E10.4)//)
   21 CONTINUE
   22 STOP
      END
```

APPENDIX B

B.1. MODIFIED SCPRF NATIONAL TESTING PROGRAM TEST RESULTS[42]

(a) Crushing Strength of Brickwork Prisms

Perforated bricks: 3-hole, 4.77 to 19.80%, mean = 14.25%

@ 10-hole brick

\+ solid brick

Mortar mix S $1:\frac{1}{2}:4\frac{1}{2}$

	Code No	Mortar Cube Strength (lbf/sq. in)	Brick Comp. Strength (lbf/sq. in)	Brickwork Prism Comp. Strength (lbf/sq.in)
	LL	1439	6066	3805
	LM	1439	6306	4553
	FL	1773	6340	2658
@	KM	1773	6868	4230
	GM	1157	7504	4243
	JM	1319	7806	4790
	MM	1665	8039	4849
	DM	1748	8717	4584
	FM	1440	9161	6516
	AL	1580	9267	4002
@	KH	1773	9708	5880
	EM	1748	9730	5891
	CL	1440	9810	4583
	MH	1319	10711	5851
	CM	1363	11502	4689
	AH	1319	12015	6186
	GH	1157	12138	6439
	DH	1665	12264	4413
	LH	1166	12336	6105
	FH	1773	12782	6087
	JH	1665	13052	6474
	AM	1580	14388	6349
	EH	1748	16440	5595
	CH	1363	17838	6808
+	NL	1491	4489	1964
+	NH	1580	6370	4292
+	NM	1580	3968	1314
	SCR	1287	11771	6281
	mean =	1513		

Uniaxial compressive strength of mortar = $\frac{1513}{1.25}$ = 1210 lbf/in^2

(b) Effect of Mortar Joint Thickness

SCR brick: 8 in x 4 in x 2 5/8 in

Perforation: 14.25%

Crushing strength: gross area = 11771 lbf/in^2

net area. = 13727 lbf/in^2

Uniaxial compression strength = 13727/1.25 = 10982 lbf/in^2

Mortar mix S 1:$\frac{1}{2}$:4$\frac{1}{2}$, uniaxial compression str. = 1210 lbf/in^2

Mortar Joint Thick (in)	Mortar/ Brick Thick	Brickwork Prism Comp. Strength (lbf/sq. in)		Brickwork/ Brick Strength
		gross	net	
$\frac{1}{4}$	0.0952	6550	7638	0.6955
3/8	0.1429	5850	6822	0.6212
$\frac{1}{2}$	0.1905	4900	5714	0.5203
5/8	0.2381	4050	4723	0.4301
$\frac{3}{4}$	0.2857	3150	3673	0.3345

B.2 MODIFIED BCRA SPECIAL PUBLICATION NO. 60 TEST RESULTS (62)

Crushing Strength of Brickwork Cubes

(a) Solid Bricks

Code No	Brick Comp. Strength (lbf/sq. in)	Mortar Cube Strength (lbf/sq. in)		Brickwork Cube Strength (lbf/sq. in)	
		1:¼:3	1:1:6	1:¼:3	1:1:6
AS	15120	1947	699	7072	6433
BS	11980	2022	806	6007	5083
CS	13060	2127	661	6050	6030
ES	6060	1693	722	3213	3157
FS	6640	2217	980	3363	3175
GS	4580	2135	919	2160	2165
HS	12450	1925	844	6570	6053
	mean =	2009	804		

Uniaxial compression strength of mortar:

for 1:¼:3 mix, $2009/1.25 = 1607$ lbf/in^2

for 1:1:6 mix, $804/1.25 = 643$ lbf/in^2

(b) Perforated Bricks

Code No.	% Perf.	Brick Comp. Strength on net area (lbf/sq.in)	Mortar Cube Strength (lbf/sq.in)		Brickwork Cube Strength on net area (lbf/sq.in)	
			1:¼:3	1:1:6	1:¼:3	1:1:6
A3	13.8	13805	1795	775	5487	5151
A11	13.9	13566	2332	738	5265	4057
B3	6.8	15129	2140	709	5523	4764
B11	17.8	14039	3206	850	4837	4221
C3	10.1	14472	1703	563	6170	6220
C7	19.8	10100	2353	670	4418	3289
C16	18.7	12632	1773	719	4383	3280
D3	9.5	12906	1632	609	6251	6033
D7	21.5	11541	1997	814	4557	3869
D14	17.7	11555	1532	458	4394	3666
E3	4.8	7332	1900	784	2976	2713
E16	6.5	6877	1615	725	3725	3137
F3	12.3	8643	2693	840	3352	2417
F5	17.1	7084	2013	804	3000	2203
G3	3.6	7739	2087	794	2409	2907
G14	7.6	4740	2427	720	2000	1517
H16	18.6	10762	1640	677	4445	3839
		mean =	2049	720		

Uniaxial compression strength of mortar:

for 1:¼:3 mix, 2049/1.25 = 1639 lbf/in^2

for 1:1:6 mix, 720/1.25 = 576 lbf/in^2

B.3 MODIFIED FRANCIS ET. AL. TEST RESULTS[19]

Effect of Mortar Joint Thickness

(a) Solid Bricks

Dimensions: 8.85 in x 4.18 in x 2.91 in
Crushing strength = 9530 lbf/in^2
Uniaxial compressive strength = 9530/1.25 = 7624 lbf/in^2
Mortar mix 1:1:6 Cube strength = 927 lbf/in^2
Uniaxial compressive strength = 742 lbf/in^2

Mortar Joint Thickness (in)	Mortar/Brick Thickness	Brickwork Prism Comp. Strength (lbf/sq.in)	Brickwork/ Brick Strength
0.022	0.0069	4198	0.5506
0.403	0.1385	2980	0.3909
0.651	0.2237	2751	0.3608
1.000	0.3436	2158	0.2831

(b) Perforated Bricks

Dimensions: 8.97 in x 4.28 in x 2.98 in
Perforation: 17-0.95 in dia. holes, 31.25%
Crushing strength: gross area = 8070 lbf/in^2
net area = 11738 lbf/in^2
Uniaxial compressive strength = 11738/1.25 = 9390 lbf/in^2
Mortar mix 1:1:6 Cube strength = 927 lbf/in^2
Uniaxial compressive strength = 742 lbf/in^2

Mortar Joint Thickness (in)	Mortar/Brick Thickness	Brickwork Prism Comp. Strength (lbf/sq.in)		Brickwork/ Brick Strength
		gross	net	
0.015	0.0050	5286	7689	0.8188
0.328	0.1101	2671	3885	0.4137
0.553	0.1856	2259	3286	0.3499
1.000	0.3356	1217	1770	0.1885